



CA' FOSCARI UNIVERSITY VENICE

PHD IN CHEMICAL SCIENCES, 22° CYCLE
(A. A. 2006/2007 – A. A. 2008/2009)

PHD THESIS
SCIENTIFIC-DISCIPLINARY SECTOR: CHIM/04

**Oxidative Carbonylation of Alkanols Catalyzed
by
Pd(II)–Phosphine Complexes**

PHD THESIS OF Emanuele Amadio, 955382

PHD COORDINATOR
PROF. Paolo Ugo

TUTOR
PROF. Luigi Toniolo

Contents

GENERAL INTRODUCTION	1
PREFACE	1
Oxidative carbonylation of alkanols.....	6
<i>General aspects.....</i>	6
<i>Industrial production of oxalates using alkyl nitrites as oxidant.....</i>	7
<i>Oxidative carbonylation of alkanols using BQ as oxidant.....</i>	9
Other oxidative reactions using BQ	11
<i>Oxidative carbonylation of styrene.....</i>	11
<i>1,4 Dialkoxylation of conjugated dienes.....</i>	14
<i>Oxidation of ethene to acetaldehyde (Wacker process).....</i>	15
SCOPE AND CONTENTS OF THE THESIS	17
REFERENCES	18
CHAPTER 1	21
INTRODUCTION	21
RESULTS AND DISCUSSION.....	23
Synthesis and characterization of the carboalkoxy complexes reported in Table 1	23
X-ray structure analysis of $[\text{Pd}(\text{COOMe})(\text{TsO})(\text{PPh}_3)_2] \cdot 2 \text{CHCl}_3$ (IIa).....	27
Reactivity	31
<i>Reactivity with alkanols.....</i>	31
<i>Reactivity with acids HX (X = Cl, OAc, TsO).....</i>	32
<i>Reactivity with water and with water/TsOH.....</i>	32
<i>Reactivity with ethene and catalytic properties of complexes (Ia–g) in the hydrocarboalkoxylation of ethene.....</i>	33
CONCLUSIONS.....	38

EXPERIMENTAL SECTION	39
Instrumentation and materials	39
Preparation of the complexes	39
<i>Synthesis of trans-[Pd(COOR)(.....</i>	39
<i>Synthesis of trans-[Pd(COOR)(OH₂)(PPh₃)₂](TsO) with R bulkier than Et.</i>	39
Reactivity tests	40
Experiments of hydroesterification of ethene using the carboalcoxy complexes reported in Table 1 as catalyst precursors in the relevant ROH	40
X-ray data collection, structure solution and refinement.....	41
REFERENCES	42
CHAPTER 2	48
INTRODUCTION	48
RESULTS AND DISCUSSION.....	50
Synthesis and characterization of I, Ia, II, III and IIIa.....	50
Reactivity and catalytic properties of I, Ia, II, III, and IIIa	59
Structural characterization of Ia and of I·CH ₂ Cl ₂	65
CONCLUSIONS.....	74
EXPERIMENTAL SECTION	75
Instrumentation and materials	75
Preparation of the complexes	76
<i>Synthesis of cis-[Pd(ONO₂)₂(PPh₃)₂] (I).</i>	76
<i>Synthesis of trans-[Pd(COOMe)(ONO₂)(PPh₃)₂] (Ia).</i>	76
<i>Synthesis of trans-[Pd(COOMe)₂(PPh₃)₂] (II).</i>	77
<i>Synthesis of [Pd(ONO)₂(PPh₃)₂] (III).</i>	78
<i>Synthesis of trans-[Pd(COOMe)(ONO)(PPh₃)₂] (IIIa).</i>	78
<i>Synthesis of cis-[Pd(C₂O₄)(PPh₃)₂] (IV).</i>	79
Reactivity tests	80
X-ray structure determinations	80
REFERENCES	82

CHAPTER 3	86
INTRODUCTION	86
RESULTS AND DISCUSSION.....	88
NMR investigations on the reactivity of I, II and III.....	88
<i>Reactivity of I.</i>	90
<i>Reactivity of II.</i>	103
<i>Reactivity of III.</i>	108
Catalytic oxidative carbonylation of methanol using I, II and III	115
On the catalytic cycle of the oxidative carbonylation reaction of alkanols.....	117
CONCLUSIONS.....	121
EXPERIMENTAL SECTION	121
Instrumentation and materials	121
Preparation of the complexes	122
<i>Synthesis of trans-[Pd(COOMe)₂(PPh₃)₂] (II).</i>	122
<i>Synthesis of [Pd(COOMe)(PPh₃)₃](TsO).</i>	122
High pressure NMR experiments	122
REFERENCES	124
CHAPTER 4.....	126
INTRODUCTION	126
RESULTS AND DISCUSSION.....	127
Influence of counter anion on the activity and selectivity of [PdX ₂ (PPh ₃) ₂].....	127
Effect of promoters on the activity and selectivity of [PdX ₂ (PPh ₃) ₂].....	128
<i>Effect of NEt₃.</i>	128
<i>Effect of added halides.</i>	129
<i>Influence of added PPh₃.</i>	131
Effect of operative conditions on the activity and selectivity of <i>trans</i> -[PdBr ₂ (PPh ₃) ₂] ...	132
<i>Effect of reaction time and of BQ.</i>	132
<i>Effect of temperature.</i>	133
<i>Effect of the pressure of CO.</i>	134
Electronic and steric effects of the phosphine ligands	134
On the catalytic cycle of the oxidative carbonylation of <i>i</i> PrOH.....	136
<i>On the coordination of L to the palladium centre during catalysis.</i>	136

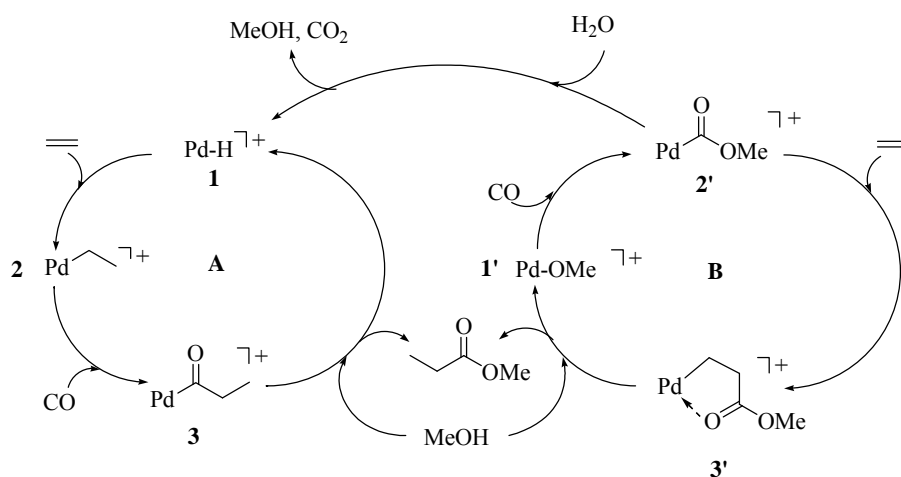
<i>Product forming step and attempted reformation of the precursor.</i>	141
<i>Reactivity with LiBr.</i>	144
<i>Proposed catalytic cycle.</i>	146
CONCLUSIONS	147
EXPERIMENTAL SECTION	148
Instrumentation and materials	148
Preparation of the complexes	148
<i>Synthesis of [PdCl₂L₂] (L = (zY-C₆H₄)₃P (z = o, m, p; Y= CH₃, CH₃O, F);</i> <i>[o,o'-(CH₃O)₂(C₆H₃)₃P).</i>	148
<i>Synthesis of [PdBr₂L₂] (L = PPh₃, (zY-C₆H₄)₃P (z = o, m, p; Y= CH₃, MeO, F),</i> <i>[o,o'-(MeO)₂(C₆H₃)₃P).</i>	149
<i>Synthesis of cis-[Pd(SO₄)(PPh₃)₂].</i>	150
<i>Synthesis of trans-[PdBr(COOiPr)(PPh₃)₂].</i>	150
Synthesis of H ₂ BQ–BQ adduct	150
Catalytic oxidative carbonylation of <i>i</i> PrOH	152
Reactivity of <i>trans</i> -[PdBr ₂ (PPh ₃) ₂] in oxidative carbonylation conditions	152
High pressure NMR experiments	153
REFERENCES	154
CHAPTER 5	156
INTRODUCTION	156
RESULTS AND DISCUSSION	157
Influence of the anion of the catalyst precursor [PdX ₂ (dppf)] (dppf = 1,1'– bis(diphenylphosphino)ferrocene	157
Effect of the pressure of carbon monoxide	159
Influence of the natural bite angle of the diphosphine ligands	161
Electronic and steric effects of the diphosphine ligand	166
Reactivity of [Pd(COOR) ₂ (P∩P)]	169
CONCLUSIONS	173
EXPERIMENTAL SECTION	174
Instrumentation and materials	174
Catalytic oxidative carbonylation of <i>i</i> PrOH	175
Preparation of the ligand	175

<i>Synthesis of pCF₃-dppf</i>	175
Preparation of the complexes	176
<i>Synthesis of cis-[Pd(OAc)₂(P∩P)] (P∩P = dppe, dppb, dppf, dippf, dtbpf, dcypf, pCF₃-dppf, DPEphos, Xantphos)</i>	176
<i>Synthesis of [PdCl₂(P∩P)] (P∩P = pCF₃-dppf, pMeO-dppf, SPANphos)</i>	177
<i>Synthesis of [Pd(OH₂)_n(OTs)_{2-n}(P∩P)](TsO)_n (n = 0, 1; P∩P = dppe, dppb, dppf, dippf, dtbpf, dcypf, pCF₃-dppf, DPEphos, Xantphos, pMeO-dppf, SPANphos)</i>	178
<i>Synthesis of cis-[Pd(C₂O₄)(dppf)]</i>	180
<i>Synthesis of cis-[Pd(SO₄)(dppf)]·H₂O</i>	180
<i>Synthesis of cis-[Pd(COOMe)₂(P∩P)] (P∩P = dppe, dppp)</i>	180
<i>Synthesis of trans-[Pd(COOMe)(OTs)(SPANphos)]</i>	181
<i>In situ NMR study on the preparation of [Pd(COOMe)₂(P∩P)] (P∩P = dppe, dppp, dppb, dppf, DPEphos, Xantphos, SPANphos) by exchange reaction</i>	181
REFERENCES	185
SHORT FINAL COMMENT	188
ABSTRACT/RIASSUNTO	189

General Introduction

Preface

My thesis work for the Master Degree in Industrial Chemistry dealt with a NMR study on the mechanism of the hydrocarbomethoxylation (HMC) of ethene (E) to methyl propanoate (MP), catalyzed by cationic complex of Pd(II) based on the precursors $[\text{Pd}(\text{OH}_2)_2(\text{PPh}_3)_2](\text{TsO})_2 \cdot 2(\text{H}_2\text{O})$ (**I**),¹ *trans*- $[\text{Pd}(\text{COEt})(\text{TsO})(\text{PPh}_3)_2]$ (**II**)² and *trans*- $[\text{Pd}(\text{COOMe})(\text{OH}_2)(\text{PPh}_3)_2](\text{TsO})$ (**III**).³ The last two are related to the acyl and the carbomethoxy intermediates of the proposed catalytic cycles shown below. The aim was to elucidate whether catalysis occurs *via* the so called hydride mechanism or the carbomethoxy one (Scheme 1).

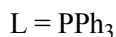
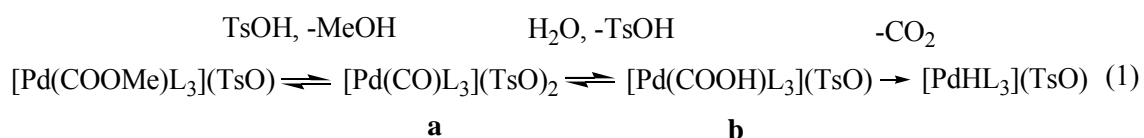


Scheme 1. Proposed catalytic cycles for the HMC of ethene. The “hydride” (**A**) and the “carbomethoxy” (**B**) cycles, with shift from the latter to the first through the action of water.

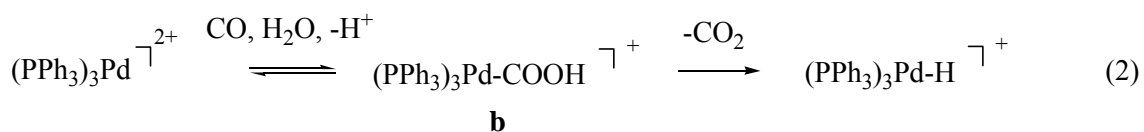
The reactivity of these complexes was studied by NMR spectroscopy under conditions close to those used in catalysis, *i. e.* in the presence of PPh₃ and TsOH, under E and CO.

The main findings are hereafter summarized. **I** in CD₂Cl₂/MeOH (10/1, v/v) in combination with PPh₃ and TsOH·H₂O (Pd/P/S = 1/4/6) and under E and CO (CO/E = 1/1, 6 bar) promotes catalysis starting from 20 °C (*ca.* 4 mol MP/mol Pd after 30 min between 30 and 60 °C). During catalysis the hydride *trans*-[PdH(PPh₃)₃](TsO) and the acyl *trans*-[Pd(COEt)(PPh₃)₃](TsO) complexes have been detected. These are related to the hydride mechanism.

In the absence of E, **I** reacts at -78 °C with CO and MeOH giving *trans*-[Pd(COOMe)(PPh₃)₃](TsO), which is unstable at 20 °C, because it reacts with TsOH, giving the hydride *trans*-[PdH(PPh₃)₃](TsO) probably *via* the intermediacy of **a** and **b** (1):



In the absence of both E and MeOH, but in the presence of CO and better in the presence of TsOH, **I** gives [PdH(PPh₃)₃](TsO) even at -78 °C. Therefore MeOH is not the source of the hydride. This might form as schematized (2):

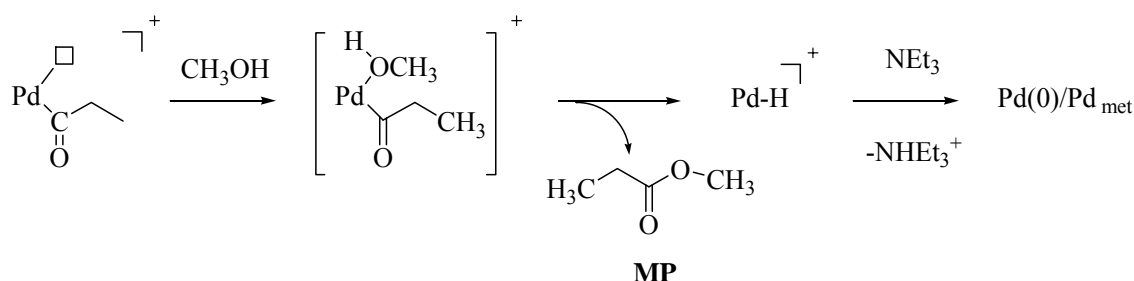


The acid stabilizes the hydride against deprotonation. When, after the formation of [PdH(PPh₃)₃](TsO), MeOH and E are added, HMC is observed starting from 20 °C. NEt₃ deprotonates [PdH(PPh₃)₃](TsO), with formation of Pd(0) complexes; in this case in the presence of E and CO, HMC does not occur.

When **II**, isolated after catalysis,² related to “hydride” mechanism, is used under HMC

conditions catalysis is observed starting from 20 °C (ca. 4 mol MP/mol Pd after 30 min between 30 and 60 °C) with gradual formation of $[\text{PdH}(\text{PPh}_3)_3](\text{TsO})$. In the absence of TsOH catalysis is slower (ca. 2 mol MP/mol Pd after 30 min between 30 and 60 °C) accompanied by the appearance of $[\text{PdH}(\text{PPh}_3)_3](\text{TsO})$, though in a lower concentration.

In the presence of PPh_3 and TsOH, but in the absence of CO and E, **II** is converted in $[\text{Pd}(\text{COEt})(\text{PPh}_3)_3](\text{TsO})$, which reacts rapidly with MeOH giving MP and $[\text{PdH}(\text{PPh}_3)_3](\text{TsO})$. When, after the formation of $[\text{PdH}(\text{PPh}_3)_3](\text{TsO})$, E is added, the hydride is slowly converted to *trans*- $[\text{Pd}(\text{Et})(\text{OTs})(\text{PPh}_3)_2]$ starting from 20 °C. By adding CO at -50 °C the Pd-ethyl complex is converted immediately into **II**. Under HMC conditions, but in the presence of NEt_3 instead of TsOH, **II** decomposes to $[\text{Pd}(\text{CO})(\text{PPh}_3)_3]$ with concomitant formation of MP already at -78 °C; however no catalytic HMC to MP was observed even upon increasing the temperature up to 60 °C, at which temperature decomposition to Pd metal is evident (Scheme 2). The base deprotonates the Pd-H⁺ species, thus preventing catalysis. All these experimental evidences are in favor of the hydride mechanism.



Scheme 2. Simplified scheme for the methanolysis of the palladium-acyl complex.

When **III**, related to “carbomethoxy” mechanism (**B** Scheme 1), is used under HMC conditions, catalysis is observed at 20 °C, but through the formation of $[\text{PdH}(\text{PPh}_3)_3](\text{TsO})$. In the absence of TsOH, catalysis is not observed up to 60°C, nor formation of any MP. Moreover there are not evidences of the insertion of E into the Pd-COOMe bond (carbomethoxy mechanism B) even in absence of PPh_3 , CO and MeOH. Again, these experimental evidences are in favor of the hydride mechanism A.

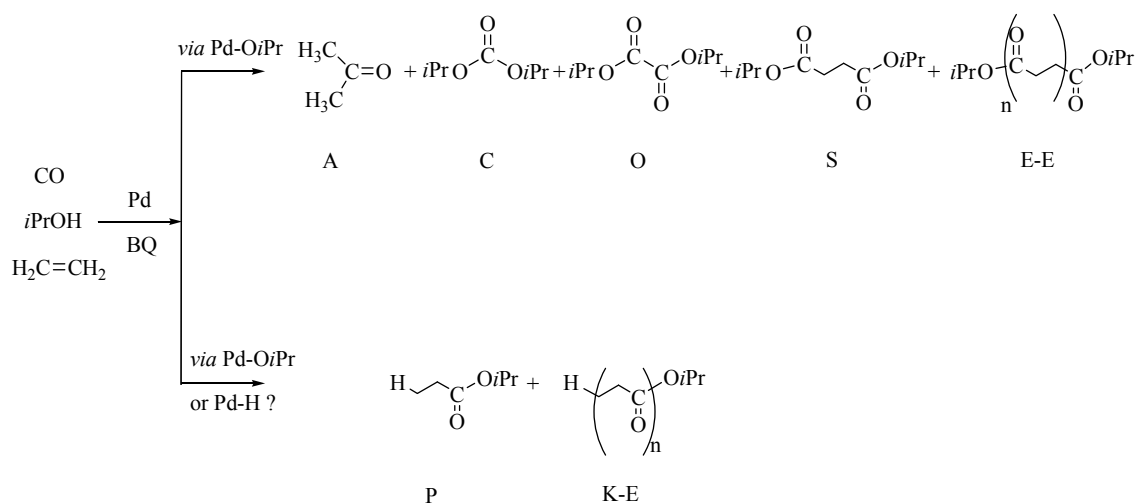
Other evidences in favor of the Pd–H mechanism have been reported. Recycled **II**, isolated after catalysis, promotes the HMC, whereas **III** promotes catalysis only in the presence of H₂O, which converts (**III**) to a hydride.^{*, 3} It was also found that a hydride source like H₂O, acid and molecular hydrogen have an enhancing effect on the HMC.⁴

In addition, phosphine degradation side reactions with formation of phosphonium cations such as MePPh₃, EtPPh₃ and EtCOCH₂CH₂PPh₃, isolated as TsO⁻ salts, provide further evidences for the “hydride” path.⁵

At the beginning of my doctorate thesis we were still interested in the HMC of ethene. Using *cis*-[Pd(SO₄)(PPh₃)₂] as precursor in *i*PrOH and in the presence of benzoquinone (BQ) we found that propanoate formed together with succinate and light CO–ethene oligomers having ester–ester ending groups (Scheme 3 and Table 1). Clearly the diesters are formed *via* initial insertion of the olefin into a Pd–COOR bond. Thus HMC of ethene catalyzed by monophosphine–Pd(II) based catalysts may also start *via* the insertion of the olefin into a Pd–COOR bond (mechanism **B**[†]).⁶ Note however, that this was achieved only when using BQ, which is known to convert a Pd–H species into a Pd–COOR one in the presence of CO.⁷ In addition, there was formation of other carbonylation products *i. e.* carbonate and oxalate and of acetone, a side product of the dehydrogenation of *i*PrOH.

* The H₂O displaces MeOH from the carbomethoxy complex **2'**, with formation of a Pd–COOH⁺ species, which upon evolution of CO₂ gives the hydride **1** that starts the catalytic cycle which undergoes through an acyl type intermediate. After catalysis, in place of the starting complex, the acyl complex is recovered

[†] When using Pd(II)–diphosphine based catalysts the carbonylation proceeds *via* both the Pd–H and Pd–COOR mechanisms even in the absence of BQ.



Scheme 3. Products of the carbonylation of ethene in *iPrOH* in the presence of BQ.

Table 1. Catalytic carbonylation of E in *iPrOH* in the presence of BQ

Entry	<i>P</i>		Activity TOF						
	[atm]		[mol/(mol*h)]						
	<i>CO</i>	<i>E</i>	<i>A</i>	<i>C</i>	<i>O</i>	<i>S</i>	<i>E-E</i>	<i>P</i>	<i>K-E</i>
1	60	10	1.8	4.6	24.4	–	–	–	–
2	35	35	2.0	3.1	21.0	0.78	–	–	–
3	20	50	11.4	1.5	12.0	1.37	–	–	–
4	10	60	7.0	1.1	11.4	5.6	3.8	12.0	9.1
5 ^a	35	35	0.2	–	0.45	0.41	–	–	–

Conditions: [Pd] = $2 \cdot 10^{-4}$ mol/L, Pd/PPh₃/BQ/NEt₃ = 1/4/500/2, T = 90 °C, 1 h, *iPrOH* anhydrous, 5 mL. ^a Same conditions above reported but without BQ and NEt₃.

Since the oxidative carbonylation of ethene occurs also with formation of carbonate and oxalate, we took into consideration first the use Pd(II) catalysts for the synthesis of only these products, *i. e.* in the absence of ethene. The aim was to take advantage of the knowledge gained by studying this simpler system for studying later the oxidative carbonylation of ethylene.

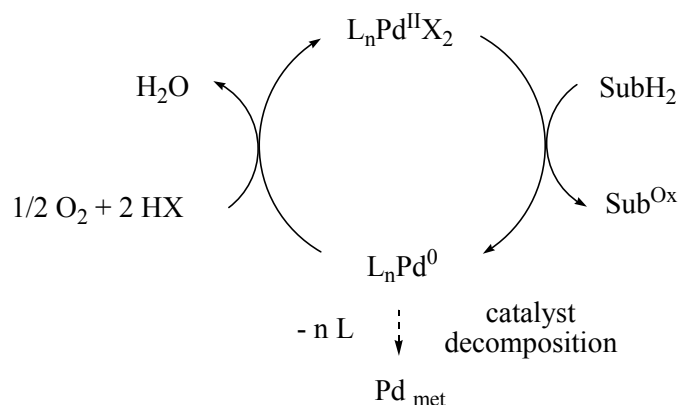
Preliminary experiments of the oxidative carbonylation of alkanols, in absence of ethene, showed that oxalate was the main product. In the literature a relatively low number of articles

deal with this subject, in spite of the recognized importance. Hereafter, we report the most significant results.

Oxidative carbonylation of alkanols

General aspects. A crucial step in the oxidative reactions catalyzed by palladium is the effective regeneration of Pd(II) from Pd(0) which is formed in the product-forming step. Generally, it is quite difficult to reoxidize Pd(0) to Pd(II) by molecular oxygen.

Since the mid-1990s, many research groups have reported palladium-catalyzed oxidation reactions that proceed with dioxygen in the absence of redox-active cocatalysts and other stoichiometric oxidants.⁸ A simplified catalytic cycle for these reactions consists of the two key steps: (i) palladium(II)-mediated reduced of the organic substrate followed by (ii) regeneration of the oxidized catalyst by molecular oxygen (Scheme 4).

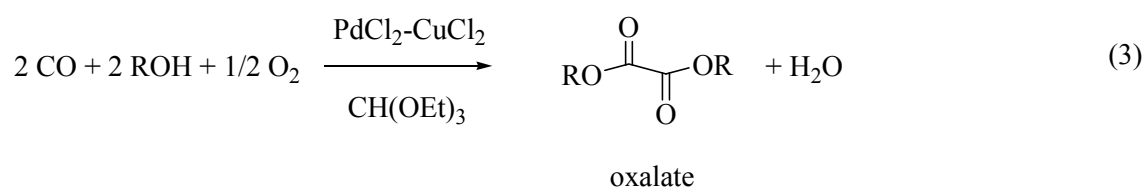


Scheme 4. Simplified catalytic cycle for palladium-catalyzed aerobic oxidation reactions.

Despite some advances, reoxidation of palladium(0) during catalytic turnover remains a critical challenge. Inefficient reaction of dioxygen with the reduced form of the catalyst, L_nPd^0 , results in catalyst decomposition *via* aggregation of palladium(0) into bulk metal (*e. g.*, palladium black). In addition, the use of oxygen leads to the formation of water which is not allowed on the oxidation process of many organic substrates.

Consequently, most of the palladium-mediated oxidation reactions do not use O₂ as the terminal oxidant, but rather stoichiometric oxidants such as copper salts, alkyl nitrites or BQ.

Industrial production of oxalates using alkyl nitrites as oxidant. The synthesis of diethyl oxalate by oxidative carbonylation of ethanol with O₂ in the presence of a PdCl₂-CuCl₂ catalyst was originally discovered by D. M. Fenton *et al.*⁹



Water that is formed causes the formation of carbon dioxide (reaction (4)) and prevents further formation of diethyl oxalate. Thus it is necessary to use a considerable excess of ethyl orthoformate (CH(OEt₃)) as the dehydrating agent.



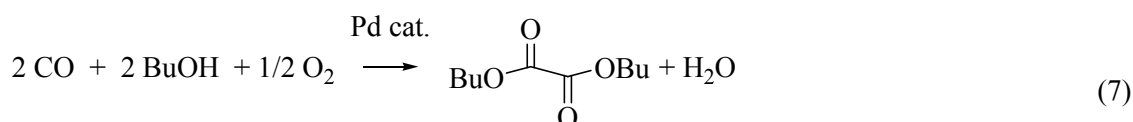
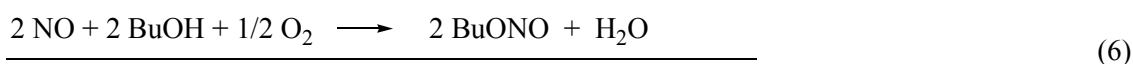
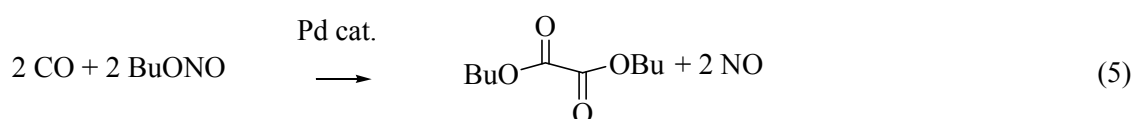
The research for the development of a new industrial process without using expensive orthoformate led to the discovery of the catalytic systems reported in Table 2 systems which give oxalate even in the presence of water.¹⁰ However they present several drawbacks.

Table 2. Catalyst systems for dialkyl oxalate synthesis

(1) PdCl ₂ -CuCl ₂ -K ₂ CO ₃	(2) PdCl ₂ -CuCl ₂ -R ₃ N
(3) Pd(NO ₃) ₂ -HNO ₃	(4) PdCl ₂ -NO
(5) Pd(0)/activated carbon-HNO ₃	(6) Pd(0)/activated carbon-NO

Systems (1) and (2) exhibit low reactivity and selectivity. Moreover, precipitation of insoluble cupric oxalate leads to deactivation. Systems (5) and (6) show higher reactivity and selectivity and long catalyst life. It was later found that nitric oxide and nitric acid were

converted to alkyl nitrite (butyl nitrite in butanol). A promising improvement of the catalyst efficiency was observed when butyl nitrite was used in place of HNO₃ or NO. Dibutyl oxalate was obtained even under low CO pressure and at lower temperature.¹¹ The lifetime of the catalyst became much longer. Small amounts of dibutyl carbonate and carbon dioxide were obtained as by-products. Butanol is indispensable for the formation of oxalate. The elementary reactions of dibutyl oxalate formation are shown below.¹¹



Reactions (5) and (6) are carried out in two separated steps, so that water is not present in the carbonylation step. In the second step the generated NO is transformed into alkyl nitrite. Water, generated at the same time, is removed azeotropically.

In the industrial production, palladium metal supported on activated carbon was the catalyst of choice to prevent loss of palladium and to maintain adequate suspended state of the liquid phase in which reactions occur. TOF (mol/mol_{Pd}·h) is higher than 10⁴. Palladium loss due to the dissolution is extremely small, catalytic life is fairly long.

The outline of production process is shown in Figure 1.

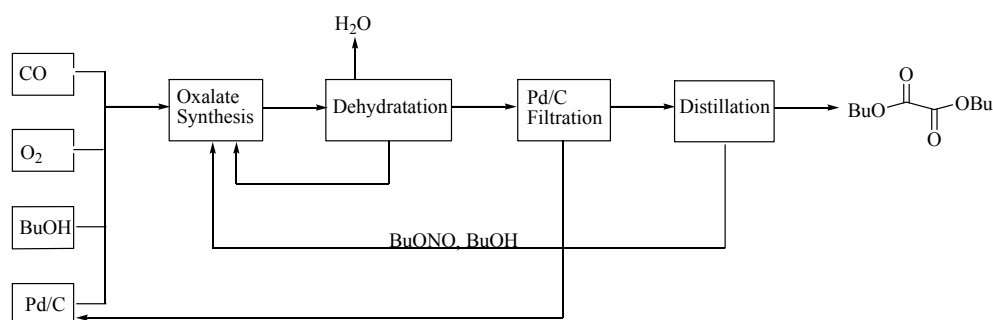
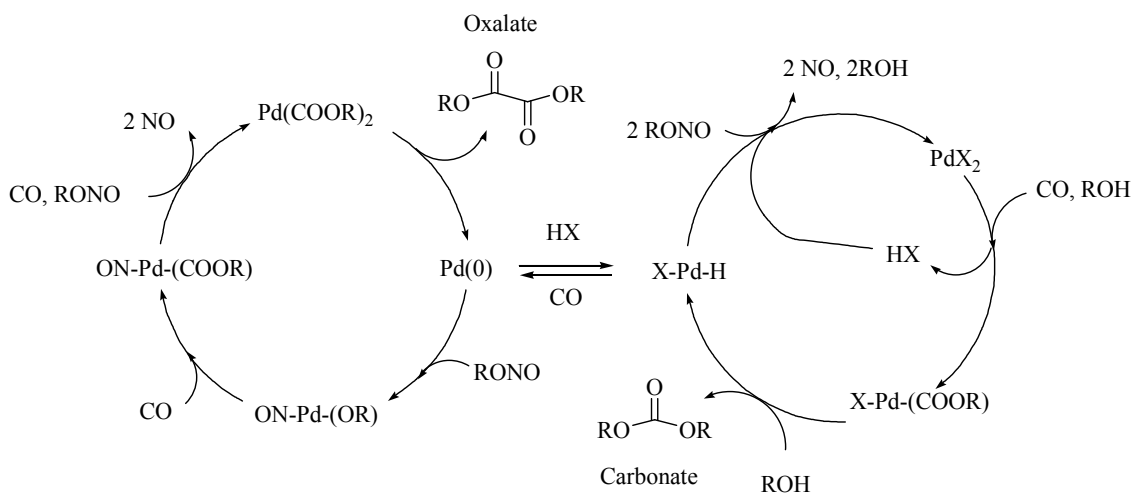


Figure 1. Flow diagram of UBE liquid phase process of dibutyl oxalate.

Scheme 5 shows the proposed mechanisms for the formation of oxalate and carbonate.¹²



Scheme 5. Proposed reaction mechanism for oxidative carbonylation of alcohols utilizing alkyl nitrite.

Oxidative carbonylation of alkanols using BQ as oxidant. The use of alkyl nitrites presents several drawbacks because they are toxic and require to be handled with much care. We have seen that, although molecular oxygen is the most convenient from an economical point of view, however water coproduced consumes CO and causes deactivation of the catalyst. These problems can be solved by using an organic oxidant such as benzoquinone (BQ) which has been found, at least in a laboratory scale, to be more effective than molecular oxygen or alkyl nitrites.¹³ The use of BQ totally avoids the formation of water because the reduction product is H₂BQ. H₂BQ can be reoxidized to BQ with molecular oxygen in a separated step.

BQ finds use both as oxidant and electron carrier in selective palladium-catalyzed oxidations.¹⁴ It can also play other roles participating in both formation and transformation stages of key intermediates into the reaction products by interaction with the catalytically active metal complex.^{15, 16} It can change properties of the reaction centre and, simultaneously, the mechanism and direction of the reaction. Hereafter, some examples are reported.

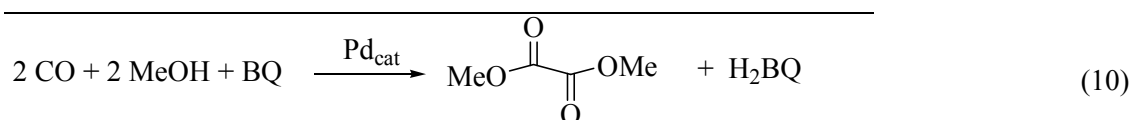
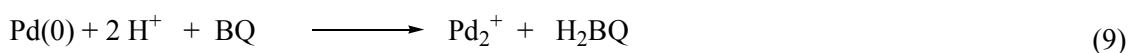
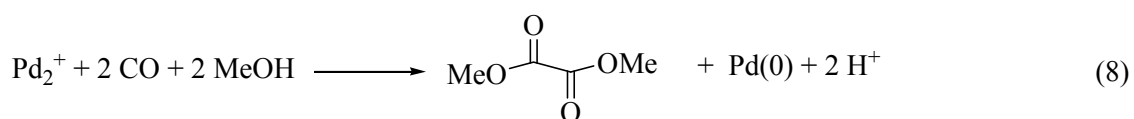
The use of BQ as oxidant in the oxidative carbonylation of alcohols has been firstly performed also by M. Fenton *et al.* using PdCl₂ as catalyst precursor (BQ/Pd = 100), at 125 °C under 35–70 bar of CO (eventually in presence also of triethyl orthoformate or triethyl ortoacetate as dehydrating agent). However, activity and selectivity were not satisfactory (*ca.* 0.3–6 TOF of carbonate and 0.8–0.06 TOF of oxalate).⁹

It was later reported that the system Pd(OAc)₂/Co(OAc)₂·4H₂O/PPh₃ in the ratio 1/4/3 was moderately active at 90 °C and 95 atm of carbon monoxide and oxygen in the ratio 18/1 for the oxidative carbonylation of MeOH to dimethyl oxalate (DMO). However, both activity and selectivity dropped substantially after 1 hour reaction, because of other products, dimethyl carbonate (DMC) and methyl formate (MF), were formed. A significant improvement in activity resulted from the addition of catalytic amounts of BQ to the above system. Most importantly, no more than trace amounts of either DMC and MF were observed.¹⁷

However, as already mentioned, by using oxygen, in addition to the desired products, there is formation of water, which gives rise to a parasite reaction consuming carbon monoxide.

These problems could be solved using the above system but in the presence of BQ only, *i. e.* without Co and oxygen. Using the system Pd(OAc)₂/PPh₃/BQ in the ratio 1/3/100 at 65 °C, 70 atm of CO, high yield of oxalate could be achieved (TOF 83 h⁻¹, selectivity 99%).¹⁷

The elementary reactions of dimethyl oxalate formation are shown below:

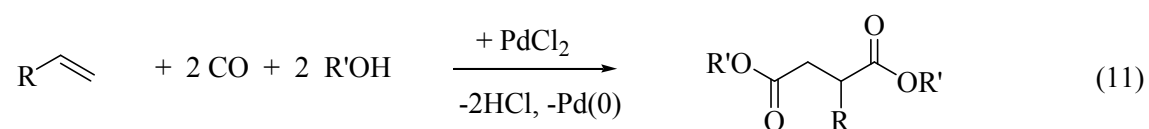


These results show that the choice of BQ as oxidant is not determined only by the benefits resulting from the exclusion of oxygen from the system, but it is also due to its capacity of directing the catalysis toward the formation of one product. For example, when using PdCl₂ or [Pd(CO)Cl]_n in the presence of BQ, dimethyloxalate was selectively produced in the oxidative carbonylation of methanol at atmospheric pressure and 40 °C while dimethylcarbonate was the reaction product in the absence of BQ.¹⁸

Other oxidative reactions using BQ

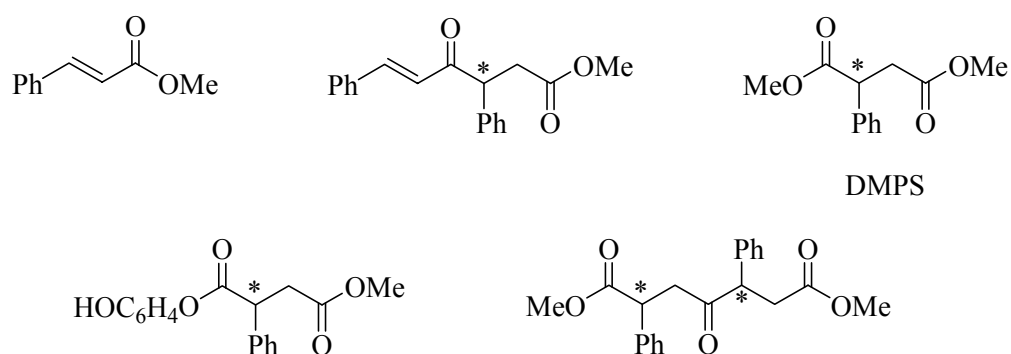
The Pd(II)–BQ catalytic system has been applied to several other reactions, such for example (i) oxidative carbonylation of styrene,¹⁹ (ii) oxidative carbonylation of alkynes,²⁰ (iii) oxidation of conjugated dienes to 1,4 diol derivatives,^{14, 21} (ii) oxidation of terminal olefins (Waker type reaction).²²

Oxidative carbonylation of styrene. At the beginning of the 1970s a convenient procedure was described for converting olefins into substituted butanedioates, namely through a Pd(II)–catalyzed bis–alkoxycarbonylation reaction (11).²³



In order to reoxidize the Pd(0) species formed and render this oxidative carbonylation catalytic, a stoichiometric amount of an oxidant is necessary.

Consiglio *et al.* using the system BQ/[Pd(L∧L')(S)₂]₂X (where L∧L' is diphosphine chelating ligand with C₂ symmetry, S is a solvent molecule, and X is a weakly coordinating anion) in the oxidative carbonylation of styrene in MeOH, showed that catalysis proceeds both enantio– and chemo–selectively forming esters of α,β–unsaturated carboxylic acids and dialkyl succinate acid type (Scheme 6).^{19b}



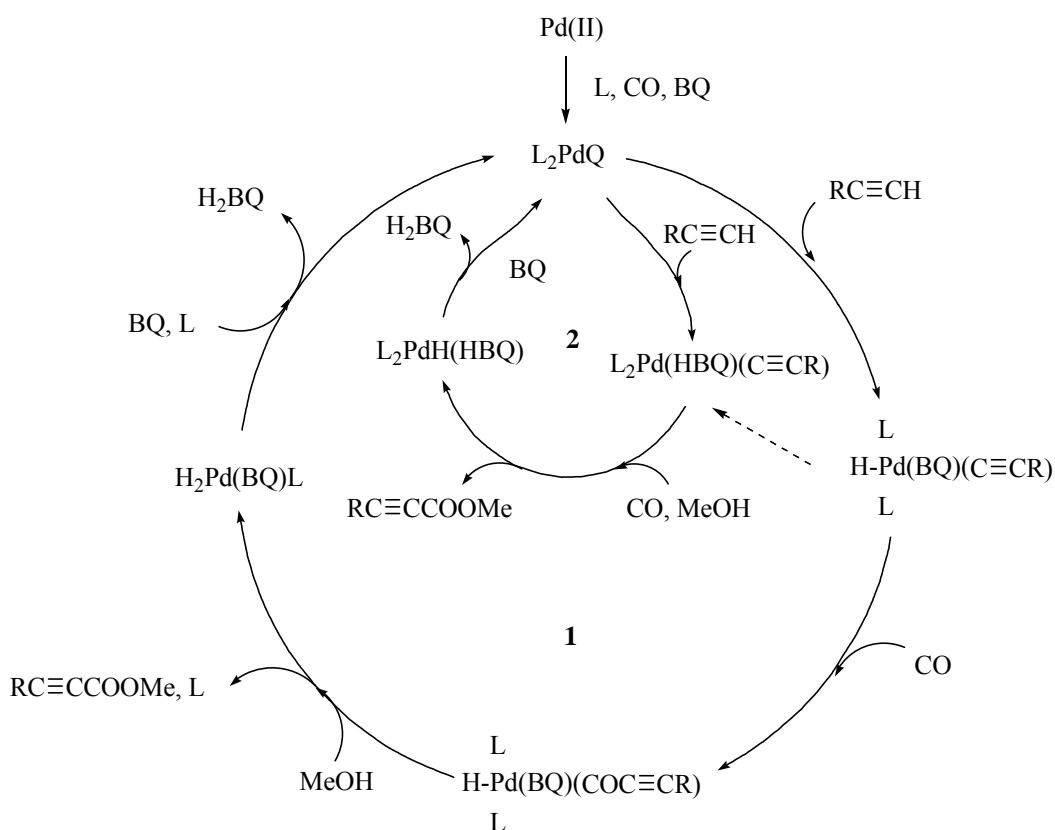
Scheme 6. Product of the bis-methoxycarbonylation of styrene.

Bianchini *et al.*, using novel diphosphine-modified Pd(II) catalysts and BQ in the oxidative carbonylation of styrene in MeOH, found that diesters and an unsaturated monoester formed.^{19a} More recently Chan *et al.* showed that chiral dipyridylphosphines Pd(II) complexes in presence of BQ, catalyze the asymmetric bis-methoxycarbonylation of styrene, reaching up to 84% e.e. and 79 % chemoselectivity for dimethyl-2-phenylsuccinate (DMPS in Scheme 7).²⁴

Oxidative carbonylation of alkynes. The catalytic oxidative carbonylation of terminal alkynes at the C–H bond, which yields esters of arylpropionic and alkylpropionic acids, has been performed using a Pd(OAc)₂/PPh₃/BQ system in MeOH.²⁰



Two mechanisms have been proposed in which a Pd(0) complex with coordinated BQ is formed through reduction of Pd(OAc)₂ in reactions with PPh₃, CO and MeOH (Scheme 7).^{15, 20}



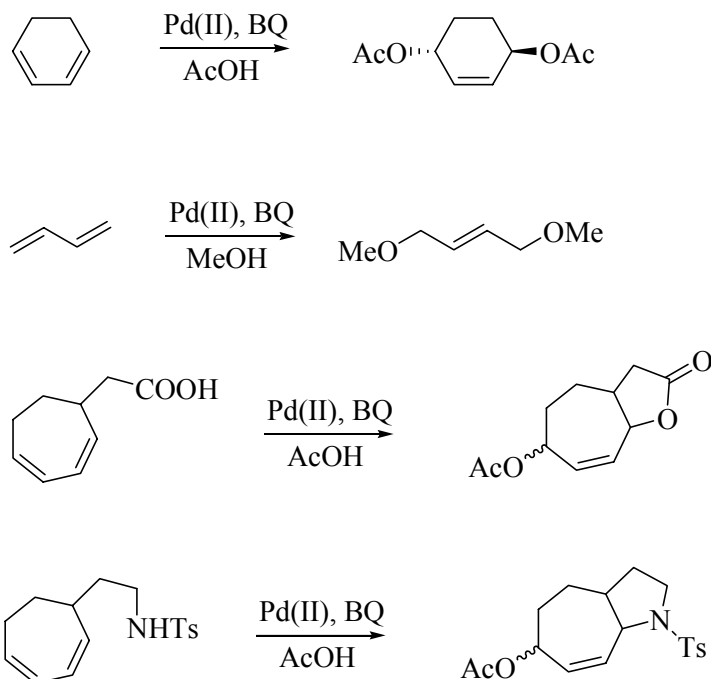
Scheme 7. Proposed mechanisms of the oxidative carbonylation of terminal alkynes.

In mechanism **1** (outer cycle) oxidative addition of phenylacetylene to the $\text{Pd(0)L}_2(\text{BQ})$ gives a $\text{Pd(II)-(hydrobenzoquinolate)}$ species, which may follow two different pathways. In one, the insertion of CO into the Pd–alkynyl σ -bond, followed by methanolysis, yields the product and $\text{PdH}_2(\text{BQ})\text{L}_2$. Oxidation of the hydride ligands by coordinated BQ yields H_2BQ with concomitant reformation of Pd(BQ)L_2 , which starts another cycle. In the other pathway intramolecular transfer of the hydride ligand to coordinated BQ gives a $\text{Pd(II)-(hydrobenzoquinolate)}$ which takes part of mechanism **2** (inner cycle).

In mechanism **2** the proton of coordinated alkyne is transferred to coordinated BQ of Pd(BQ)L_2 , giving the $\text{Pd(II)-(hydrobenzoquinolate)}$ intermediate common to both mechanisms. CO insertion into the Pd–alkynyl σ -bond, followed by methanolysis, yields the product and

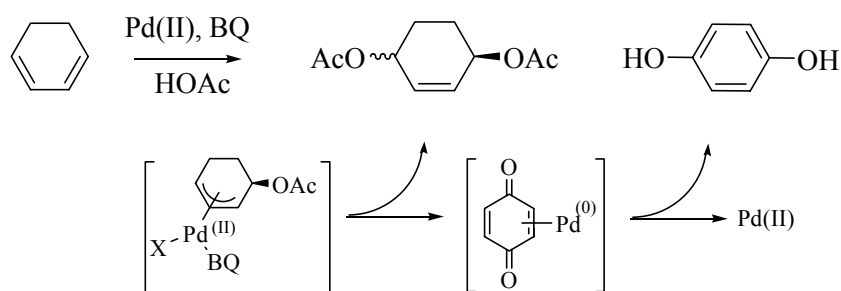
$\text{PdH}(\text{HBQ})\text{L}_2$, which undergoes reductive elimination of H_2BQ with reformation of $\text{Pd}(\text{BQ})\text{L}_2$ ready to start a new cycle.

1,4 Dialkoxylation of conjugated dienes. The palladium-catalyzed 1,4-dialkoxylation of 1,3 dienes was performed in the corresponding alcohol as solvent with BQ as the oxidant.¹⁴ In Scheme 8 are reported some application of this reactions in organic synthesis.



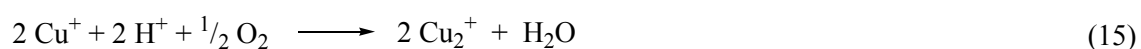
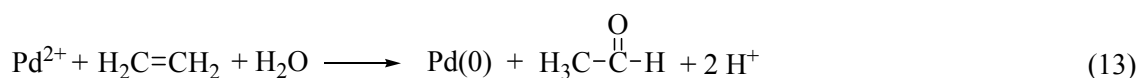
Scheme 8. Oxidation of conjugated dienes.

It has been demonstrated that BQ coordinates the (π -allyl)palladium intermediate enhancing the product forming-nucleophilic attack to produce a $\text{Pd}(0)$ -benzoquinone complex, which would undergo a redox reaction to give $\text{Pd}(\text{II})$ and hydroquinone (Scheme 9).²¹ The electron transfer in $\text{Pd}(0)$ -BQ complex is favored by acid condition.²¹



Scheme 9. Detail of the oxidation of conjugated dienes mechanism.

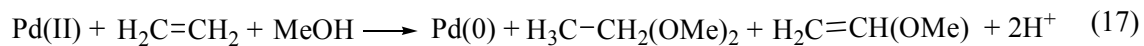
Oxidation of ethene to acetaldehyde (Wacker process). The most prominent Pd-catalyzed oxidation reaction is the conversion of ethene to acetaldehyde, with a PdCl₂ catalyst, in the presence of CuCl₂ cocatalyst and molecular oxygen as the stoichiometric oxidant.²⁵ Pd(II) oxidizes ethene to acetaldehyde in the presence of water (13). The reoxidation of Pd(0) by molecular oxygen is slow, whereas Cu(II) promptly reoxidizes it (14). Cu(I) is immediately reoxidized by molecular oxygen (15).



Since their development in 1958, the catalytic systems based on palladium have emerged as the mainstream oxidative catalyst used in industry. For example, vinyl acetate and allyl acetate are produced by the oxidation of ethylene, and propylene, respectively. Several reviews concerning these industrial processes are found in the literature.²⁶

The Wacker type reaction has been carried out also using BQ as an oxidant in place of molecular oxygen. Henry *et al.* found that ethylene is oxidized by Pd(II) in anhydrous methanol

to give dimethylacetal and methyl vinyl ether (17). At 25 °C, the major product was the acetal (*ca.* 95 % yield, based on the amounts of reoxidant and palladium salts used). The reaction can be made catalytic by adding a reoxidant such as BQ (18).^{22b}



Wacker-type products were obtained also in the oxidation of allyl alcohol by PdCl_4^{2-} in aqueous solution with BQ as reoxidant for Pd(0), to form β -hydroxypropanal and α -hydroxyacetone (19).^{22a}



Scope and contents of the thesis

The main goal of this thesis was to gain a deeper understanding of the factors ruling the activity and selectivity of Pd(II)-based catalysts in the oxidative carbonylation of alkanols. The final goal was the development of highly active and selective catalytic systems.

In **Chapter 1** the synthesis and characterization of the new cationic carboalkoxy complexes *trans*-Pd(COOR)(OH₂)(PPh₃)₂](TsO) (R = Et, *n*Pr, *i*Pr, *n*Bu, *i*Bu, *sec*Bu). Their reactivity in the catalytic hydrocarbomethylation of ethene is also reported. In addition, the X-ray structure of *trans*-[Pd(COOMe)(TsO)(PPh₃)₂]-CH₂Cl₃ is presented.

Chapter 2 deals with the synthesis, characterization and reactivity of [Pd(COOMe)_nX_{2-n}(PPh₃)₂] (n = 1, 2; X = ONO₂, ONO). The catalytic properties of [Pd(COOMe)_nX_{2-n}(PPh₃)₂] (n = 0, 1, 2; X = ONO₂, ONO, Cl, OAc) in the oxidative carbonylation of MeOH is also reported together with the X-ray structure of *trans*-[Pd(COOMe)(ONO₂)(PPh₃)₂] and of *cis*-[Pd(ONO₂)₂(PPh₃)₂]-CH₂Cl₂.

In **Chapter 3** mechanistic studies of the oxidative carbonylation of MeOH using a [P(X)_n(Y)_{2-n}(PPh₃)₂] (X = COOMe, Y = OTs, n = 0, 1, 2) complexes and BQ as oxidant are reported.

In **Chapter 4** the catalytic oxidative carbonylation of *i*PrOH catalyzed by Pd(II)-monophosphine complexes is described. The influence of (i) monophosphine ligands, (ii) anion, (iii) additives and (iv) operative conditions on activity and selectivity toward oxalate is presented.

Chapter 5 deals with the oxidative carbonylation of alkanols catalyzed by Pd(II)-diphosphine ligands on the oxidative carbonylation reaction. The influence of the anion, pressure of carbon monoxide and properties of the ligands (bite angle, electronic and steric parameters) on the activity and selectivity toward oxalate is discussed.

References

- (1) Cavinato, G.; Vavasori, A.; Toniolo, L.; Dolmella, A. *Inorg. Chim. Acta.* **2004**, *257*, 2737.
- (2) Cavinato, G.; Toniolo, L.; Vavasori, A. *J. Mol. Catal. A: Chem.* **2004**, *219*, 233.
- (3) Cavinato, G.; Vavasori, A.; Toniolo, L.; Benetollo, F. *Inorg. Chim. Acta* **2003**, *343*, 183.
- (4) (a) Pugh, R. I.; Drent, E. *Adv. Synth. Catal.* **2002**, *344*, 837. (b) Vavasori, A.; Cavinato, G.; Toniolo, L.; *J. Mol. Catal. A: Chem.* **2001**, *176*, 11. (c) Zudin, V. N.; Chinakov, V. D.; Nekipelov, V. M.; Rogov, V. A.; Likholobov, V. A.; Yermakov, Y. I. *J. Mol. Catal.* **1989**, *52*, 27.
- (5) Tooze, R. P.; Whiston, K.; Malyan, A. P.; Taylor, M. J.; Wilson, N. W. *J. Chem. Soc. Dalton. Trans.* **2000**, 3441.
- (6) (a) Bianchini, C.; Meli, A.; Oberhauser, W.; van Leeuwen, P. W. N. M.; Zuideveld, M. A.; Freixa, Z.; Kamer, P.; Spek, A. L.; Gusev, O. V.; Kal'sin, A. M. *Organometallics* **2003**, *22*, 2409. (b) Drent, E.; Budzelaar, P. H. M. *Chem. Rev.* **1996**, *96*, 663
- (7) Drent, E.; van Broekhoven, Doyle, M. J. *J. Organomet. Chem.* **1991**, *417*, 235. Vavasori, A.; Toniolo, L. *J. Mol. Catal.* **1996**, *110*, 13.
- (8) (a) Stahl, S. S. *Angew. Chem. Int. Ed.* **2004**, *43*, 3400. (b) Stoltz, B. M. *Chem. Lett.* **2004**, *33*, 362. (c) Sigman M. S.; Schultz, J. M. *Org. Biomol. Chem.* **2004**, *2*, 2551. (d) Nishimura, T.; Uemura, S. *Synlett* **2004**, 201. (e) Dams, M.; De Vos, D. E.; Celen, S.; Jacobs, P. A. *Angew. Chem. Int. Ed.* **2003**, *42*, 3512. (f) Toyota M.; Ihara, M. *Synlett* **2002**, 1211. (g) Sheldon, R. A.; Arends, I.W.C.E.; ten Brink G.-J.; Dijkman, A. *Acc. Chem. Res.* **2002**, *35*, 774. (h) van Benthem, R.A.T.M.; Hiemstra, H.; Michels, J.J.; Speckamp, W.N. *J. Chem. Soc. Chem. Commun.* **1994**, 357. (i) Larock, R.C.; Hightower, T.R. *J. Org. Chem.* **1993**, *58*, 5298.
- (9) Fenton, D. M.; Steinwand, P. J. *J. Org. Chem.* **1974**, *39*, 701.

-
- (10) Uchiumi, S.; Yamashita, M. *Jpn. Petrol. Inst.* **1982**, *25*, 197.
- (11) Nishimura, K.; Uchiumi, S.; Fujii, K.; Nishihira, K.; Yamashita, M.; Itatani, H.; Matsuda, M. JP 54-41813, 54-100312, **1979**, US Patent 4229589, 4229591, *Chem. Abstr.* **1979**, *91*, 4958, UBE Industries, Ltd..
- (12) Waller, F. J. *J. Mol. Catal.* **1985**, *31*, 123.
- (13) (a) Bar, G.L.J.; Lloyd-Jones, G.C.; Booker-Milburn, K.I. *J. Am. Chem. Soc.* **2005**, *127*, 7308. (b) Zhang, H.; Ferreira, E.M.; Stoltz, B. M. *Angew. Chem. Int. Ed.* **2004**, *43*,
- (14) Backvall, J. E. *Pure Appl. Chem.* **1992**, *64*, 429.
- (15) Kulik, A. V.; Bruk, L. G.; Temkin, O. N.; Khabibulin, V. R.; Belsky, V. K.; Zavodnik, V. E. *Mendeleev Commun.* **2002**, *12*, 47.
- (16) Backvall, J.; Hopkins, R. B.; Grennberg, H.; Mader, M. M.; Awasthi, A. K. *J. Am. Chem. Soc.* **1990**, *112*, 5160.
- (17) Current, S. P. *J. Org. Chem.* **1983**, *48*, 1780.
- (18) (a) Zhir-Lebed, L. N.; Temkin, O. N. *Kinet. Katal. (Engl. Transl.)* **1984**, *25*, 255. (b) Zhir-Lebed, L. N.; Temkin, O. N. *Kinet. Katal. (Engl. Transl.)* **1984**, *25*, 263.
- (19) (a) Bianchini, C.; Mantovani, G.; Meli, A.; Oberhauser, W.; Bruggeller, P.; Stampfl, T. *J. Chem. Soc. Dalton Trans.* **2001**, 690. (b) Sperle, M.; Consiglio, G. *J. Mol. Catal. A: Chem.* **1999**, *143*, 263.
- (20) (a) Khabibulin, V. R.; Kulik, A. V.; Oshanina, I. V.; Bruk, L. G.; Temkin, O. N.; Nosova, V. M.; Ustynyuk, Y. A.; Bel'skii, V. K.; Stash, A. I.; Lysenko, K. A.; Antipin, M. Y. *Kinet. Katal.* **2007**, *48*, 228. (b) Bruk, L. G.; Temkin, O. N. *Inorg. Chim. Acta* **1998**, *280*, 202.
- (21) (a) Grennberg, H.; Gogoll, A.; Backvall, J. E. *Organometallics* **1993**, *12*, 1790. (b) Backvall, J. E.; Vagberg, J. O. *J. Org. Chem.* **1988**, *53*, 5695.

-
- (22) (a) Wan, W. K.; Zaw, K.; Henry, P. M. *Organometallics* **1988**, *7*, 1677. (b) Lee, B.-H.; Henry, P. M. *Can. J. Chem* **1976**, *54*, 1726.
- (23) Heack, R. F. *J. Am. Chem. Soc.* **1972**, *94*, 2712.
- (24) Wang, L.; Kwok, W.; Wu, J.; Guo, R.; Au-Yeung, T. T.-L.; Zhou, Z.; Chan, A. S. C.; Chan, K.-S. *J. Mol. Catal. A: Chem.* **2003**, *196*, 171.
- (25) Smidt, J.; Hafner, W.; Jira, R.; Sedlmeier, J.; Sieber, R.; Rüttinger, R.; Kojer, H. *Angew. Chem.* **1959**, *71*, 176.
- (26) (a) Tsuji, J. *Palladium Reagents and Catalysts* Wiley, Chichester **1995**. (b) J. Tsuji, *Synthesis* **1990**, 739. (c) Waller, F. J. *J. Mol. Catal.* **1985**, *31*, 123.

Chapter 1

New Carboalkoxybis(triphenylphosphine)palladium(II) Cationic Complexes. Synthesis, Characterization, Reactivity and Role in the Catalytic Hydrocarboalkoxylation of Ethene. X-ray Structure of *trans*-[Pd(COOMe)(TsO)(PPh₃)₂]·2CHCl₃

Introduction

Palladium(II)-carboalkoxy complexes are intermediates in several important catalytic carbonylation reactions carried out in the presence of an alkanol,¹ such for example the alkene-carbon monoxide copolymerisation to polyketones,² the oxidative carbonylation of alkenes or alkanols to unsaturated esters or diesters³ or to carbonates and oxalates.^{3m, 4} These complexes have been proposed as intermediates also in the catalytic hydrocarboalkoxylation of alkenes to monoesters.⁵

During the course of catalysis, they reenter in the catalytic cycle through interaction of carbon monoxide and the alkanol, or an alkoxy species, on the metal centre. This interaction allows the isolation of Pd(II)-carboalkoxy complexes, when sufficiently stable. This represents

the most direct way for their synthesis.⁶ The insertion of CO into a Pd–OCH₃ bond to give a Pd–COOMe species has been demonstrated.^{5a, 6h, 7}

Other methods of synthesis include the oxidative addition of chloro- or cyano-formate, or of phenylcarbonate to Pd(0) complexes,⁸ the decarbonylation of alkoxalyl complexes,⁹ or the exchange with HgCl(COOMe).¹⁰

Most of the syntheses reported up to now are relevant to carbomethoxy derivatives. The synthesis of neutral Pd(II) complexes of the type *trans*–[Pd(COOR)X(PPh₃)₂] (X = Cl, CN) with R bulkier than Me (up to cyclohexyl) has been also reported.^{6c, i, 8a–d}

The cationic carbomethoxy complex *trans*–[Pd(COOMe)(OH₂)(PPh₃)₂](TsO) has been synthesized from the neutral *trans*–[Pd(COOMe)Cl(PPh₃)₂] by methathetical exchange with Ag(TsO). Its role in the catalytic hydrocarbomethylation of ethene to propanoate product has been investigated and were suggested that the carbomethoxy complex plays only a minor role in catalysis. Indeed, the catalysis does not occur *via* a Pd–carboalcoxy species but takes place *via* Pd–hydride ones.^{6b}

As mentioned in General Introduction, our preliminary experiments on the oxidative carbonylation of ethene in *i*PrOH using *cis*–[Pd(SO₄)(PPh₃)₂] as precursor in *i*PrOH and in the presence of BQ showed the formation of propanoate together with succinate and light CO–ethene oligomers having ester–ester ending groups. Clearly these products can form only *via* the Pd–carboalcoxy mechanism. Thus, for the first time, it was proved that the hydrocarboalkoxylation of ethene catalysed by monophosphine–Pd(II) based catalysts can start also *via* the insertion of the olefin into a Pd– carboalcoxy bond.

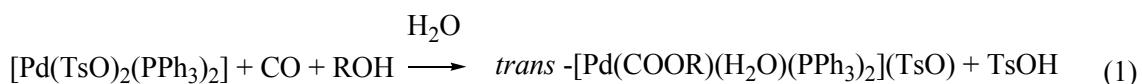
In order to gain a deeper understanding on the mechanism of the hydrocarbomethylation of ethene we decide to extend the study to the synthesis and characterization of the new cationic carboalkoxy complexes *trans*–[Pd(COOR)(OH₂)(PPh₃)₂](TsO), with R = Et, *n*Pr, *i*Pr, *n*Bu, *i*Bu, *sec*Bu, and to the reactivity of these new complexes as well as the methyl analogue in relation to the catalytic hydrocarbomethylation of ethene. We also report the X–ray diffraction structure

of *trans*-[Pd(COOMe)(TsO)(PPh₃)₂] \cdot 2CHCl₃.

Results and discussion

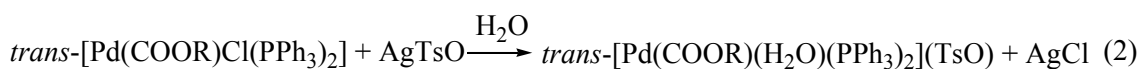
Synthesis and characterization of the carboalkoxy complexes reported in Table 1

Complexes **Ia** and **Ib** have been prepared by reacting [Pd(TsO)₂(PPh₃)₂] or [Pd(OH₂)₂(PPh₃)₂](TsO) \cdot 2H₂O with CO in ROH (R = Me or Et) (2 atm, r. t.):



The reaction with MeOH takes place in a few minutes, whereas with EtOH is significantly slower as it takes 20–30 minutes.

Reaction (1) with bulkier alkanols gives unsatisfactory results. An attempt to synthesize complex **If** failed. The carboalkoxy complexes (**Ic–g**) with bulkier R (Table 1) have been prepared *via* methathetical exchange of the corresponding neutral chloride with AgTsO, as already experienced for the synthesis of (**Ia**)^{6b}



It is noteworthy to point out that the synthesis based on reaction (1) does not require the presence of a tertiary base, at difference of the analogous synthesis of the corresponding chloride *trans*-[Pd(COOR)Cl(PPh₃)₂] starting from *trans*-[PdCl₂(PPh₃)₂], in which case the use of the base is necessary in order to neutralize HCl that forms during the reaction and that otherwise reverses the reaction.^{6i, p}

Selected IR and NMR data are reported in Table 1. The IR spectra of (**Ia–g**) show a

strong absorption band in the 1684–1670 cm^{-1} region due to $\nu_{\text{C=O}}$ of the carboalkoxy ligand. In the corresponding neutral chloride the $\nu_{\text{C=O}}$ absorption appears at slight lower frequency,⁶ⁱ which might be due to a stronger π -back donation from the metal to the carboalkoxy moiety in the neutral complexes.

Absorption bands due to coordinated water are observed in the 3640–3142 cm^{-1} region.^{11a} Complexes (**Ia–c, e**) show two sharp bands of low intensity; complex **If** shows one band of low intensity at 3637 cm^{-1} and an unresolved broad absorption centered at 3142 cm^{-1} ; complexes **Id, g** show a broad unresolved band centered at 3220 and at 3144 cm^{-1} , respectively. Those at lower frequency suggest the presence of a hydrogen-bond between water and TsO^- , with consequent lowering of $\nu_{\text{O-H}}$.¹¹ The absorptions in the ranges 1273–1222, and 1014–1007 cm^{-1} are identified as some of the characteristic bands of the anionic $-\text{SO}_3^-$ group.¹² The band in the 1037–1025 cm^{-1} region is assignable to the C–O–C stretch of the alkoxycarbonyl group.^{6i, k, n}

The ^1H -NMR spectra of (**Ia–g**) show signals in the range 0.20–3.69 ppm assigned to the alkoxy group protons.⁶ⁱ The singlets observed at 2.36 ppm is assigned to the CH_3 protons of the TsO^- anion. Two well separated multiplets for the aromatic protons are centered at about 7.6 and 7.3 ppm. The ^{31}P NMR spectrum shows a singlet in the range 19.01–19.27 ppm, close to that of the relevant neutral chloride complex.⁶ⁱ

As reported in the experimental section, complexes (**Ia–g**) have been precipitated by pouring their alkanol solution into cold water. When warm water has been used to precipitate the carbomethoxy complex, a different derivative has been obtained, (**IIa**). The IR spectrum of (**IIa**) does not show absorption bands due to coordinated water. The ν_{CO} and $\nu_{\text{C-O-C}}$ are shifted from 1685 and 1036 cm^{-1} to 1668 and 1029 cm^{-1} and the bands of the $-\text{SO}_3^-$ group are shifted from 1230 and 1013 cm^{-1} to 1263 and 1001 cm^{-1} and are assignable to a coordinated anion.¹² The ^1H and ^{31}P NMR spectra of complexes (**Ia**) and (**IIa**) in CD_3OD do not differ appreciably, probably due to the fast exchange of labile water, TsO^- , solvent. The X-ray crystal structure of the CHCl_3 clathrated of complex (**IIa**) shows that it has a *trans* geometry, in which TsO^-

coordinates the metal (in place of H₂O) in (**Ia**);⁶ⁱ the ³¹P NMR spectrum for this complex in CDCl₃ shows a singlet at 18.51 ppm slightly lower than in CD₃OD. On the basis of these data complex (**IIa**), precipitated from MeOH/H₂O is formulated as *trans*-[Pd(COOMe)(TsO)(PPh₃)₂]. A *trans* geometry is assigned also to all the new cationic complexes (**Ib–g**).

The IR spectrum of the solid precipitated by addition of cold water to the ethanol solution of the carboethoxy derivative shows double absorptions in the ν_{CO} , $\nu_{\text{C-O-C}}$ and ν_{SO_3} regions, suggesting that this solid is a mixture of *trans*-[Pd(COOMe)(OH₂)(PPh₃)₂](TsO), (**Ib**) and *trans*-[Pd(COOMe)(TsO)(PPh₃)₂], (**IIb**).

Table 1. Selected IR, ¹H NMR and ³¹P{¹H}NMR data of *trans*-[Pd(COOR)(OH₂)(PPh₃)₂](TsO) (**Ia–g**), *trans*-[Pd(COOMe)(TsO)(PPh₃)₂] (**IIa**) and *trans*-[Pd(COOEt)(TsO)(PPh₃)₂] (**IIb**)

R	IR^a		¹H^b	³¹P^c
	ν	cm^{-1}	δ (ppm)	δ (ppm)
Me (Ia) ^{6b}	H ₂ O	3489, 3412	2.58 (s, 3 H, CH ₃ -PdCOMe)	19.04 (s) ^d
	C=O	1685	2.36 (s, 3 H, CH ₃ -TsO)	
	C-O-C	1070		
	SO ₃	1230, 1035, 1013		
(IIa)	C=O	1668	2.58 (s, 3 H, CH ₃ -PdCOMe)	19.04 (s)
	C-O-C	1086	2.36 (s, 3 H, CH ₃ -TsO)	
	SO ₃	1263, 1029, 1000		
Et (Ib)	H ₂ O	3671, 3441	2.87 (q, 2 H, CH ₂ -PdCOEt)	19.01 (s)
	C=O	1684	2.36 (s, 3 H, CH ₃ -TsO)	
	C-O-C	1057	0.49 (t, 3 H, CH ₃ -PdCOEt)	
	SO ₃	1222, 1036, 1011.		
(IIb)	C=O	1663	2.87 (q, 2 H, CH ₂ -PdCOEt)	19.01 (s)
	C-O-C	1088	2.36 (s, 3 H, CH ₃ -TsO)	
	SO ₃	1268, 1029, 999	0.49 (t, 3 H, CH ₃ -PdCOEt)	
<i>n</i> Pr (Ic)	H ₂ O	3640, 3485	2.81 (t, 2 H, CH ₂ O-PdCONPr)	19.12 (s)
	C=O	1671	2.36 (s, 3 H, CH ₃ -TsO)	

	C–O–C	1083	0.88 (m, 2 H, CH ₂ –PdCO <i>n</i> Pr)	
	SO ₃	1257, 1031, 1008	0.51 (t, 3 H, CH ₃ –PdCO <i>n</i> Pr)	
<i>i</i> Pr (Id)	H ₂ O	3220	3.82 (t, 1 H, CH–PdCO <i>i</i> Pr)	19.08 (s)
	C=O	1674	2.36 (s, 3 H, CH ₃ –TsO)	
	C–O–C	1051	0.31 (d, 3 H, CH ₃ –PdCO <i>i</i> Pr)	
	SO ₃	1223, 1038, 1014		
<i>n</i> Bu (Ie)	H ₂ O	3640, 3488	2.87 (t, 2 H, CH ₂ O–PdCO <i>n</i> Bu)	19.13 (s)
	C=O	1672	2.36 (s, 3 H, CH ₃ –TsO)	
	C–O–C	1081	0.87 (m, 4 H, CH ₂ –PdCO <i>n</i> Bu)	
	SO ₃	1246, 1030, 1007	0.68 (t, 3 H, CH ₃ –PdCO <i>n</i> Bu)	
<i>i</i> Bu (If)	H ₂ O	3142	2.63 (t, 2 H, CH ₂ O–PdCO <i>i</i> Bu)	19.27 (s)
	C=O	1669	2.36 (s, 3 H, CH ₃ –TsO)	
	C–O–C	1068	1.08 (m, 1 H, CH–PdCO <i>n</i> Bu)	
	SO ₃	1218, 1036, 1012	0.47 (d, 6 H, CH ₃ –PdCO <i>n</i> Bu)	
<i>sec</i> Bu (Ig)	H ₂ O	3144	3.69 (m, 1 H, CHO–PdCO <i>sec</i> Bu)	19.10 (s)
	C=O	1671	2.36 (s, 3 H, CH ₃ –TsO)	
	C–O–C	1059	0.67 (m, 2 H, CH ₂ –PdCO <i>sec</i> Bu)	
	SO ₃	1231, 1037, 1013	0.41 (t, 3 H, CH ₃ –PdCO <i>sec</i> Bu)	
			0.20 (d, 3 H, CH ₃ –PdCO <i>sec</i> Bu)	

Abbreviations: s, singlet; t, triplet; q, quartet; m, multiplet. NMR spectra were recorded in CD₃OD at 25 °C. ^a Nujol mull. ^b δ (¹H) values in ppm referenced to CD₃OD; ^c δ (³¹P{¹H}) values in ppm from external 85 % H₃PO₄, downfield being taken as positive; ^d in ^{6b} it was erroneously reported 16.51 ppm.

X-ray structure analysis of [Pd(COOMe)(TsO)(PPh₃)₂] \cdot 2 CHCl₃ (**IIa**)

The ORTEP¹³ drawing of the complex is shown in Figure 1, together with the numbering scheme used, while relevant bond lengths and angles are reported in Table 2.

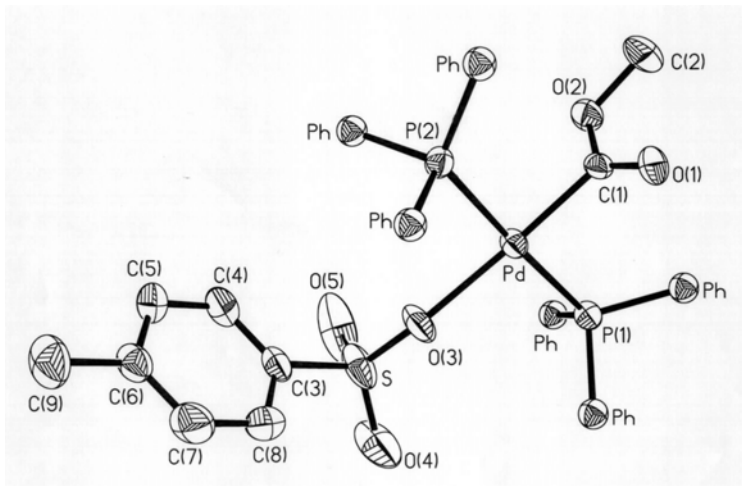


Figure 1. A drawing of the complex **IIa** with the selected numbering scheme. Ellipsoids are at the 50% level; hydrogen atoms are represented by spheres of arbitrary size. The phenyl rings and the CHCl₃ molecules have been omitted for clarity.

Table 2. Relevant bond distances (Å) and angles (°)

Pd–P(1)	2.353(2)	Pd–O(3)	2.160 (4)
Pd–P(2)	2.342(2)	Pd–C(1)	1.978 (6)
S–O(3)	1.452(4)	C(1)–O(1)	1.187 (7)
S–C(3)	1.789(6)	C(1)–O(2)	1.336 (7)
		O(2)–C(2)	1.458 (7)
P(1)–Pd–P(2)	177.2(1)	C(1)–Pd–O(3)	170.8 (2)
P(1)–Pd–O(3)	98.1 (1)	P(2)–Pd–O(3)	84.3 (1)
P(1)–Pd–C(1)	89.2 (2)	P(2)–Pd–C(1)	88.3 (2)
Pd–O(3)–S	151.9(3)	O(3)–S–C(3)	104.5 (3)
Pd–C(1)–O(1)	124.6(5)	Pd–C(1)–O(2)	110.0 (4)
		O(1)–C(1)–O(2)	125.4 (6)

The solid state investigation revealed three sets of atoms lying in well defined planes: P(1)–C(1)–P(2)–O(3), C(1)–C(2)–O(1)–O(2) and O(3)–S–C(3). The atoms in the set P(1)–C(1)–P(2)–O(3) (basal plane) are virtually coplanar within 0.04 Å, with the Pd centre out by 0.06 Å. The set C(1)–C(2)–O(1)–O(2) is strictly planar, and is almost orthogonal to the basal plane, the two planes making a dihedral angle of 88.9°. Instead, the O(3)–S–C(3) set is tilted from both the previous plane, being inclined of 28.6° in respect of the basal plane and of 69.8° in respect of the C₂O₂ set.

Looking at bond distances and angles, it appears worth noting that the Pd–O(3)–S angle is very wide, 151.9(3)°; this is the largest value reported to date for a mononuclear Pd(II) complex. A search in the Cambridge Structural Database (CCD)¹⁴ showed that the closest values found in (trifluoromethanesulfonato)(3-(diethylamino)propionyl)(diethylamine)palladium(II) and (2-(benzene-1,1-diyl)-2-methyl-propyl)-(trifluoromethanesulfonato)trimethylphosphine-palladium(II),¹⁵ were 150.5° and 146.0°, respectively. In ref 15b, the abnormal widening of the Pd–O–S angle was attributed to van der Waals contacts between the other oxygen atoms of the sulfone with hydrogen atoms of nearby ligands. In the present case, the large Pd–O(3)–S angle might be due to the very efficient interaction involving O(4) and the hydrogen atom of a CHCl₃ molecule, as indicated in Figure 2 (the contact distance is 1.99 Å, and the pertinent O(4)···H–C(11) angle is 164°), and only to a limited extent to steric interactions with the PPh₃ group.

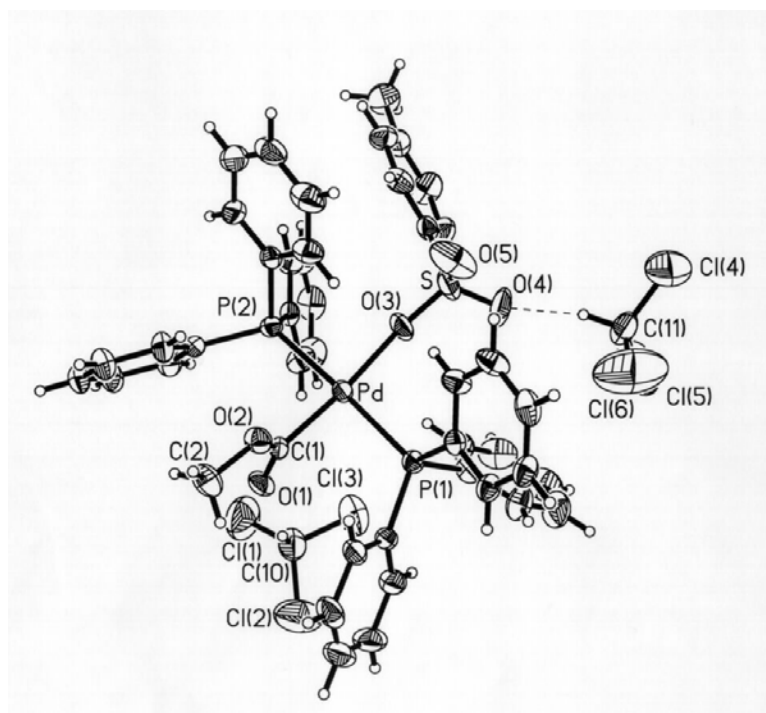


Figure 2. The interaction between the sulfonato moiety of **IIa** and one of the CHCl_3 solvent molecules described in text.

The CCD exploration returned about twenty Pd mononuclear complexes with the metal showing a Pd–O–S–C moiety and a Pd environment similar to the one found in our compound.¹⁶ The Pd–O(3) (2.160(4) Å) and O(3)–S (1.452(4) Å) distances agree reasonably with the average values found in such complexes (2.175 and 1.461 Å, respectively).^{15, 16} Similar considerations also apply to other geometrical parameters involving the sulfur atom of the *p*-toluenesulfonato ligand. In fact, in the present complex the S–C(3) distance and the O(4)=S=O(5), O(3)–S–C(3) angles are 1.789(6) Å, 115.7(4) and 104.5(3)°, whereas the corresponding average parameters found in about thirty Pd square planar complexes showing at least one sulfonato ligand are 1.809 Å, 116.4 and 102.1°, respectively.¹⁴

In the CCD there are also about fifteen structures in which a mononuclear tetracoordinated Pd atom is bound by a –C(=O)–O–C moiety,^{6a, b, k, 8b, 15b, 17} most of them also showing the metal coordinated by two phosphine ligands. The average Pd–C distance and the

Pd–C(=O), Pd–C–O angles in the reported structures are 1.979 Å, 126.6 and 112.9°, respectively. These values compare quite well with 1.978(6) Å, 124.6(5) and 110.0(4)° in the complex described here. Among known structures, the complexes most closely resembling these values are *trans*–aqua–carbomethoxy–bis(triphenylphosphine)–palladium (1.975 Å, 124.5 and 111.4°),^{6b} *trans*–carbomethoxy–chloro–bis(triphenylphosphine)palladium (1.972 Å, 125.3 and 111.9°)^{17g} and chloro–(3–hydroxypropoxycarbonyl–C)–(2–(pyridin–2–yl)ethyl)diphenylphosphine–N,P)–palladium(II) (1.964 Å, 124.5 and 112.7°).^{6a}

The two CHCl₃ molecules in the unit cell are animated by high thermal motions, and only one of them, as said above, seems to interact with the complex inner core. Instead, the phenyl ring of the *p*–toluenesulfonato moiety establishes a rather long–range (4.22 Å) π –interaction with a phenyl ring bound to P(2). Other structural parameters, like the six P–C_{ph} distances (average value 1.819 Å) do not show any new feature, and the same can be said of the two Pd–PPh₃ bonds, that match quite well the average value of 2.33(3) Å found in 227 square planar Pd(II) complexes bearing two PPh₃ groups.¹⁴

A summary of the X–ray analysis of **IIa** is listed in Table 3.

Table 3. Crystal and refinement data

<i>Complex</i>	
Formula	C ₄₇ H ₄₂ O ₅ P ₂ SCl ₆ Pd
Molecular wt	1099.9
Colour	colourless
Crystal system	monoclinic
Space group	<i>P</i> ₂ ₁ / <i>n</i> (No. 14)
<i>a</i> (Å)	19.558(3)
<i>b</i> (Å)	12.155(2)
<i>c</i> (Å)	21.453(4)

β (°)	103.87(1)
V (Å ³)	4951(1)
Z	4
D_{calc} (g cm ⁻³)	1.476
$F(000)$	2232
Crystal dimens (mm)	0.20×0.20×0.20
Θ limits (°)	3.5 / 29.6
No. of independent data	11938
No. of data with $I > 2\sigma(I)$	3892
No. of variables	560
$R(F)$ ^a	0.058
$wR(F^2)$ ^b	0.110
Largest peak in $(F \text{ e } \text{Å}^{-3})$	0.824
GOF ^c	0.763

$$^a R(F) = \sum ||F_o| - |F_c|| / \sum |F_o|$$

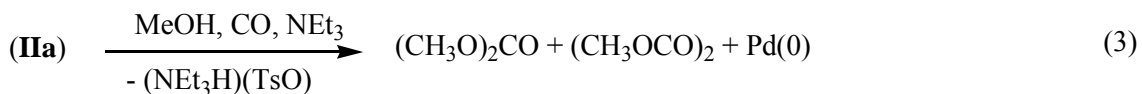
$$^b wR(F^2) = [\sum w (|F_o|^2 - |F_c|^2)^2 / \sum w (|F_o|^2)^2]^{1/2}$$

$$^c \text{GOF} = [\sum w (|F_o|^2 - |F_c|^2)^2 / (n - p)]^{1/2}$$

Reactivity

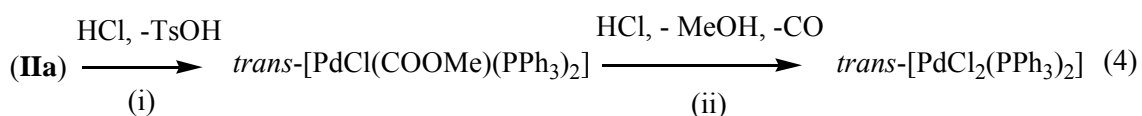
The reactivity has been tested with both the carbomethoxy complexes (**Ia**) and (**IIa**). They behave the same way, therefore for the sake of simplicity here below we report the tests done with (**IIa**) only, if not otherwise indicated.

Reactivity with alkanols. At 80 °C, under 45 atm of CO, the carbomethoxy complex reacts with R'OH (R' = *n*Pr, *i*Pr), used also as a solvent, giving complexes (**Ic-d**). These complexes react with MeOH under the same conditions giving the carbomethoxy derivative. Under the above conditions and in the presence of a base such as triethylamine, complex (**IIa**) in MeOH is reduced to Pd(0) complexes, [Pd₃(CO)₃(PPh₃)₃] and [Pd(CO)(PPh₃)₃], the latter forms prevalently when the reaction is carried out also in the presence of one mole of PPh₃ per Pd atom. The reduction occurs with concomitant formation of dimethyl carbonate (DMC) and oxalate (DMO), as here below schematized:



Under similar conditions the analogous complexes *trans*-[Pd(COOMe)Cl(PPh₃)₂] and *trans*-[Pd(OAc)(COOMe)(PPh₃)₂] give DMC or DMO, respectively.^{6g, 17a, 18}

Reactivity with acids HX (X = Cl, OAc, TsO). The reactions have been carried in MeOH. At r. t. **(IIa)** reacts with one equivalent of HCl affording *trans*-[Pd(COOMe)Cl(PPh₃)₂], whereas when treated with two equivalents of acid the carboalkoxy moiety evolves with formation of MeOH and CO, according to reaction (4) in which step (ii) practically reverses the reaction that leads to the synthesis of *trans*-[Pd(COOMe)Cl(PPh₃)₂] from [PdCl₂(PPh₃)₂], CO and MeOH in the presence of NEt₃.^{6i, p}

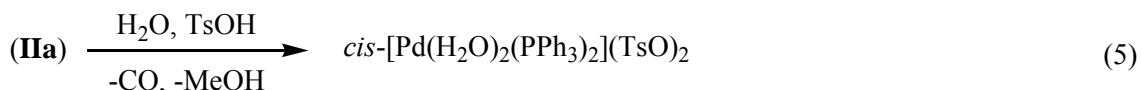


At r. t. the carboalkoxy moiety is stable when treated with AcOH or TsOH, even in excess; with the first acid, in the ratio Pd/AcOH = 1/1, **(IIa)** is partially converted to the corresponding acetate, *trans*-[Pd(COOMe)(OAc)(PPh₃)₂], whereas the conversion is complete using an excess of AcOH.

When treated at 50°C with TsOH (Pd/TsOH = 1/6–1/10), complex **(IIa)** is unstable yielding [Pd(TsO)₂(PPh₃)], analogously to reaction (4), step(ii).

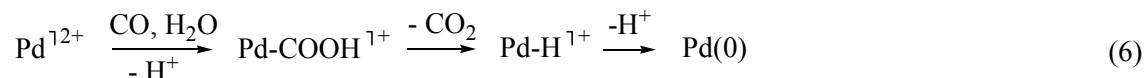
The complexes *trans*-[Pd(COOMe)X(PPh₃)₂] (X = Cl, AcO) are easily obtained also by adding one equivalent of LiX to **(IIa)** dissolved in MeOH.

Reactivity with water and with water/TsOH. Complex **(IIa)** in MeOH/H₂O (10/1, v/v) does not react significantly in one hour even at 50°C, as it is recovered unreacted upon adding cold water to the solution, whereas when to this MeOH/H₂O solution TsOH is added (Pd/TsOH = 1/6) the carbomethoxy moiety is unstable and **(IIa)** is converted to [Pd(OH₂)₂(PPh₃)₂](TsO)₂].



Taking into account the reactivity of **(IIa)** with TsOH above reported, it appears that i) the acid promotes the demethoxylation of the carbomethoxy moiety, probably through protonation of the oxygen atom of the methoxy group, and that ii) water does not play a significant role in the demethoxylation step.

When the same experiment is carried out under CO pressure (20 atm), reduction to Pd(0) complexes occurs, with formation of $[\text{Pd}_3(\text{CO})_3(\text{PPh}_3)_3]$ or $[\text{Pd}(\text{CO})(\text{PPh}_3)_3]$, the latter forming when the reaction is carried out also in the presence of 1 equivalent of PPh_3 . The reduction occurs with concomitant formation of CO_2 , probably *via* a reaction closely related to the water gas shift reaction through the intermediary of a Pd(II)–(COOH) species:¹⁹



Reactivity with ethene and catalytic properties of complexes (Ia–g) in the hydrocarboalkoxylation of ethene. After pressuring a methanol solution of **(IIa)** with ethene (1–40 atm) at r. t. for 1 hour, the complex has been recovered unreacted, together with a minor amount of Pd(0) complexes (*ca.* 10%). In the MeOH solution no methyl propanoate was detected by GC; nor any insertion was observed in $\text{CD}_2\text{Cl}_2/\text{MeOH}$ from $-78\text{ }^\circ\text{C}$ up to $50\text{ }^\circ\text{C}$ in a NMR tube pressurized with 6 atm of ethene. In principle, ethene could insert into the Pd–(COOMe) bond with formation of a Pd–(CH₂–CH₂–COOMe) moiety, which may be in equilibrium with a so-called β–esterchelate, as it has been found to occur promptly with cationic *cis*-chelated diphosphine Pd(II) complex $[\text{Pd}(\text{COOCH}_3(\text{CH}_3\text{CN})(\text{dibpp}))](\text{TfO})$ (dibpp = 1,3–(*i*Bu₂P)₂C₃H₆) in $\text{CH}_2\text{Cl}_2/\text{MeOH}/\text{CH}_3\text{CN}$ even at $-30\text{ }^\circ\text{C}$ at ambient pressure, as established by NMR multinuclear spectroscopy.^{5a} It has been also found that upon rising the temperature up

to 25 °C the β -esterchelate reacts with MeOH yielding methyl propanoate and the starting carbomethoxy complex, thus the “carboalkoxy” cycle for the hydromethoxycarbonylation of ethene was demonstrated under the conditions just reported.^{5a}

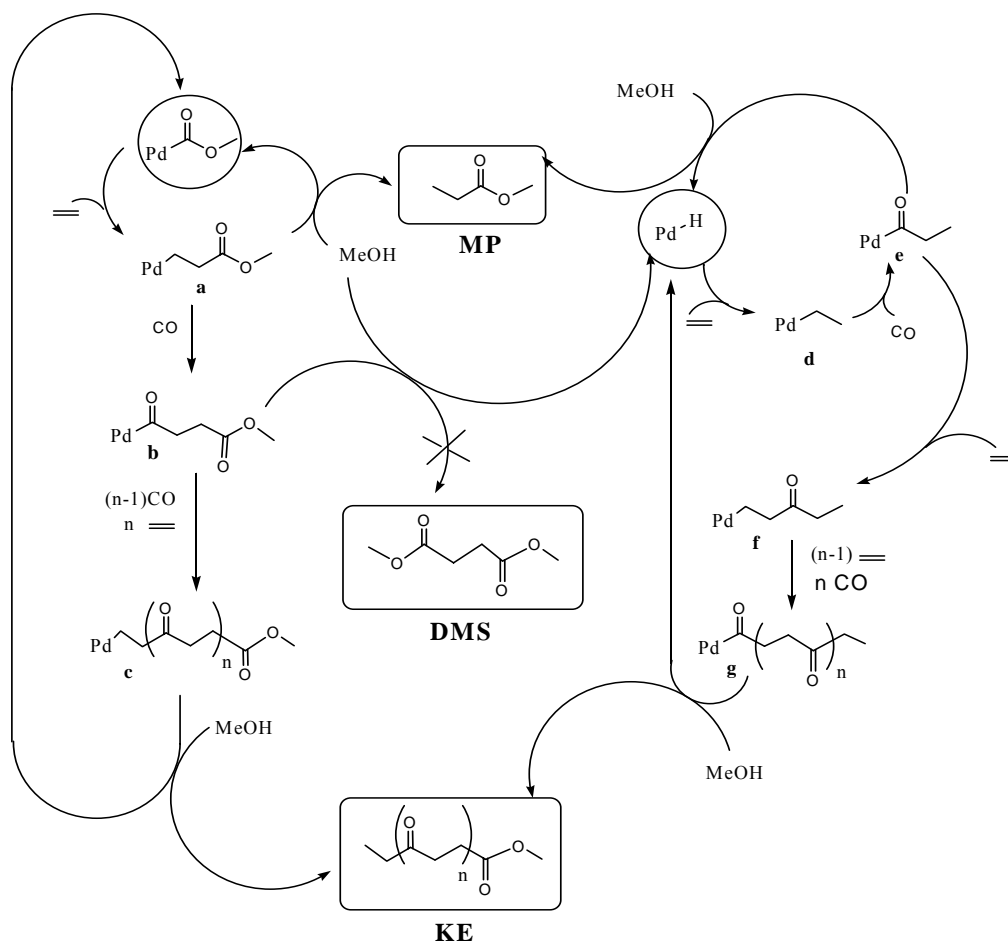
The catalytic activity of complex (**Ia**) in the hydroesterification of ethene in MeOH has been already reported.^{6b, 20} Under standard conditions (40 atm, CO/ethene = 1/1, 70–100 °C) significant catalytic activity is shown only in the presence of both PPh₃ and TsOH (Pd/P/TsOH = 1/8/8). After catalysis the starting complex was recovered (65%) as *trans*-[Pd(COEt)(TsO)(PPh₃)₂], related to the “hydride” cycle (Scheme 1).²⁰ This acyl complex reacts with MeOH to give the expected methyl propanoate (MP) in an almost stoichiometric amount and it is a catalyst precursor for the methoxycarbonylation of a different olefin to give the expected ester and an almost stoichiometric amount of MP. This proves that the acyl complex is sufficiently stable to be isolated while being reactive enough to enter the catalytic cycle. Using [Pd(TsO)₂(PPh₃)₂] as catalyst precursor, it was found that a hydride source, such as H₂, H₂O, or TsOH, present a promoting effect on the catalysis.²¹ All these experimental evidences are more in favor of the “hydride” cycle rather than of the “carbomethoxy” cycle.²² In addition, other researchers found that using a closely related system, derived from Pd(AcO)₂ in combination with an excess of PPh₃ and of TsOH,²³ there was the formation of phosphine degradation products such as MePPh₃⁺, EtPPh₃⁺ and EtCOCH₂CH₂PPh₃⁺, isolated as TsO⁻ salts, thus providing further evidences for the “hydride” mechanism, the last two being Pd mediated side products of the “hydride” route.²⁴

In the present case, we found that also complexes (**Ib–g**), tested in the relevant alkanol at 100 °C and 40–50 atm, do not present any significant catalytic activity and that extensive decomposition to palladium metal occurs at 100°C. Only in the presence of both added PPh₃ and TsOH catalytic activity is observed. Qualitative observations indicate that the activity lowers with increasing bulkiness of the alkanol.

That being said, in addition to the fact that ethene does not insert into the Pd–COOMe

bond under the condition reported in above, we present here further evidences that are more in favor of the “hydride” cycle. In an experiment carried out under conditions in which complex **(Ia)** is relatively stable, *i. e.* 40 °C and in the presence of 2 equivalents of added PPh₃, catalysis is not observed even under 80 atm total pressure (CO/ethene 1/1). Unlike, under these conditions, but also in the presence of 10 equivalents of TsOH, there is formation of MP (TOF = 10 h⁻¹), together with minor, though significant, amounts of light CO/ethene co-oligomers having only keto-ester end groups (KE in Scheme 1), the most abundant of them being 4-oxohexanoate (n = 2). Even more significant, no dimethyl succinate (DMS) or higher diesters co-oligomers were detected by GC of the reaction mixture.

Both the “carbomethoxy” and the “hydride” cycles lead to the formation of MP and KE co-oligomers. Though it is well known that intermediates arising from the insertion of ethene **(a)**, **(c)** and **(f)** are in equilibrium with the so-called β-chelates, and those arising from the insertion of CO **(b)** and **(g)** are in equilibrium with the so-called γ-chelates, the omission of these chelates do not question the validity of the reasoning that follows, therefore they are omitted for the shake of clarity.



Scheme 1. Proposed reaction mechanism.

In the “carbomethoxy” cycle, insertion of ethene into a Pd–COOMe bond gives intermediate (**a**), which upon protonolysis by MeOH yields MP and a Pd–OMe species, which inserts CO to continue the catalytic cycle. Protonolysis competes with the further subsequent insertion of CO and ethene, with formation of intermediates (**b**) and (**c**), which, after protonolysis with MeOH, give the KE cooligomers and again a Pd–OMe species, that continues the catalysis. It should be noted that the copolymerization process stops after the insertion of a few molecules of monomers, *i. e.* the termination process competes effectively with the chain growing process. However, since it has been found that in the copolymerization process CO insertion is faster than ethene insertion,²⁵ it is hard to explain why after CO insertion into intermediate (**a**) (or (**c**)) there is not formation of dimethyl succinate (or of higher diesters). Formation of the diesters would occur *via* methanolysis with formation of a Pd–H species which

can start the “hydride” cycle. The shift from one mechanism to the other has been demonstrated by multinuclear NMR spectroscopy.^{5a} For balance requirements of the two cycles there should be also formation of diethylketone or of cooligomers having only keto ending groups for any molecule having only ester ending groups. However, cooligomers of this type did not form diethyl ketone.

Therefore is more likely that MP and the ketoesters form through a catalytic cycle that starts from a Pd–H species and terminates *via* attack of MeOH to a Pd–acyl bond of intermediates (e) and (g), with concomitant reformation of the hydride species. The hydride would form after decarbomethoxylation of the Pd–COOMe bond promoted by TsOH/H₂O (see above), followed by the interaction of H₂O with CO (*cf.* reaction (6): under catalytic conditions ethene would insert into the Pd–H bond before deprotonation).

These results do not exclude that, under the conditions in which catalysis occurs as just reported, ethene insertion into a Pd–COOMe bond might take place to some extent. As a matter of fact it has been found that the dibpp–based cationic complex under NMR conditions, both the acyl complex, related to the “hydride”, and the β–ester chelate, related to the “carbomethoxy” cycle, easily form at – 60 °C and at – 30 °C, respectively. In addition, it has been found that the acyl complex undergoes methanolysis at –30 °C in a few minutes to give the ester as required from the “hydride” cycle, whereas methanolysis of the β–ester chelate, required to give MP from the “carbomethoxy” cycle, is slow on a timescale of days, at 25 °C. It was suggested that slow methanolysis of the β–ester chelate, rather than slow insertion of an alkene into the Pd–COOMe bond, directs the catalysis towards the “hydride” mechanism.^{5a}

However, it should be underlined that the dibpp– and the PPh₃–based systems are too different to consent a straightforward comparison. A part that dibpp acts only as *cis*–chelating ligand and that the acyl– and carbomethoxy–complexes isolated after catalysis using the PPh₃–based system have a *trans*–geometry (this is the preferred geometry, however in solution it is likely that *cis*–species are also present, as it is well known that this geometry favors the

insertion reactions as well as the product-forming step²⁶), the two systems work under different conditions. The second one requires the use of an excess of PPh₃ in order to prevent deactivation to Pd metal. When PPh₃ is added to the dibpp system the insertion of ethene into the Pd–COOMe bond is inhibited.^{5a} In addition, the PPh₃ system, in order to be catalytically efficient, requires also the use of an excess of TsOH and H₂O, which lead to decarbomethoxylation of the Pd–COOMe bond.

Not only, but the evidences here reported for the “hydride” mechanism, together with those reported in previous studies,^{6b, 20, 21, 27, 23, 24} refer to actual catalysis conditions.

It is worth mentioning that also neutral *trans*-[Pd(COOMe)Cl(PPh₃)₂] treated at 95 °C with 1-hexene does not insert the olefin into the Pd–COOMe bond.^{6j} In this case the much greater coordination capacity of the chloride ligand and the bulkier 1-hexene might prevent the insertion.

Conclusions

The new cationic complexes *trans*-[Pd(COOR)(OH₂)(PPh₃)₂](TsO (R = Me, Et, *n*Pr, *i*Pr, *n*Bu, *i*Bu, *sec*Bu)) have been synthesized and characterized by IR, ¹H NMR and ³¹P NMR spectroscopies.

The structure of *trans*-[Pd(COOMe)(TsO)(PPh₃)₂]·2CHCl₃ has been determined by X-ray diffraction studies.

The reactivity of the carbomethoxy complex with alkanols, TsOH/H₂O and ethene has been studied in relation with the catalytic hydrocarbomethoxylation of the olefin. All the carboalkoxy complexes are catalyst precursors for the carboalkoxylation of ethene if used in combination of PPh₃ and TsOH, better in the presence of some water. Experimental evidences are more in favor of the so-called “hydride” mechanism rather than the “carbomethoxy” mechanism.

Experimental section

Instrumentation and materials

The IR spectra were recorded in nujol mull on a Nicolet FTIR instruments mod. Nexus. ^1H and ^{31}P NMR spectra were recorded on a Bruker AMX 300 spectrometer equipped with a BB multinuclear probe operating in the FT mode at 300 and 121.5 MHz for ^1H and ^{31}P respectively. All the samples were dissolved in deuterated methanol used also as internal reference for the assignment of the chemical shifts.

Carbon monoxide and ethene (purity higher than 99%) were supplied by SIAD Spa (Italy). Methanol was purchased from Baker (purity > 99.5%, 0.01% of water) and $\text{Pd}(\text{OAc})_2$, $\text{Ag}(\text{TsO})$, NEt_3 , PPh_3 and *p*-toluenesulfonic acid were purchased from Aldrich Chemicals. NEt_3 and the solvents were commercial grade and used without further purification. $[\text{Pd}(\text{COOR})\text{Cl}(\text{PPh}_3)_2]$,^{6b} $[\text{PdCl}_2(\text{PPh}_3)_2]$ ²⁸ $[\text{Pd}(\text{OH}_2)_2(\text{PPh}_3)_2(\text{TsO})_2]$ ²⁷ and $[\text{Pd}(\text{TsO})_2(\text{PPh}_3)_2]$ ²⁷ complexes were prepared according to methods reported in the literature.

Preparation of the complexes

All the IR and NMR data of the synthesized complexes are reported in Table 1.

Synthesis of *trans*- $[\text{Pd}(\text{COOR})(\text{OH}_2)(\text{PPh}_3)_2](\text{TsO})$ (R = Me, Et). 0.1 mmol of $[\text{Pd}(\text{OH}_2)_2(\text{PPh}_3)_2](\text{TsO})_2$ was dissolved in 2 ml of MeOH or EtOH, previously saturated with CO at r. t. The solution was kept under 2 atm of CO for 5–10 minutes and then poured into 20 ml of cold water under vigorous stirring. A white precipitate formed immediately. The suspension was filtered, the solid was washed with cold water, *n*-pentane, and dried under vacuum (yield 77%).

Synthesis of *trans*- $[\text{Pd}(\text{COOR})(\text{OH}_2)(\text{PPh}_3)_2](\text{TsO})$ with R bulkier than Et. AgTsO was slowly added to *trans*- $[\text{Pd}(\text{COOR})\text{Cl}(\text{PPh}_3)_2]$ (0.1 mmol) suspended in 2 ml of ROH. The solution was stirred for a few minutes at 15 °C till complete precipitation of AgCl and then

quickly filtered using a micro-filter system. The solution was dropped directly into 20 ml of cold water, under vigorous stirring. A white solid precipitates which was separated by filtration, washed with cold water, *n*-pentane and dried under vacuum (yield 75%). This procedure gives good results also when R = Me or Et. If the filtered methanol solution is poured into warm water (50 °C), the complex *trans*-[Pd(COOR)(TsO)(PPh₃)₂] separates.

Reactivity tests

The reactivity tests under pressure higher than 2 atm were carried out dissolving the carboalkoxy complex (0.1 mmol) in the appropriate alkanol (2 ml) in a 5–10 ml glass bottle placed in an autoclave of *ca.* 50 ml volume. The autoclave was first washed several times with the appropriate gas (CO or ethene), then pressurized and warmed to the desired pressure and temperature. The solution was stirred with a magnetic bar. After the desired reaction time was over the autoclave was rapidly cooled to r. t. (or even to 0 °C) and then slowly depressurized. A small sample was taken apart for GC analysis. The rest was quickly poured into water. The precipitate was collected on a filter, washed with cold water and *n*-heptane and dried under vacuum. The solid was characterized by IR and NMR spectroscopy.

The reactivity was tested with alkanols, acids (HCl, AcOH and TsOH), water, water/TsOH and with ethene. In order not to be redundant, the conditions of the tests are reported together with the results and the discussion in the next section.

Experiments of hydroesterification of ethene using the carboalkoxy complexes reported in Table 1 as catalyst precursors in the relevant ROH

The precursor was used as such or also in combination with PPh₃ and PPh₃/TsOH as reported in the discussion of the results. All the experiments were carried out in a stainless steel autoclave of *ca.* 250 ml of capacity following the same procedure already reported, using the solvent with 800 ppm of water in order to compare the activity with that previously reported

using related precursors.^{6b, 20, 21}

X-ray data collection, structure solution and refinement

The X-ray data collection was performed at room temperature with a STADI 4 CCD STOE area detector diffractometer on single-crystal mounted in a thin-walled glass capillary with graphite-monochromated Mo-K α radiation ($\lambda = 0.71073 \text{ \AA}$). The crystals were obtained by slow evaporation of a CHCl₃/*n*-hexane solution of the complex at $-10 \text{ }^\circ\text{C}$. The structure was solved by direct methods and refined by full-matrix least-squares based on F^2 , where all non-hydrogen atoms were assigned anisotropic displacement parameters. As commented in 3. 2., the solvent molecules suffer from high thermal motions. The final Fourier difference maps showed no significant features, the largest maxima (less than one electron) close to the chlorine atoms. All calculations were made with programs of the SHELXTL/PC system and SHELXL93 program.²⁹

References

- (1) *Metal–Catalysis in Industrial Organic Processes*, Chiusoli; G. P.; Maitlis P. M., Eds; RSCP Publishing, **2006**.
- (2) (a) Sen, A. *Catalytic Synthesis of Alkene–Carbon Monoxide Copolymers and Cooligomers*, Sen, A., Ed.; Kluwer Academic Publishers, Dordrecht, **2003**. (b) Drent, E; Budzelaar, P. H. M. *Chem. Rev.* **1966**, *96*, 663.
- (3) (a) Kalck, Ph; Urrutigoity, M; Dechy–Cabaret, O. “Catalytic Carbonylation Reactions” in *Top. Organomet. Chem.*, Beller, M., Ed.; Springer, **2006**, *18*, 97. (b) Sesto, B.; Consiglio, G. *J. Am. Chem. Soc.* **2001**, *123*, 4097. (c) Bianchini, C.; Mantovani, G.; Meli, A.; Oberhauser, W.; Bruegeller, P.; Stampfl *J. Chem. Soc., Dalton Trans.* **2001**, 690. (d) Gambs, C.; Chaloupka, S.; Consiglio, G.; Togni, A. *Angew. Chem. Int. Ed.* **2000**, *39*, 2486. (e) Sperrle, M.; Consiglio, G. *J. Mol. Catal. A* **1999**, *143*, 5064. (f) Sperrle, M.; Consiglio, G. *J. Organomet. Chem.* **1996**, *506*, 177. (g) Sperrle, M.; Consiglio, G. *J. Am. Chem. Soc.* **1995**, *117*, 12130. (h) Consiglio, G.; Nefkems, S. C. A.; Pisano, C. *Inorg. Chim. Acta* **1994**, *220*, 273. (i) Pisano, C.; Nefkems, S. C. A.; Consiglio, G. *Organometallics* **1992**, *11*, 1975. (j) Pisano, C.; Mezzetti, A.; Consiglio, G. *Organometallics* **1992**, *11*, 20. (k) Barsacchi, M.; Consiglio, G.; Medici, L.; Petrucci, G.; Suter, U. W. *Angew. Chem. Int. Ed.* **1991**, *30*, 989. (l) Brechot, Ph.; Chauvin, Y.; Commereuc, D.; Saussine, L. *Organometallics* **1990**, *9*, 26. (m)) Fenton, D. M.; Steiwand, P. J. *J. Org. Chem.* **1974**, *37*, 1972. (n) Medema, D.; Van Helden, R.; Kohl, C. F. *Inorg. Chim. Acta* **1969**, *3*, 255.
- (4) (a) Delledonne, D.; Rivetti, F.; Romano, U. *Appl. Catal. A* **2001**, *221*, 241. (b) Uchiumi, S.; Ataka, K.; Matsuzaki, T. *J. Organomet. Chem.* **1999**, *576*, 279. (c) Beller, M.; Tafesh, A. M. in: Cornils, B.; Hermann, W. A. (Eds.), *Applied Homogeneous Catalysis with*

-
- Organometallic Compounds, I; VCH, Weinheim, **1996**, 187. (d) Current, S. P. *J. Org. Chem.* **1983**, *48*, 1779. (e) Fenton, D. M.; Steiwand, P. J. *J. Org. Chem.* **1974**, *39*, 1974.
- (5) (a) Liu, J.; Heaton, B. T.; Iggo, J. A.; Whyman, R.; Bickley, J. F.; Steimer, A. *Chem. Eur. J.* **2006**, *12*, 4417. (b) Milsteim, D. *Acc. Chem. Res.* **1988**, *21*, 428. (c) James, D. E., Hines, L. F.; Stille, J. K. *J. Am. Chem. Soc.* **1976**, *98*, 1806. (d) Fenton, D. M. *J. Org. Chem.* **1973**, *38*, 3192.
- (6) (a) Giannoccaro, P.; Cornacchia, D.; Doronzo, S.; Mesto, E.; Quaranta, E.; Aresta, M. *Organometallics* **2006**, *25*, 2872. (b) Cavinato, G.; Vavasori, A.; Toniolo, L.; Benetollo, F.; *Inorg. Chim. Acta* **2003**, *343*, 183. (c) Dervisi, A.; Edwards, P. G.; Newmam, P. D.; Tooze, R. P.; Coles, S. J.; Hursthouse, M. B. *J. Chem. Soc., Dalton Trans.* **1999**, 1113. (d) Santi, R.; Romano, A. M.; Garrome, R.; Millini, R. *J. Organomet. Chem.* **1998**, *566*, 37. (e) Bertani, R.; Cavinato, G.; Facchin G.; Toniolo, L.; Vavasori, A. *J. Organomet. Chem.* **1994**, *466*, 273. (f) Giannoccaro, P.; Ravasio, M.; Aresta, M. *J. Organomet. Chem.* **1993**, *451*, 243. (g) Cavinato, G.; Toniolo, L. *J. Organomet. Chem.* **1993**, *444*, C65. (h) Smith, G. D.; Hansom, B. E.; Merola, J. S.; Waller, F. J. *Organometallics* **1993**, *12*, 568. (i) Bertani, R.; Cavinato, G.; Toniolo, L.; Vasapollo, G. *J. Mol. Catal.* **1993**, *84*, 165. (j) Cavinato, G.; Toniolo, L. *J. Organomet. Chem.* **1990**, *398*, 187. (k) Sacco, A.; Vasapollo, G.; Nobile, C. F.; Piergiovanni, A.; Pellinghelli, M. A.; Lanfranchi, M. *J. Organomet. Chem.* **1988**, *356*, 397. (l) Vasapollo, G.; Nobile, C. F.; Sacco, A. *J. Organomet. Chem.* **1985**, *296*, 435. (m) Rivetti, F.; Romano, U. *Chim. Ind.* **1980**, *62*, 7. (n) Rivetti, F.; Romano, U. *J. Organomet. Chem.* **1978**, *154*, 323. (o) Stille, J. K.; Wong, P. K. *J. Org. Chem.* **1975**, *40*, 532. (p) Hidai, M.; Kokura, M.; Uchida, Y. *J. Organomet. Chem.* **1973**, *52*, 431. (q) Otsuka, S.; Nakamura, A.; Yoshida, T.; Naruto, M.; Ataka, K. *J. Am. Chem. Soc.* **1973**, *95*, 3180. (r) v. Werner, K; Beck, W. *Chem. Ber.* **1972**, *105*, 3947. (s) Beck, W.; v. Werner, K. *Chem. Ber.* **1971**, *104*, 2901.

-
- (7) (a) Ruiz, J.; Martinez, M. T.; Florenciano, F.; Rodriguez, V.; Lopez, G. *Inorg. Chem.* **2003**, *42*, 3650. (b) Bianchini, C.; Meli, A.; Oberauser, W.; van Leeuwen, P. W. M. M.; Zuideveld, M. A.; Freixa, Z.; Kamer, P. C. J.; Spek, A. L.; Gusev, O. V.; Kal'sim, A. M. *Organometallics* **2003**, *22*, 2409. (c) Toth, I.; Elsevier, C. J. *J. Chem. Soc. Chem. Commun.* **1993**, 529. (d) Dekker, G. P. C. M.; Elsevier, C. J.; Vrieze, K.; van Leeuwen, P. W. M. M.; Roobeek, C.F. *J. Organomet. Chem.* **1992**, *430*, 357. (e) Kim, Y-J.; Osakada, K.; Sugita, K.; Yamamoto, T.; A. Yamamoto, *Organometallics* **1988**, *7*, 2182.
- (8) (a) Nishihara, Y.; Miyasaka, M.; Inoue, Y.; Yamaguchi, T.; Kojima, M.; Takagi, K. *Organometallics* **2007**, *26*, 4054. (b) Hua, R.; Takeda, H.; Onozawa, S.; Abe, Y.; Tanaka, M. *J. Am. Chem. Soc.* **2001**, *123*, 2899. (c) Keim, W.; Becker, J.; Trzeciak, A.M. *J. Organomet. Chem.* **1989**, *372*, 447. (d) Otsuka, S.; Nakamura, A.; Yoshida, T.; Naruto, M.; Ataka, K. *J. Am. Chem. Soc.* **1973**, *95*, 3180. (e) Fitton, P.; Johnson, M. P.; McKeon, J. E. *J. Chem. Soc. Chem. Commun.* **1968**, 6.
- (9) (a) Dobrzynsky, E. D.; Angelici, R. J. *Inorg. Chem.* **1975**, *14*, 59. (b) Fayos, J.; E. Dobrzynsky, D.; Angelici, R. J.; Clardy, J. *J. Organomet. Chem.* **1973**, *59*, C33.
- (10) Milsteim, D. *J. Chem. Soc. Chem. Commun.* **1986**, 817.
- (11) (a) Vicente, J.; Arcas, A.; Bautista, D.; Jones, P. G. *Organometallics* **1997**, *16*, 2127. (b) Kubas, G. J.; Burns, C. J.; Khaisa, G. R. K.; Van Der Sluys, L. S.; Kiss, G.; Hoff, C. D. *Organometallics* **1992**, *11*, 3390. (c) Branan, D. M.; Hoffman, N. W.; McElroy, E. A.; Prokopuk, N.; Salazar, A. B.; Robbins, M. J.; Hill, W. E.; Webb, T. R. *Inorg. Chem.* **1991**, *30*, 1200.
- (12) (a) Lasser, W.; Thewalt, U. *J. Organomet. Chem.* **1986**, *302*, 201. (b) Bohner, U.; Zundel, G. *J. Phys. Chem.* **1985**, *89*, 1408. (c) Bailey, O. H.; Ludi, A. *Inorg. Chem.* **1985**, *24*, 2582. (d) Horn, E.; Snow, M. R. *Aust. J. Chem.* **1984**, *37*, 1375. (e) Robinson, E. A. *Can. J. Chem.* **1961**, *391*, 247.

-
- (13) Johnson, C. K. ORTEP, Report ORNL-5138, Oak Ridge National Laboratory, Oak Ridge, TN, **1976**.
- (14) (a) Cambridge Crystallographic Database (Version 5.29 of November 2007). (b) Allen, F. H. *Acta Crystallogr. B* **2002**, *58*, 380. (c) Allen, F. H.; Motherwell, W.D.S. *Acta Crystallogr. B* **2002**, *58*, 407.
- (15) (a) Campora, J.; Lopez, J. A.; Palma, P.; Valerga, P.; Spillner, E.; Carmona, E. *Angew. Chem., Int. Ed. Engl.* **1999**, *38*, 147. (b) Anderson, O. P.; Packard, A. B. *Inorg. Chem.* **1979**, *18*, 1129.
- (16) (a) Newsham, D. K.; Borkar, S.; Sen, A.; Conner, D. M.; Goodall, B. L. *Organometallics* **2007**, *26*, 3636. (b) Weng, W.; Chen, C-H.; Foxman, B. M.; Ozerov, O. V. *Organometallics* **2007**, *26*, 3315. (c) Agostinho, M.; Braunstein, P.; *C. R. Chim.* **2007**, *10*, 666. (d) Agostinho, M.; Braunstein, P.; Welter, R. *J. Chem. Soc., Dalton Trans.* **2007**, 759. (e) Agostinho, M.; Braunstein, P.; *Chem. Commun.* **2007**, 58. (f) Yamashita, M.; Takamiya, I.; Jin, K.; Nozaki, K. *Organometallics* **2006**, *25*, 4588. (g) Grotjahn, D. B.; Gong, Y.; Zakharov, L.; Golen, J. A.; Rheingold, A. L. *J. Am. Chem. Soc.* **2006**, *28*, 438. (h) Chapman, C. J.; Frost, C. G.; Mahon, M. F. *J. Chem. Soc., Dalton Trans.* **2006**, 2251. (i) Kochi, T.; Yoshimura, K.; Nozaki, K. *J. Chem. Soc., Dalton Trans.* **2006**, 25. (j) Bedford, R. B.; Cazin, C. S. J.; Coles, S. J.; Gelbrich, T.; Horton, P. N.; Hursthouse, M. B.; Light, M. E. *Organometallics* **2003**, *22*, 987. (k) Burrows, A. D.; Mahon, M. F.; Varrone, M. *J. Chem. Soc., Dalton Trans.* **2003**, 4718.
- (17) (a) Nishihara, Y.; Inoue, Y.; Itazaki, M.; Takagi, K. *Organic Letters* **2005**, *7*, 2639. (b) Ruiz, J.; Martinez, M. T.; Florenciano, F.; Rodriguez, V.; Lopez, G.; Perez, J.; Chaloner, P. A.; Hitchcock, P. B. *Inorg. Chem.* **2003**, *42*, 3650. (c) Gallo, E.; Ragaini, F.; Cenini, S.; Demartin, F. *J. Organomet. Chem.* **1999**, *586*, 190. (d) Santi, R.; Romano, A. M.; Garrone, R.; Millini, R. *J. Organomet. Chem.* **1998**, *566*, 37. (e) Smith, G. D.; Hanson, B.

-
- E.; Merola, J. S.; Waller, F. J. *Organometallics* **1993**, *12*, 568. (f) Del Piero, G.; Cesari, M. *Acta Crystallogr. B* **1979**, *35*, 2411. (g) Zhir–Lebed, L. N.; Kuz'mina, L. G.; Struchkov, Y. T.; Temkin, O. N.; Golodov, V. A. *Koord. Khim.* **1978**, *4*, 1046.
- (18) Rivetti, F.; Romano, U. *J. Organomet. Chem.* **1979**, *174*, 221.
- (19) (a) Zudin, V. N.; Chinakov, V. D.; Nekipelov, V. M.; Rogov, V. A.; Likholobov, V. A.; Yermakov, Y. I. *J. Mol. Catal.* **1989**, *52*, 27. (b) Zudin, V. N.; Chinakov, V. D.; Nekipelov, V. M.; Likholobov, V. A.; Yermakov, Y. I. *J. Organomet. Chem.* **1985**, 289, 425. (c) Zudin, V. N.; Il'inich, G. N.; Likholobov, V. A.; Yermakov, Y. I. *J. Chem. Soc. Chem. Commun.* **1984**, 545.
- (20) Cavinato, G.; Toniolo, L.; Vavasori, A. *J. Mol. Catal. A: Chem.* **2004**, *219*, 233.
- (21) Vavasori, A.; Cavinato, G.; Toniolo, L. *J. Mol. Catal. A: Chem.* **2001**, *176*, 11.
- (22) Cavinato, G.; Toniolo, L.; Vavasori, A. "Catalytic Carbonylation Reactions" in *Top. Organomet. Chem.* Beller, M., Ed.; Springer, **2006**, *18*, 125.
- (23) Reman, W. G.; De boer, G. B. J.; Van Langen, S. A. J.; Nahuijsen A. (Shell) Eur. Pat., EP 411 721 A3.
- (24) Tooze, R. P.; Whiston, K.; Malyan, A. P.; Taylor, M. J.; Wilson, N. W. *J. Chem. Soc., Dalton Trans.* **2000**, 3441.
- (25) (a) Drent, E.; Budzelaar, P. H. M. *Chem. Rev.* **1996**, *96*, 663. (b) Sen, A. *Acc. Chem. Res.* **1993**, *26*, 303.
- (26) van Leeuwen, P. W. N. M.; Zuideveld, M. A.; Swennenhuis, B. H. G.; Freixa, Z.; Kamer, P. C. J.; Goubitz, K.; Fraanje, J.; Lutz, M.; Spek, A. L. *J. Am. Chem. Soc.* **2003**, *125*, 5523.
- (27) Cavinato, G.; Vavasori, A.; Toniolo, L.; Dolmella, A. *Inorg: Chim. Acta* **2004**, *357*, 2737.
- (28) Jenkins, J. M.; Verkade, J. C. *Inorg. Synth.* **1968**, *11*, 108.
- (29) Sheldrick, G. M. SHELXTL/PC, Version 5.03, Siemens Analytical X-ray Instruments

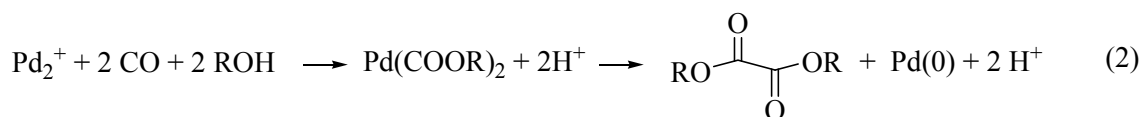
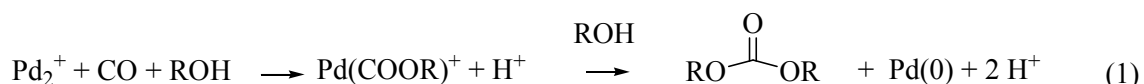
Inc., Madison, WI, 1994; G.M. Sheldrick, SHELXL-93, Program for the Refinement of
Crystal Structures, University of Göttingen, Germany, **1993**.

Chapter 2

Synthesis, Characterization, Reactivity of
[Pd(COOMe)_nX_{2-n}(PPh₃)₂] (n = 1, 2; X = ONO₂, ONO).
Catalytic Properties of [Pd(COOMe)_nX_{2-n}(PPh₃)₂] (n = 0,
1, 2; X = ONO₂, ONO, Cl, OAc) in the Oxidative
Carbonylation of MeOH. X-ray Structure of
trans-[Pd(COOMe)(ONO₂)(PPh₃)₂] and of
cis-[Pd(ONO₂)₂(PPh₃)₂]

Introduction

It has been reported that PdCl₂ promotes the non-catalytic carbonylation of ethyl alcohol to diethyl carbonate with simultaneous reduction to palladium metal, under room conditions in the presence of a base.¹ Also Pd(OAc)₂ is reduced to palladium metal with CO in MeOH with formation of dimethyl oxalate (DMO), together with minor amounts of dimethyl carbonate (DMC). The presence of a phosphine, such as PPh₃, prevents the formation of palladium black, instead Pd(0) complexes, such as [Pd(CO)(PPh₃)₃] and [Pd(CO)(PPh₃)₃] form.² It has been proposed that the formation of the esters occurs through the intermediacy of *trans*-[Pd(COOMe)_n(OAc)_{2-n}(PPh₃)₂] (n = 1 or 2).^{2,3}



As already mentioned in the General Introduction, in order to make the carbonylation catalytic, a reoxidant of Pd(0), such as oxygen, Cu²⁺, Fe³⁺, benzoquinone (BQ) or an organic nitrite or a combination of them, must be used.⁴ In principle also an inorganic–nitrate or –nitrite can act as a reoxidising agent.

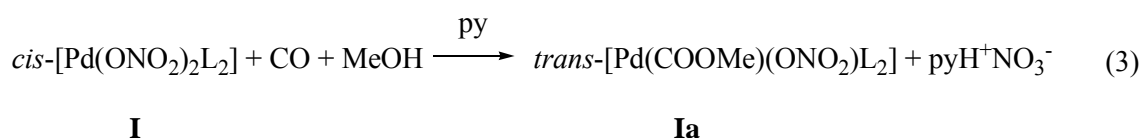
Taking advantage of our experience in the synthesis of carbomethoxy complexes of the type *trans*-[Pd(COOR)X(PPh₃)₂] (R = Me, Et, *n*-Pr, *i*-Pr, *n*-Bu, *i*-Bu, *s*-Bu; X = Cl, OTs) (Chapter 1 and ref 5) and *cis*-[Pt(COOMe)₂(dppf)] (dppf = 1,1'-bis(diphenylphosphino)ferrocene)⁶ we took into account the possibility of synthesising analogous complexes having X = NO₂,³ with the aim of finding whether these ligands could act as reoxidants after formation of carbonate and/or oxalate. The reactivity of [PdX₂(PPh₃)₂] (X = NO₂,³) with CO has been already explored, but in the absence of MeOH. It has been reported that [Pd(ONO₂)₂(PPh₃)₂] reacts with CO in dichloromethane under ambient conditions affording [Pd(ONO)₂(PPh₃)₂] without further deoxygenation of NO₂⁻.⁷ Further reduction with formation of the cluster [Pd₄(CO)₅(PPh₃)₄] occurs by prolonging the reaction time to 72 h.⁸

Here, we report the synthesis, characterization, and reactivity of the complexes *cis*-[Pd(ONO₂)₂(PPh₃)₂] (**I**), *trans*-[Pd(COOMe)(ONO₂)(PPh₃)₂] (**Ia**), *trans*-[Pd(COOMe)₂(PPh₃)₂] (**II**), [Pd(ONO)₂(PPh₃)₂] (**III**) and *trans*-[Pd(COOMe)(ONO)(PPh₃)₂] (**IIIa**) and their catalytic activity in the oxidative carbonylation of MeOH in the presence of BQ, together with that of related complexes having X = Cl, OAc. In addition, we report the X-ray diffraction structures of *trans*-[Pd(COOMe)(ONO₂)(PPh₃)₂] and of *cis*-[Pd(ONO₂)₂(PPh₃)₂].

Results and discussion

Synthesis and characterization of **I**, **Ia**, **II**, **III** and **IIIa**

Complex **I**, suspended in MeOH, in the presence of pyridine, reacts with CO under mild conditions to yield the carbomethoxy–nitrate complex **Ia** in 77% yield. The formation of the product occurs through the interaction of CO with MeOH on the metal centre with releasing of a proton. Pyridine is necessary in order to neutralize the proton that otherwise reverses the reaction. As a matter of fact complex **Ia**, suspended in MeOH containing HNO₃, gives back complex **I**. Although of the two nitrate ligands of **I**, the fate of the one that does not remain coordinated has not been investigated, the formation of **Ia** is schematized as below:

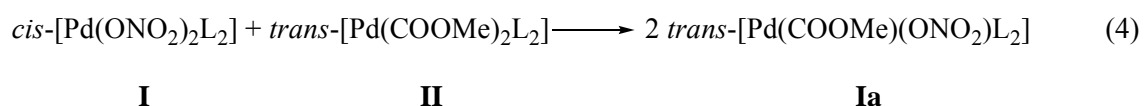


Normally, a trialkyl amine is used as a base, for example in the synthesis of the analogous complex *trans*-[Pd(COOMe)Cl(PPh₃)₂] by carbonylation of *trans*-[PdCl₂(PPh₃)₂] in MeOH. In this case the formation of the carbomethoxy complex is reversed by HCl.^{5d, 9}

When NEt₃ is used in place of pyridine, the solid that is recovered after reaction is a mixture of **Ia**, the dicarbomethoxy complex **II**, [Pd(CO)(PPh₃)₃] (IR, ν_{CO} 1860 cm⁻¹)¹⁰, and unreacted **I**. After reaction, no DMC or DMO was detected by GC; instead there was formation of OPPh₃. This suggests that the Pd(0) complex is not formed *via* attack of MeOH or MeO⁻ on **Ia** or **II** (see below), or *via* reductive elimination of DMO from **II**, but probably it might be formed through oxygen transfer from the nitrate ligand to CO with formation of nitro–complex and subsequent oxygen transfer from this complex to PPh₃, which consumes part of PPh₃ and ultimately leads to Pd(0).^{7, 8} OPPh₃ formation and reduction of Pd(II) may occur also through interaction with H₂O present in the solvent.¹¹ Pd(0) can be formed also through a reaction closely related to the water–gas shift reaction.¹²

Thus the stronger base NEt_3 promotes the formation of a second carbomethoxy ligand, probably increasing the concentration of MeO^- . As a matter of fact, complex **II** has been previously prepared by reacting *trans*- $[\text{Pd}(\text{COOMe})\text{Cl}(\text{PPh}_3)_2]$ with the strong base NaOCH_3 in MeOH under CO (2–3 atm, 0 °C, 4–5 h reaction).^{3b} NEt_3 was used also to form $[\text{Pd}(\text{MeCN})(\text{OMe})(\text{dibpp})](\text{OTf})$ from $[\text{Pd}(\text{MeCN})_2(\text{dibpp})](\text{OTf})_2$ in $\text{CD}_2\text{Cl}_2/\text{MeCN}/\text{MeOH}$ ($\text{dibpp} = 1,3\text{-}(i\text{-Bu}_2\text{P})_2\text{C}_3\text{H}_6$).¹³

Complex **II** is not formed *via* disproportionation of complex **Ia** to complexes **I** and **II**, but rather it occurs the opposite, that is **I** and **II** interchange a carbomethoxy and a nitrate ligand giving **Ia**:



The reaction has been followed by NMR (Figure 1), by dissolving equimolar amounts of **I** and **II** in CD_2Cl_2 at -78 °C, under argon (3 atm). The two singlets for **I** and **II** that are still present at 0 °C, at 33.73 ppm and at 21.40 ppm, respectively, disappear at 10 °C, to make place to a singlet at 18.53 ppm for complex **Ia**. The transformation is irreversible, because upon cooling, only this last signal remains present. It is also quantitative with complete retention of the integrity of the carbomethoxy ligand, in particular without loss of any carbon monoxide, as proved by the ^1H NMR spectrum showing that the $\text{H}(\text{PPh}_3)/\text{H}(\text{COOMe})$ ratio is 60/6 before and after transmetallation.

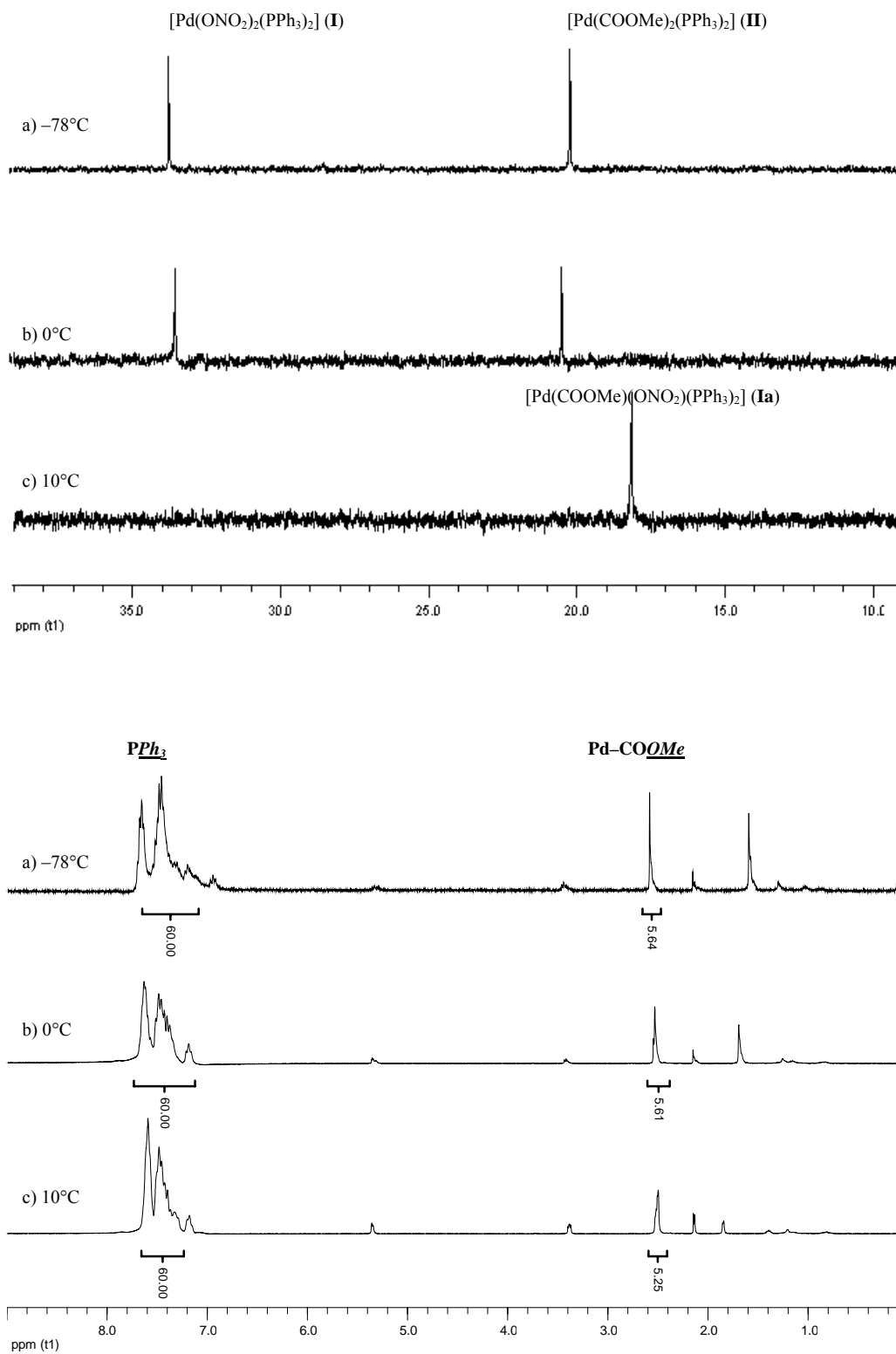
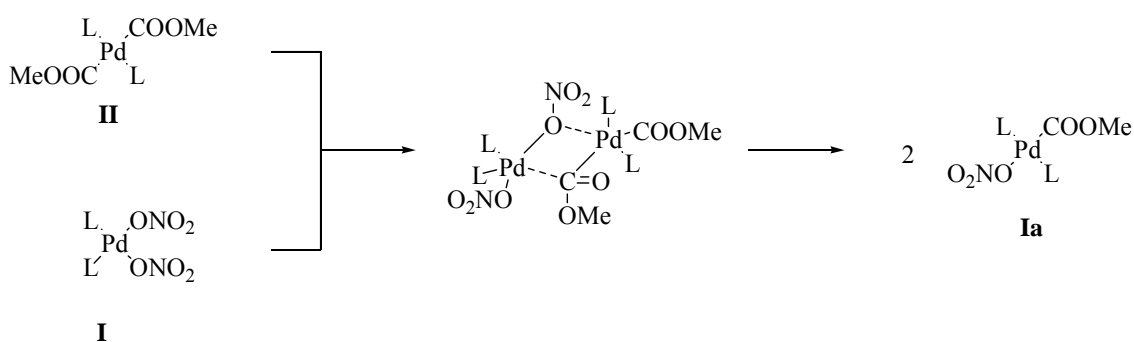


Figure 1. $^{31}\text{P}\{^1\text{H}\}$ and ^1H NMR spectra of the transmetalation between **I** and **II**.

The transfer of an aryl¹⁴ or an alkyl¹⁵ group between palladium atoms is well known, whereas the transfer of a carbomethoxy group from a palladium centre to another, to the best of our knowledge, has not been reported to date.

The mechanism through reaction (4) occurs has not been investigated, however it has been supposed that probably involves the *in situ* formation of a dinuclear Pd(II) intermediate in which the oxygen of the anion and the carbon sp² of the COOMe are bridging two different palladium centres (Scheme 1). Indeed, dinuclear intermediate seems to be involved in the transmetallation reactions. For the transmetallation of [Pd(P-P)(Ph)(CF₃)] with [Pd(P-P)(Ph)I] the intermediary of a species having two five-coordinate palladium centres bridged by a iodine and a phenyl ligand has been proposed.¹⁶ Detailed mechanistic studies on the *trans-cis* isomerisation of *trans*-[Pd(CH₃)₂L₂] (L = tertiary monophosphine) and scrambling with its CD₃ analogue lead to postulate that the reaction proceeds *via* a methyl-bridged intermediate formed between a partially L-dissociated three coordinate species and an undissociated complex. In this dinuclear species one palladium atom is four-coordinate, the other is five-coordinate.¹⁵ An analogous intermediate has been postulated also for the interchange between *trans*-[PdAr₂L₂] and *trans*-[PdMe(I)L₂].¹⁷



Scheme 1. Putative mechanism of the transmetallation between **I** and **II**.

As mentioned in the introduction, it was reported that the di-nitrate complex **I** is reduced by CO in CH₂Cl₂ under ambient conditions, in absence of any base, affording reasonable good yields (49%) of the corresponding di-nitro complex **III** after just 1 h reaction.⁷ Thus substitution of a NO₃ ligand of complex **I** with a COOMe one brings to stabilization of the other NO₃ ligand of the resulting complex **Ia** against further reduction. That in the present case the product of reaction (1) is not the corresponding reduced nitro complex **IIIa** (or a nitrite complex *trans*-[Pd(COOMe)(ONO)(PPh₃)₂]) has been unambiguously proved by the fact that i) the IR, ¹H MMR, and ³¹P{¹H} spectra of complex **Ia** are identical to those of the carbomethoxy complex prepared by metathetical exchange of *trans*-[Pd(COOMe)Cl(PPh₃)₂] with AgNO₃ or by reacting the cationic carbomethoxy complex *trans*-[Pd(COOMe)(OTs)(PPh₃)₂] with LiNO₃ and ii) differ from the spectra of the carbomethoxy-nitro complex **IIIa** prepared from *trans*-[Pd(COOMe)Cl(PPh₃)₂] and AgNO₂ and from *trans*-[Pd(COOMe)(OTs)(PPh₃)₂] and NaNO₂.

The assignment of the IR absorptions for the nitrate-, nitro- and carbomethoxy-ligands of complexes **Ia**, **II** and **IIIa** has been made by comparison with data reported in the literature of analogous complexes. Compared to the IR of *trans*-[Pd(COOMe)Cl(PPh₃)₂],^{5d} in complex **Ia** new absorptions are present, consistent with the presence of O-coordinate monodentate nitrate (in the stretching region at 1465 (ν_{asym} NO₂), 1285 (ν_{sym} NO₂) and 1018 (ν_{N-O}) cm⁻¹ and in the deformation region at 803 cm⁻¹(δ_{ONO}))^{7, 18} (see also the X-ray structure of **Ia**). In addition there is a band of strong intensity at 1385 cm⁻¹, which is characteristic of ionic nitrate.¹⁹ This band is present both in the spectrum taken in KBr and in Nujol mull, therefore it cannot be of the nitrate ligand displaced, even partially, from coordination to Pd(II) by Br⁻ of KBr in the solid.

The ν_{CO} region of **Ia** is characterized by a band of strong intensity at 1671 cm⁻¹ and a band of weak intensity at 1655 cm⁻¹. At 1075 cm⁻¹ a rather broad band of strong intensity can be attributed to ν_{COC}. Also the complex *trans*-[Pd(COOMe)Cl(PPh₃)₂] shows two absorptions in the ν_{CO} region, attributed to the possibility of the presence of conformational isomers with *cis* and *trans* geometry.^{5d}

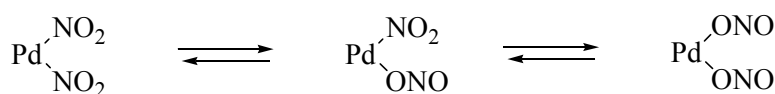


Another possible explanation may be the following: in the X-ray crystal structure (see the structural characterization below for a detailed description) two independent, similar, but not identical molecules are present in the asymmetric unit. The two molecules differ for the reciprocal orientation of the nitrate and –COOMe ligands as well as for the relative position of the –COOMe moiety with respect to the PPh₃ ligands, and appear to be stabilized by a network of nonbonding contacts. If such arrangements coexist in the conditions under which the IR spectrum is taken, they might be the cause of the appearance of the two bands in the ν_{CO} region.

If two conformational isomers are present in the solid state, they cannot be distinguished by NMR as the ¹H NMR and the ³¹P{¹H} spectra in CD₂Cl₂ show only one sharp singlet even at –78 °C, at 19.12 and 2.52 ppm, respectively (18.55 and 2.58 ppm at r. t.).

The IR spectrum of the analogous nitro–carbomethoxy complex **IIIa** presents a band of strong intensity at 1656 cm⁻¹ and at 1055 cm⁻¹ for ν_{CO} and ν_{COC} , respectively. The frequencies relevant to the NO₂ ligand appear at 1413 ($\nu_{\text{asym NO}_2}$), 1331 ($\nu_{\text{sym NO}_2}$), 821 (δ_{ONO}) cm⁻¹; in the NO₂ wagging region (ρ_{w} 600–550 cm⁻¹) there are several bands of weak intensity which prevents to make an unambiguous assignment. Both $\nu_{\text{asym NO}_2}$ and $\nu_{\text{sym NO}_2}$ have been raised with respect to the free ion values, 1328 and 1261 cm⁻¹.²⁰ Moreover, the band at 1331 cm⁻¹ is characteristic of the N–bonded nitro–group.²¹ This leaves little doubt that the NO₂ ligand is coordinated through the nitrogen atom.

The NMR spectra of **IIIa** deserve some comments. The NO₂⁻ ligand may exhibit the phenomenon of linkage isomerism as it can coordinate through the N atom or the O (Scheme 2).



Scheme 1. Equilibria involving N– (nitro) and O– (nitrite) bonded complexes.

Diphosphine complexes of the type *cis*-[Pd(P-P)(NO₂)₂] (P-P = dppm, dppe, dppp) have been found to be fluxional at room temperature, as no resonance appeared, but on cooling to - 53 °C, NMR signals due to three species (N-bonded, O-bonded, and the mixed coordination compound) could be detected.²² On the contrary, the ³¹P{¹H} and ¹H MMR spectra of **IIIa** show only one sharp resonance in the range - 78 ÷ - 40 °C, therefore it is unlikely that **IIIa** is fluxional, as it has been found for other monophosphine complexes of the type *trans*-[Pd(NO₂)₂(PMePh₂)₂], in which the NO₂⁻ ligand is also N-coordinated.²²

The previously synthesized dicarbomethoxy complex **II** was characterized by IR and ¹H NMR, no ³¹P{¹H} NMR data were reported.^{3b} As shown below, complex **II** can be isolated in mixture with **Ia** and Pd(0) by treating **I** with CO in MeOH in the presence of NEt₃.

The formation of complex **II** occurs even at - 78 °C and has been followed by ³¹P{¹H} NMR in CD₂Cl₂ starting from **I** or **Ia**. Figure 2 shows the signal of **I** at 33.55 ppm. Upon admission of CO (4 atm) and MeOH (10% with respect of CD₂Cl₂), a signal at 18.50 ppm, relevant to **Ia** appears immediately. Only upon addition of NEt₃ (Pd/N = 1/10) there is formation of complex **II** (signal at 20.91 ppm). In this solution, complex **II** is stable up to 0 °C, however, at r. t. one displaced nitrate ion reenters in the coordination sphere of Pd(II) giving back **Ia** probably because of the high coordinating capacity of NO₃⁻. Upon warming at 60 °C the decomposition to palladium metal is evident, accompanied with the formation of trace amounts of DMO and DMC, and OPPh₃.

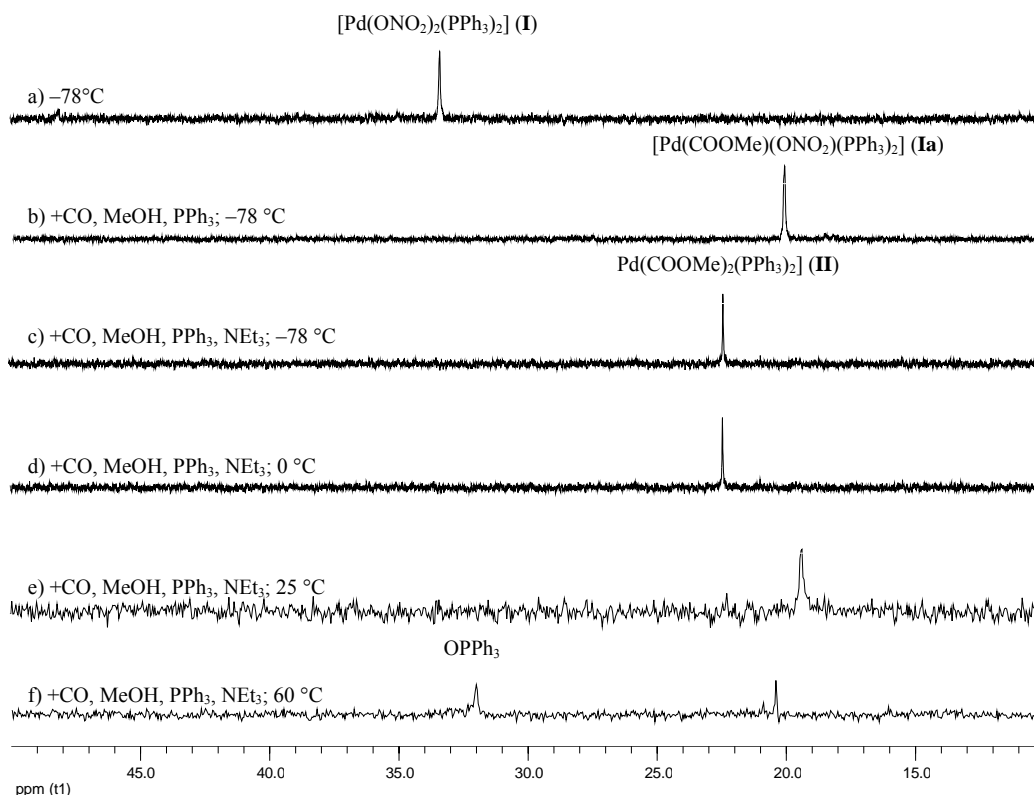
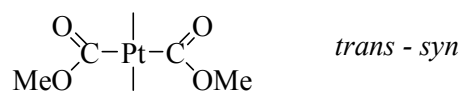


Figure 2. $^{31}\text{P}\{^1\text{H}\}$ NMR spectra of the formation of **II** at $-78\text{ }^\circ\text{C}$ starting from **I** and stability of complex **II**.

In order to explain the presence of two absorptions at 1632.5 and 1629.5 cm^{-1} for ν_{CO} of the analogous dicarbomethoxy–platinum complex *trans*-[Pt(COOMe)₂(PPh₃)₂] a *trans*–*syn* configuration was proposed.²³ The ^1H and $^{31}\text{P}\{^1\text{H}\}$ NMR spectra of **II** in CD₂Cl₂ show a sharp singlet even at $-78\text{ }^\circ\text{C}$ at 2.49 ppm and at 20.91 ppm , respectively. Therefore, the presence of possible conformational isomers for **II** is not evidentiable, nor by IR (only one band at 1630 cm^{-1} for ν_{CO} , consistent with a *trans*–geometry of **II** and a *trans*–configuration for the Pd(COOMe)₂ moiety).



The comparison of ν_{CO} of **Ia** and **IIIa** gives some insights on the nature of the *trans*–[Pd(COOMe)(NO₃)] and *trans*–[Pd(COOMe)(ONO)] moieties. The nitrate ligand is coordinated

through a Pd–oxygen σ bond. The nitro ligand is coordinated through a nitrogen atom, the Pd–N bond has σ – add π –character and it is known to exert a moderately strong *trans* effect.²⁴ The σ –donating effect should decrease the ν_{CO} stretching frequency, whereas the π –back donation effect should increase this frequency. The fact that ν_{CO} of **Ia** is higher than that of **IIIa** suggests that the σ effect prevails over the π effect.

The comparison of ν_{CO} of **IIIa** and **II** is also interesting. In the latter complex ν_{CO} is significantly lower. This fact suggests that i) the (COOMe) ligand presents a σ effect stronger than that of the (ONO) ligand and ii) also with the (COOMe) ligand the σ effect prevails over the π effect.

The comparison of the (ONO) IR frequencies of **III** and **IIIa** gives some more insights. If **III** has a *trans*–geometry, the fact that the frequencies differ little suggests that the (COOMe) and the (ONO) ligands exert a similar effect on the (ONO) ligand in *trans*–position.

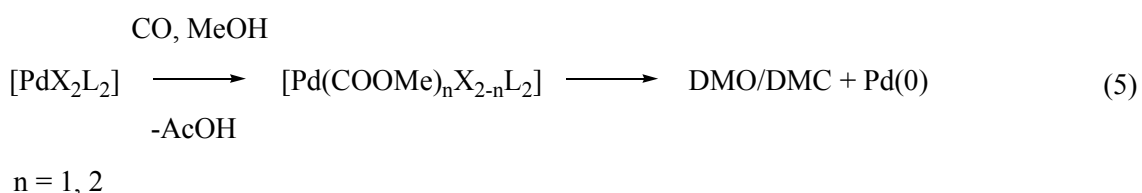
The stereochemistry of Pd(II) complexes of the type $[\text{PdX}_2(\text{PR}_3)_2]$ (R = alkyl and/or aryl) in solution can be conveniently established by NMR studies when PR_3 is dimethylphenylphosphine, as the ^1H (methyl) resonance consists of a 1 : 1 doublet for the *cis*–isomer or of a 1 : 2 : 1 triplet for the *trans*–isomer.²⁵ In the present case PR_3 is triphenylphosphine, the $^{31}\text{P}\{^1\text{H}\}$ NMR spectrum of complexes of the type *trans*– $[\text{PdXY}(\text{PPh}_3)_2]$ (X = or \neq Y) shows only one singlet as well as complexes of the type *cis*– $[\text{PdXY}(\text{PPh}_3)_2]$ when X = Y, so that in this case the geometry cannot be unambiguously assigned. We have observed that complexes having *trans*– or *cis*–geometry, as unambiguously established, for example by X–ray diffraction– or by IR–studies, the $^{31}\text{P}\{^1\text{H}\}$ signal appears around 18 \div 25 ppm or 30 \div 38 ppm, respectively (*cf.* all the complexes here reported and others, see for example reference ²⁶). Moreover, the ^{31}P MMR spectrum of the oxalate complex $[\text{Pd}(\text{C}_2\text{O}_4)(\text{PPh}_3)_2]$ (**IV**), having *cis*–geometry both in solid as well in solution, shows one singlet at 33.94 ppm.²⁷ Based on these

observations, we propose that **Ia**, **I-CH₂Cl₂**, and **II**, having *trans*-, *cis*-, and *trans*-geometry in solid state, respectively, maintain the same geometry also in solution.

Reactivity and catalytic properties of **I**, **Ia**, **II**, **III**, and **IIIa**

Part of the reactivity of **I** and **II** has been reported above. Here, we deal with the possibility of using these complexes as catalyst precursors for the oxidative carbonylation of MeOH.

It was reported that *trans*-[Pd(OAc)₂(PPh₃)₂], in MeOH under 20–50 atm of CO at r. t. gives *trans*-[Pd(COOMe)(OAc)(PPh₃)₂], whereas at 50–80 °C it gives phosphine–palladium(0) complexes and DMO together with minor amounts of DMC.^{3b} In addition, it was reported that complex **II** at 50 °C under CO atmosphere in MeOH decomposes yielding oxalate and Pd(0) complexes.^{3b} It has been also reported that *trans*-[Pd(COOMe)Cl(PPh₃)₂] is rather stable at 90–100 °C, 20–80 atm, and that under these conditions and in the presence of NEt₃, it gives Pd(0) and DMC together with minor amounts of DMO.^{5c} The formation of these products can be so schematized:



It has been also reported that the Pd(OAc)₂/PPh₃ system (Pd/P = 1/3) can be made catalytic by the use of an oxidant, such as BQ, capable of reoxidize Pd(0) to Pd(II), and that CH₃COOH has a beneficial effect of the catalytic activity.^{4d} In principle also the (NO₂, ₃)⁻ ligands of **I**, **Ia**, **III**, and **IIIa** can act as oxidants. As a matter of fact, it has been reported that the stoichiometric carboxylation of aromatic compounds promoted by Pd(OAc)₂ in CF₃COOH as a solvent occurs with reduction to palladium metal, and that it can be turned catalytic by the use of NaNO_{2,3} as oxidants.²⁸

Thus, we tested the reactivity of **I**, **Ia**, **III**, and **IIIa** with MeOH to check whether i) these complexes are able to promote the formation of DMC and/or DMO according to reaction (5), and ii) the $(\text{NO}_2)_3^-$ ligands are able to reoxidize Pd(0) to Pd(II), so that there can be formation of more than one mol of DMC/DMO *per* palladium atom. We chose the operative conditions under which the particularly stable *trans*-[Pd(COOMe)Cl(PPh₃)₂] gives DMC/DMO and Pd(0).^{5c} Upon heating these complexes up to 90 °C in 2 mL MeOH, in presence of PPh₃ and NEt₃ (Pd/P/N = 1/4/10), under 40 atm of CO for 1 hour, there was formation of [Pd(CO)(PPh₃)₃] (*ca.* 70%), OPPh₃ (OPPh₃/Pd = 0.5÷1) and only trace amounts of expected DMC/DMO, even with complexes **Ia** and **IIIa** having a preformed carbomethoxy ligand. The same results were obtained in the presence of added NaNO_{2,3} (Pd/salt = 1/100). These attempts were repeated by warming the autoclave up to 90 °C at a low rate, hopefully to give the possibility of spending enough time in the range of temperatures more favorable to the formation of the DMO/DMC, however unsuccessfully. Addition of 20 equivalents of CH₃COOH to the system **I**/PPh₃/NaNO_{2,3} in the ratio 1/1/100, under 60–70 atm of CO at 65 °C, led to decomposition to palladium metal, without formation of DMC or DMO.

The reactivity of **Ia** and **IIIa** has been followed by NMR (Figure 3). At –78 °C **Ia**, in combination with NEt₃ and PPh₃ (Pd/P/N = 1/4/10), under 4 atm of CO, in CD₂Cl₂ with 10 % of MeOH, gives **II**, which is stable up to 0 °C. At r. t. it gives back **Ia**. Upon warming at 60 °C decomposition occurs with formation of trace amounts of DMC and DMO, and OPPh₃. A broad peak centered at 12.60 ppm indicates the presence of several complexes, probably of Pd(0). This gives further evidence that substitution of a NO₃ ligand of complex **I** with a COOMe inhibits reduction of the other NO₃ ligand of the resulting complex **Ia**, as **I** is readily reduced to **III** at r. t. in CH₂Cl₂.⁷ **IIIa** is more stable than **Ia**, it does not give **II**, however, at 60 °C its ³¹P{¹H} signal lowers of intensity, a new signal appears at 20.04 ppm, probably due to isomerisation of the nitro–complex to a nitrite–one. This variation is accompanied with formation of only DMC, *ca.* 7 %, and OPPh₃ and Pd(0) complexes.

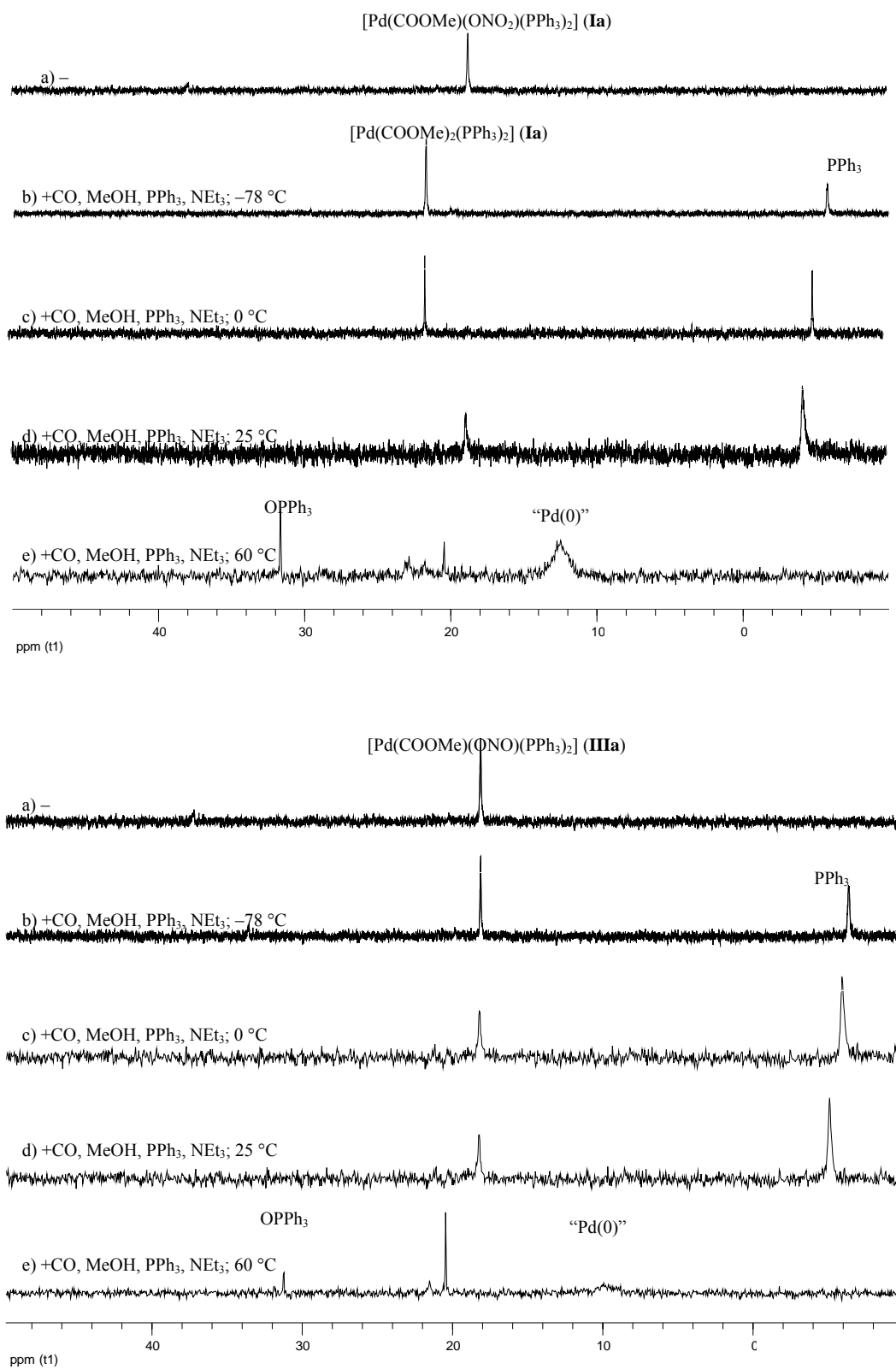


Figure 3. $^{31}\text{P}\{^1\text{H}\}$ NMR spectra of the reactivity of **Ia** and **IIIa** in combination with PPh_3 and NEt_3 in CD_2Cl_2 with 10% of MeOH under 4 atm of carbon monoxide.

Instead, when complexes **I**, **Ia**, **II**, **III**, and **IIIa** are pressurized with CO in the presence of NEt₃ and of an oxidant such as BQ, selective catalysis to DMO was observed, no other carbonylation product formed in detectable amounts (Table 1). The reaction conditions are those experienced by Current using the system Pd(OAc)₂/PPh₃ in the ratio 1/3 as catalyst precursor, except that in his case the concentration of the catalyst precursor was 12 times higher and NEt₃ was not used.^{4d} For comparative purposes the results obtained with other catalyst precursors are also reported. It can be noticed that in general the precursors [PdX₂(PPh₃)₂] give better results than the corresponding monocarbomethoxy complexes and complex **II**. In addition, it can be seen that the nature of the anion does not appear to be discriminant. However, it should be said that these results are valid mainly only an indication that the complexes are actual catalyst precursors. The comparison of their activity is not so straightforward because at the end of catalysis it was found that some decomposition to Pd metal occurred and that the consumption of BQ was higher than that expected for the amount of DMO formed. Current reported that an insoluble solid was produced by BQ polymerization promoted by a PPh₃-BQ adduct that forms *in situ*. He stated that *DMO yields could be variable, depending on the extent of these unrelated side reactions*.^{4d} Another BQ consuming reaction could be the oxidation of MeOH to formal, which in turn can give rise to many derivatives (methyl hemi-formal and di-formal, formal oligomers, methyl formate, 4-hydroxyphenyl formate, pitches).²⁹ However, after reaction formal was present only in trace amounts, practically as in the MeOH used as solvent, and no methyl formate was detected, nor trioxane. We did not investigate any further these aspects, because the main purpose was to establish whether NO_{2,3}⁻ could act as stoichiometric oxidants. The results on Table 1 are valid mainly only as an indication that i) **I**, **Ia**, **III**, and **IIIa** can be effective catalyst precursors when used with BQ and ii) when using them either as such or in the presence NaNO_{2,3}, catalysis does not occur because NO_{2,3}⁻ fail to act as reoxidants.

Table 1. Oxidative carbonylation of methanol

<i>Entry</i>	<i>Catalyst precursor</i>	<i>TOF</i> _{DMO} [h ⁻¹]
1	I ^a	38
2	Ia ^a	25
3	II ^a	19
4	III ^a	12
5	IIIa ^a	21
6	<i>trans</i> -[PdCl ₂ (PPh ₃) ₂] ^a	34
7	<i>trans</i> -[PdCl(COOMe)(PPh ₃) ₂] ^a	15
8	<i>trans</i> -[Pd(OAc) ₂ (PPh ₃) ₂] ^a	33
9	<i>trans</i> -[Pd(COOMe)(OAc)(PPh ₃) ₂] ^a	11
10	[Pd(CO)(PPh ₃) ₃] ^b	38
11	[Pd(CO)(PPh ₃) ₃] ^b	37
12	[Pd(CO)(PPh ₃) ₃] ^c	19

Run conditions: ^a 10⁻² mmol Pd, Pd/PPh₃/NEt₃/BQ = 1/3/2/100, 5 mL of anhydrous MeOH, 65 atm of CO, 65 °C, 1h; ^b the same as in ^a, but without added PPh₃ and with HNEt₃⁺X⁻ (X = Cl, AcO) in place of NEt₃; ^c the same as in ^a, but without added PPh₃.

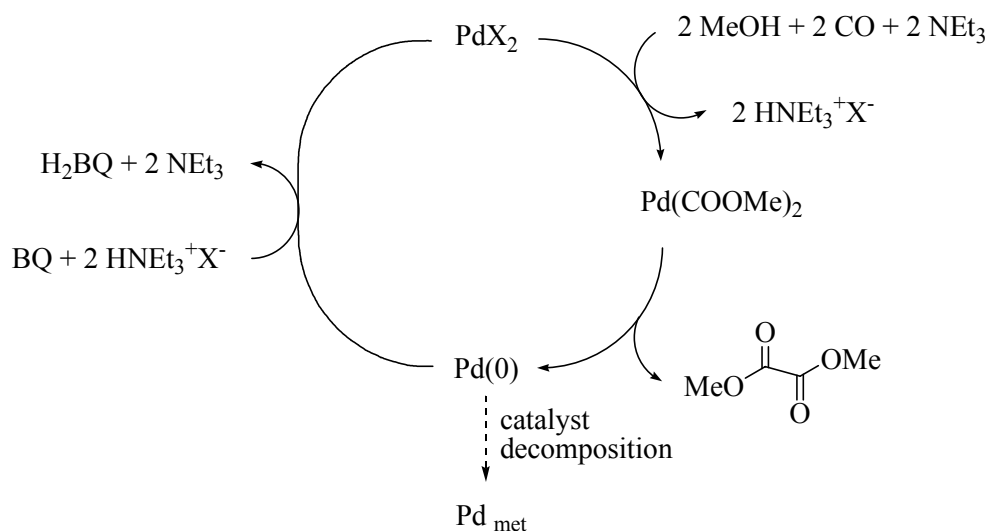
It is interesting to observe that DMO forms selectively also in the case when a preformed mono-carbomethoxy precursor is used. This fact suggests that carbon monoxide and MeOH interacts with a monocarbomethoxy species to form a dicarbomethoxy species which gives DMO before any interaction of MeOH with any carbomethoxy species which would give DMC. In addition, it suggests also that under relatively high pressure of CO, the dicarbomethoxy intermediate does not undergoes decarbonylation of one carbomethoxy ligand, which would lead to the formation of DMC.

It is worthy pointing out that also *trans*-[Pd(COOMe)Cl(PPh₃)₂] gives good results even though this complex under these conditions, but in the absence of BQ, is stable. As a matter of fact it can be prepared in high yield by carbonylation of *trans*-[PdCl₂(PPh₃)₂] in MeOH in the

presence of NEt_3 even at $70\text{ }^\circ\text{C}$.^{5d} Therefore, BQ can also change properties of the reaction centre and, simultaneously, the mechanism and direction of the reaction.

In order to make easier the recovery of the precursor after catalysis we carried out a reaction using a relatively large amount of **I** or **II** (0.1 mmol) with just 5 mmol of BQ, enough to ensure catalysis and, hopefully, not enough to cause the coprecipitation of the solid mentioned by Current. The solid recovered after catalysis was recognized by IR as a mixture of $[\text{Pd}(\text{CO})(\text{PPh}_3)_3]$ and $[\text{Pd}(\text{CO})(\text{PPh}_3)]_3$.¹⁰ $[\text{Pd}(\text{CO})(\text{PPh}_3)_3]$ was reused as precursor. In two experiments (entries 10 and 11) it was used in combination with two equivalents of $\text{HNEt}_3^+\text{X}^-$ ($\text{X} = \text{Cl}, \text{AcO}$) in place of two equivalents of NEt_3 and in the absence of one equivalent of added PPh_3 , which is relevant to the conditions of experiments 6 and 8 of Table 1. In another experiment (entry 12) the precursor was used in combination of NEt_3 , again in the absence of one equivalent of added PPh_3 , which is relevant to the conditions of experiment 2. Again selective catalysis to DMO was observed, with TOF close to those of experiments 6, 8 and 2. These results, together with those of the attempted catalysis using NaNO_2 , confirm that in the latter case catalysis does occur because the salts fails to reoxidize $\text{Pd}(0)$ species.

Scheme 3 shows a simplified catalytic cycle, in which a $\text{Pd}(\text{COOMe})_2$ species gives the product and $\text{Pd}(0)$, which is reoxidized by BQ to $\text{Pd}(\text{II})$, which interacts with CO and MeOH giving back the dicarbomethoxy- $\text{Pd}(\text{II})$ species. In Scheme 3, when using **II** as precursor, X^- is formally CH_3O^- . Further studies on elementary reactions relating to a putative catalytic cycle are in progress.



Scheme 3. Simplified catalytic cycle for the oxidative carbonylation of methanol.

Structural characterization of **Ia** and of **I·CH₂Cl₂**

In **Ia** the Pd atom exhibits square planar (*sp*) coordination, with the two phosphorous donor atoms mutually *trans* (as evidenced also in solution) and monodentate η^1 -nitrate *trans* to the monodentate η^1 -methoxycarbonyl ($-\text{C}(\text{O})-\text{OMe}$) ligand. The compound crystallizes with two independent molecules (from now on Mol 1 and Mol 2) in the asymmetric unit, differing in the orientation of the nitrate and $-\text{COOMe}$ ligands with respect to the coordination / basal plane. The orientation is such that the nitrogen atom and the ester oxygen in one molecule are at opposite sides with respect to the basal plane and their position is reversed in the other molecule. Besides, the nitrate and $-\text{COOMe}$ moieties assume a *cisoid* arrangement with respect to the same plane. The structure of Mol 1 is depicted in Figure 4.

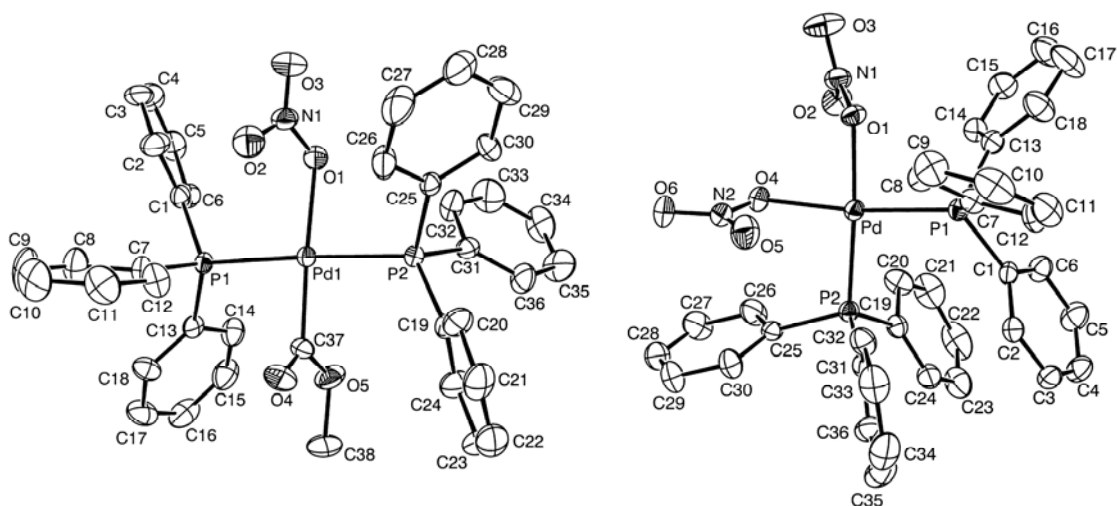


Figure 4. The ORTEP representation of one of the two independent molecules (Mol 1) in complex **Ia** (left) and of complex **I·CH₂Cl₂** (right), with the selected numbering schemes. Ellipsoids are at the 50% level; hydrogen atoms and the dichloromethane solvation molecule of **I·CH₂Cl₂** have been omitted for clarity.

The atoms in basal plane and Pd in Mol 1 and 2 are coplanar within ± 0.04 Å and ± 0.02 Å, respectively, whereas the sum of the angles about Pd is of 360.0° in both Mol 1 and 2, revealing very little distortion of the square planar environment. The nitrate anions in Mol 1 and 2 are strictly planar and roughly orthogonal to the coordination plane, making with it dihedral angles of 70.5° and 81.6° , respectively. Likewise, the $-\text{COOMe}$ ligands are planar within ± 0.03 Å and ± 0.02 Å and they make angles of 82.9° and 75.6° with the basal plane in Mol 1 and 2, respectively. The mean planes of the nitrate and of the $-\text{COOMe}$ ligand of each molecule in Mol 1 make a dihedral angle of 12.5° , while in Mol 2 it reduces to 6.2° . Besides, the nitrate ligands in Mol 1 and 2 are oriented so that one of the formally terminal oxygen atoms of each group lies rather close to the palladium atoms (2.884 and 2.920 Å, respectively), a rather common arrangement for monodentate nitrate anions.

The reciprocal orientation of the two PPh_3 ligands corresponds almost exactly to a staggered conformation; in this way, the contact interactions between faced phenyl groups are kept to a minimum. It is also noteworthy that Mol 1 and 2, with the exception of the arrangement of the nitrate and $-\text{COOMe}$ ligands share the same overall geometry. A fitting of

the *ipso*-carbons of the phenyl rings, plus the Pd and the P atoms made with the *Structure Overlay* routine in Mercury³⁰ gives a RMS value of 0.08 Å, thus yielding a nice superimposition of the main body of the two molecules, in which the coupled phenyl rings of the two PPh₃ units show only minor displacement with respect to each other. As for the nitrate and –COOMe ligands, by examining the overlapped two molecules looking down the P(1)–Pd–P(2) axis, it turns out that the mean planes containing Pd, P(1), P(2), O(1), C(37) in Mol 1 and 2 make with each other an angle of about 35°. In this way, always looking down the P(1)–Pd–P(2) axis, the Pd–C(37) bond nearly overlaps the P(2)–C(19) link in Mol 1 and the P(1)–C(13) one in Mol 2 (see the above interpretation for the presence of two bands in the ν_{CO} region of **Ia**).

Despite the huge number of known *sp* Pd complexes, –COOR ligands appear in a limited number of instances. Careful searches in the CCDC database³¹ yielded about twenty structural reports³², mostly *trans*-bis(phosphine) complexes like **Ia**. In reported structures, that in all the following text will be identified by means of the pertinent CCDC refcodes, the average structural parameters, notably, Pd–C distance, Pd–C–(O) and Pd–C–O angles are 1.985 Å, 126.3° and 112.4°, comparing with 1.948(8)/1.927(8) Å, 126.4(7)/129(1)°, 111.9(7)/111(1)° in Mol 1 and 2, respectively.

The bond distances found by us and those reported in CCDC for analogous compounds again support the idea of a partial double-bond character of the Pd–C link; such behavior will help in stabilizing, at least partially, the afore described Mol 1 and Mol 2 arrangements and may be invoked in the explanation of the IR spectrum (again, see the above interpretation for the presence of two bands in the ν_{CO} region of **Ia**).

By considering the same parameters among known compounds, molecules AMXPPD (1.983 Å, 127.4° and 110.7°)^{32d}, ENAXAS (1.961 Å, 129.6° and 109.6°)^{32b}, FAWQUP (1.967 Å, 127.9° and 110.5°)³³ and PEJWAD (1.964 Å, 124.5° and 112.0°)³⁴ show the closest similarities with **Ia**. In the same set, the shortest Pd–C distance is 1.909 Å in PEJVUW³⁴ however, in this complex two independent molecules are present in the unit cell, with an

average Pd–C bond length of 1.964 Å. Not considering PEJVUW, the values found in **Ia** are, to the best of our knowledge, the shortest Pd–C distances so far reported in Pd–COOR complexes.

This finding stimulated us to analyze published data looking for a possible relation between Pd–C bond length and IR C=O stretching frequencies. The two parameters, however, do not appear to be correlated on the basis of available data. By restricting the comparison to *trans*-bis(phosphine) complexes it appears that the Pd–C distance is related only to the *trans* effect of the donor facing the –COOR moiety, so that a presence of a hard donor results in longer Pd–C bond lengths and *vice versa*. The same reason explains the larger mean Pd–O(N) bond in **Ia**, 2.150 Å, compared with the average of 2.086 Å calculated over 35 reported entries in the CCDC database of Pd–nitrate complexes.

The Pd–O(N) values found in **Ia** fit with the upper quintile of known data, close to those found in compounds IJIMIX (2.150, 2.153, 2.160 Å)³⁵, QELQUT (2.159 Å)^{35b} and VALKEZ (2.148 Å)^{35c}. Interestingly, in all these cases and in **Ia** the η^1 -nitrate is *trans* to a σ -bonded C donor atom. With respect to the Pd–O–N angle, the mean value found in **Ia** (116.4°) agrees well with the average for CCDC reported entries (117.0°). The P–C_{phenyl} distances (average: 1.825 Å) are unexceptional and do not deserve any comment; Pd–P distances (average: 2.355 Å) are somewhat longer than the mean for *sp trans*-bis(phosphine) complexes deposited in CCDC (2.328 Å), and fall in the upper decile of the known range. As for nonbonding contacts, almost all oxygens in Mol 1 and 2 are involved in some intermolecular contacts. Those for which the distance between interacting atoms is at least 0.1 Å shorter than the sum of the pertinent vdW radii are listed in Table 2.

Table 2. Selected Bond Lengths (Å) and Angles (deg) for complexes **Ia** (molecules 1 and 2) and **I·CH₂Cl₂**

	<i>Ia</i>		<i>I·CH₂Cl₂</i>
	<i>Mol 1</i>	<i>Mol 2</i>	
Pd–P(1)	2.349(3)	2.340(3)	2.272(1)
Pd–P(2)	2.364(3)	2.367(3)	2.255(1)
Pd–O(1)	2.150(6)	2.149(6)	2.088(3)
Pd–C(37)	1.948(8)	1.927(8)	
Pd–O(4)			2.111(4)
P–C	1.829(8)	1.822(8)	1.817(5)
	1.80(1)	1.819(9)	1.826(5)
	1.832(8)	1.846(8)	1.833(5)
	1.836(8)	1.844(8)	1.818(5)
	1.804(8)	1.812(9)	1.831(5)
	1.83(1)	1.83(1)	1.817(5)
P(1)–Pd–P(2)	176.8(1)	176.0(1)	96.2(1)
O(1)–Pd–P(1)	94.6(2)	88.1(2)	86.6(1)
O(1)–Pd–P(2)	88.6(2)	96.0(2)	175.2(1)
O(1)–Pd–C(37)	175.8(3)	177.7(5)	
P(1)–Pd–C(37)	86.8(2)	85.9(3)	
P(2)–Pd–C(37)	90.0(2)	90.1(3)	
O(1)–Pd–O(4)			86.2(1)
O(4)–Pd–P(1)			172.8(1)
O(4)–Pd–P(2)			91.0(1)

In **I·CH₂Cl₂**, the Pd nucleus shows *sp* coordination and it is surrounded by a P₂O₂ donor set in which the two triphenylphosphine ligands and the two η¹-nitrate are *cis*-disposed. The asymmetric unit contains only one molecule, which is accompanied by a dichloromethane crystallization solvent molecule. The two nitrate ligands are at opposite sides with respect to the basal plane, so that the N(1) and N(2) atoms respectively lie 0.974 Å above and 1.163 Å below such plane. The atoms in basal plane and Pd are coplanar within ±0.04 Å. The sum of the angles

about Pd is of 360.01° , while the P(1)–Pd–P(2) and the O(1)–Pd–O(4) planes make with each other an angle of only 3.92° , revealing again almost no distortion of the *sp* environment.

The nitrate anions are also strictly planar and their mean planes make angles of 68.1° (N(1)) and 84.9° (N(2)), respectively, with the coordination plane and an angle of 76.9° with each other. Also in this case, one of the formally terminal oxygen atoms of each nitrate ligand lies close to Pd (2.922 and 2.818 Å for O(1) and O(5), respectively, in agreement with the values found in **Ia**). The PPh₃ ligands are in a *synclinal* staggered conformation with respect to each other (torsion angle C(1)–P(1)–P(2)–C(19) of 42.6°); furthermore, the C(1) and C(19) phenyl rings are involved in a rather long-range π – π stacking interaction, with a centroid-to-centroid distance of 3.685 Å (compared with 3.354 Å in graphite) and a dihedral angle between the mean planes of the two phenyl rings of 7.7° .

The *cis*-disposition of the two PPh₃ ligands is not very common. There are less than 80 entries for bis(triphenylphosphine) Pd complexes in CCDC, most of which Pd chelates. Non-chelates are just a tenth of structures, in which the *cis*- arrangement is either due to favorable nonbonding interactions among the ligands (mostly, π – π stackings), or, conversely, to the absence of steric repulsions, such as in the case of coordinating water molecule;³⁶ **I·CH₂Cl₂** seems to better fit in the last group.

Among the 35 reported entries in the CCDC database for *sp* nitrate Pd complexes, 16 are bis(nitrate) derivatives. In these structures, the average structural parameters, notably, Pd–O and O–N distances and Pd–O–N angle are 2.054 Å, 1.298 Å and 115.9° , comparing with 2.088(3)/2.111(4) Å, 1.304(5)/1.302(7) Å, $115.2(3)/111.8(4)^\circ$ for N(1) and N(2) nitrate, respectively. By restricting the comparison to CCDC-deposited bis(nitrate)–phosphine complexes^{7, 37} the mean values of the same parameters (Pd–O, O–N, Pd–O–N) are 2.092 Å, 1.297 Å and 115.2° , with a better agreement between our and existing data, and the compound showing the closest overall similarity with **I·CH₂Cl₂** are the diphenylphosphinoethane chelate

ADEBUH (2.103/2.114 Å, 1.292/1.289 Å, 114.4/111.2°)^{37a} and the phosphole WIJVEQ (2.102/2.124 Å, 1.293/1.290 Å, 115.6/113.0°).^{37b}

The Pd–O distances in **I**·CH₂Cl₂ are shorter than those above seen for **Ia** and the shortest reported so far for bis(nitrate) bis(phosphine) complexes after those found in DUVSOC (2.030/2.031 Å).⁷ The latter, however, is a *trans*-bis(nitrate) derivative. In addition, the comparison of the Pd–ONO₂ bond distance of **Ia** and of **I**·CH₂Cl₂ indicates that the (COOMe) ligand has a stronger *trans* influence than the PPh₃ one (see above the comparison of ν_{CO} of **Ia**, **II**, and **IIIa**).

The Pd–P distances (2.272(1) and 2.255(1) Å) are shorter than the mean for nearly 1700 CCDC–deposited *cis*-bis(phosphine) complexes (2.291 Å), yet, they are longer than the values found in the other deposited bis(nitrate)–phosphine complexes,³⁷ and the closest match (especially if considering all bond distances around Pd) is given by the phosphole WIJVEQ (2.247 and 2.243 Å).^{37b} The longer Pd–P distances in **I**·CH₂Cl₂ with respect to WIJVEQ can be attributed to the more sterically demanding PPh₃ ligand. The P–C_{phenyl} distances (average: 1.824 Å) are instead unexceptional, like for **Ia** above.

Interestingly, a recent work by Longato *et al.*³⁸ reports the crystal structure of the Pt analogous (PIZMOB) of **I**·CH₂Cl₂. The platinum derivative is isostructural and isomorphous with **I**·CH₂Cl₂ and shows a similar pattern in terms of the bond distances around the metal. Moreover, also the Pt compound shows a crystallization solvent molecule (chloroform instead of dichloromethane), which turns out to occupy a position in the crystal similar to that found in **I**·CH₂Cl₂. Among CCDC–reported phosphine/nitrate complexes of Pd and Pt, other similar couples are given by complexes ADEBUH^{37a} and QIHTOQ³⁹ and WIJVEQ and WIJVER.^{37b} In all these cases, metal–P distances in Pt complexes are shorter, thus highlighting the better ability of Pt to establish π -back bonding with phosphorous. A comparison of **I**·CH₂Cl₂ and PIZMOB with the *Structure Overlay* routine of Mercury by fitting the *ipso*-carbons of the phenyl rings,

the Pd and the P₂O₂ donor set (eleven atoms), gives a RMS value of 0.05 Å, revealing a nice superimposition of the two molecules.

Both the nitrate anions and the dichloromethane crystallization solvent molecules are engaged in some intermolecular contacts, however, despite the presence of the crystallization solvent molecule, the network appears to be less extended than that seen for **Ia** above. The contacts for which the distance between interacting atoms is at least 0.1 Å shorter than the sum of the pertinent vdW radii are listed in Table 3.

Table 3. Tighest nonbonding contacts for Mol 1 and 2 of complex **Ia** (above) and for complex **I·CH₂Cl₂** (below). Atoms marked with a final 'A' belong to Mol 2. Atom1 and Atom2 are the atoms participating in contact; Atom 3 is the atom bonding H

<i>Ia</i>				
<i>Atom1</i>	<i>Atom2</i>	<i>Atom3</i>	<i>Symmetry</i>	<i>Length</i>
O(1A)	H(65)	C(15)	x, y, z	2.534
H(27A)	O(5)	C(27A)	x, y, z	2.604
O(2)	H(15A)	C(15A)	$l + x, y, -l + z$	2.513
O(4)	H(35A)	C(35A)	$-l - x, -l/2 + y, l - z$	2.559
O(5A)	H(53)	C(27)	$-l + x, y, l + z$	2.564
O(2A)	H(45)	C(21)	$x, y, l + z$	2.567
O(3A)	H(74B)	C(38A)	$l + x, y, z$	2.593
O(3)	H(76A)	C(38)	$l + x, y, z$	2.609
O(2A)	H(57)	C(9)	$-x, l/2 + y, l - z$	2.615
<i>I·CH₂Cl₂</i>				
<i>Atom1</i>	<i>Atom2</i>	<i>Atom3</i>	<i>Symmetry</i>	<i>Length</i>
O(5)	H(37A)	C(37)	$l/2 + x, l/2 - y, l/2 + z$	2.353
O(3)	H(21)	C(21)	$l - x, -y, 2 - z$	2.366
O(6)	H(37A)	C(37)	$l/2 + x, l/2 - y, l/2 + z$	2.617

A summary of the main crystallographic data are listed in Table 4 (see below for selected bond lengths and angles).

Table 4. Crystallographic Data of complexes **Ia** and **I·CH₂Cl₂**

	Ia	I·CH₂Cl₂
Empirical formula	C ₃₈ H ₃₃ NO ₅ P ₂ Pd	C ₃₇ H ₃₂ N ₂ O ₆ P ₂ Cl ₂ Pd
Formula weight	751.99	839.89
Crystal size (mm ³)	0.24 × 0.20 × 0.15	0.30 × 0.25 × 0.18
Crystal system	monoclinic	monoclinic
Space group	<i>P</i> 2 ₁ (No. 4)	<i>P</i> 2 ₁ / <i>n</i> (No. 14)
<i>a</i> (Å)	11.011(3)	11.975(2)
<i>b</i> (Å)	19.446(3)	20.127(3)
<i>c</i> (Å)	16.276(3)	15.479(3)
β (deg)	91.85(3)	95.06(3)
Volume (Å ³)	3483(1)	3716(1)
<i>Z</i>	4	4
<i>T</i> (K)	294	294
Calculated density (Mg m ⁻³)	1.434	1.501
Absorption coefficient (cm ⁻¹)	6.68	7.77
<i>F</i> (000)	1536	1704
θ range (deg)	3.04–26.00	3.31–25.00
Independent (unique) reflections / <i>R</i> _{int}	6803 / 0.0377	6487 / 0.0179
Observed reflections [<i>I</i> > 2 σ (<i>I</i>)]	6306	5786
Data / parameters	6803 / 849	6487 / 451
<i>R</i> indices [<i>I</i> > 2 σ (<i>I</i>)]	<i>R</i> ₁ ^b = 0.0447; <i>wR</i> ₂ ^c = 0.0980	<i>R</i> ₁ ^b = 0.0523; <i>wR</i> ₂ ^c = 0.1194
<i>R</i> indices (all data)	<i>R</i> ₁ ^b = 0.0522; <i>wR</i> ₂ ^c = 0.1050	<i>R</i> ₁ ^b = 0.0635; <i>wR</i> ₂ ^c = 0.1278
Goodness-of-fit a on <i>F</i> ²	1.190	1.245
Largest difference peak; hole (eÅ ⁻³)	0.697; -0.690	0.675; -0.792

^a Goodness-of-fit = $[\sum (w (F_o^2 - F_c^2)^2) / (N_{\text{obsvns}} - N_{\text{params}})]^{1/2}$, based on all data;

^b $R_1 = \sum (|F_o| - |F_c|) / \sum |F_o|$;

^c $wR_2 = [\sum [w (F_o^2 - F_c^2)^2] / \sum [w (F_o^2)^2]]^{1/2}$.

Conclusions

In summary, we have shown that complex **Ia** can be prepared by reacting complex **I** in MeOH with carbon monoxide under mild conditions in the presence of pyridine, and that no reduction of the nitrate ligand occurs. The reactivity of these complexes and of complexes **III** and **IIIa** has been also studied. Complexes **I** and **II** interchange a carbomethoxy and a nitrate ligand giving **Ia**. The transformation is irreversible and occurs with complete retention of the integrity of the carbomethoxy ligand. Complex **II** forms even at $-78\text{ }^{\circ}\text{C}$ starting from **I**, **Ia** in $\text{CD}_2\text{Cl}_2/\text{MeOH}$, under CO and in the presence of NEt_3 . In this solution complex **II** is stable up to $0\text{ }^{\circ}\text{C}$, at r. t. one displaced nitrate ion reenters in the coordination sphere of Pd(II) giving **Ia**.

Complexes **I**, **Ia**, **III**, and **IIIa**, in combination with PPh_3 and NEt_3 in MeOH, at $90\text{ }^{\circ}\text{C}$, 40 atm of carbon monoxide, and with a potential oxidant such NaNO_2 or NaNO_3 , give $[\text{Pd}(\text{CO})(\text{PPh}_3)_3]$, OPPh_3 and only trace amounts of expected DMC and DMO. On the contrary, using BQ as an oxidant, these complexes or **II** or *trans*- $[\text{Pd}(\text{COOMe})_{2-n}\text{X}_n(\text{PPh}_3)_2]$ ($\text{X} = \text{Cl}$, OAc ; $n = 1, 2$) promote selective catalysis to DMO. Using **I** or **II** as catalyst precursors, the Pd(0) complexes $[\text{Pd}(\text{CO})(\text{PPh}_3)_3]$ and $[\text{Pd}(\text{CO})(\text{PPh}_3)]_3$ have been recovered after catalysis. Using $[\text{Pd}(\text{CO})(\text{PPh}_3)_3]$ as precursor, in combination with 2 equivalents of NEt_3 or $\text{HNEt}_3^+\text{X}^-$ ($\text{X} = \text{Cl}$, AcO) and with BQ, selective catalysis to DMO was observed. In general the precursors $[\text{PdX}_2(\text{PPh}_3)_2]$ give better results than the corresponding monocarbomethoxy complexes and than complex **II**. In addition, the nature of the anion does not appear to be discriminant. Also *trans*- $[\text{Pd}(\text{COOMe})\text{Cl}(\text{PPh}_3)_2]$ gives good results even though this complex under these conditions, but in the absence of BQ, is stable. In conclusion, using $\text{NaNO}_{2,3}$ catalysis does not occur because these salts fail to act as reoxidants.

The X-ray structures of **Ia** and **I-CH₂Cl** have also been described. In **Ia** there are two molecules in the asymmetric unit showing small, but appreciable, differences in the overall molecular arrangement. The Pd-C distances found in **Ia** appear to be among the shortest so far

reported in sp Pd–COOMe complexes. In **I·CH₂Cl₂** the two PPh₃ ligands show the rather uncommon *cis* disposition, favored by the absence of strong steric repulsion from the nitrate ligands and, to a lesser extent, by a long–range π – π interaction involving the C(1) and C(19) phenyl rings. Both complexes show a 3D–network of nonbonding contacts, however, despite the presence of a crystallization solvent molecule, the one found in **I·CH₂Cl** appears to be less efficient than the one present in the solid state of **Ia**.

Experimental section

Instrumentation and materials

The IR spectra were recorded in nujol mull or in KBr on a Nicolet FTIR instrument mod. Nexus. ¹H and ³¹P{¹H} NMR spectra were recorded on a Bruker AMX 300 spectrometer equipped with a BB multinuclear probe operating in the FT mode at 300 and 121.442 MHz for ¹H and ³¹P{¹H}, respectively. NMR under pressure was performed using a special glass tube (resistant up to 13 atm) purchased from the Wilmad Lab Glass. All the samples were dissolved in deuterated solvents. ¹H chemical shifts are reported in ppm downfield (positive) of the deuterated solvent used as internal standard. ³¹P{¹H} chemical shifts are reported in ppm downfield (positive) of externally referenced to 85% H₃PO₄. GC analysis was performed on a Hewlett–Packard Model 6890 chromatograph fitted with a HP5, 30 m × 0.32 μ m × 0.25 μ m column (detector: FID; carrier gas: N₂, 0.7 mL/min; oven: 40 °C (3.5 min) to 250 °C at 15 °C/min). For the detection of methyl formate a 80/120 Carbowax 20M, 6 ftX1/4” OD 2mm ID glass column was used, temp 50 °C to 170 °C, 5 °C/min, detector: FID, carrier N₂ 20 mL/min; for the detection of formal by the EPA 8315A method, <http://www.epa.gov/epawaste/hazard/testmethods/sw846/pdfs/8315a.pdf>, a Agilent HPLC–UV/VIS instrument equipped with a Zorbax ODS column 5 μ m, 4.6x250 mm, at 30 °C, wave length 360 nm was used.

CD₂Cl₂ and the solvents (Aldrich) used for the preparation of the complexes were used as received. Pd(OAc)₂, AgTso, AgNO₃, AgNO₂, PPh₃, *p*-toluensulfonic acid, NEt₃, and BQ were also Aldrich products; only BQ was purified before use (from ethyl ether). Carbon monoxide (purity higher than 99%) was supplied by SIAD Spa (Italy). The complexes *trans*-[Pd(COOMe)(OTs)(PPh₃)₂] (reported in Chapter 1) *trans*-[Pd(COOMe)Cl(PPh₃)₂],^{5d} *trans*-[PdCl₂(PPh₃)₂],⁴⁰ *trans*-[PdOAc)₂(PPh₃)₂]⁴¹ were prepared according to methods reported in the literature.

Preparation of the complexes

All the NMR data of the synthesized complexes **I**, **Ia**, **II**, **III**, **IIIa** and **IV** are reported in Table 5.

Synthesis of *cis*-[Pd(ONO₂)₂(PPh₃)₂] (I). Several procedures for preparing this complex have been already reported in the literature, by treatment of [Pd(NO₂)₂(PPh₃)₂] with NO₂,⁷ from [Pd(O₂)(PPh₃)₂] and N₂O₄⁴² or from [PdCl₂(PPh₃)₂] and AgNO₃.⁴³

We followed a more direct procedure. To a solution of 0.4 mmol of Pd(AcO)₂ in 4 mL of acetone 0.91 mmol of PPh₃ were added at r. t. under stirring. A yellow precipitate formed in a few seconds. To this suspension 160 mg of HNO₃ 65% was added drop wise at room temperature. The mixture was stirred for 30', after which the yellow precipitate was filtered, washed with ether and dried under vacuum. Yield 93%. Elem anal. Calcd for C₃₆H₃₀N₂O₆P₂Pd: C, 57.27; H, 4.01; N, 3.71. Found: C, 57.65; H, 3.92; N, 3.87. IR data are reported in reference 7.

Synthesis of *trans*-[Pd(COOMe)(ONO₂)(PPh₃)₂] (Ia). 5 mL of MeOH containing 0.1 mmol of **I** together with 0.1 mmol of PPh₃ and 0.12 mmol of pyridine were added to a glass tube introduced in a 60 mL autoclave. After washing with CO at room temperature, the autoclave was warmed at 50 °C for 2 hours under 5 atm of CO. After filtering, 20 mL of ethyl ether was added under stirring. The suspension that formed after a few minutes was allowed to

stir for about 30', after which the white precipitate was filtered, washed with ether and dried under vacuum. Yield 77%. Elem anal. Calcd for $C_{38}H_{33}NO_5P_2Pd$: C, 60.69; H, 4.42; N, 1.86. Found: C, 60.21; H, 4.70; N, 1.78. IR (KBr): 1671 s (ν_{CO}), 1655 w (ν_{CO}), 1465 s ($\nu_{asym NO_2}$), 1385 s, 1285 s ($\nu_{sym NO_2}$), 1075 br (ν_{COC}), 1018 w (ν_{N-O}), 803 w (δ_{ONO}) cm^{-1} .

In a different procedure, 0.1 mmol of *trans*-[Pd(COOMe)Cl(PPh₃)₂], suspended in 2 mL of MeOH, was treated with a slight excess of AgNO₃ in 4 mL of CH₂Cl₂ under stirring at room temperature. The white precipitate that formed after a few minutes was filtered and washed with CH₂Cl₂. To the solution 70 mL of ethyl ether and petrol ether (2/5) was added under stirring. After a few minutes a white precipitate formed. The suspension was stirred for 30 more minutes, filtered, the solid was washed with a mixture of the two ethers, dried under vacuum. Yield 92%. The product was recrystallized by dissolving it in CH₂Cl₂ and addition of petrol ether.

In another procedure, 0.25 mmol of LiNO₃ dissolved in 10 mL of water was added to 0.1 mmol of the "cationic" complex *trans*-[Pd(COOMe)(OTs)(PPh₃)₂] dissolved in 2 mL of MeOH at room temperature under stirring. A white precipitate formed immediately. The suspension was stirred for 30 minutes, then filtered. The solid was washed with ethyl ether and dried under vacuum. Yield 93%.

Synthesis of *trans*-[Pd(COOMe)₂(PPh₃)₂] (II). This complex forms when **I** is allowed to react with CO in MeOH, as described above for the preparation of **Ia**, but using NEt₃ in place of pyridine and in the presence of 0.05 mmol of PPh₃. Starting from 0.1 mmol (75 mg) of **I**, after 2 hours reaction under 5 atm of CO at room temperature, the yellow solid that formed was filtered, washed with water, Et₂O–MeOH and Et₂O and dried under vacuum (53 mg). The IR spectrum showed that it was a mixture of **II**, **Ia**, [Pd(CO)(PPh₃)₃],¹⁰ together with minor amounts of unreacted **I**. Further washing with Et₂O dissolved the Pd(0) complex and remained 43 mg of the other three complexes.

Pure complexes **II** was synthesized following a reported method.^{3b} Elem anal. Calcd for C₄₀H₃₆O₄P₂Pd: C, 64.14; H, 4.84. Found: C, 63.78; H, 4.94. IR (KBr): 1630 s (ν_{CO}), 1014 br (ν_{COC}) cm⁻¹.

Synthesis of [Pd(ONO)₂(PPh₃)₂] (III). Also for this complex several procedures have been already reported, including treatment of K₂[Pd(NO₂)₄] (in turn prepared from PdCl₂ and KNO₂)⁸ with PPh₃ in water/ethanol,⁴⁴ or of [Pd(O₂)(PPh₃)₂] with NO in dichloromethane⁴² or of [Pd(PPh₃)₄] (in turn prepared by reduction of *trans*-[PdCl₂(PPh₃)₂] with hydrazine)⁴⁵ with N₂O₃.⁴⁶

We followed a simpler procedure. 0.1 mmol of Pd(OAc)₂ was stirred in 5 mL of acetonitrile at room temperature for 10', after which 0.22 mmol of AgNO₂ was added and stirred for 30 more minutes. The white precipitate that formed was filtered. To the solution 0.2 mmol of PPh₃ dissolved in 10 mL of ethyl ether were added with stirring for another half hour. The resulting suspension was filtered. The white-ivory solid was washed with ether, dried under vacuum. Yield 89%. NaNO₂ dissolved in water can be used in place of AgNO₂. Yield 81%. Elem anal. Calcd for C₃₆H₃₀N₂O₄P₂Pd: C, 59.80; H, 4.18; N, 3.87. Found: C, 60.21; H, 4.24; N 3.57. IR data are reported in reference 8.

The dinitro complex can be prepared also by using 0.1 PdCl₂ dissolved in 0.2 mL of acetic acid in place of Pd(OAc)₂, following the procedure just reported. Yield 72%.

Synthesis of *trans*-[Pd(COOMe)(ONO)(PPh₃)₂] (IIIa). Several attempts to prepare this complex by direct carbonylation of the corresponding dinitro-complex in MeOH, as reported for **Ia**, gave unsatisfactory results. Nor it could be prepared by treatment of [PdCl(NO₂)(PPh₃)₂] with carbon monoxide in MeOH/tri-*n*-octylamine, which yields the Pd(0) complex [Pd(CO)₃(PPh₃)₃] (53 % yield) and *trans*-[Pd(COOMe)Cl(PPh₃)₂] (37 % yield).⁹

Complex **IIIa** was prepared from a preformed Pd-carbomethoxy complex as follows. To 0.14 mmol of *trans*-[Pd(COOMe)Cl(PPh₃)₂] dissolved in 3 mL of MeOH, 0.16 mmol of AgTsO were added at room temperature under stirring for 30'. After filtering, 0.4 mmol of

NaNO₂ in 10 mL of water were added. The white precipitate was collected on a filter, washed with water and ethyl ether and dried under vacuum. Yield 89%. Elem anal. Calcd for C₃₈H₃₃NO₄P₂Pd: C, 62.01; H, 4.52; N, 1.86. Found: C, 62.33; H, 4.69; N, 1.90. IR (KBr): 1656 s (ν_{CO}), 1413 s (ν_{asym NO2}), 1331 s (ν_{sym NO2}), 1055 br (ν_{COC}), 821 w (δ_{ONO}), 600–550 w (ρ_{w ONO}) cm⁻¹.

In a different procedure 0.1 mmol of *trans*-[Pd(COOMe)Cl(PPh₃)₂], dissolved in 4 mL of acetonitrile/CH₂Cl₂, (1/3) 0.1 mmol of AgNO₂ was added at room temperature under stirring. The suspension that formed was filtered. After collecting on a filter the white solid that precipitated upon adding ethyl ether and petrol ether, and after usual work up, the yield was 82%.

Synthesis of *cis*-[Pd(C₂O₄)(PPh₃)₂] (IV). This complex has been prepared by treating with oxalic acid the carbonate complex [Pd(CO₃)(PPh₃)₂],²⁷ in turn prepared by bubbling a mixture of oxygen and carbon dioxide through a benzene solution of [Pd(PPh₃)₄].⁴⁷

We followed a more direct procedure. 0.1 mmol of *trans*-[Pd(OAc)₂(PPh₃)₂] in 50 mL EtOH was treated with a slight excess of oxalic acid. After *ca.* 10 minutes an ivory solid precipitated. The suspension was stirred for 2 more hours. After adding 50 mL petrol ether, the solid was collected on a filter, washed with EtOH, petrol ether and dried. Yield 66 %. Elem anal. Calcd for C₃₈H₃₀O₄P₂Pd: C, 63.48; H, 4.21. Found: C, 63.07; H, 3.95.

Table 5. NMR spectroscopic data for **I**, **Ia**, **II**, **III**, **IIIa** and **IV**

<i>Complex</i>	$\delta^1\text{H NMR}$ [ppm]	$\delta^{31}\text{P}\{\text{H}\}$ NMR [ppm]
<i>cis</i> -[Pd(ONO ₂) ₂ (PPh ₃) ₂] (I)	7.69–7.63 (m, 30 H, Ar)	33.61 (s)
<i>trans</i> -[Pd(COOMe)(ONO ₂)(PPh ₃) ₂] (Ia)	7.65–7.42 (m, 30 H, Ar) 2.58 (s, 3 H, CH ₃ -PdCOOMe)	18.55 (s)
<i>trans</i> -[Pd(COOMe) ₂ (PPh ₃) ₂] (II)	7.68–7.37 (m, 30 H, Ar) 2.55 (s, 6H, CH ₃ -PdCOOMe)	21.76 (s)
[Pd(ONO) ₂ (PPh ₃) ₂] (III)	7.69–7.47 (c m, 30H, PPh ₃)	16.41 (s)
<i>trans</i> -[Pd(COOMe)(ONO)(PPh ₃) ₂] (IIIa)	7.63–7.37 (c m, 30H, Ar) 2.50 (s, 3H, CH ₃ -PdCOOCH ₃)	18.82 (s)
<i>cis</i> -[Pd(C ₂ O ₄)(PPh ₃) ₂] (IV)	7.49–7.28 (c m, 30H, PPh ₃)	33.94 (s)

Abbreviations: s, singlet; m, multiplet. NMR spectra were taken in CD₂Cl₂ at 25 °C.

Reactivity tests

The reactivity tests under CO pressure higher than 2 atm were carried out using a stainless autoclave of ca. 60 mL in which a glass bottle containing solvent and reagents was introduced. The autoclave was first flushed several times with CO, then pressurized and warmed to the desired pressure and temperature. The solution was stirred with a magnetic bar. After the desired reaction time was over the autoclave was rapidly cooled to 0 °C and then slowly depressurized. The content was analyzed by GC, IR and NMR.

X-ray structure determinations

Crystals of both complexes **I** and **Ia**, suitable for X-ray analyses, were obtained by slow recrystallisation from CH₂Cl₂/*n*-hexane solutions. Complex **I** crystallizes with a dichloromethane molecule and is indicated hereafter as **I**·CH₂Cl₂. The selected specimens of both compounds were lodged into Lindemann glass capillaries and mounted on the goniometer head of a four-circle Philips PW1100 diffractometer made available by Colleagues of the

C.M.R.–I.C.I.S. Institute of Padua, Italy. Raw diffraction data were collected at room temperature with the ω - 2θ technique, using graphite monochromated MoK α radiation ($\lambda = 0.71073$ Å). Intensities were corrected for Lorentz and polarization effects, as well as for absorption (ψ -scans).⁴⁸

Unit cell parameters were determined by least squares refinement of 30 well-centred high-angle reflections. Three standard reflections were checked every 150 measurements to assess crystal stability; no sign of decay was noticed. The structures were solved with a combination of direct methods and Fourier difference syntheses (SIR program)⁴⁹ and subsequently refined by standard full-matrix least-squares based on F_o^2 with the SHELXL-97⁵⁰ and SHELXTL-NT⁵¹ programs. In the last cycles of refinement, all non-hydrogen atoms were allowed to vibrate anisotropically. Hydrogen atoms were introduced in calculated positions in their described geometries and refined as “riding model”, with fixed isotropic thermal parameters set at 1.2 times the U_{equiv} of the appropriate carrier atom.

For the structure of **Ia**, the Flack parameter⁵² has also been refined. The graphical representation of the two complexes have been obtained through the ORTEP module of the WinGX software.⁵³

References

- (1) Graziani, M.; Uguagliati, P.; Carturan, G. *J. Organomet. Chem.* **1971**, *27*, 275.
- (2) Rivetti, F.; Romano, U. *J. Organomet. Chem.* **1979**, *174*, 221.
- (3) (a) Rivetti, F.; Romano, U. *Chim. Ind.* **1980**, *62*, 7. (b) Rivetti, F.; Romano, U. *J. Organomet. Chem.* **1978**, *154*, 323.
- (4) (a) Delledonne, D.; Rivetti, F.; Romano, U. *Appl. Catal. A* **2001**, *221*, 241. (b) Uchiumi, S.; Ataka, K.; Matsuzaki, T. *J. Organomet. Chem.* **1999**, *576*, 279. (c) Beller, M.; Tafesh, A. M. in: Cornils, B.; Hermann, W. A. (Eds.), *Applied Homogeneous Catalysis with Organometallic Compounds*, I; VCH, Weinheim, **1996**, 187. (d) Current, S. P. *J. Org. Chem.* **1983**, *48*, 1779. (e) Fenton, D. M.; Steiwand, P. J. *J. Org. Chem.* **1974**, *39*, 1974. (f) Fenton, D. M.; Steiwand, P. J. *J. Org. Chem.* **1974**, *37*, 1972.
- (5) (a) Cavinato, G.; Vavasori, A.; Toniolo, L.; Benetollo, F.; *Inorg. Chim. Acta* **2003**, *343*, 183. (b) Bertani, R.; Cavinato, G.; Facchin G.; Toniolo, L.; Vavasori, A. *J. Organomet. Chem.* **1994**, *466*, 273. (c) Cavinato, G.; Toniolo, L. *J. Organomet. Chem.* **1993**, *444*, C65. (d) Bertani, R.; Cavinato, G.; Toniolo, L.; Vasapollo, G. *J. Mol. Catal.* **1993**, *84*, 165.
- (6) Vasapollo, G.; Toniolo, L.; Cavinato, G.; Bigoli, F.; Lanfranchi, M.; Pellinghelli, M. A. *J. Organomet. Chem.* **1994**, *481*, 173.
- (7) Jones, C. J.; McCleverty, J. A.; Rothin, A. S.; Adams, H.; Bailey, M. A. *J. Chem. Soc. Dalton Trans.* **1986**, 2055.
- (8) Feltham, R. D.; Elbaze G.; Ortega R.; Eck C.; Dubrawsky, J. *Inorg. Chem.* **1985**, *24*, 1503.
- (9) M. Hidai, M. Kokura, Y. Uchida, *J. Organomet. Chem.* **1973**, *52*, 431.

-
- (10) (a) Misono, A.; Uchida, Y.; Hidai, M.; Kudo, K. *J. Organomet. Chem.* **1969**, *20*, P7. (b) Kudo, K.; Hidai, M.; Uchida, Y. *J. Organomet. Chem.* **1971**, *33*, 393.
- (11) Benetollo, F.; Bertani, R.; Bombieri, G.; Toniolo, L. *Inorg. Chim. Acta* **1995**, *233*, 5.
- (12) (a) Zudin, V. M.; Likholobov V. A.; Yermakov, Y. I.; Yeremenko, M. K. *Kinet. Katal.* **1997**, *18*, 524. (b) Laine, R. M.; Craford, E. J. *J. Mol. Catal.* **1988**, *44*, 357.
- (13) Liu, J.; Heaton, B. T.; Iggo, J. A.; Whyman, R.; Bickley, J. F.; Steimer, A. *Chem. Eur. J.* **2006**, *12*, 4417.
- (14) Albénitz, A. C.; Espinet, P.; Lopez-Cimas, O.; Martín-Ruiz, B. *Chem. Eur. J.* **2005**, *11*, 242.
- (15) Ozawa, F.; Ito, T.; Nakamura, Y.; Yamamoto, A. *Bull. Chem. Soc. Jpn* **1981**, *54*, 1868.
- (16) Grushin, V. V.; Marshall, W. J. *J. Am. Chem. Soc.* **2006**, *128*, 4632.
- (17) Ozawa, F.; Fujimori, M.; Yamamoto, T.; Yamamoto, A. *Organometallics* **1986**, *5*, 2144.
- (18) Rosenthal, M. R. *J. Chem. Educ.* **1973**, *50*, 331.
- (19) Gatehouse, B. M.; Livingstone, S. E.; Nyholm, R. S. *J. Chem. Soc.* **1957**, 4222.
- (20) Weston, R. E.; Brodasky, T. F. *J. Chem. Phys.* **1957**, *27*, 683.
- (21) K. Nakamoto, "Infrared and Raman Spectra of Inorganic and Coordination Compounds", Wiley, New York, **1986**, *4th ed.*, 221.
- (22) Moser, J. A.; Stockland, R. A.; Anderson, G. K. *Polyhedron* **2000**, *19*, 1329.
- (23) Werner, K; Beck, W. *Chem. Ber.* **1972**, *105*, 3947.
- (24) Basolo, F.; Pearson, R. G. "Mechanisms of Inorganic Reactions", Wiley, New York, **1967**, *2nd ed.*, 351.
- (25) Shaw, B. L.; Jenkins, J. M. *J. Chem. Soc. (A)* **1966**, 770.
- (26) Garrou, Ph. E.; Heck, R. F. *J. Am. Chem. Soc.* **1976**, *98*, 4115.
- (27) Blake, D. M.; Nyman, C. J. *J. Am. Chem. Soc.* **1970**, *92*, 5359.
- (28) Ugo, R.; Chiesa, A. *J. Chem. Soc., Perkin Trans.* **1987**, 2625.

-
- (29) Pearson, D. M. ; Waymouth R. M. *Organometallics* **2009**, *28*, 3896.
- (30) Macrae, C. F.; Bruno, I. J.; Chisholm, J. A.; Edgington, P. R.; McCabe, P.; Pidcock, E.; Rodriguez–Monge, L.; Taylor, R.; van de Streek, J.; Wood, P. A. *J. Appl. Crystallogr.* **2008**, *41*, 466; Mercury CSD 2.0.
- (31) Allen, F. H. *Acta Crystallogr., Sect. B* **2002**, *58*, 380; Cambridge Structural Database (Version 5.30 of November 2008 + 2 updates).
- (32) (a) Khabibulin, V. R.; Kulik, A. V.; Oshanina, I. V.; Bruk, L. G.; Temkin, O. M.; Mosova, V. M.; Ustynyuk, Yu. A.; Belsky, V. K.; Stash, A. I.; Lyssenko, K. A.; Antipin, M. Yu. *Kinetics Catal. (Russ.)* **2007**, *48*, 244. (b) Yasuda, H.; Maki, N.; Choi, J.–C.; Sakakura, T. *J. Organomet. Chem.* **2003**, *682*, 66. (c) Gallo, E.; Ragaini, F.; Cenimi, S.; Demartin, F. *J. Organomet. Chem.* **1999**, *586*, 190. (d) Del Piero, G.; Cesari, M. *Acta Crystallogr., Sect. B* **1979**, *35*, 2411. (e) Zhir–Lebed, L. N.; Kuz'mina, L. G.; Struchkov, Yu. T.; Temkin, O. M.; Golodov, V. A. *Coord. Chem. (Russ.)* **1978**, *4*, 1046.
- (33) Dervisi, A.; Edwards, P. G.; Newmam, P. D.; Tooze, R. P.; Coles, S. J.; Hursthouse, M. *B. J. Chem. Soc., Dalton Trans.* **1999**, 1113.
- (34) Giannoccaro, P.; Cornacchia, D.; Doronzo, S.; Mesto, E.; Quaranta, E.; Aresta, M. *Organometallics* **2006**, *25*, 2872.
- (35) (a) Li, Y.; Ng, K.–H.; Selvaratnam, S.; Tan, G.–K.; Vittal, J. J.; Leung, P.–H. *Organometallics* **2003**, *22*, 834. (b) Li, Y.; Selvaratnam, S.; Vittal, J. J.; Leung, P.–H. *Inorg. Chem.* **2003**, *42*, 3229. (c) Gul, N.; Nelson, J. H. *Organometallics* **2000**, *19*, 91.
- (36) Qin, Z.; Jennings, M. C.; Puddephatt, R. J. *Inorg. Chem.* **2001**, *40*, 6220.
- (37) (a) Adrian, R. A.; Zhu, S.; Damnels, L. M.; Tiekink, E. R. T.; Walmsley, J. A. *Acta Crystallogr., Sect. E* **2006**, *62*, m1422. (b) Redwine, K. D.; Wilson, W. L.; Moses, D. G.; Catalano, V. J.; Nelson, J. H. *Inorg. Chem.* **2000**, *39*, 3392. (c) Rath, N. P.; Stockland, R. A. Junior; Anderson, G. K. *Acta Crystallogr., Sect. C* **1999**, *55*, 494.

-
- (38) Montagner, D.; Zangrando, E.; Longato, B. *Inorg. Chem.* **2008**, *47*, 2688.
- (39) Arendse, M. J.; Anderson, G. K.; Rath, M. P. *Acta Crystallogr., Sect. C* **2001**, *57*, 237.
- (40) Jenkins, J. M.; Verkade, J. C. *Inorg. Synth.* **1968**, *11*, 108.
- (41) Stephenson, T. A.; Morehouse, S. M.; Powell, A. R.; Heffer, J. P.; Wilkinson, G. *J. Chem. Soc.* **1965**, 3632.
- (42) (a) Levison, J. J.; Robinson, S. D. *Inorg. Nucl. Chem. Letters* **1968**, *4*, 407. (b) Levison, J. J.; Robinson, S. D. *J. Chem. Soc. (A)* **1971**, 762.
- (43) Coulson, D. R. *Inorg. Synth.* **1972**, *13*, 121.
- (44) Burmeister, J. L.; Timmer, R. C. *J. inorg. nucl. Chem.* **1966**, *28*, 1973.
- (45) Malatesta, L.; Angoletta, M. *J. Chem. Soc.* **1957**, 1186.
- (46) Jain, K. C.; Pandey, K. K.; Agarwala, U. C. *Z. anorg. Allg. Chem.* **1981**, *472*, 217.
- (47) Nyman C. J.; Wymore, C. E.; Wilkison, G. *J. Chem. Soc. (A)* **1968**, 561.
- (48) North, A. T. C.; Philips, D. C.; Mathews, F. S. *Acta Crystallogr., Sect. A* **1968**, *24*, 351.
- (49) Altomare, A.; Burla, M. C.; Camalli, M.; Cascarano, G. L.; Giacovazzo, C.; Guagliardi, A.; Moliterni, A. G. G.; Polidori, G.; Spagna, R. "SIR-97" *J. Appl. Crystallogr.* **1999**, *32*, 115.
- (50) Sheldrick, G. M. "SHELXL-97", Program for the Refinement of Crystal Structures, University of Göttingen, Germany, **1997**.
- (51) SHELXTL/MT, Version 5.10; Bruker AXS Inc.: Madison, WI, **1999**; Sheldrick, G. M. *Acta Crystallogr., Sect. A* **1990**, *A46*, 467.
- (52) (a) Bernardinelli, G.; Flack, H. D. *Acta Crystallogr., Sect. A* **1985**, *41*, 500 (b) Flack, H. D. *Acta Crystallogr., Sect. A* **1983**, *39*, 876.
- (53) Farrugia, L. J. *J. Appl. Crystallogr.* **1999**, *32*, 837.

Chapter 3

Mechanistic Studies on the Oxidative Carbonylation of MeOH using a $[\text{Pd}(\text{X})_n(\text{Y})_{2-n}(\text{PPh}_3)_2]$ ($\text{X} = \text{COOMe}$, $\text{Y} = \text{OTs}$, $n = 0, 1, 2$) Complexes and *p*-Benzoquinone as an Oxidant

Introduction

In Chapter 2 it has been shown that NaNO_2 or NaNO_3 fail as stoichiometric oxidants for the catalytic oxidative carbonylation of MeOH when using $[\text{Pd}(\text{X})_n(\text{Y})_{2-n}(\text{PPh}_3)_2]$ ($\text{X} = \text{COOMe}$, $\text{Y} = \text{ONO}_2$ or ONO , $n = 0, 1$) as catalyst precursors in combination with PPh_3 and NEt_3 . Instead, when using BQ as an oxidant these complexes promote selective catalysis to oxalate already at 65 °C and 65 atm of CO. It was also found that with the precursor *trans*- $[\text{Pd}(\text{COOMe})\text{Cl}(\text{PPh}_3)_2]$ selective catalysis to O occurs with comparable TOF, even though this complex under these conditions, but in the absence of BQ, is stable. As a matter of fact it can be prepared in high yield by carbonylation of *trans*- $[\text{PdCl}_2(\text{PPh}_3)_2]$ in MeOH in the presence of NEt_3 even at 70 °C.¹ Thus, BQ is not only an oxidant but indeed may play different roles in the course of a catalytic reaction. It can be involved in both formation and transformation stages of key intermediates into reaction products by interaction with the catalytically active metal

complex.² It can change properties of the reaction centre and, simultaneously, the mechanism and direction of the reaction.³

In order to understand better the role of BQ and of the other components of the catalytic system and to shed light on the catalytic cycle of the oxidative carbonylation reaction, the reactivity of the precursors *cis*-[Pd(OTs)₂(PPh₃)₂] (**I**), *trans*-[Pd(COOMe)(OTs)(PPh₃)₂] (**II**) and *trans*-[Pd(COOMe)₂(PPh₃)₂] (**III**) has been investigated.

Among all the precursors used in the previous chapter, “cationic” **I** and **II** have been chosen because they were expected to be particularly reactive. The choice of **III** was compulsory because catalysis is selective to DMO, which is likely to form from a dicarbomethoxy species.

Hereafter, the results are presented and discussed.

Results and discussion

NMR investigations on the reactivity of I, II and III

In Table 1 and Table 2 the list of the multicomponent systems studied and the relevant NMR data are reported, respect.

Table 1. Multicomponent systems studied by NMR spectroscopy

<i>Designation</i>	<i>System</i>
	<i>cis</i> -[Pd(OTs) ₂ (PPh ₃) ₂] (I)
1.1	(10 % MeOH, 1 PPh ₃) + (8 NEt ₃) + (10 BQ, CO)
1.2	(10 % MeOH, 6 PPh ₃ , 10 BQ) + (CO)
1.3	(1 PPh ₃) + (CO) + (10 % MeOH) + (8 NEt ₃)
1.4	(CO) + (10 % MeOH) + (8 NEt ₃)
1.5 ^a	(MeOD, 10 BQ, CO) + (8 NEt ₃)
1.6 ^b	(MeOH, 8 NEt ₃) + (CO)
	<i>trans</i> -[Pd(COOMe)(OTs)(PPh ₃) ₂] (II)
2.1	(10 % MeOH, 1 PPh ₃) + (CO) + (8 NEt ₃)
2.2	(MeOH, 1 PPh ₃ , 10 BQ, CO)
2.3	(MeOH, 6 PPh ₃ , 10 BQ, CO)
	<i>trans</i> -[Pd(COOMe) ₂ (PPh ₃) ₂] (III)
3.1	(CO) + (1 TsOH) + (1 TsOH) – (CO)
3.2	
3.3	(2 PPh ₃)
3.4	(CO)
3.5	(BQ, CO) + (MeOH)

Note: The components that were mixed or added together are bracked; the value near the component represents the equivalent with respect Pd added or mixed; MeOH 10 % in volume with respect the CD₂Cl₂, except in ^a (CD₃OD). ^b in only MeOH and in synthesis scale.

Table 2. ^1H and $^{31}\text{P}\{^1\text{H}\}$ NMR data of **I**, **II**, **III** and other complexes/compounds identified during the NMR experiments

<i>Compound</i>	$\delta^1\text{H NMR}$ [ppm]	$\delta^{31}\text{P}\{^1\text{H}\}$ NMR [ppm]
<i>cis</i> -[Pd(TsO) ₂ (PPh ₃) ₂] (I)	7.48–6.99 (m, 38 H, Ar) 2.28 (s, 6 H, CH ₃ -TsO)	38.3 (s)
<i>trans</i> -[Pd(COOMe)(OTs)(PPh ₃) ₂] (II)	7.61–6.67 (m, 38H, Ar) 2.36 (s, 3 H, CH ₃ -PdCOOMe) 2.19 (s, 3 H, CH ₃ -TsO)	18.9 (s)
<i>trans</i> -[Pd(COOMe) ₂ (PPh ₃) ₂] (III)	7.68–7.37 (m, 30H, Ar) 2.55 (s, 6 H, CH ₃ -PdCOOMe)	21.76 (s)
[Pd(OTs)(PPh ₃) ₃](TsO)	7.71–7.01 (m, 53 H, Ar) 2.34 (s, 6 H, CH ₃ -TsO)	35.3 (t, 1 P) 31.1 (d, 2 P) J _{p-p} = 13.2
[Pd(COOMe)(PPh ₃) ₃](TsO)	7.61–6.67 (m, 38H, Ar) 2.33 (s, 3 H, CH ₃ -TsO) 1.91 (s, 3 H, CH ₃ -PdCOOMe)	19.9 (d, 2P) 15.7 (t, 1 P) J _{p-p} = 39.2 Hz
BQ	6.80 (s, 4 H, CH)	
HQ	6.65 (s, 4 H, CH) 9.00 (brs, 2 H, OH)	
DMC	3.73 (s, 6 H, CH ₃)	
DMO	3.89 (s, 6 H, CH ₃)	
PPh ₃	7.50–7.20 (m, 30 H, Ar)	- 4.81 (s)
OPPh ₃	7.64–7.46 (m, 30 H, Ar)	30.31 (s)
PPh ₃ -BQ adduct		22.3, 16.4 (s) ^a
[Pd(COOMe)(OMe)(PPh ₃) ₂]	3.25 (t, 3 H, OMe)	19.7 (s); 20.3 (s) ^b
[Pd(CO)(PPh ₃) ₃]		28.5 (s)
[Pd(CO)(PPh ₃) ₃]		22.6 (s) ^c
[Pd(BQ)(PPh ₃) ₂]		32.9 (s) ^d

NMR spectra were taken in CD₂Cl₂ at -78 °C. Abbreviations: s, singlet; d, doublet; t, triplet; vt, virtual triplet; dt, doublet of triplet; m, multiplet ; brs, broad singlet.

^a in CD₂Cl₂/MeOH 10% in presence of CO, BQ or even NEt₃ (system 1.1, 1.2, 2.2 and 2.3).

^b in CD₂Cl₂/MeOH 10% in presence of PPh₃, CO, NEt₃ (system 1.3 and 2.1).

^c in CD₂Cl₂/MeOH 10% with CO, NEt₃ (system 1.3).

^d in CD₂Cl₂/MeOH 10% in presence of CO, NEt₃, BQ (system 1.1).

Reactivity of I. When **I** at $-78\text{ }^{\circ}\text{C}$ (Table 1, system 1.1) has been allowed to react with PPh_3 ($\text{Pd}/\text{PPh}_3 = 1/1$) a cationic complex having three coordinated PPh_3 ligands identified as $[\text{Pd}(\text{OTs})(\text{PPh}_3)_3](\text{TsO})$ is formed. The $^{31}\text{P}\{^1\text{H}\}$ NMR spectrum of this complex shows two signals, one at 35.3 ppm (triplet, 1P) and the other at 31.1 ppm (doublet, 2P), both arising from the spin spin system AX_2 ($J_{\text{P-P}} = 13.2\text{ Hz}$).

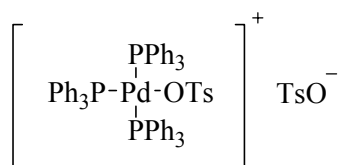
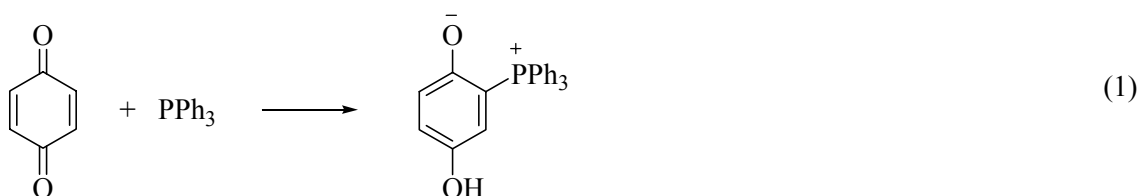


Figure 1. Complex formed in the system 1.1.

Upon addition of NEt_3 at $-78\text{ }^{\circ}\text{C}$ new signals appear (Figure 2, spectra c), attributed to several cationic species of general formula $[\text{Pd}(\text{X})(\text{S})(\text{PPh}_3)_2]^+$, $[\text{Pd}(\text{S})_2(\text{PPh}_3)_2]^{2+}$, $[\text{Pd}(\text{X})(\text{PPh}_3)_3]^+$ or $[\text{Pd}(\text{S})(\text{PPh}_3)_3]^{2+}$ ($\text{X} = \text{OH}, \text{OCH}_3^*$; $\text{S} = \text{OH}_2, \text{MeOH}, \text{NEt}_3$).⁴ Upon addition of BQ and of CO, Pd(0) complexes are formed *i. e.* $[\text{Pd}(\text{BQ})(\text{PPh}_3)_2]$ ⁵ and $[\text{Pd}(\text{CO})(\text{PPh}_3)_3]$ ^{4a, 6} together with a “betaine” BQ– PPh_3 adduct. As was demonstrated in earlier studies,^{5, 7} PPh_3 reacts with BQ yielding (2,5–dihydroxyphenyl)phosphonium betaine (1), which is readily identifiable by NMR (singlet at *ca.* 22.1 ppm in $\text{CD}_2\text{Cl}_2/\text{MeOH}$ (10/1, v/v)). In the reaction mixture this phosphonium compound is successively converted into another unidentified compound⁵ ($^{31}\text{P}\{^1\text{H}\}$ resonance at *ca.* 16.4 ppm in $\text{CD}_2\text{Cl}_2/\text{MeOH}$ (10/1, v/v)).



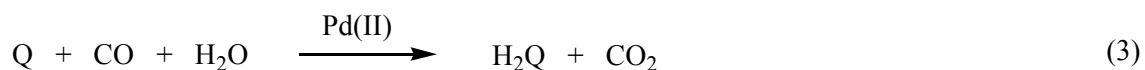
Quite interestingly, no mono- **II** or di-carbomethoxy **III** species have been detected. Upon warming at $60\text{ }^{\circ}\text{C}$, traces of DMO are detectable only after a prolonged time (*ca.* 1 hour).

* OCH_3 is unlikely otherwise a Pd–COOMe would form upon admission of carbon monoxide.

There is also formation of H₂BQ in a larger amount than that expected for the formation of DMO (Figure 1d). BQ could be reduced by MeOH giving H₂BQ and formaldehyde (2) (formal presents signals at 9.5 ppm⁸), which in turn can give rise to many derivatives (methyl hemi-formal and di-formal, formal oligomers, methyl formate, 4-hydroxyphenyl formate, pitches)⁹ However, these products were not detected.



In addition it is known that Pd(II) complexes catalyze the reduction of quinones (Q) with carbon monoxide in the presence of H₂O:¹⁰



However, the solvent used was dried in advance over molecular sieves, so it is not clear how H₂BQ forms in a so unexpected high amount. In conclusion, the above NMR experiment allowed us to establish the presence in solution of the Pd(0) complex [Pd(BQ)(PPh₃)₂].

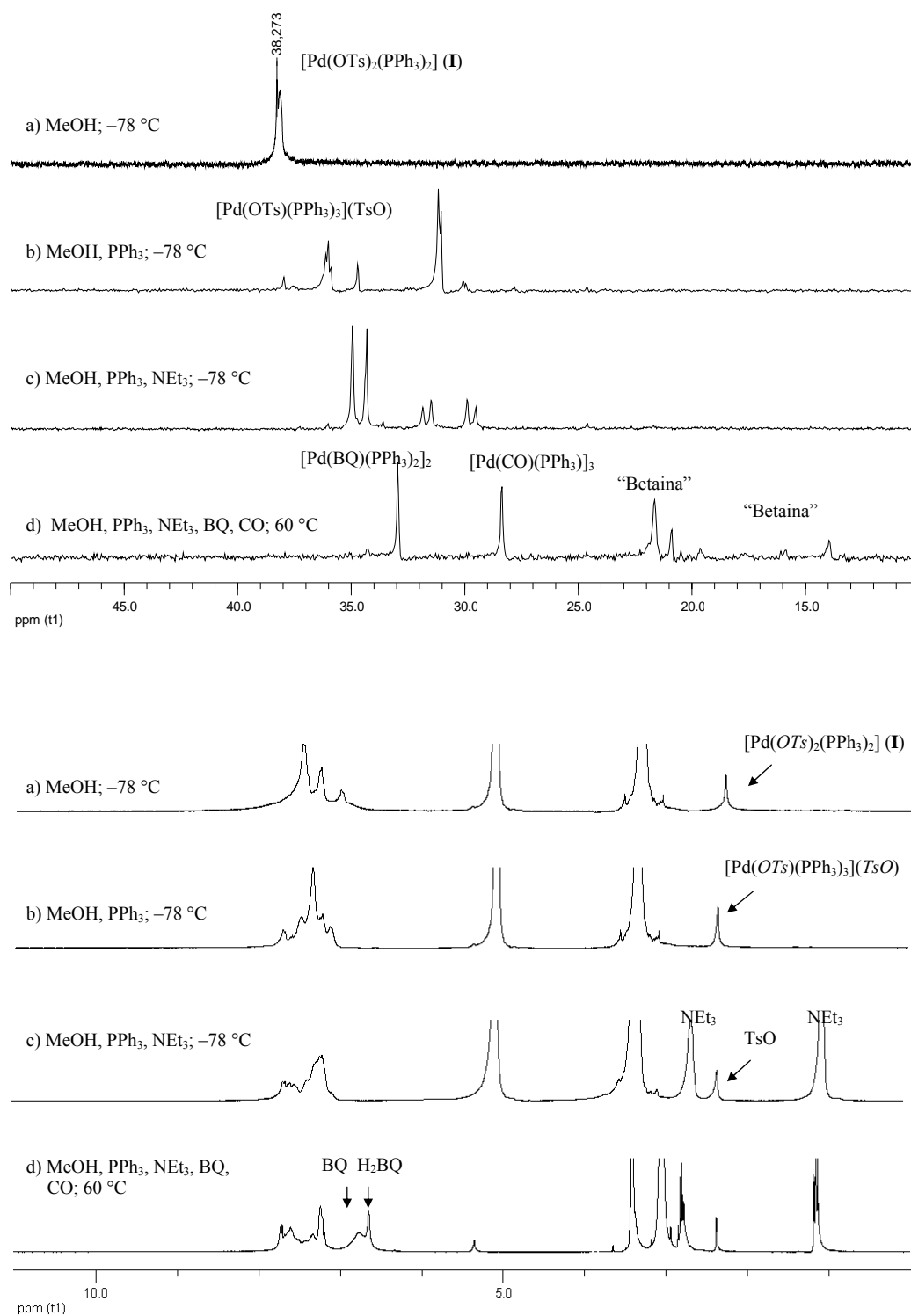
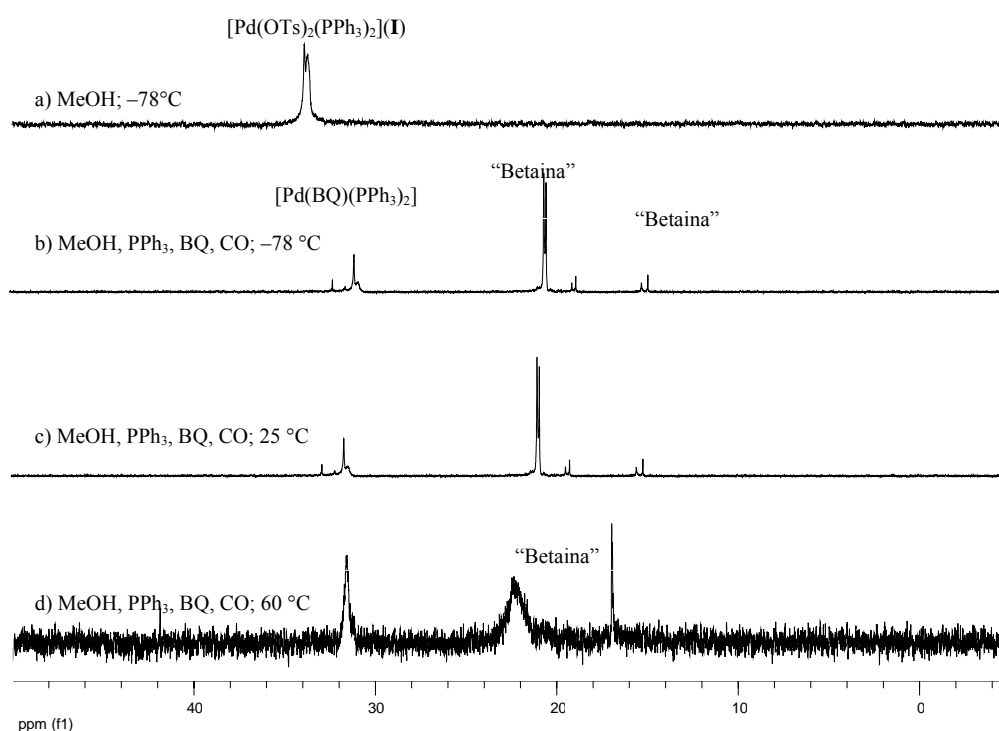


Figure 2. Selected $^{31}\text{P}\{^1\text{H}\}$ and ^1H NMR spectra in CD_2Cl_2 of the reactivity of **I** in system 1.1.

To gain more insights, **I** dissolved in $\text{CD}_2\text{Cl}_2/\text{MeOH}$ (10% MeOH v/v), was treated with a BQ, PPh_3 ($\text{Pd}/\text{PPh}_{3\text{added}}/\text{BQ} = 1/6/10$) and then pressurized with CO, 4 atm (Table 1, system 1.2). All the operations were carried out at -78°C . As shown in Figure 3, **I** already at -78°C was converted to $[\text{Pd}(\text{BQ})(\text{PPh}_3)_2]$, no other Pd(0) complex formed in detectable amount. All PPh_3 disappeared because of the reaction with BQ forming betaine. At 25°C the $^{31}\text{P}\{^1\text{H}\}$ and ^1H spectra did not change significantly. Neither DMO nor DMC formed even at 60°C .



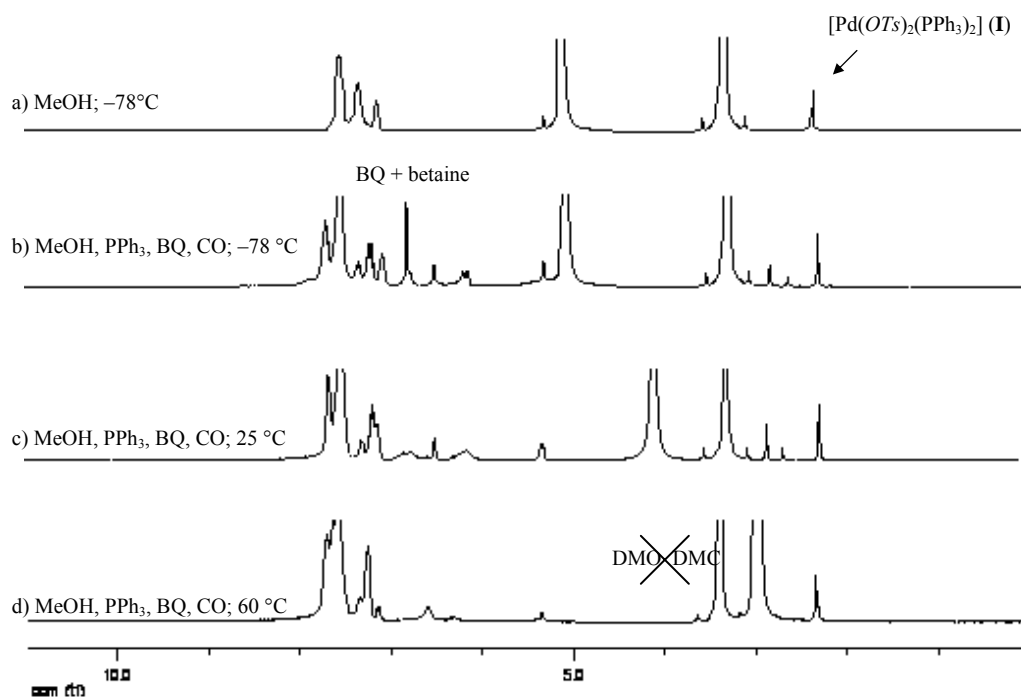


Figure 3. Selected $^{31}\text{P}\{^1\text{H}\}$ and ^1H NMR spectra in CD_2Cl_2 of the reactivity of **I** in system 1.2.

In another experiment (Table 1, system 1.3; Figure 1.), **I** was allowed first to react with PPh_3 (1/1) in CD_2Cl_2 . At -78°C there is formation of $[\text{Pd}(\text{OTs})(\text{PPh}_3)_3](\text{OTs})$. Upon admission of CO (4 atm) at the same temperature, new signals appear, indicating that CO interacts with this complex. These new species were not identified. Then MeOH was added give rise to a new carbomethoxy complex having three coordinated PPh_3 ligands $[\text{Pd}(\text{COOMe})(\text{PPh}_3)_3](\text{TsO})$ already at -78°C (*cf.* Experimental). The $^{31}\text{P}\{^1\text{H}\}$ NMR spectrum of this complex shows two signals, one at 19.9 ppm (doublet, 2P) and the other at 15.7 ppm (triplet, 1P), both arising from the AX_2 spin system ($J_{\text{P-P}} = 39.2$ Hz).

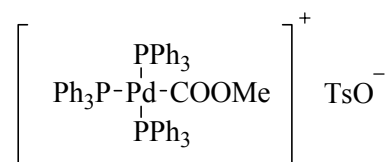
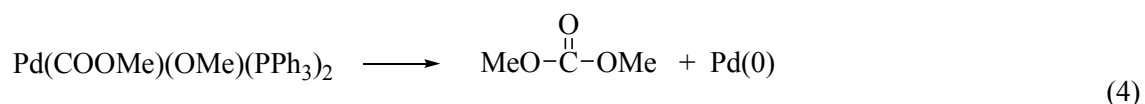


Figure 5. Complex formed in the system 1.3.

Only by subsequent addition of NEt_3 ($\text{Pd/N} = 1/8$) the $[\text{Pd}(\text{COOMe})(\text{PPh}_3)_3](\text{TsO})$ reacts with CO and MeOH to give $\text{trans-}[\text{Pd}(\text{COOMe})_2(\text{PPh}_3)_2]$ and PPh_3 . Above $40\text{ }^\circ\text{C}$ this complex begins to be unstable and decomposes to $[\text{Pd}(\text{CO})(\text{PPh}_3)_3]$,¹¹ OPPh_3 and $\text{trans-}[\text{Pd}(\text{COOMe})(\text{OMe})(\text{PPh}_3)]$ ($^{31}\text{P}\{^1\text{H}\}$ NMR at 20.3 ppm). The assignment of this last complex is based on the facts that *i*) the same ^{31}P signal has been observed in the decomposition of **III** complexes in CD_2Cl_2 (*cf.* system 3.2) and in this case the signal of the Pd-OMe moiety of the supposed $\text{trans-}[\text{Pd}(\text{COOMe})(\text{OMe})(\text{PPh}_3)]$ complex is visible at 3.25 ppm as triplet*¹² and *ii*) at $60\text{ }^\circ\text{C}$ decomposition is accompanied by the formation of DMO and DMC , 15% each, the latter is likely to form from a carbomethoxy-methoxy species of the type $\text{trans-}[\text{Pd}(\text{COOMe})(\text{OMe})(\text{PPh}_3)_2]$ *via* an intramolecular migratory nucleophilic attack of the coordinated methoxide at the carbomethoxy group (4).¹³



* Pd-OMe complexes of the type $\text{trans-}[\text{Pd}(\text{OMe})(\text{R})(\text{PPh}_3)_2]$ ($\text{R} = \text{C}_6\text{F}_5, \text{CCl}=\text{CCl}_2$) shows ^1H signal as a triplet at 3.08 and 2.78 ppm respectively for the MeO ligand coordinated to palladium.

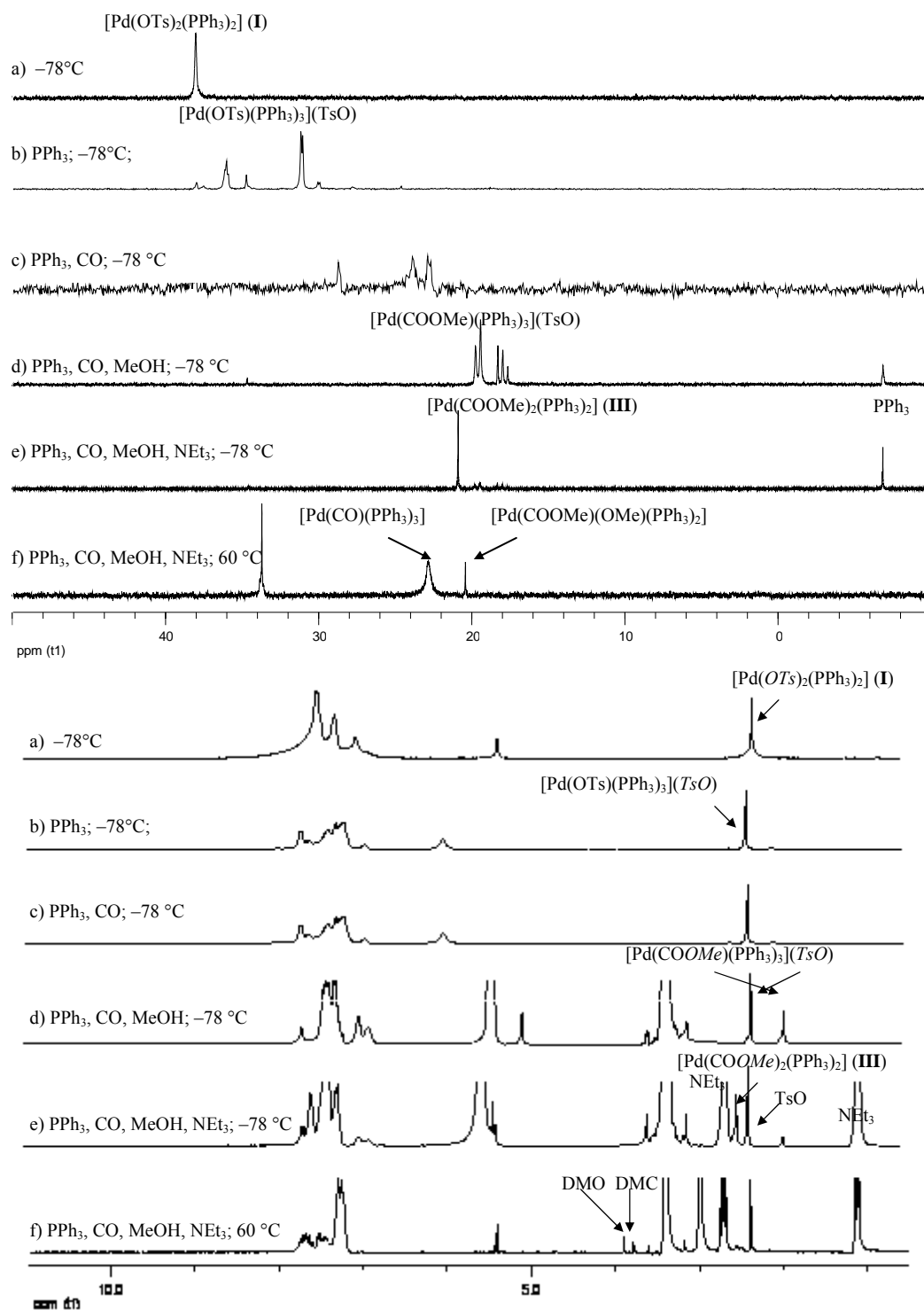
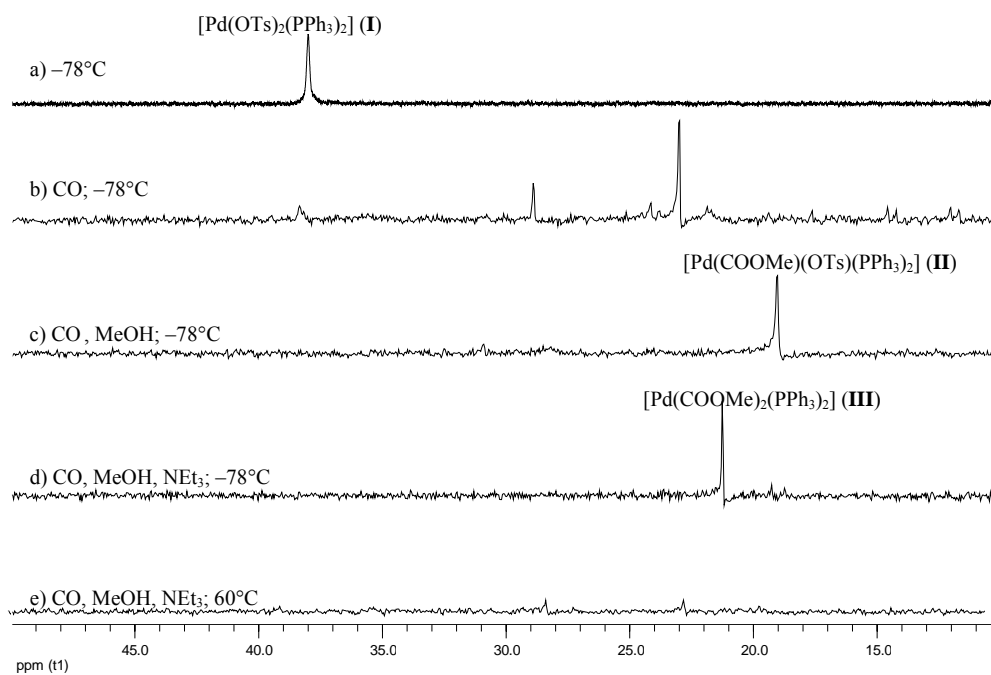


Figure 4. Selected $^{31}\text{P}\{^1\text{H}\}$ and ^1H NMR spectra in CD_2Cl_2 of the reactivity of **I** in system 1.3.

Following the procedure just above reported, **III** is formed from **I** also in the absence of added PPh₃ (Table 1, system 1.4; Figure 6). **I** in CD₂Cl₂ at -78 °C reacts with CO (4 atm) giving a new unidentified species (³¹P{¹H} NMR at 23.01 ppm), whose value suggests that it is related to a species having *trans*-geometry (*cfr.* Chapter 2). At -78 °C upon addition of MeOH (10% with respect to CD₂Cl₂), **II** is formed immediately. At the same temperature only upon addition of NEt₃ (Pd/N = 1/10) **III** is formed. Above 40 °C the dicarbomethoxy complex begins to be unstable, at 60 °C decomposition to palladium metal is evident, accompanied with the formation of DMO and DMC in approximately equal amount, 15 % of each one.



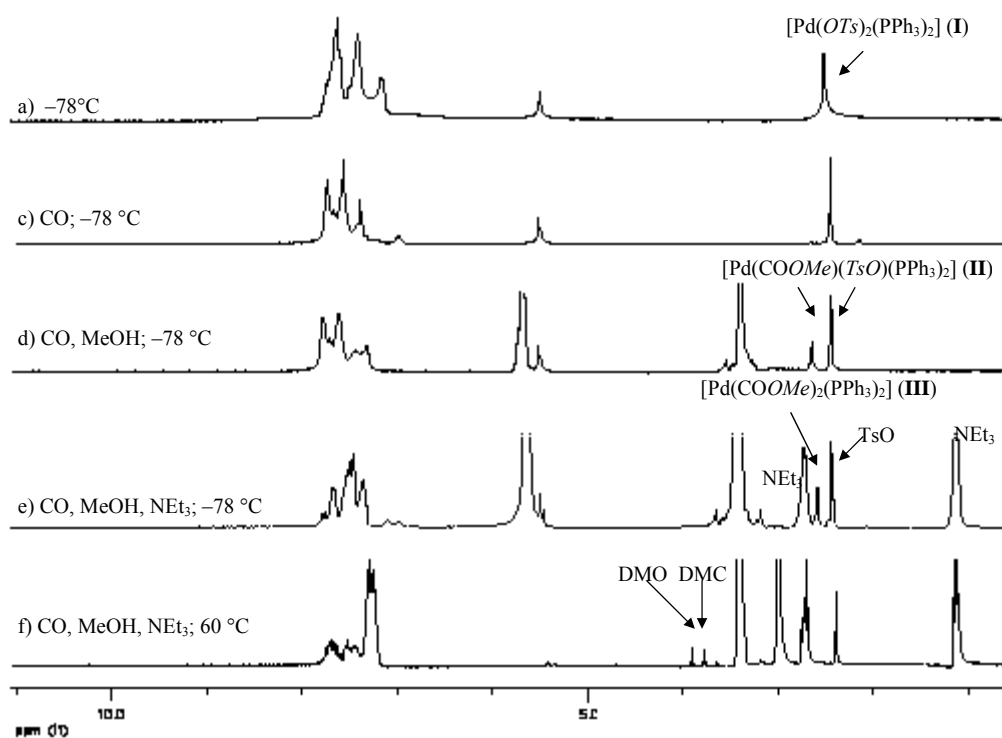


Figure 6. Selected $^{31}\text{P}\{^1\text{H}\}$ and ^1H NMR spectra in CD_2Cl_2 of the reactivity of **I** in system 1.4.

In another experiment (Table 1, system 1.5) **I** and BQ were dissolved in CD_3OD and then carbon monoxide was admitted at 25 °C. There was immediate formation of the monocarbonyl complex (**II**), converted to $[\text{Pd}(\text{BQ})(\text{PPh}_3)_2]$ by subsequent addition of NEt_3 (Figure 7). No change was observed at 50 °C. Probably, in this case after addition of NEt_3 **II** is converted in the di-carbonyl **III**, which reacts with BQ giving immediately DMO-D_6 (which is not relievable by NMR) and $[\text{Pd}(\text{BQ})(\text{PPh}_3)_2]$. The comparison of this experiment (system 1.5) with the experiment just above reported (system 1.4) suggests that the reactivity of the complex **III** formed *in situ* could be strongly influenced by both the presence/or absence of BQ and the solvent used, pure CD_3OD in one case and the mixture $\text{CD}_2\text{Cl}_2/\text{MeOH}$ (MeOH 10% v) in the other.

However, it has been demonstrated that *i)* **II** may form from **I** also when in presence of BQ and *ii)* the formation of $[\text{Pd}(\text{BQ})(\text{PPh}_3)_2]$ (and probably the catalysis *via* intermediate **III**) occurs only if the base is added.

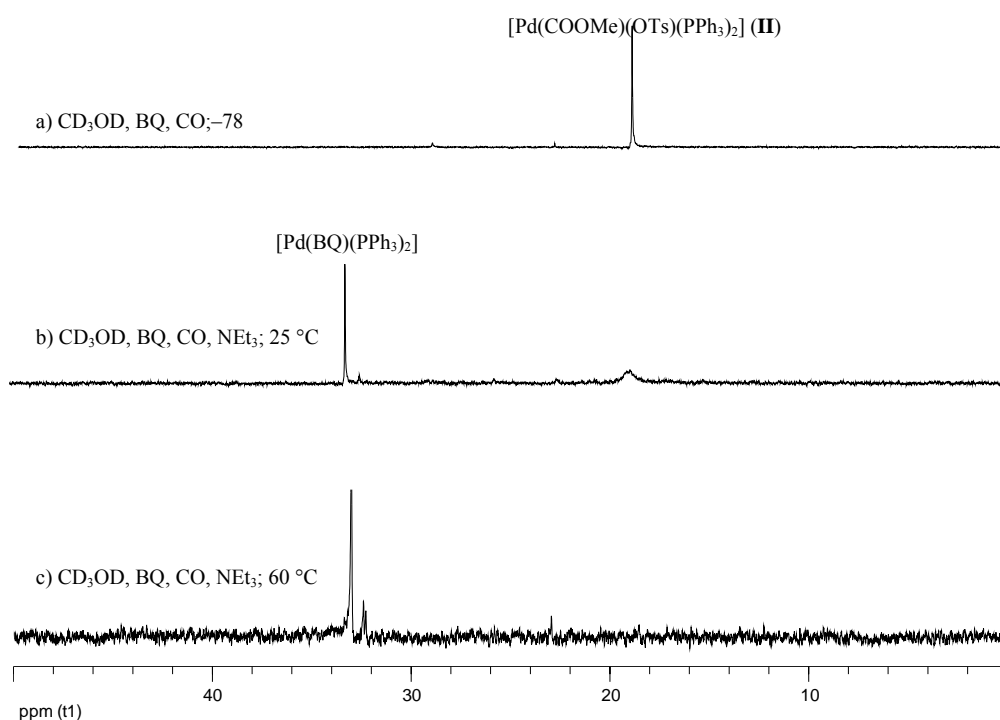
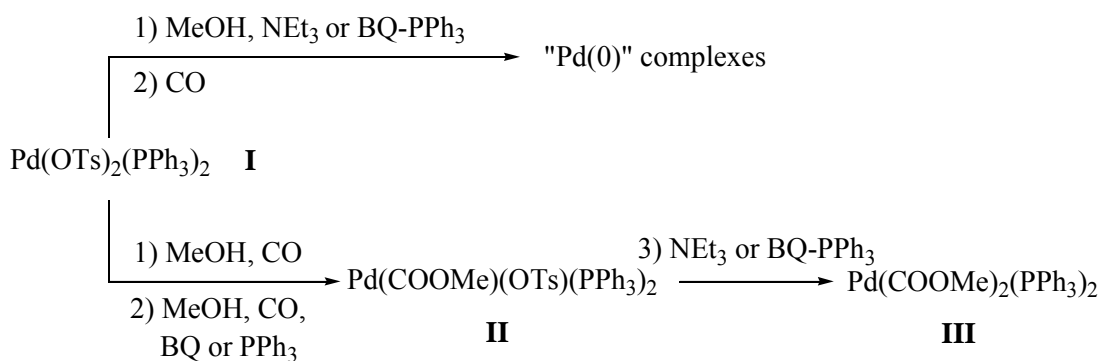


Figure 7. Selected $^{31}\text{P}\{^1\text{H}\}$ and ^1H NMR spectra in CD_3OD of the reactivity of **I** in system 1.5.

The reactivity of **I** with carbon monoxide and methanol can be summarised as follows:

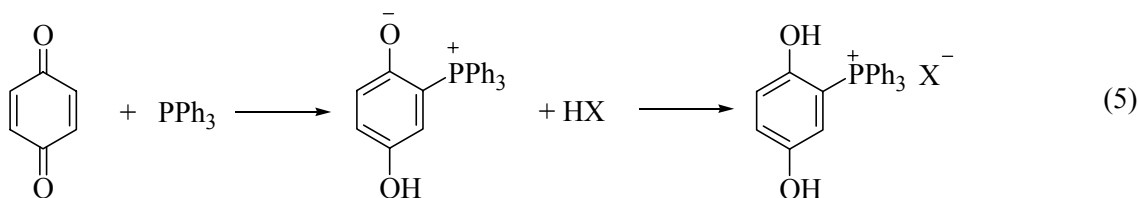
- i) When NEt_3 or BQ-PPh_3 are present before admission of carbon monoxide, $\text{Pd}(0)$ is formed without formation of any carbomethoxy complex (system 1.1, 1.2).
- ii) **II** is formed even when BQ only or PPh_3 only are present before admission of carbon monoxide (system 1.3, 1.4, 1.5).
- iii) **III** is formed only after the monocarboxy complex *trans*- $[\text{Pd}(\text{COOMe})(\text{OTs})(\text{PPh}_3)_2]$ is formed and only upon successive addition of NEt_3 (system 1.3, 1.4).
- iv) **III** is formed from **II** also when BQ-PPh_3 is added.

These results can be so schematized:



Scheme 1. Simplified scheme on the reactivity of **I**.

A reasonable explanation of these results may be the following. It is likely that, because of unavoidable presence of water, carbon monoxide reduces Pd(II) to Pd(0) before it interacts with MeOH to give a carbomethoxy species. The carbon monoxide–water interaction may lead to a Pd(II)–hydride species, which is deprotonated to Pd(0) by the base NEt₃. The couple BQ–PPh₃ yields betaine, which can also act as a base because of the presence of an Ar–O– moiety. In support of its basicity it was reported that betaine reacts with HX giving the corresponding phosphonium salt (5):⁷



However, it should be noticed that the NMR experiments were carried out with MeOH diluted in CH₂Cl₂. We have found that in MeOH with dissolved NEt₃ (Pd/N = 1/8), in the absence of CD₂Cl₂, **I** reacts with carbon monoxide (2 atm) at 0 °C to give [Pd(CO)(PPh₃)₃] together with both the mono– **II** and the di–carbomethoxy **III** complexes (Table 1, system 1.6). When using 0.1 mmol of the complex in 2 mL of MeOH the solution at 0 °C, initially light brown, turns orange–red in a few minutes and at the same time a precipitate is formed. After 20' the solution was analyzed by GC: no DMO or DMC was detected. The NMR and IR spectra of

the solid (A) (40 mg) recovered after filtration show the presence of $[\text{Pd}(\text{CO})(\text{PPh}_3)_3]$ and of **III** (Figure 8 and Figure 9). Upon adding cold water to the filtrate a white solid (B) precipitated (8 mg), that was identified as **II** (Figure 10, Figure 11). These results show that in MeOH the carbomethoxy complexes are formed even when NEt_3 is present before the admission of carbon monoxide, at difference of what observed in a NMR tube in which MeOH is diluted with CD_2Cl_2 . Thus the concentration of MeOH (and probably also the polarity of the medium) plays an important role in directing the reactivity.

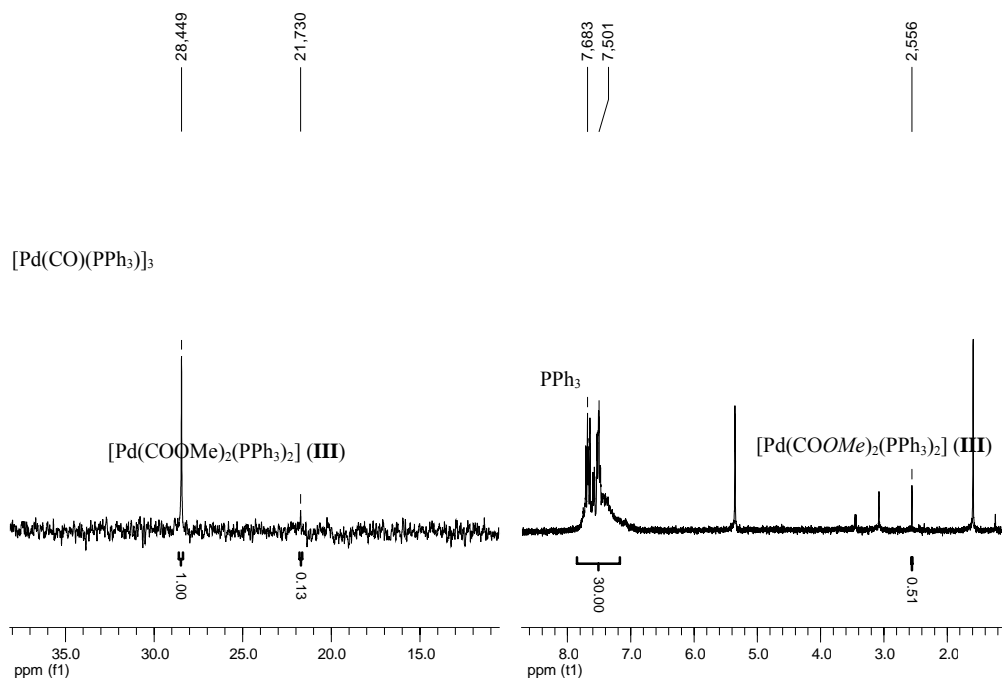


Figure 8. $^{31}\text{P}\{^1\text{H}\}$ and ^1H spectra in CD_2Cl_2 at 25°C of the solid A formed in system 1.6.

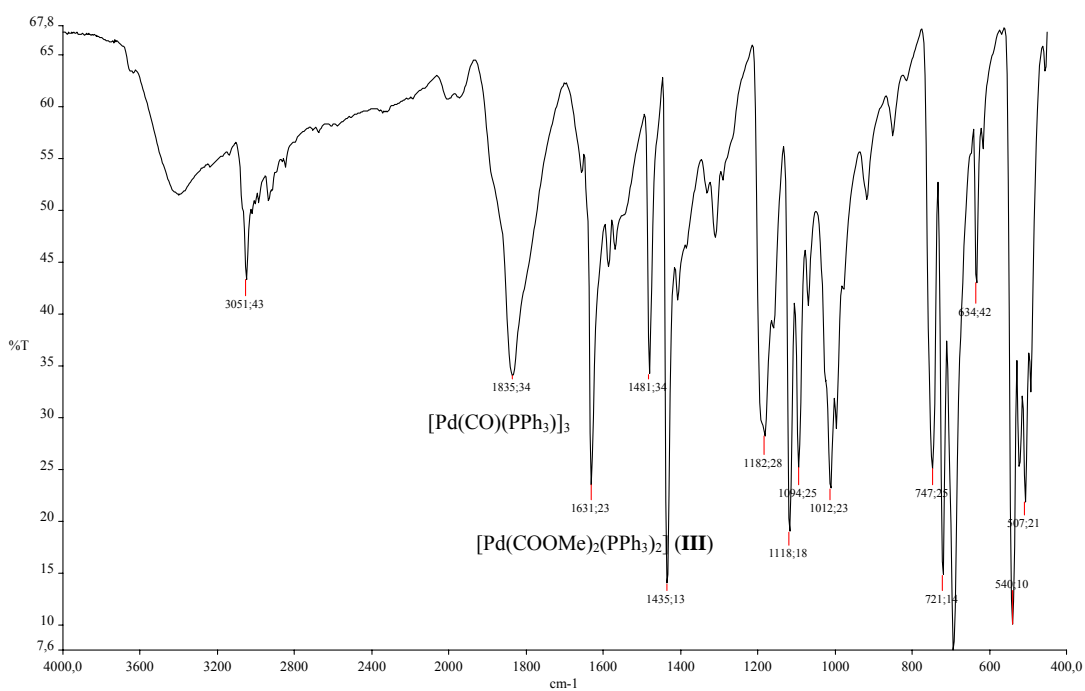


Figure 9. IR spectra in KBr of the solid A formed in system 1.6.

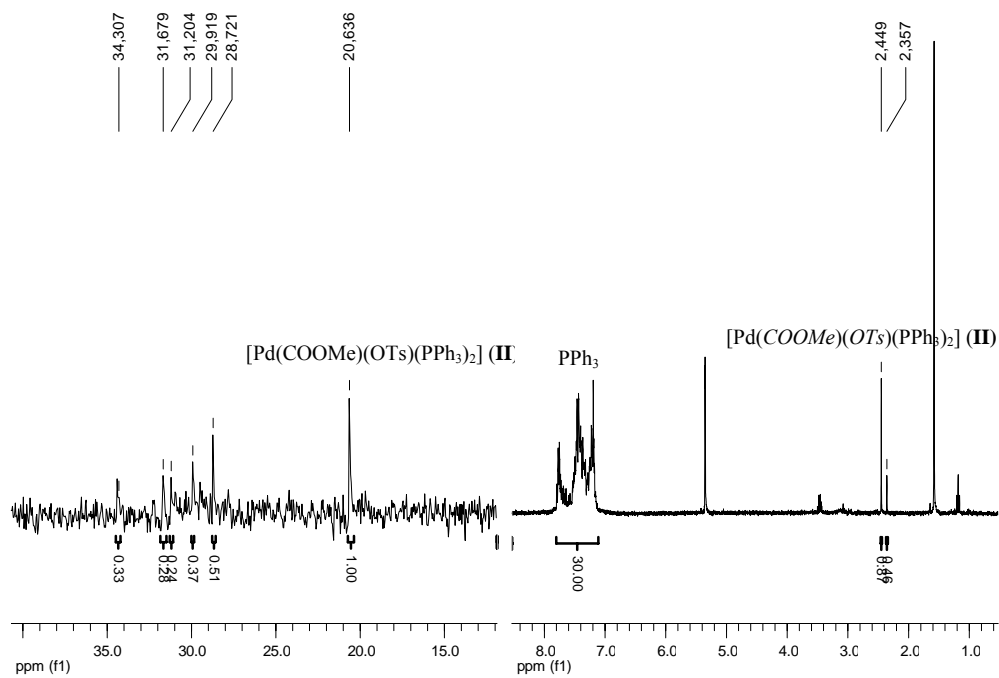


Figure 10. ³¹P{¹H} and ¹H spectra in CD₂Cl₂ at 25 °C of the solid B formed in system 1.6.

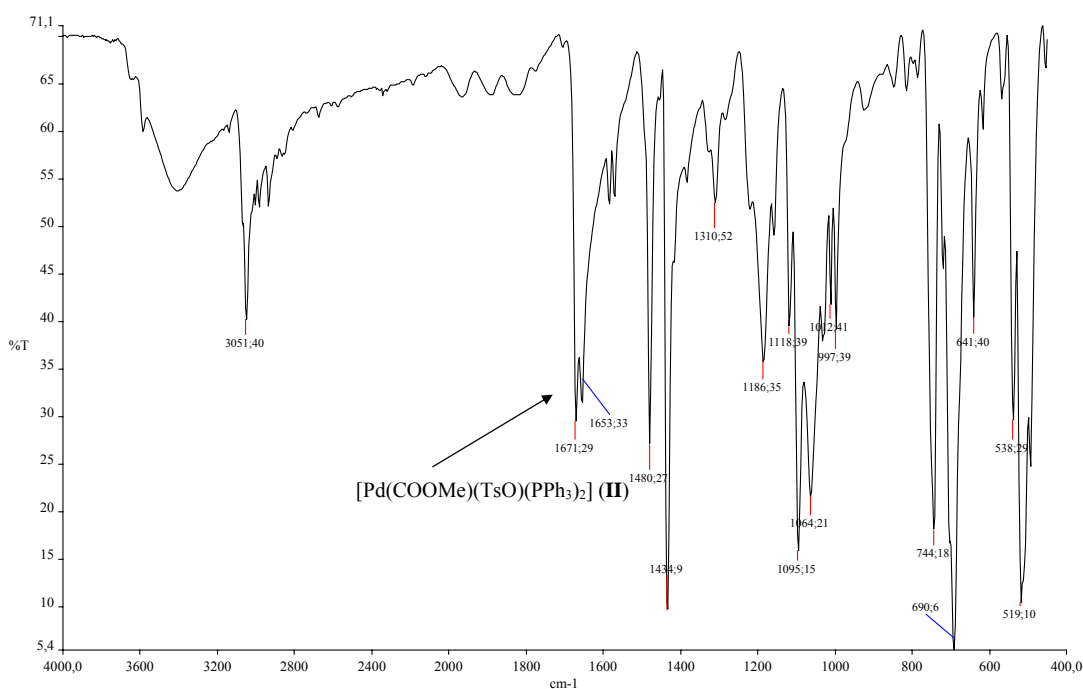


Figure 11. IR spectra in KBr of the solid B formed in system 1.6.

Reactivity of II. In the HP-NMR tube at $-78\text{ }^{\circ}\text{C}$, **II** was dissolved first in $\text{CD}_2\text{Cl}_2/\text{MeOH}$ (10% MeOH v/v), then PPh_3 was added ($\text{Pd}/\text{PPh}_3_{\text{added}} = 1/1$) and then CO was admitted (4 atm) (Table 1, system 2.1). As shown in Figure 12, **II** reacts with PPh_3 to give $[\text{Pd}(\text{COOMe})(\text{PPh}_3)_3](\text{TsO})$ even at $-78\text{ }^{\circ}\text{C}$. Only upon subsequent addition of NEt_3 ($\text{Pd}/\text{NEt}_3 = 1/8$) further reactions occur: a PPh_3 ligand is displaced from the coordination of Pd(II) and carbon monoxide and methanol interacts giving **III**. This complex is stable in solution up to $25\text{ }^{\circ}\text{C}$, but at $40\text{ }^{\circ}\text{C}$ (better at $60\text{ }^{\circ}\text{C}$) it decomposes with formation of *ca.* 15 % of both DMO and DMC, accompanied with formation of *trans*- $[\text{Pd}(\text{COOMe})(\text{OMe})(\text{PPh}_3)_2]$ and $[\text{Pd}(\text{CO})(\text{PPh}_3)_3]$.

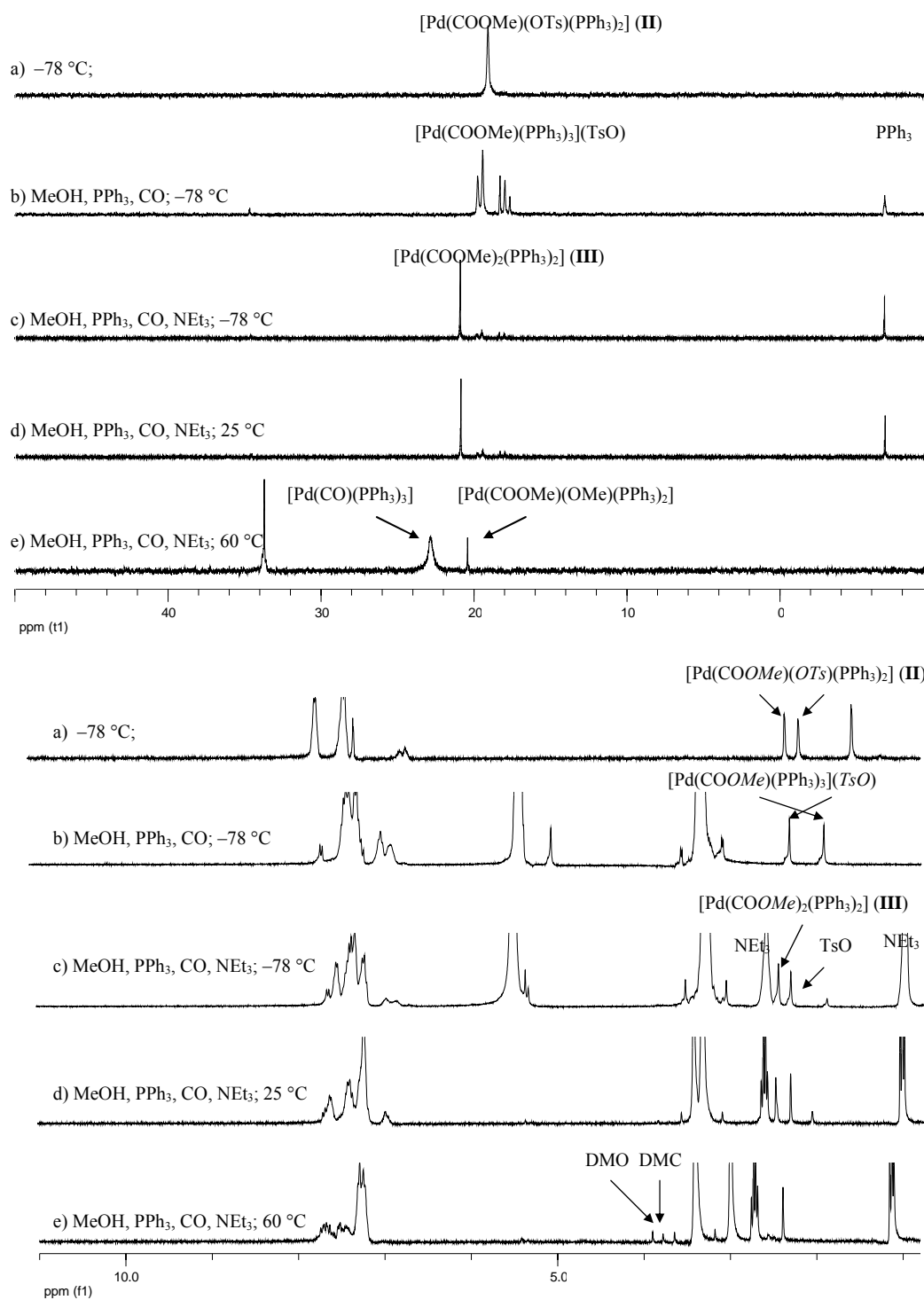
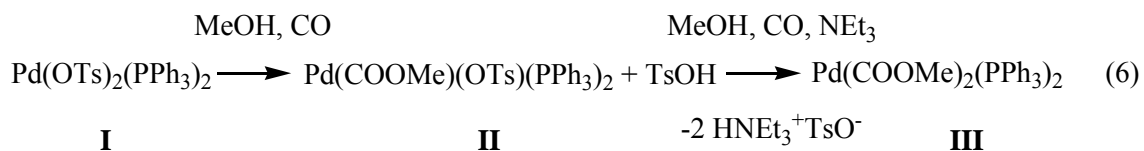


Figure 12. Selected $^{31}\text{P}\{^1\text{H}\}$ and ^1H NMR spectra in CD_2Cl_2 of the reactivity of **II** in system 2.1.

Thus, starting from both **I** or **II** the dicarbomethoxy complex **III** is formed only after the addition of NEt_3 (*cf.* system 1.3, 1.4, 2.1). The main difference is that when the

monocarboxy complex **II** is formed from **I** one equivalent of TsOH is also formed, so that one equivalent of acid is present before the addition of the base:



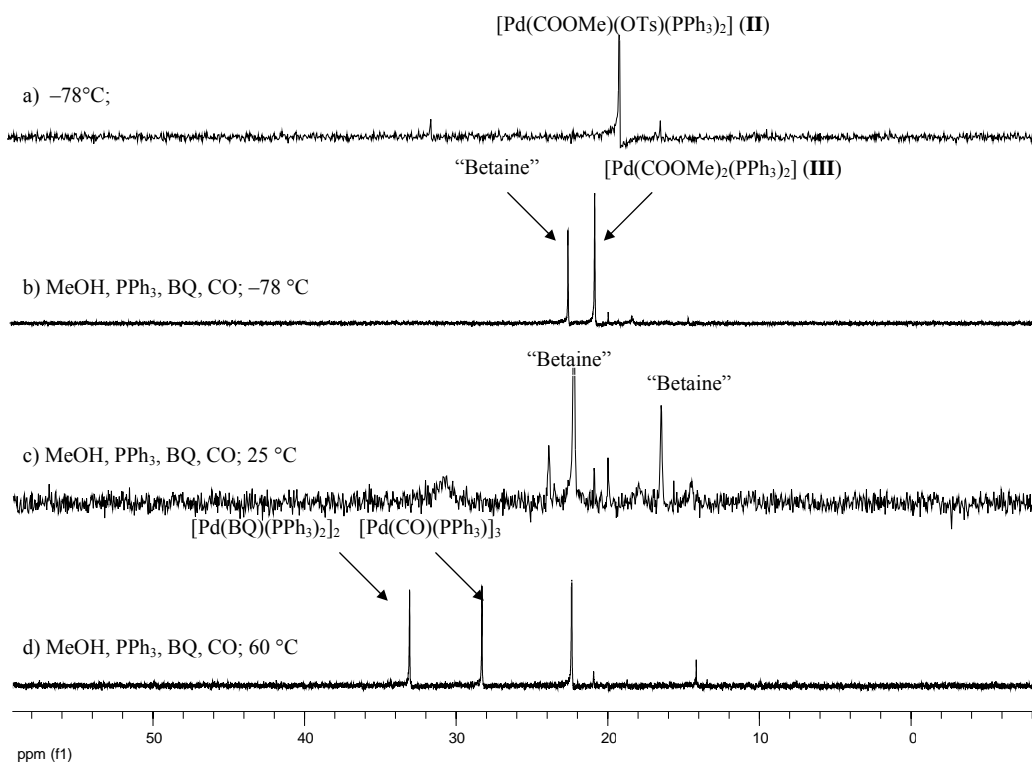
When in absence of base the acid prevents the formation of the dicarboxy complex. As a matter of fact the dicarboxy complex in the presence of one equivalent of acid is unstable and gives the monocarbomethoxy one as below reported (system 3.1).

The reactivity of **II** has been studied also with BQ under conditions closer to those of catalysis (Table 1, system 2.2). In the HP-NMR tube **II** was first dissolved in CD₂Cl₂/MeOH (10% MeOH v/v), then PPh₃ and BQ were added (**II**/PPh_{3 added}/BQ = 1/1/10) and then CO was admitted (4 atm). All operations were carried out at -78 °C. As shown in Figure 13, **II** reacts immediately with CO and MeOH to give the dicarbomethoxy complex **III**. It is interesting to point out that starting from **I** and BQ there is the formation of the monocarbomethoxy **II** complex only, without formation of the dicarbomethoxy **III** one (*cf.* system 1.5). This observation suggests that BQ does not act as a base. Since in the presence of PPh₃ the monocarbomethoxy complex coordinates the ligand giving [Pd(COOMe)(PPh₃)₃](OTs), again without formation of any dicarbomethoxy complex (*cf.* system 1.3), it follows that is the couple BQ-PPh₃ that acts as a base. This gives further support to the suggestion that “betaine”, the BQ-PPh₃ adduct, can act as a base.

III is stable in solution up to 25 °C, temperature at which it starts decomposing giving 20 % of DMO. Only upon increasing the temperature up to 60 °C there is formation of [Pd(BQ)(PPh₃)₂], [Pd(CO)(PPh₃)₃] and of *ca.* 1,5 equivalent of DMO, an amount larger than of the starting complex. Thus for the first time we observed catalysis. The catalytic activity is not

so high, but in any case is significant considering that in the absence of BQ, DMO is formed in 15 % yield with respect to **III** (*cf.* system 2.1).

The same results have been obtained also using a larger amount of free ligand (Table 1, system 2.3; Pd/PPh₃ added = 1/6). In both cases in fact, added PPh₃ does not interact with the complexes, but rather it reacts immediately with BQ forming the 1/1 “betaine” adduct.



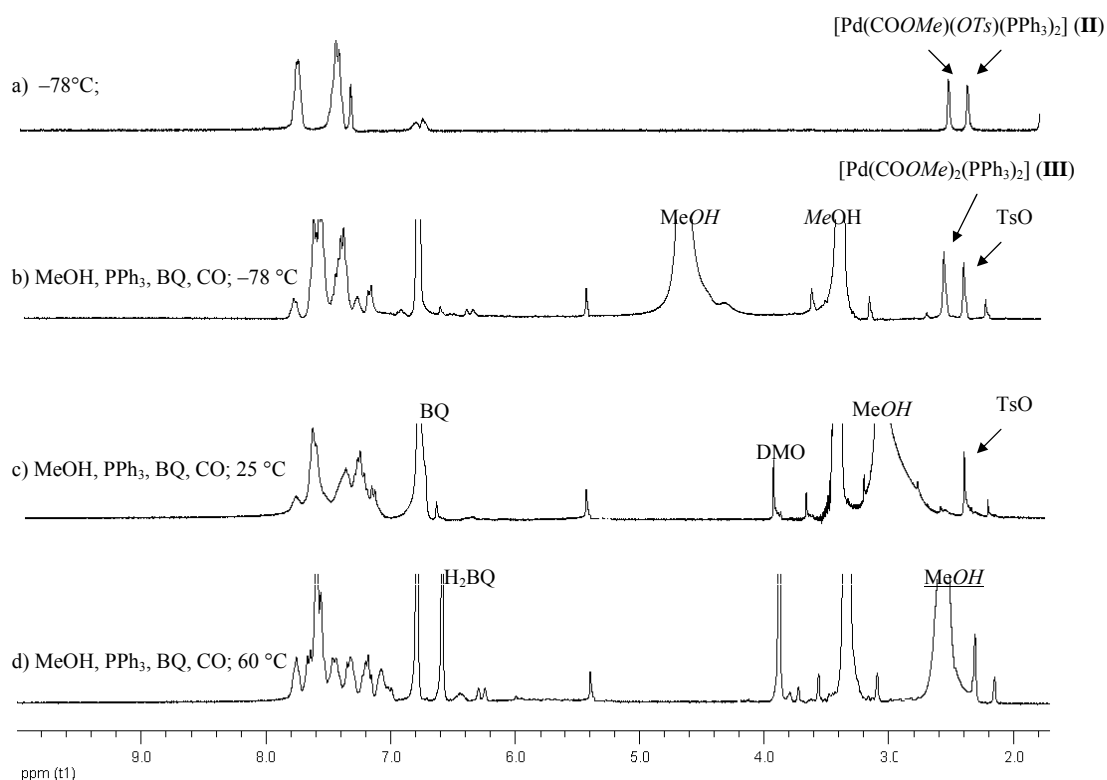


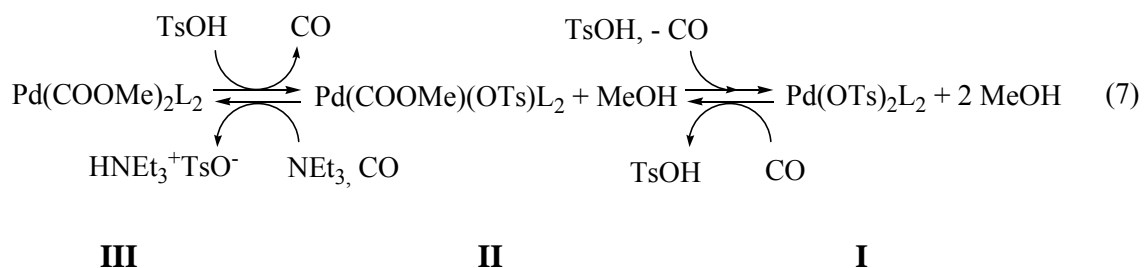
Figure 13. Selected $^{31}\text{P}\{^1\text{H}\}$ and ^1H NMR spectra in CD_2Cl_2 of the reactivity of **II** in system 2.2.

The reactivity of **II** with carbon monoxide and methanol can be summarised as follows:

- i) The dicarbomethoxy complex **III** is formed only when the monocarboxy complex **II** is in presence of a base (NEt_3 or the BQ-PPh_3 adduct) (*cfr.* systems 2.1, 2.2, 2.3).
- ii) Only in the presence of BQ (*cfr.* systems 2.2 and 2.3) DMO is formed from **III** already at 25°C , together with $\text{Pd}(0)$ complexes $[\text{Pd}(\text{CO})(\text{PPh}_3)_3]$ and $[\text{Pd}(\text{BQ})(\text{PPh}_3)_2]$, and without any formation of DMC . At 60°C catalysis occurs. In the absence of BQ (*cfr.* system 2.1) **III** is unstable at 40°C with formation of DMO , DMC , $\text{trans-}[\text{Pd}(\text{COOMe})(\text{OMe})(\text{PPh}_3)_2]$ and $[\text{Pd}(\text{CO})(\text{PPh}_3)_3]$.

From these evidences it is possible to sustain that the presence of BQ modifies the reactivity of the system and in particular the reactivity of **III** toward the formation of oxalate.

Reactivity of III. As above reported for the formation of **III** from both **I** and **II** it is required the addition of base, which role is subtracting the acid that is formed. The acid might be the cause of the instability of the dicarbomethoxy complex. Indeed, when TsOH is added to **III** (Pd/S= 1/1) in CD₂Cl₂/MeOH (10 % MeOH v/v) under 4 atm of CO at -78 °C (Table 1, system 3.1), the formation of **II** is observed (Figure 14). **II** is stable up to 50 °C even in the absence of CO. By addition of one more equivalent of TsOH (Pd/S_{tot} = 1/2), **II** is stable, under pressure of CO, from -78 °C up to 50 °C. However, at 50 °C by replacing of CO with argon a slow conversion to **I** takes place. Considering that **I** in MeOH and CO gives **II**, which is converted to **III** upon addition of NEt₃, the following equilibria may establish in solution:



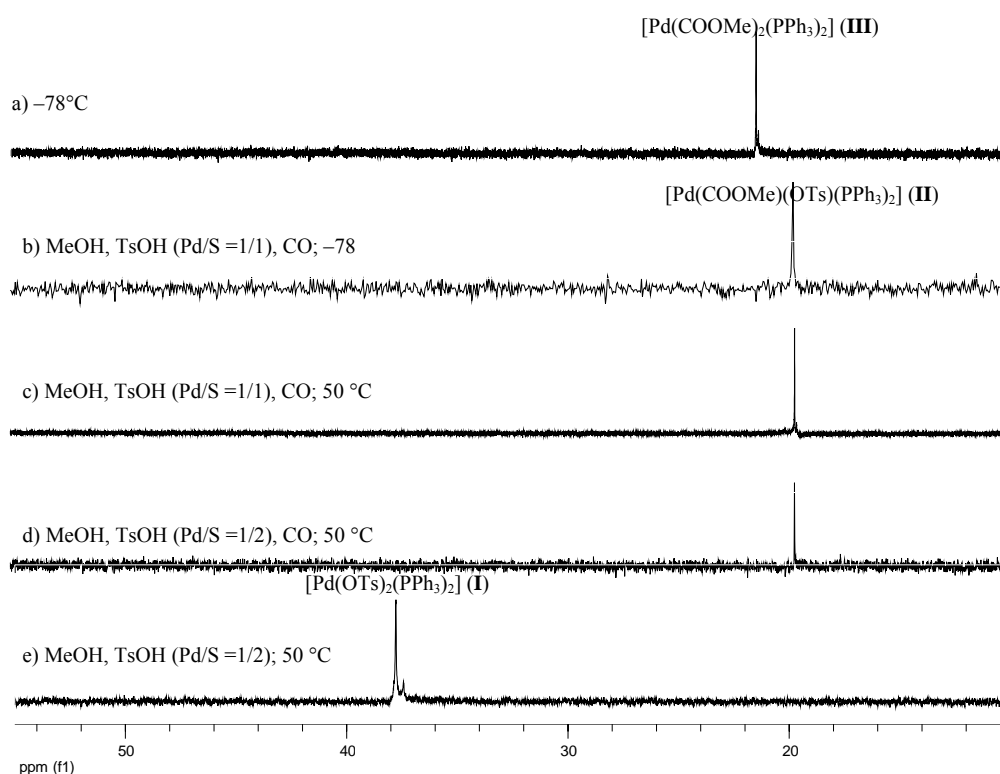


Figure 14. Selected $^{31}\text{P}\{^1\text{H}\}$ and ^1H NMR spectra in CD_2Cl_2 of the reactivity of **III** in system 3.1.

III is likely to be involved in the product-forming step. Therefore, the study of its stability and reactivity is of paramount importance.

In the HP-NMR tube **III** was dissolved in CD_2Cl_2 and then the solution was pressurized with 3 atm of Ar (Table 1, system 3.2). As reported in Figure 15 the complex is stable from -78 °C up to 40 °C, temperature at which partial decarbonylation of one Pd-COOMe moiety occurs giving rise to a complex already observed in the system 1.3 which has been tentatively formulated as *trans*- $[\text{Pd}(\text{COOMe})(\text{OCH}_3)(\text{PPh}_3)_2]$. There is concomitant formation *ca.* 10 % of DMC. Complete decomposition of both carbomethoxy complexes with formation of Pd metal occurs at 60 °C, however without formation of additional carbonylated products. No formaldehyde,⁸ that could form from Pd-OMe decomposition *via* β -H elimination,⁹ nor its

derivatives (methyl hemi-formal and di-formal, formal oligomers, methyl formate, 4-hydroxyphenyl formate, pitches)⁹ have been detected.

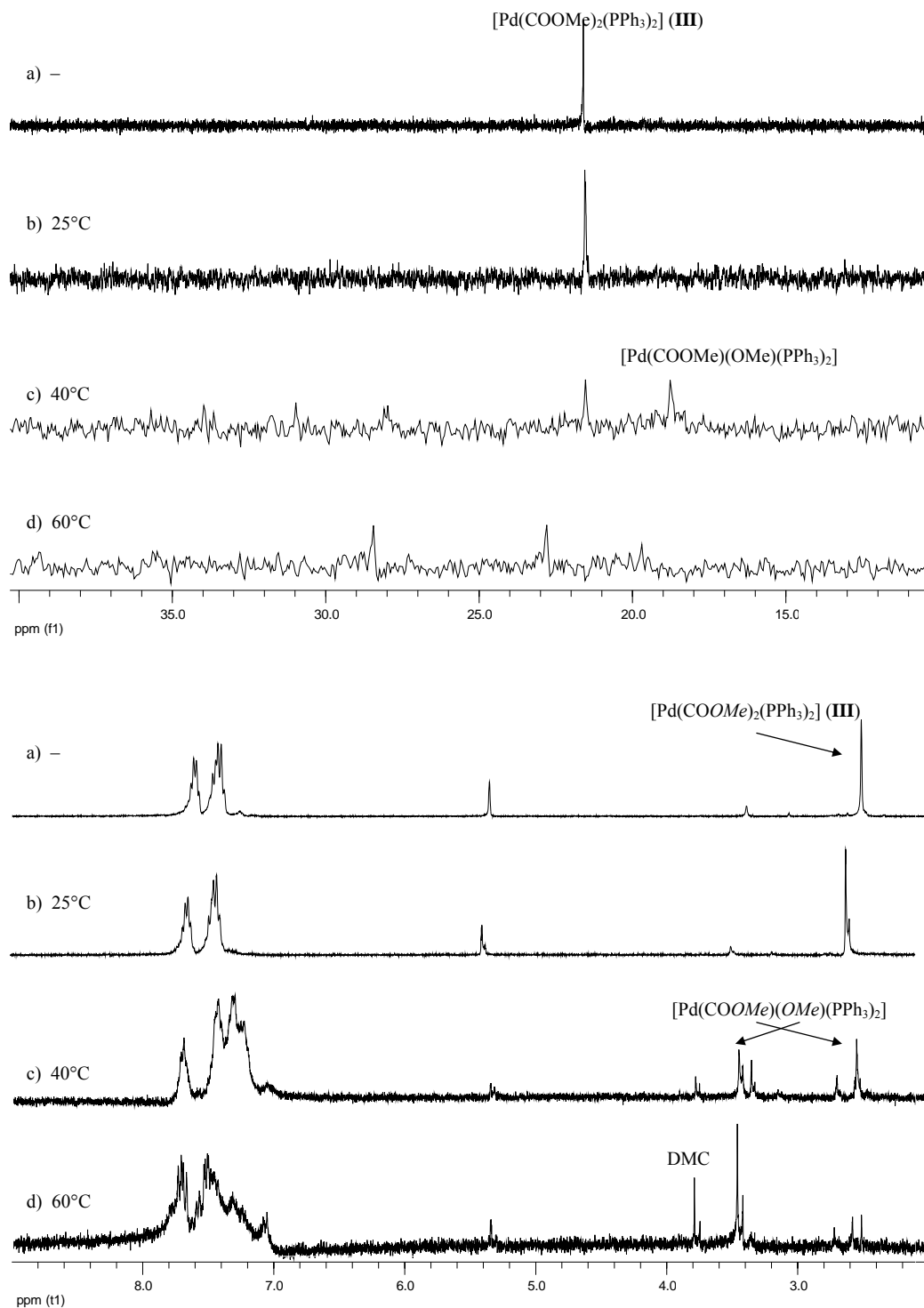
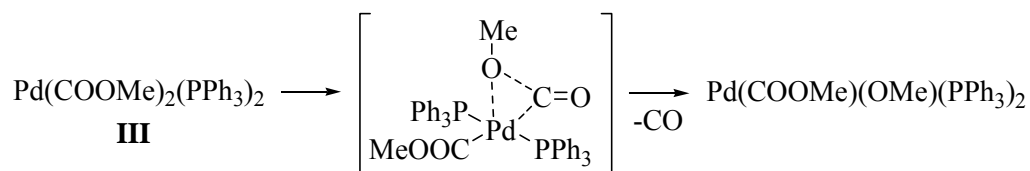


Figure 15. Selected $^{31}\text{P}\{^1\text{H}\}$ and ^1H NMR spectra in CD_2Cl_2 of the reactivity of **III** in system 3.2.

Concerning the identification of $[\text{Pd}(\text{COOMe})(\text{OMe})(\text{PPh}_3)_2]$ complex it has been observed that i) the conversion occurs with decreasing of the intensity of the signal to Pd–COOMe moiety at 2.52 ppm from the ratio $\text{H}(\text{PPh}_3)/\text{H}(\text{COOCH}_3)$ of 30/6 in **III** to 30/3 due to the formation of $[\text{Pd}(\text{COOMe})(\text{Y})(\text{PPh}_3)_2]$; ii) a new broad ^1H signal appears at *ca.* 3.25 ppm close to that of the Pd–OMe moiety for similar *trans* monophosphine complexes;¹² iii) the position of the $^{31}\text{P}\{^1\text{H}\}$ signal at *ca.* 19 ppm, close to that of *trans*- $[\text{Pd}(\text{COOMe})(\text{X})(\text{PPh}_3)_2]$ (X = Cl, ONO_2 , ONO, OTs) (Chapters 1, 2, and ref. 1) suggests that this complex has a *trans* geometry. $[\text{Pd}(\text{COOMe})(\text{OMe})(\text{PPh}_3)_2]$ is formed probably *via* intermolecular deinsertion of CO involving the fifth coordination site of Pd(II).



Scheme 2. Putative pathway of formation of $[\text{Pd}(\text{COOMe})(\text{OMe})(\text{PPh}_3)_2]$ from **III**.

This hypothesis was supported by repeating the experiment in presence of PPh_3 ($\text{Pd}/\text{PPh}_3 \text{ added} = 1/2$; Table 1, system 3.3). As shown in Figure 16, **III** is stable from $-78\text{ }^\circ\text{C}$ up to $60\text{ }^\circ\text{C}$, temperature at which slowly it decomposes giving *ca.* 15 % of DMC only. The $^{31}\text{P}\{^1\text{H}\}$ spectrum shows signals of OPPh_3 , $[\text{Pd}(\text{CO})(\text{PPh}_3)_3]$, and *trans*- $[\text{Pd}(\text{COOMe})(\text{OMe})(\text{PPh}_3)_2]$. No formation of palladium metal was observed.

In conclusion the presence of PPh_3 slightly stabilizes complex **III**, which decomposes only at $60\text{ }^\circ\text{C}$, whereas in absence of PPh_3 decomposition occurs at $40\text{ }^\circ\text{C}$, probably because PPh_3 competes for a coordination site with CO deinserting from the Pd–COOMe moiety.

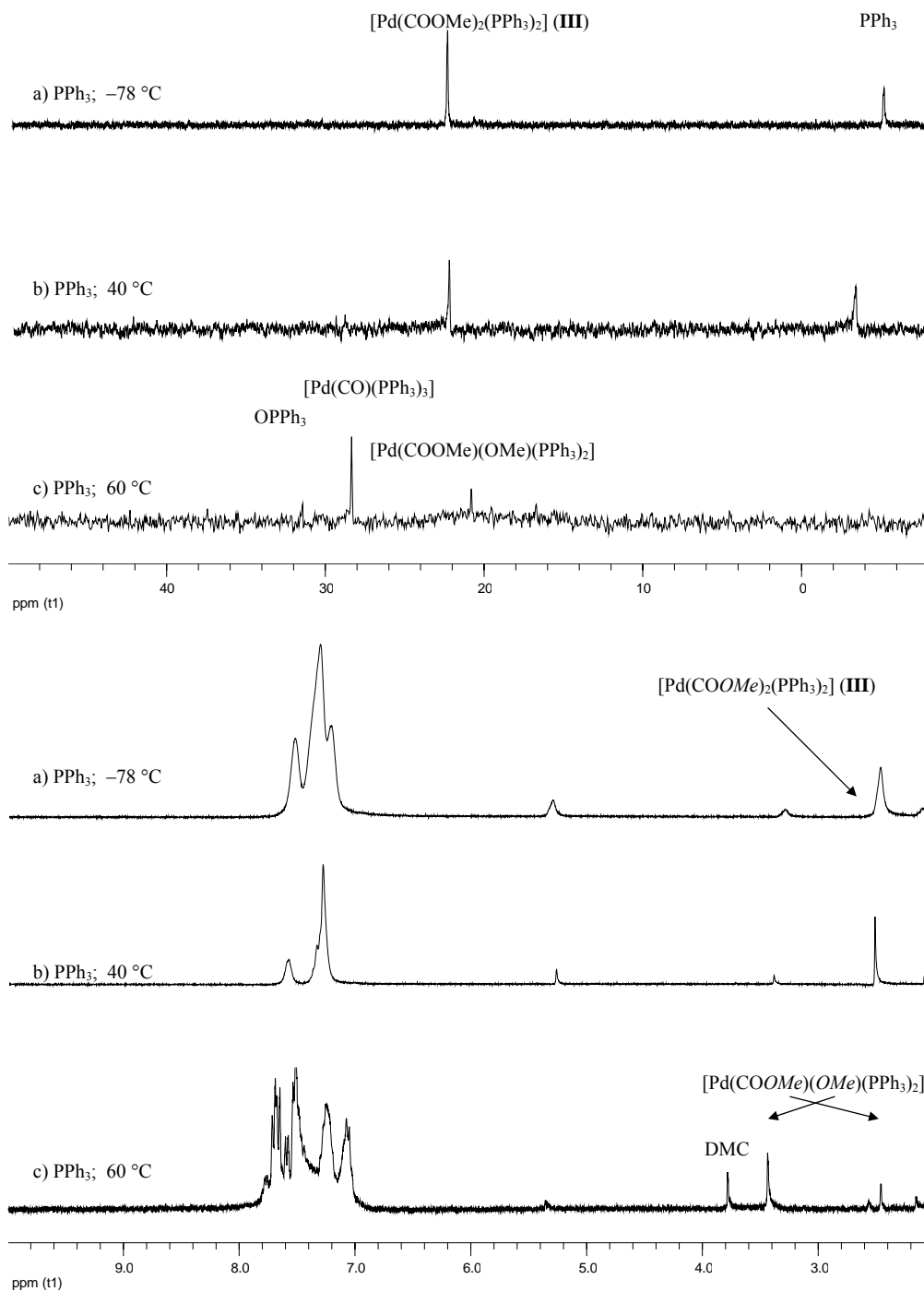
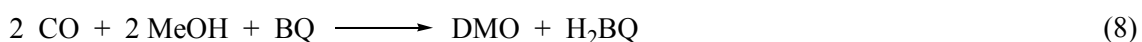


Figure 16. Selected $^{31}\text{P}\{^1\text{H}\}$ and ^1H NMR spectra in CD_2Cl_2 of the reactivity of **III** in system 3.3.

In another experiment (Table 1, system 3.4), the stability of **III** has been tested under 4 atm of CO starting from $-78\text{ }^\circ\text{C}$. **III** is relatively stable, but at $40\text{ }^\circ\text{C}$ it gives DMC and DMO,

ca. 10 % of each, and *trans*-[Pd(COOMe)(OMe)(PPh₃)₂]. At 60 °C the dicarboalcoxy species is completely converted to the monocarboxy one, which does not decompose.

The reactivity of **III** has been studied also with BQ under conditions similar to those of catalysis (Table 1, system 3.5). In a HP-NMR tube **III** and BQ were dissolved in the ratio Pd/BQ = 1/10 in CD₂Cl₂. The resulting solution was pressurized with 4 atm of CO. All the operations were carried out at -78 °C. As shown in Figure 17, the complex is stable in solution from -78 °C up to 25 °C, temperature at which new signals appear attributable to [Pd(BQ)(PPh₃)₂] and *trans*-[Pd(COOMe)(OMe)(PPh₃)₂]. At this temperature the formation of DMO becomes evident (ca. 10 %)*. Although DMO is formed in a lower amount than that expected from the disappearance of the starting complex, it can be said that BQ destabilises the dicarbomethoxy complex and promotes both the reductive elimination of DMO as well as the decarbonylation of one Pd-COOMe moiety. At this point, in order to observe catalysis, MeOH (10 % v with respect CD₂Cl₂) was added at -78 °C and CO was readmitted (4 atm). No change in the NMR spectra was observed from -78 °C up to 40 °C, whereas at 60 °C [Pd(BQ)(PPh₃)₂] and *trans*-[Pd(COOMe)(OMe)(PPh₃)₂] slowly disappeared with concomitant formation of DMO (ca. 1.2 TON) and of hydroquinone H₂BQ. These last two are formed in the ratio 1.2/2.5, different from expected 1/1 ratio according to reaction 8, suggesting that some oxidation of MeOH may occur. However, no ¹H signal for formaldehyde was detected. After reaction the ³¹P{¹H} spectra showed several signals that were not identified.



* Even though in the ¹H region of DMC (ca. 3.80–3.60 ppm) some signals are present, the formation of DMC could not be confirmed by addition of some DMC, which gave rise to a new signal in this region.

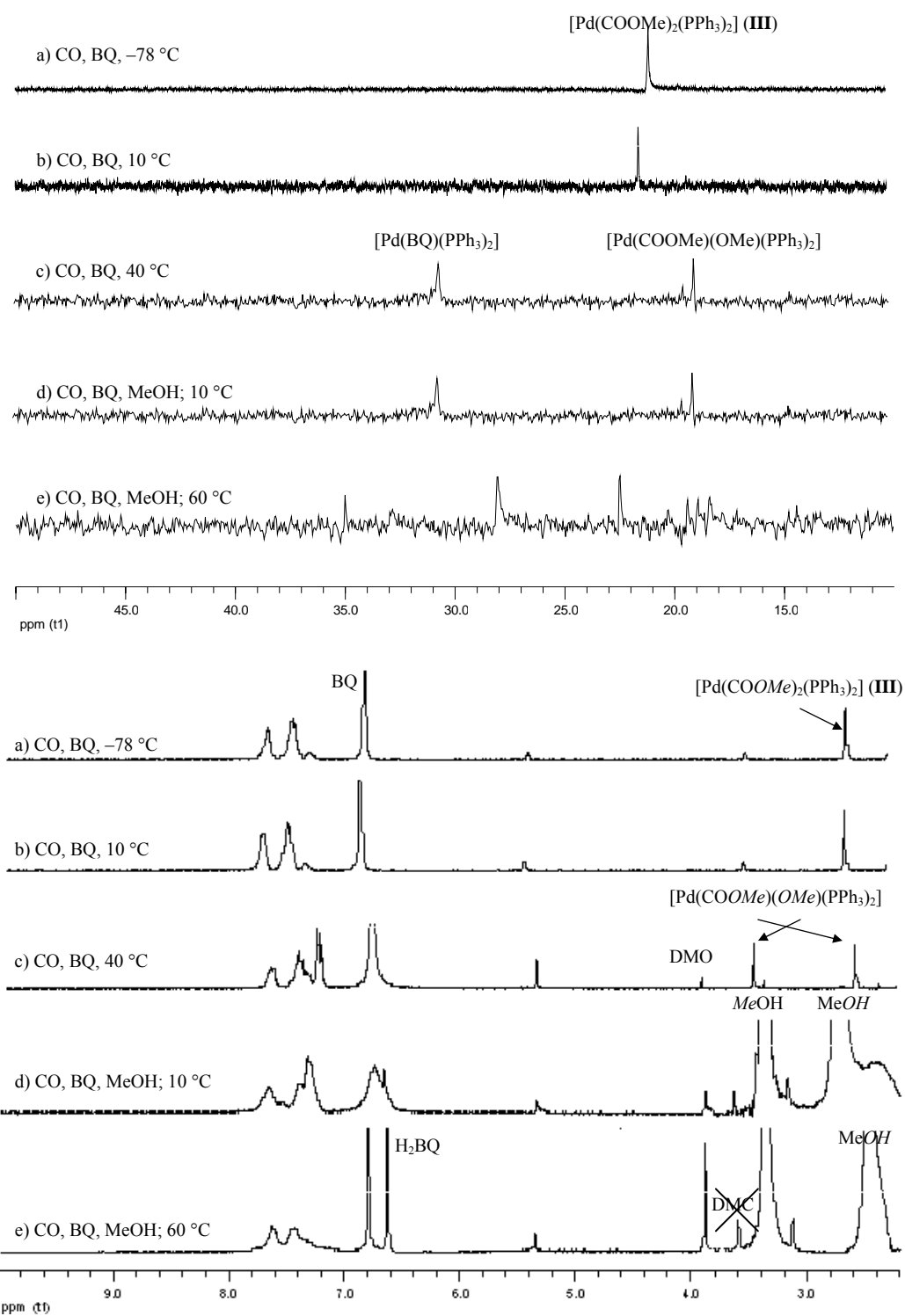


Figure 17. Selected $^{31}\text{P}\{^1\text{H}\}$ and ^1H NMR spectra in CD_2Cl_2 of the reactivity of **III** in system 3.5.

The results above reported on the reactivity of the dicarboalcoxy complex with BQ in the presence of MeOH and CO, gives significant insights into the basic aspects of the catalytic cycle, that can be schematised as follows:

- i) In order to observe catalysis it is necessary that complex **III**^{*} or [Pd(BQ)(PPh₃)₂] are formed. Starting from **II** complex **III** is formed even at -78 °C, but only after addition of NEt₃ or the PPh₃-BQ adduct. **II** is formed from **I** also at -78 °C.
- ii) Complex **III**^{*} is stable up to 25 °C.
- iii) In the presence of BQ complex **III**^{*} is converted to [Pd(BQ)(PPh₃)₂] with formation of DMO at *ca.* 25 °C, temperature significantly lower than that necessary to observe catalysis.
- iv) Catalysis occurs only at 60 °C.

Therefore the formation of complex **III**^{*} or the product forming step are not the slow step of the catalysis. The slow step has to deal with the reformation of **III**^{*} from [Pd(BQ)(PPh₃)₂].

Catalytic oxidative carbonylation of methanol using I, II and III

In order to confirm the NMR results above reported and to demonstrate that the **I**, **II** and **III** are effectively catalyst precursors, the oxidative carbonylation of MeOH using BQ as an oxidant has been performed. It has been decided to use milder condition (25 °C, 2 atm CO) than those previously reported in Chapter 2 (65 °C, 65 atm CO), hopefully to avoid the decomposition to Pd metal. This decomposition to palladium metal was one of the problem that did not make possible the comparison of the activity the different catalytic systems.

The catalysis is quite selective to DMO, being this the only carbonylation product. In Table 3 the catalytic activity is reported.

* Or any other dicarbomethoxy species. For simplicity indicated as **III**.

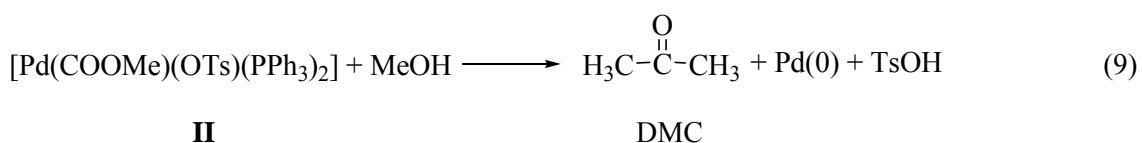
Table 3. Effect of time and base on the activity of the oxidative carbonylation reaction toward oxalate using **I**, **II** and **III**

<i>time</i> [h]	<i>I</i>		<i>II</i>	<i>III</i>
	TON_{DMO}	TON_{DMO}	TON_{DMO}	TON_{DMO}
0,5	0	0	5	6
1	0	0	10	14
1.5	11 ^a	9 ^b	26 ^a	30 ^a
2	21 ^a	20 ^b	37 ^a	39 ^a

Operative conditions: [Pd] = $1.2 \cdot 10^{-2}$ mol/L, Pd/BQ = 1/100, P_{CO} 2 atm, 25 °C, MeOH anhydrous, 5 mL. ^a NEt₃ (Pd/NEt₃ = 1/2) has been added after 1h of reaction. ^b PPh₃ (Pd/ PPh_{3 added} = 1/1) has been added after 1h of reaction. TON = [mol product/mol Pd].

In the absence of a base (such as NEt₃ or betaine which is formed *in situ* after the addition of PPh₃ (*cf.* Eq (1)) only **II** and **III** are active. Since the only carbonylation product is DMO, it is quite reasonable to suppose that the product-forming step involves a di-carbomethoxy species. Since **III** is stable in MeOH, either in the presence of CO or in its absence, it is likely that BQ promotes the transformation of **III** into a species having the two carbomethoxy ligands in *cis*-position, more favorable for the formation of DMO.

It is worth to point out that DMC does not form even when using the monocarbomethoxy complex **II** as catalyst precursor, in spite of the fact that this “cationic” complex presents an easily available site for the coordination of MeOH, which in principle could lead to DMC, as schematized:



Thus **II** is transformed into a dicarbomethoxy species before any reaction of type (9) takes place. This transformation occurs with concomitant formation of one equivalent of TsOH. We observed by NMR that **III** in CD₂Cl₂ is unstable at room conditions when in the presence of one

equivalent of TsOH and gives **II**, thus practically reversing the above transformation (*cf.* system 3.1). Thus, starting from **II**, it is likely that a dicarbomethoxy or $[\text{Pd}(\text{BQ})(\text{PPh}_3)_2]$ species form at least to some extent, enough to observe catalysis.

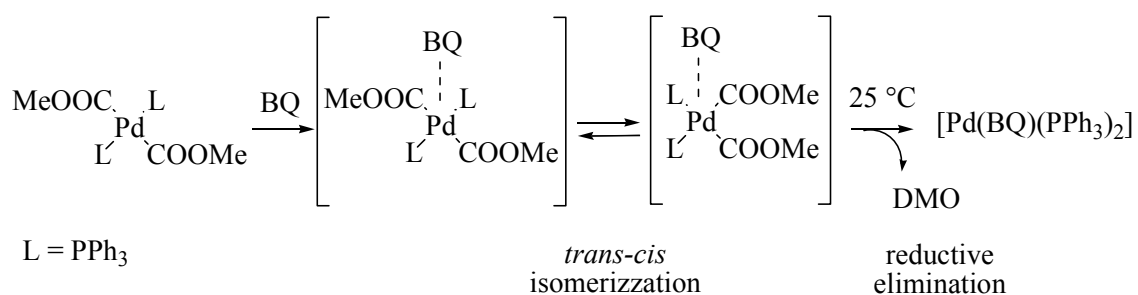
Despite the uncertainty of the GC analysis we are tempted to say that after the first hour of reaction, **III** is *ca.* 40% more active than **II** (TOF 14 h^{-1} *versus* 10 h^{-1}), which might be due to the presence of TsOH when starting from the latter precursor.

At difference, starting from **I** no catalytic activity is observed. When after 1 hour of catalysis, 2 equivalents of a base such as NEt_3 are added, **II** and **III** show a significant increment in the catalytic activity. **I** becomes active, too, also when PPh_3 is used in place of NEt_3 giving further demonstration that betaine acts as a base (*cf.* Eq (5)). In this case the role of the base is to neutralize the acid. In the first half an hour, the activity increments for **II** and **III** are practically the same, from 10 to 26 and from 14 to 30 mol of DMO/mol of Pd respectively. This reinforces the above explanation on the retarding effect of TsOH. The base neutralizes TsOH and favors the formation of a di-carbomethoxy species **III**, so that the two systems become equivalents and show the same increment of catalytic activity.

On the catalytic cycle of the oxidative carbonylation reaction of alkanols

Summarizing, the NMR evidences show that in absence of BQ **III** (preformed or formed *in situ*) is stable up to 40–60 °C.

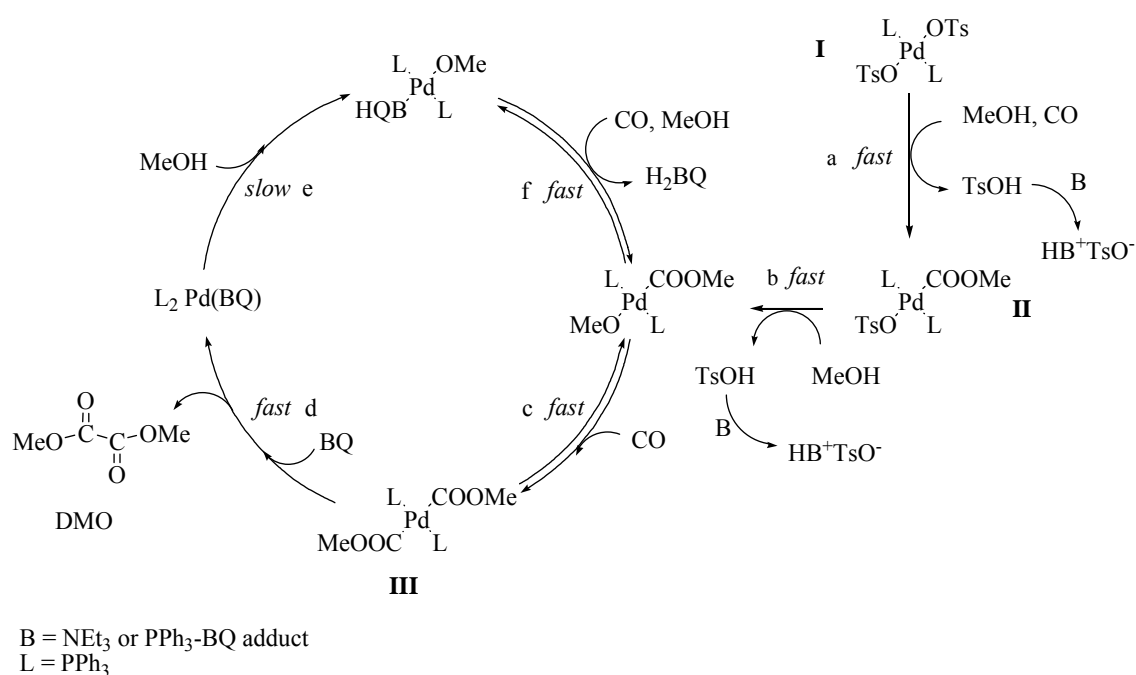
In presence of BQ **III** gives selectively DMO and $[\text{Pd}(\text{BQ})(\text{PPh}_3)_2]$, a significantly lower temperature, *i. e.* 25 °C. It is proposed that BQ, an electron withdrawing olefin, coordinates the metal centre of the dicarbomethoxy complex and promotes the formation of a species having two $\text{Pd}(\text{COOMe})_2$ moieties in *cis*-position, favourable to the reductive elimination of DMO. The last step may occur through the following sequence (Scheme 3 and Scheme 4 step d):



Scheme 3. Pathway for the reductive elimination of DMO from **III** assisted by BQ.

Catalysis occurs at a significantly higher temperature, *i. e.* 60 °C, suggesting that the slow step of the catalysis is the reoxidation of this complex (Scheme 4 step e). The last step may occur through the following sequence:

- i) Interaction of MeOH with the Pd(0)–BQ moiety to give a Pd(II)(methoxy)(*p*-hydroxyphenoxy) species (Scheme 4 step e).
- ii) Insertion of CO into the Pd–OMe bond to give a Pd(II)(carbomethoxy)(*p*-hydroxyphenoxy) species and displacement of the *p*-hydroxyphenoxy ligand by MeOH with formation of a Pd(II)(carbomethoxy)(methoxy) species (Scheme 4 step f).
- iii) CO insertion into the Pd–OCH₃ bond with reformation of **III** (also without the presence of a base when starting from **II** or **III**) (Scheme 4 step c).



Scheme 4. Simplified mechanism of the oxidative carbonylation of MeOH toward oxalate catalyzed by Pd(II) complexes in presence of BQ.

It is known that the oxidation of “Pd(0)BQ” is favored by an acid.¹⁵ When starting from **III**, MeOH plays the role of both reagent and acid. When starting from **II**, during the first hour of reaction, TsOH is the acid. The above mechanism basically holds in this case, too, because eventually the catalysis occurs after the formation of [Pd(COOMe)(OMe)(PPh₃)₂] intermediate, indeed i) a Pd–OTs species is in equilibrium with a Pd–OMe one (Scheme 4 step b); ii) a dicarbomethoxy species **III** forms from **II** in pure MeOH with BQ or in presence of base when in CD₂Cl₂/MeOH 10 % and BQ. The concentration of MeOH and probably also the polarity of the medium play an important role in directing the reactivity.

Also when starting from **I** TsOH is the acid and in this case it has been observed that **I** reacts with CO in MeOH (pure or with CD₂Cl₂) either in the presence or in the absence of BQ even at –78 °C forming only **II** (Scheme 4 step a), but not **III**. This fact may be explained considering that the transformation of **I** into **II** occurs with concomitant formation of TsOH

(Scheme 4 step a). The mono-carbomethoxy complex **II** is stable in the presence of one equivalent of TsOH.

Further transformation of **II** into **III** would occur with formation of another equivalent of TsOH, and this is unlikely because **III** is unstable in the presence of just one equivalent of acid. In order to promote the catalysis it is necessary the presence of a base which promotes the formation of **III** or directly of $[\text{Pd}(\text{BQ})(\text{PPh}_3)_2]$. Again the above proposed mechanism holds also in this case.

The facts just above reported explain why catalysis cannot occur starting from the **I** and BQ and why it occurs only after addition of a base. The fact that in the presence of a base the catalytic activity significantly increases also when starting from **III** (in this case no TsOH may form) suggests that the base:

- i) neutralizes TsOH formed when starting from **I** and **II** favoring the formation of a di-carbomethoxy species (Scheme 4 step a and b);
- ii) may increase the nucleophilicity of MeOH, thus easing the formation of Pd-(OMe) and Pd-(COOCH₃) species and/or favouring the reoxidation of $[\text{Pd}(\text{BQ})(\text{PPh}_3)_2]$ through the formation of an anionic labile species of the type $[\text{Pd}(\text{BQ})(\text{OCH}_3)(\text{PPh}_3)_2]^-$ more prone to oxidation.¹⁴

The fact that the presence of acid prevents the catalysis is rather surprising. Indeed, in the palladium catalyzed intermolecular 1,4 additions to conjugated dienes with BQ as an oxidant, it was found that the presence of acid (*e. g.* CH₃SO₃H or HClO₄) is essential, and without added acid no reaction occurred. The role of the acid, in this case, is to induce a redox reaction between BQ and metal to give Pd(II) and hydroquinone.¹⁵ However in our case starting from **I** the catalysis does not occur because even though on one hand the acid would eventually favour the reoxidation, however the acid inhibits the formation of the dicarboalcoxy intermediate, thus preventing the catalysis to take place.

Conclusions

It has been demonstrated that not only the carbomethoxy complexes but also both BQ and the base play a role of paramount importance in the oxidative carbonylation of alcohol. In particular, it has been shown that the BQ does not act only as an oxidant, but it can improve the catalytic performance by i) promoting the reductive elimination of DMO from a dicarbomethoxy species and Pd(0) and ii) stabilizing Pd(0) as [Pd(BQ)(PPh₃)₂]. In addition BQ may assist the formation of Pd(II) methoxy and carbomethoxy species in the reoxidation of Pd(0) to Pd(II).

Experimental section

Instrumentation and materials

Chemicals were purchased from Sigma–Aldrich, Acros Chimica and Eurisotop. PPh₃, NEt₃, TsOH·H₂O were used as received. MeOH, CD₂Cl₂ and CD₃OD were stored over 4 Å molecular sieves under Ar. Carbon monoxide (purity higher than 99 %) was supplied by SIAD Spa (Italy). NMR spectra were recorded on Bruker AMX 300 spectrometer. ³¹P spectra was measured ¹H decoupled. All ¹H chemical shifts are reported relative to the residual proton resonance in the deuterated solvents. ³¹P signals were referenced to an 85 % aqueous solution of H₃PO₄. NMR under pressure was performed using a 5 mm pyrex glass HP–NMR tube with Teflon head (maximum pressure tolerated 13 atm). *cis*–[Pd(OTs)₂(PPh₃)₂] (**I**),¹⁶ *trans*–[Pd(COOMe)(TsO)(PPh₃)₂] (**II**),¹⁷ and the PPh₃–BQ adduct “betaine”^{5, 7} were prepared according to literature procedures.

Preparation of the complexes

The NMR characterization of all complex is reported in Table 2.

Synthesis of *trans*-[Pd(COOMe)₂(PPh₃)₂] (II). This complex has been synthesized by treating *cis*-[Pd(OTs)₂(PPh₃)₂] (0.1 mmol), dissolved in 2 mL of MeOH, with carbon monoxide (2 atm) at 0 °C for 10' under stirring, during which time the solution turned from brownish to yellowish. NEt₃ (0.8 mmol) was then added while stirring for 10 more minutes. The light brown solid that formed was collected on a filter, washed with MeOH, Et₂O and dried under vacuum. Yield 87%. Elem anal. Calcd for C₄₀H₃₆O₄P₂Pd: C, 64.14; H, 4.84. Found: C, 63.78; H, 4.94. IR (KBr): 1630 s (ν_{CO}), 1014 br (ν_{COC}) cm⁻¹.

Synthesis of [Pd(COOMe)(PPh₃)₃](TsO). To 0.1 mmol of Pd(OAc)₂ in 2 mL of MeOH was added 0.3 mmol of PPh₃ and 0.2 mmol of TsOH·H₂O. The solution was stirred at room temperature for 10', after it was kept under 2 atm of CO for 30 minutes and then poured into 20 ml of cold water under vigorous stirring. A white precipitated formed immediately. The suspension was filtered, the solid was washed with cold water, *n*-pentane, and dried under vacuum (yield 71%). Elem anal. Calcd for C₆₃H₅₅O₅P₃SPd: C, 67.35; H, 4.93. Found: C, 67.01; H, 5.14. IR (nujol): 1661 s (ν_{CO}) cm⁻¹.

High pressure NMR experiments

Typically, a solution of 0.005 mmol of the palladium complex dissolved in CD₂Cl₂ (0.15 mL) was poured into the 5 mm pyrex glass HPNMR tube, previously evacuated by a vacuum pump, at r. t. under Ar flow. The tube was then quickly placed in a or liquid N₂/acetone bath cooled at -78 °C. To the cooled solution was added, under argon flow, a solution containing the desired amount of PPh₃ and/or BQ, NEt₃, MeOH (30 μL to reach 10 % of final volume) in 0.15 mL of CD₂Cl₂. The tube was connected with the pressure line by using the special screw top in Teflon, then purged several time (4-5) and pressurized with CO or Ar (the maximum pressure

used at this temperature was 6 atm) taking care to shake the tube to favour the solubilization of the gases. The tube was then heated at desired temperature in the NMR probe. Further addition of liquid (such as NEt_3 and MeOH) was performed injecting the desired amount by a syringe to a depressurized NMR tube cooled at $-78\text{ }^\circ\text{C}$. Similar procedure was followed for the addition of the solid compounds. In this case the solution injected was prepared solubilising the solid in a little vial cooled at $-78\text{ }^\circ\text{C}$ under CO or Ar atmosphere using a little part of the solution already present in the tube as solvent. In both case the resulting NMR tube was immediately pressurized at the desiderate pressure at $-78\text{ }^\circ\text{C}$.

Note: Although the above described high pressure tubes have been used safely in our department for years in the pressure range of 1–8 atm, it is absolutely avoid direct exposure to a charged high pressure tube without any safety device.

References

- (1) Bertani, R.; Cavinato, G.; Toniolo, L.; Vasapollo, G. *J. Mol. Catal.* **1993**, *84*, 165.
- (2) Backvall, J.; Hopkins, R. B.; Grennberg, H.; Mader, M. M.; Awasthi, A. K. *J. Am. Chem. Soc.* **1990**, *112*, 5160.
- (3) (a) Zhir–Lebed, L. N.; Temkin, O. N. *Kinet. Katal. (Engl. Transl.)* **1984**, *25*, 255. (b) Zhir–Lebed, L. N.; Temkin, O. N. *Kinet. Katal. (Engl. Transl.)* **1984**, *25*, 263.
- (4) (a) Seayad, A.; Jayasree, S.; Damodaran, K.; Toniolo, L.; Chaudhari, R. V. *J. Organomet. Chem.* **2000**, *601*, 100. (b) Amatore, C.; Jutand, A.; Medeiros, M. J. *New J. Chem.* **1996**, *20*, 1143. (c) Zudin, V. N.; Chinakov, V. D.; Nekipelov, V. M.; Rogov, V. A.; Likholobov, V. A.; Yermakov, Y. I. *J. Mol. Catal.* **1989**, *52*, 27.
- (5) (a) Khabibulin, V. R.; Kulik, A. V.; Oshanina, I. V.; Bruk, L. G.; Temkin, O. N.; Nosova, V. M.; Ustynyuk, Y. A.; Bel'skii, V. K.; Stash, A. I.; Lysenko, K. A.; Antipin, M. Y. *Kinet. Katal.* **2007**, *48*, 228. (b) Kulik, A. V.; Bruk, L. G.; Temkin, O. N.; Khabibulin, V. R.; Belsky, V. K.; Zavodnik, V. E. *Mendeleev Commun.* **2002**, *12*, 47.
- (6) Kudo, K.; Hidai, M.; Uchida, Y. *J. Organomet. Chem.* **1971**, *33*, 393.
- (7) (a) Arshad, M.; Beg, A.; M. S. Siddiquiri, M. S. *Tetrahedron* **1966**, *22*, 2203. (b) Ramirez, F. and Dershowitz, S. *J. Am. Chem. Soc.* **1956**, *78*, 5614.
- (8) Dahn, H.; Pèchy, P. *Magn. Reson. Chem.* **1996**, *34*, 723.
- (9) Pearson, D. M.; Waymouth R. M. *Organometallics* **2009**, *28*, 3896.
- (10) Querci, C.; D'Aloisio, R.; Bortolo, R.; Ricci, M.; Bianchi, D. *J. Mol. Catal. A: Chem* **2001**, *176*, 95.
- (11) del Rio, I.; Claver and van Leeuwen, P. W. N. M. *Eur. J. Inorg. Chem.* **2001**, 2718
- (12) Yoshida, T.; Okano, T.; Otsuka, S. *J. Chem. Soc. Dalton* **1976**, 993

-
- (13) van Leeuwen, P. W. N. M.; Zuideveld, M. A.; Swennenhuis, B. H. G.; Freixa, Z.; Kamer, P. C. J.; Goubitz, K.; Fraanje, J.; Luitz, M.; Spek, A. L. *J. Am. Chem. Soc.* **2003**, *125*, 5523.
- (14) (a) Amatore, C.; Bensalem, S.; Ghalem, S.; Jutand, A.; Fenech, D.; Galia, A.; Silvestri, G. *C. R. Chimie* **2004**, *7*, 737. (b) Amatore, C. and Jutand, A. *Acc. Chem. Res.* **2000**, *33*, 314.
- (15) (a) Grennberg, H.; Gogoll, A., Backval, J. E. *Organometallics* **1993**, *12*, 1790. (b) Backvall, J. E.; Vagberg, J. O. *J. Org. Chem.* **1988**, *53*, 5695.
- (16) Cavinato, G.; Vavasori, A.; Toniolo, L.; Dolmella, A. *Inorg. Chim. Acta.* **2004**, *257*, 2737.
- (17) Cavinato, G.; Vavasori, A.; Toniolo, L.; Benetollo, F. *Inorg. Chim. Acta* **2003**, *343*, 183.

Chapter 4

Pd(II)–Monophosphine Catalysts for the Oxidative Carbonylation of *i*PrOH

Introduction

In Chapter 2 it was reported that the catalyst precursors $[\text{Pd}(\text{COOMe})_n\text{X}_{2-n}(\text{PPh}_3)_2]$ ($n = 0, 1, 2$; $\text{X} = \text{AcO}, \text{Cl}, \text{ONO}_2, \text{ONO}, \text{TsO}$) used in the oxidative carbonylation of MeOH partially decompose to Pd metal under the reaction conditions (65 °C, 65 atm CO) and that the consume of BQ was higher than expected in comparison to the amount of DMO formed. For these reasons it was not possible to give an order of activity in relation to the nature of X.

BQ might be subtracted from the reaction medium by the formation of insoluble solid produced by BQ polymerization promoted by a PPh_3 –BQ adduct formed *in situ*.¹ Another BQ consuming reaction might be the oxidation of MeOH to formal, which in turn can give rise to many derivatives (methyl hemi–formal and di–formal, formal oligomers, methyl formate, 4–hydroxyphenyl formate, pitches).² However, formal and its derivatives were not detected. Therefore, we tested the catalytic activity using other alkanols.

Preliminary experiment using *i*PrOH showed that the mass balance between BQ, H_2BQ and the products (diisopropyl oxalate (**O**), diisopropyl carbonate (**C**) and acetone (**A**)) was reasonably well respected ($\pm 20\%$). Acetone does not give rise to any derivative in significant

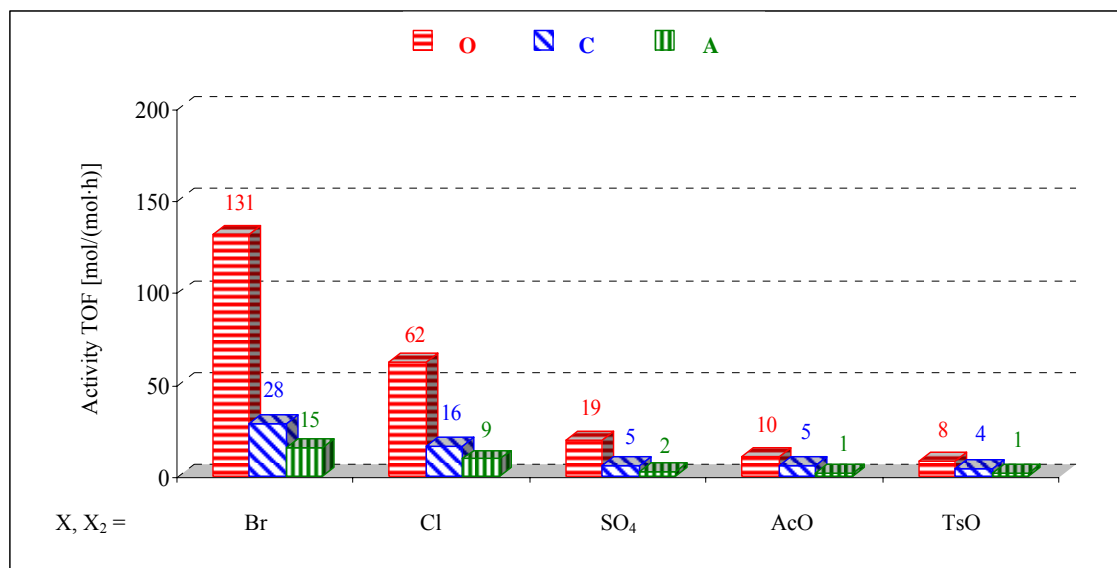
amounts and it is easily quantifiable by GC analysis. Moreover, decomposition to Pd metal did not occur even under relatively severe conditions (100 °C, 90 atm of CO, 2 h).

This chapter deals with the study of the oxidative carbonylation of *i*PrOH catalyzed by the complexes $[\text{PdX}_2\text{L}_2]$ [$\text{X} = \text{AcO}, \text{Br}, \text{Cl}, \text{TsO}$; $\text{X}_2 = \text{SO}_4$; $\text{L} = \text{P}(\text{C}_6\text{H}_4\text{Y})_3$, $\text{Y} = \text{H}, o, m, p\text{-(CH}_3, \text{CH}_3\text{O)}, p\text{-F}$; $\text{L} = \text{P}(\text{C}_6\text{H}_3\text{Y}_2)_3$, $\text{Y} = o, o'\text{-OCH}_3$].

Results and discussion

Influence of counter anion on the activity and selectivity of $[\text{PdX}_2(\text{PPh}_3)_2]$

The influence of the anion on the activity and selectivity of the title complexes has been studied using precursors having $\text{X} = \text{AcO}, \text{Br}, \text{Cl}, \text{TsO}$; and $\text{X}_2 = \text{SO}_4$. As shown in Graph 1 the highest activity and selectivity toward **O** have been obtained when X and X₂ are strongly coordinating anions ($\text{Br} \gg \text{Cl} \gg \text{SO}_4 > \text{AcO} > \text{TsO}$).

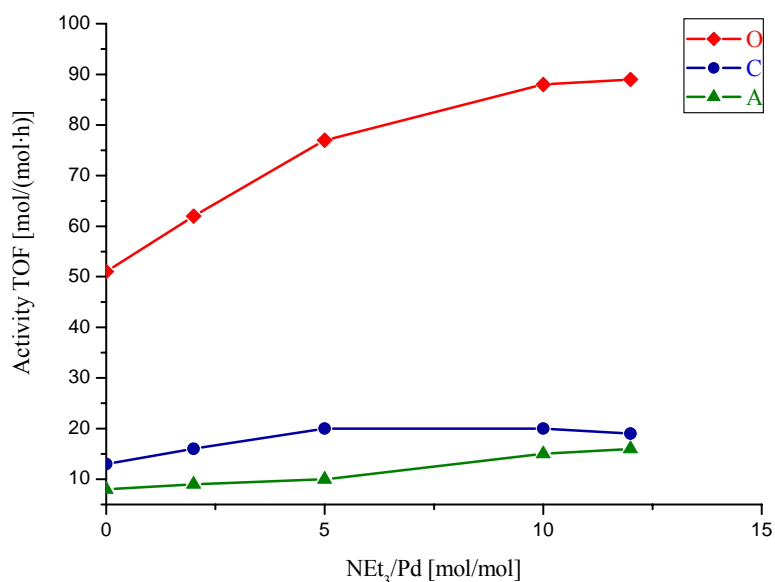


Graph 1. Influence of anion on the performance of $[\text{PdX}_2(\text{PPh}_3)_2]$ in the oxidative carbonylation of *i*PrOH. Conditions: $[\text{Pd}] = 2 \cdot 10^{-4}$ mol/L, $\text{Pd}/\text{PPh}_3/\text{NEt}_3/\text{BQ} = 1/4/2/700$, $\text{P}_{\text{CO}} = 85$ atm, $T = 90$ °C, 1 h, 5 mL anhydrous *i*PrOH.

This result is rather surprising because strongly coordinating anions compete with the reacting molecules for coordination to the metal centre, thus they were expected to inhibit the catalytic activity.

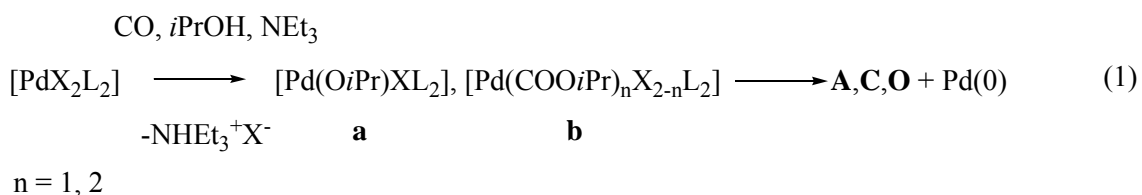
Effect of promoters on the activity and selectivity of $[\text{PdX}_2(\text{PPh}_3)_2]$

Effect of NEt_3 . Previous studies (Chapter 3) on the oxidative carbonylation of MeOH proved that a higher activity can be achieved in the presence of NEt_3 . This base presents a positive effect also when using *i*PrOH as shown in Graph 2.



Graph 2. Influence of NEt_3/Pd molar ratio on the performance of *trans*- $[\text{PdCl}_2(\text{PPh}_3)_2]$ complexes in the oxidative carbonylation of *i*PrOH. Conditions: $[\text{Pd}] = 2 \cdot 10^{-4}$ mol/L, $\text{Pd}/\text{PPh}_3/\text{BQ} = 1/4/700$, $P_{\text{CO}} = 85$ atm, $T = 90$ °C, 1 h, 5 mL anhydrous *i*PrOH.

The formation of the products **O**, **C** and of the byproduct **A** occurs through intermediate of type **a** and **b** with concomitant release of a proton. The base subtracts the proton thus favoring the formation of these intermediates.



The formation of the products occurs with concomitant reduction of Pd(II) to Pd(0). The stabilization of Pd(0) avoids the decomposition to palladium metal and eases the reoxidation of Pd(0) to Pd(II). These are important factors in order to guarantee high catalytic performance.

Effect of added halides. Amatore *et al.* and Neghishi *et al.* demonstrated that $[\text{Pd}(0)(\text{PPh}_3)_2]$ is unstable in the absence of halide ions. The partial or total saturation of the coordination shell of a zerovalent palladium complex by halide ions, with formation of anionic complexes $\text{Li}[\text{Pd}(\text{PPh}_3)_2\text{X}]$ or $\text{Li}_2[\text{Pd}(\text{PPh}_3)_2\text{X}_2]$,* prevent its deactivation.³ Not only, but the negative charge of Pd(0) coordinated by the anion enhances its reactivity toward oxidation.⁴

Therefore, it has been decided to study the influence of X (X = Cl, Br, I) on the activity and selectivity using the *trans*- $[\text{PdCl}_2(\text{PPh}_3)_2]$ as catalyst precursor in combination with LiX.

Table 1. Influence of the halide anions on the performance of *trans*- $[\text{PdCl}_2(\text{PPh}_3)_2]$ in the oxidative carbonylation of *i*PrOH

Entry	Pd/LiX [mol/mol]	Activity TOF [mol/(mol*h)]			Selectivity [%]		
		O	C	A	O	C	A
1	-	88	20	15	72	16	12
2	6 Cl	60	13	0	82	18	0
3	24 Cl	77	12	0	87	13	0
4	6 Br	125	31	0	80	20	0
5	24 Br	228	32	0	88	12	0
6	6 I	85	8	0	91	9	0
7	24 I	14	2	0	88	12	0

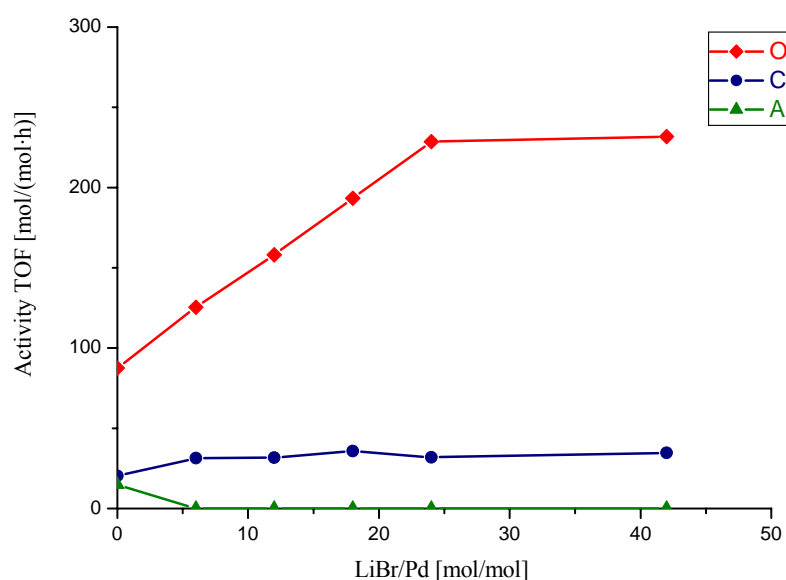
Conditions: $[\text{Pd}] = 2 \cdot 10^{-4}$ mol/L, Pd/PPh₃/NEt₃/BQ = 1/4/10/700, P_{CO} = 85 atm, T = 90 °C, 1 h, 5 mL anhydrous *i*PrOH.

Table 1 shows that the catalytic activity increases in the presence of LiBr. Cl⁻ has a minor effect, I⁻ depresses significantly the activity when used in relatively high concentration. These results may be accounted with a different coordinating capacity of the anions on the palladium

* Obtained in the presence of LiX.

centre. While the Cl^- ion is less coordinating than Br^- , I^- is too much coordinating, thus making difficult the coordination of the reagents.⁵ A similar trend has been observed in the palladium catalysed carbonylation of aryl halides.⁶

Graph 3 shows how the activity and selectivity vary with the Br/Pd ratio. The rate of formation of **O** increases up to 228 TOF at a ratio Br/Pd = 24/1, then it remains almost constant. The rate of formation of **C** is little influenced. The formation of **A** is completely inhibited at Br/Pd > 6/1.

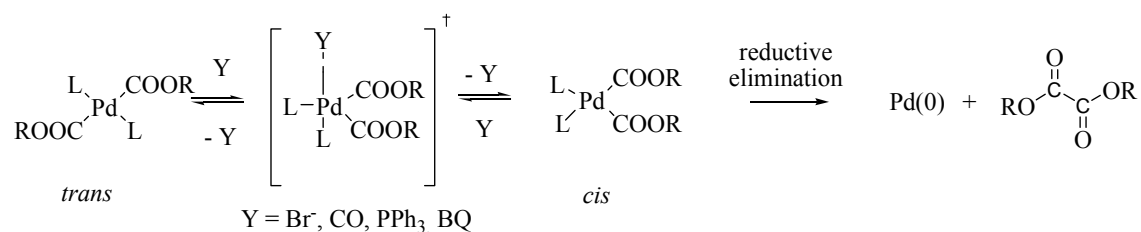


Graph 3. Influence of the LiBr/Pd molar ratio. For the other conditions see Table 1.

The fact that the formation of **A** is inhibited in the presence of any halide provides a further evidence that the halide plays an important role. The halide may compete with the β -hydride extraction of the Pd-OR species, responsible of the formation of **A**. This competition

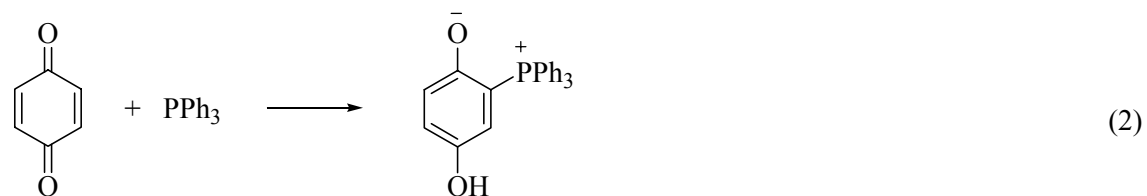
does not compromise the formation of the Pd–OR or Pd–COOR moieties because, at least when LiBr is used, the activity toward **O** and **C***⁷ is enhanced.

Summarizing, LiBr enhances the catalytic activity and the selectivity to **O** probably because Br[−] might stabilize the Pd(0) as anionic species of the type [PdBr(BQ)(PPh₃)₂][−] or [PdBr₂(BQ)(PPh₃)₂]^{2−} and enhances their reoxidation without compromising the coordination of the reagents. In addition, it might be possible that the Br[−] favors the isomerisation from *trans* to *cis* of the intermediates and hence the product forming step as schematized below for the formation of **O**.⁸ The isomerisation *trans*–*cis* might be promoted also by the presence of free ligand and/or CO^{8,9} and also by BQ (*cf.* Chapter 3).

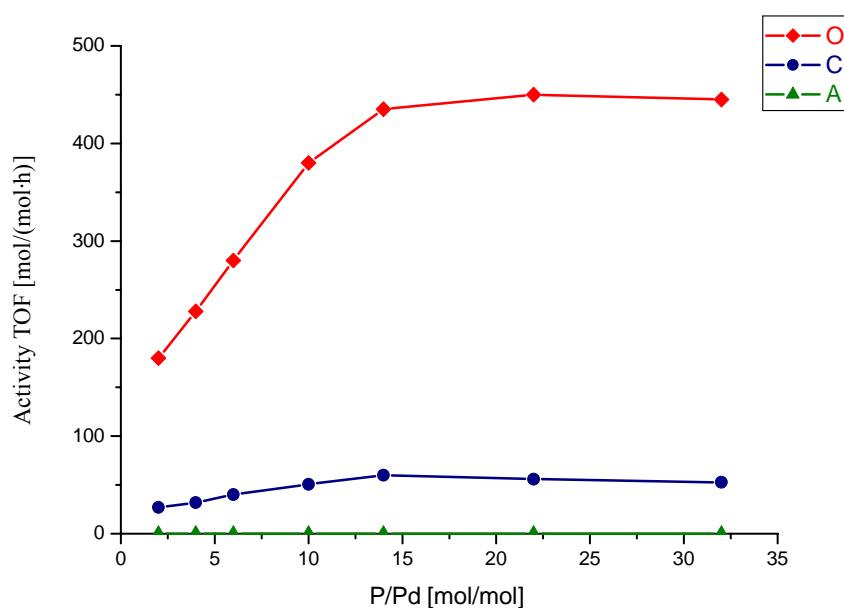


Scheme 1. Sequence proposed for the *trans*–*cis* isomerisation and formation of **O** promoted by Br[−], CO, PPh₃ and BQ.

Influence of added PPh₃. This has been studied using the best system reported above (entry 5 in Table 1). Graph 4 shows how the catalytic increases upon addition of PPh₃. As mentioned in Chapter 3, BQ gives an adduct with free PPh₃ with formation of (2,5–dihydroxyphenyl)phosphonium (betaine),¹⁰ which may act as a base because of the presence of a Ar–O– moiety.¹¹ This might explain the enhancing effect of added PPh₃.



***C** is likely to form from a carboisopropoxy–isopropoxy species of the type *trans*–[Pd(COO*i*Pr)(O*i*Pr)(PPh₃)₂] via an intramolecular migratory nucleophilic attack of the coordinated alkoxide at the carboisopropoxy group.⁷



Graph 4. Influence of PPh_3/Pd molar ratio on the performance of $\text{trans-}[\text{PdCl}_2(\text{PPh}_3)_2]$ in the oxidative carbonylation of $i\text{PrOH}$. Conditions: $[\text{Pd}] = 2 \cdot 10^{-4} \text{ mol/L}$, $\text{Pd}/\text{NEt}_3/\text{LiBr}/\text{BQ} = 1/10/24/1400$, $P_{\text{CO}} = 85 \text{ atm}$, $T = 90 \text{ }^\circ\text{C}$, 1 h, 5 mL anhydrous $i\text{PrOH}$.

Effect of operative conditions on the activity and selectivity of $\text{trans-}[\text{PdBr}_2(\text{PPh}_3)_2]$

The results reported in Graph 4 have been obtained using $\text{trans-}[\text{PdCl}_2(\text{PPh}_3)_2]$ as precursor. In the presence of an excess of the LiBr the precursor is reasonably converted to $\text{trans-}[\text{PdBr}_2(\text{PPh}_3)_2]$. As matter of fact all the bromide complexes reported in this chapter (*cfr.* Experimental) have been synthesized from the corresponding PdCl_2L_2 with an excess of LiBr. Therefore, the influence of the operative conditions (reaction time, temperature and pressure) has been studied using $\text{trans-}[\text{PdBr}_2\text{L}_2]$ as precursor, which under the conditions of entry 1 in Table 2 gives **O** with $\text{TOF} = 455 \text{ h}^{-1}$ and 91 % selectivity, close to the results obtained using $\text{trans-}[\text{PdCl}_2\text{L}_2]$ ($\text{TOF} = 450 \text{ h}^{-1}$, 89 % selectivity).

Effect of reaction time and of BQ. Upon increasing the reaction time from 1 to 3 h the TOF and the selectivity to **O** slightly decrease (Table 2). Since during the course of catalysis the concentration of BQ decreases considerably, it arises that the catalytic activity depends only slightly on the concentration of BQ. This suggests that either *i*) uncoordinated BQ is not

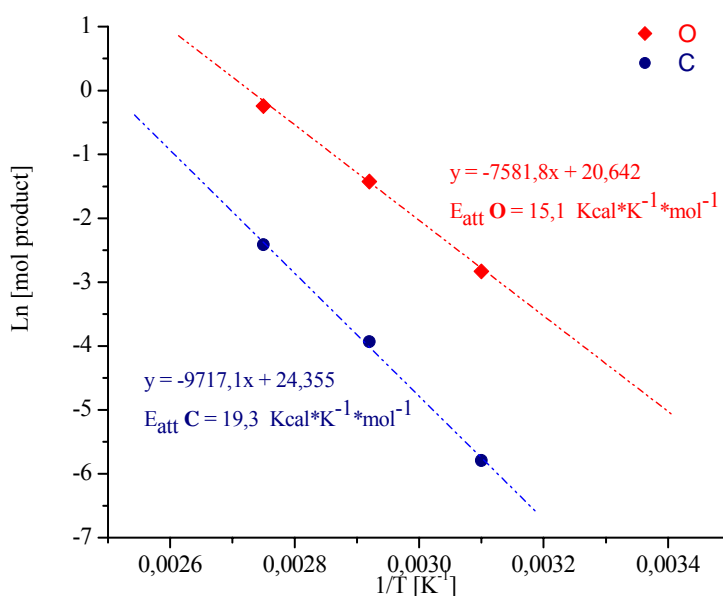
involved in the slow step of the catalysis or *ii*) the species involved in the slow step is coordinated by BQ to a large extent, practically 100%.

Table 2. Influence of time and temperature on the performance of *trans*-[PdBr₂(PPh₃)₂] in the oxidative carbonylation of *i*PrOH

Entry	<i>t</i> [h]	<i>T</i> [°C]	Activity TOF [mol/(mol*h)]			Selectivity [%]		
			O	C	A	O	C	A
1	1	90	455	45	0	91	9	0
2	2	90	386	44	0	90	10	0
3	3	90	370	40	0	90	10	0
4	2	70	120	10	0	92	8	0
5	2	50	28	2	0	93	7	0

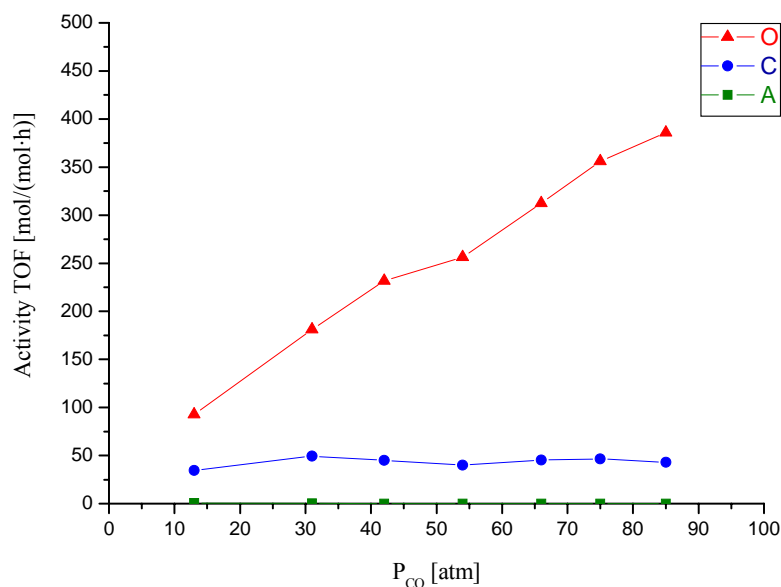
Conditions: [Pd] = 2·10⁻⁴ mol/L, Pd/PPh₃/NEt₃/LiBr/BQ = 1/22/10/24/1400, P_{CO} = 85 atm, 5 mL anhydrous *i*PrOH.

Effect of temperature. Upon decreasing the temperature, the activity decreases as expected, but the selectivity to O increases (Table 2). Indeed, the apparent activation energy is higher for the formation of C (19.3 Kcal·K⁻¹·mol⁻¹) than for O (15.1 Kcal·K⁻¹·mol⁻¹) (Graph 5).



Graph 5. Arrhenius plot. For the conditions see Table 2 above reported.

Effect of the pressure of CO. Graph 6 shows that upon increasing the pressure of CO the TOF toward **O** steadily increases, whereas that of **C** is little influenced. **A** is formed in low quantities at low CO pressure (0.7 TOF at 13 atm).



Graph 6. Influence of P_{CO} on the performance of *trans*-[PdBr₂(PPh₃)₂] in the oxidative carbonylation of *i*PrOH. Conditions: [Pd] = 2·10⁻⁴ mol/L, Pd/PPh₃/NEt₃/LiBr/BQ = 1/22/10/24/1400, T = 90 °C, 2 h, 5 mL anhydrous *i*PrOH.

Electronic and steric effects of the phosphine ligands

The results reported in Table 3 have been obtained using preformed *trans*-[PdBr₂L₂] in combination with an excess L. Figure 1 shows the phosphines used.

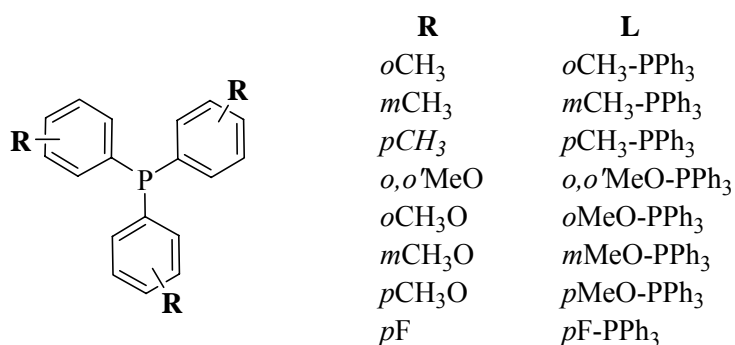


Figure 1. Modified triphenylphosphine ligands used.

Table 3. Electronic and steric effects on activity and selectivity of *trans*-[PdBr₂L₂]

Entry	L	Activity TOF [mol/(mol*h)]			Selectivity [%]		
		O	C	A	O	C	A
1	PPh ₃	455	45	0	91	9	0
2	<i>o</i> CH ₃ -PPh ₃	110	18	0	86	14	0
3	<i>m</i> CH ₃ -PPh ₃	421	57	0	88	12	0
4	<i>p</i> CH ₃ -PPh ₃	329	46	0	88	12	0
5	<i>o,o'</i> MeO-PPh ₃	2	4	0	33	67	0
6	<i>o</i> MeO-PPh ₃	29	5	0	85	15	0
7	<i>m</i> MeO-PPh ₃	384	45	0	90	10	0
8	<i>p</i> MeO-PPh ₃	226	30	0	88	12	0
9	<i>p</i> F-PPh ₃	190	20	0	90	10	0

Conditions: [Pd] = 2·10⁻⁴ mol/L, Pd/P/NEt₃/LiBr/BQ = 1/22/10/24/1400, T = 90 °C, 2 h, 5 ml anhydrous *i*PrOH.

Steric effects play a major role with respect to the electronic ones. Ortho substituents inhibit catalysis and lower the selectivity. *o,o'*OMe-PPh₃ presents the largest effect. This suggests that the ortho substituent inhibits the formation of a bulkier dicarboxy species to a larger extent with respect to the formation of a less hindered monocarboxy species, which leads to the formation of C. Also the *p*F-substituent slows down the activity. It might be that the electron withdrawing substituent makes more difficult the reoxidation of Pd(0). In all cases the formation of acetone is completely suppressed.

However, BQ reacts with added L giving the corresponding betaine, which presents a strong promoting effect (*cf.* Graph 4). The results reported in Table 3 have been achieved using a relative large amount of added L. Therefore, they do not allow to distinguish the effect of betaine from that of the actual steric and electronic effects of L coordinated to the metal centre. Other experiments must be carried out in the absence of added L.

On the catalytic cycle of the oxidative carbonylation of *i*PrOH

On the coordination of L to the palladium centre during catalysis. The highest catalytic activity has been obtained using the precursor *trans*-[PdBr₂(PPh₂)₂] in combination with relatively large amounts of added PPh₃ and LiBr. Since BQ reacts with the ligand, the question is: does coordinated phosphine dissociates during the catalysis, so that the metal centre is not any more coordinated by this ligand? In order to answer this question the catalytic activity of PdBr₂ has been compared to that of *trans*-[PdBr₂(PPh₂)₂]. As shown in Table 4, PdBr₂ is significantly less active and selective than *trans*-[PdBr₂(PPh₂)₂] (entry 1 and 3) also in the presence of added PPh₃ (entry 2). In this last case, the ligand was first added to a solution of BQ in *i*PrOH and then PdBr₂ and NEt₃ were added. With this procedure PPh₃ is subtracted in advance by BQ, so that there is not any more free ligand left to react with PdBr₂ to give *trans*-[PdBr₂(PPh₂)₂]. The comparison of the results reported in Table 4 suggests that dissociation of the ligand does not occur during catalysis.

Table 4. Effect of presence of ligand on the activity and selectivity of PdBr₂

Entry	Catalyst	Pd/PPh ₃ [mol/mol]	Activity TOF [mol/(mol*h)]			Selectivity [%]		
			O	C	A	O	C	A
1	PdBr ₂	0	87	15	0	85	15	0
2	PdBr ₂	22	170	18	0	90	10	0
3	[PdBr ₂ (PPh ₂) ₂]	22	455	45	0	91	9	0

Conditions: [Pd] = 2·10⁻⁴ mol/L, Pd/NEt₃/LiBr/BQ = 1/10/24/1400, T = 90 °C, 2 h, 5 mL anhydrous *i*PrOH.

As further demonstration we carried out a reaction using a relatively large amount of *trans*-[PdBr₂(PPh₃)₂] in *i*PrOH at 85 atm of CO, 90 °C together with relatively small amount of LiBr and BQ (Pd/Br/BQ = 1/4/5), hopefully to make easier the recovery of the precursor after catalysis and yet ensuring catalysis to some extent. GC analysis of the solution after 1 h showed

the following: i) formation of only 0.1 mol of **O** per mole of Pd (**C** and **A** did not form); ii) most of the BQ was still present (*ca.* 4.8 BQ/Pd). The mass balance was reasonably well respected. The recovered solid (**1**) was recognized by IR and NMR as the starting complex *trans*-[PdBr₂(PPh₃)₂] (Figure 2 and Figure 3). The ³¹P{¹H} spectrum of the solution after reaction (Figure 4) did not show any signal, indicating that no other complexes or betaine were present. It may be concluded that under the above conditions dissociation of the PPh₃ ligand from *trans*-[PdBr₂(PPh₃)₂] does not occur.

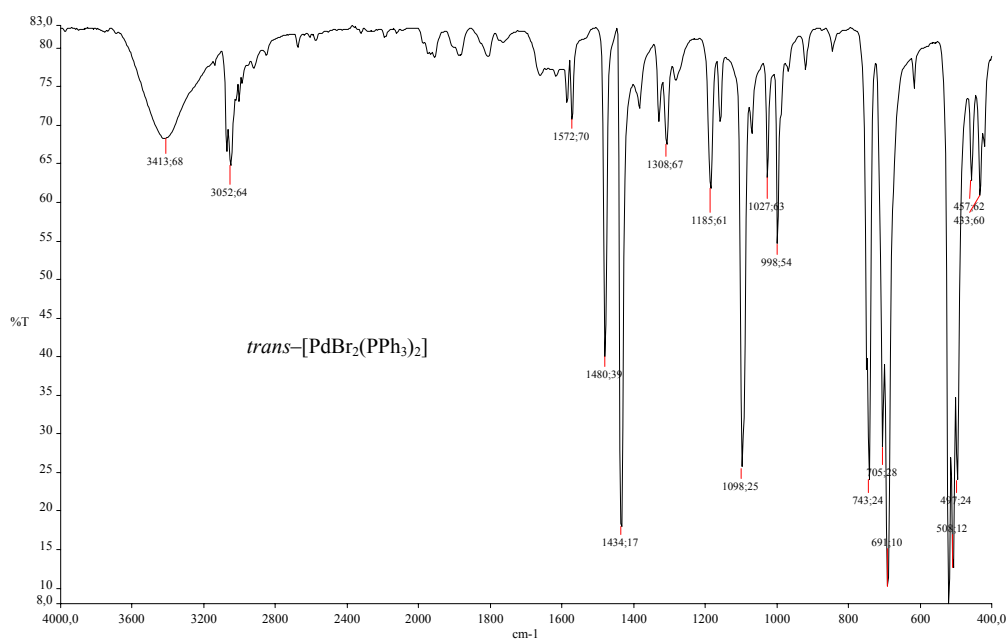


Figure 2. IR in KBr of the recovered solid **1**.

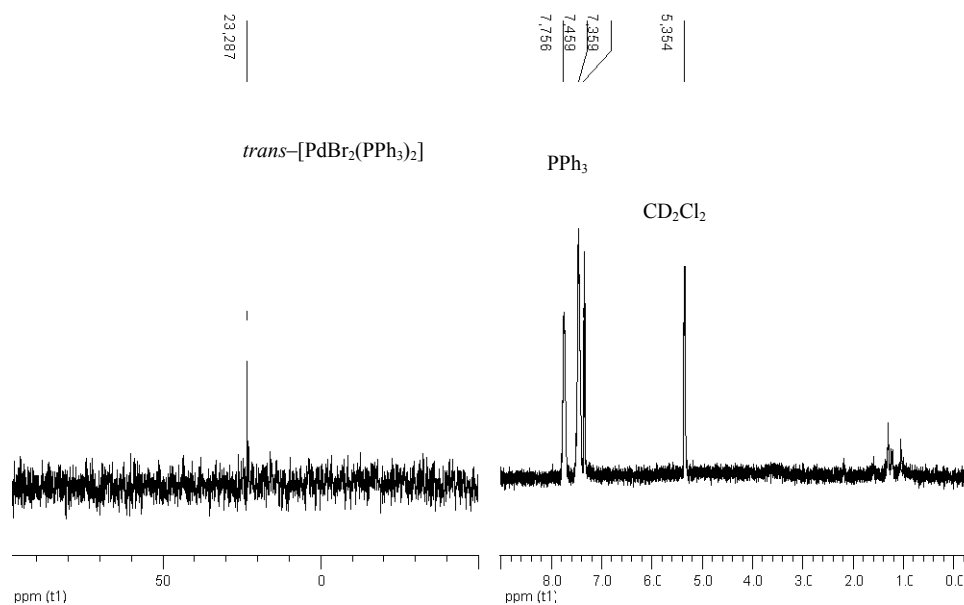


Figure 3. ^1H and $^{31}\text{P}\{^1\text{H}\}$ spectra of the recovered solid **1** in CD_2Cl_2 at r. t.

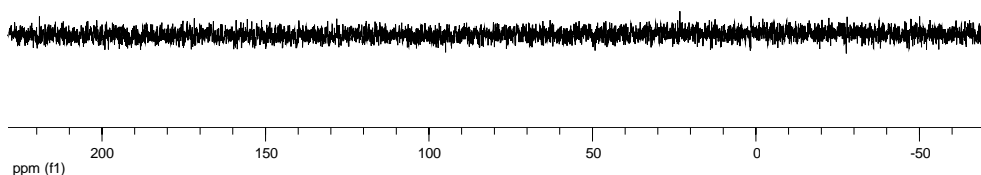


Figure 4. ^1H and $^{31}\text{P}\{^1\text{H}\}$ spectrum of solution recovered after filtration in CD_2Cl_2 at r. t.

In order to favor catalysis the above experiment was repeated but in the presence of NEt_3 ($\text{Pd/Br/NEt}_3/\text{BQ} = 1/4/2/5$). After 1 h reaction, GC analysis of the solution showed the presence of **O**, **C** and **A** (TOF 3.6, 0.1 and 1.0 h^{-1} , respectively) and of H_2BQ (*ca.* 4.3 $\text{H}_2\text{BQ/Pd}$). All BQ was consumed. Thus also in this case the mass balance was reasonably well respected. By removing the solvent from the reaction mixture, two different solids were recovered, a yellow one (**2**) and a brown pitchy residue (**3**).

2 was recognized as a mixture of the precursor *trans*-[PdBr₂(PPh₃)₂] and *trans*-[PdBr(COO*i*Pr)(PPh₃)₂] (Figure 5). [Pd(BQ)(PPh₃)₂] was also detected, though in a small amount. The IR spectrum (Figure 6) showed absorptions in the 1650–1620 cm⁻¹ region, probably of a BQ-containing species, for instance a H₂BQ–BQ adduct (*cf.* Experimental).

3 is likely to be a mixture of *trans*-[PdBr(COO*i*Pr)(PPh₃)₂] and H₂BQ and of another unidentified compound (Figure 7 and Figure 8). In both ³¹P{¹H} spectra of **2** and **3** there are no signal attributable to betaine (³¹P at 23.3 and 16.4, *cf.* Table 2, Chapter 3). Therefore, also during catalysis no dissociation of a PPh₃ ligand occurs.

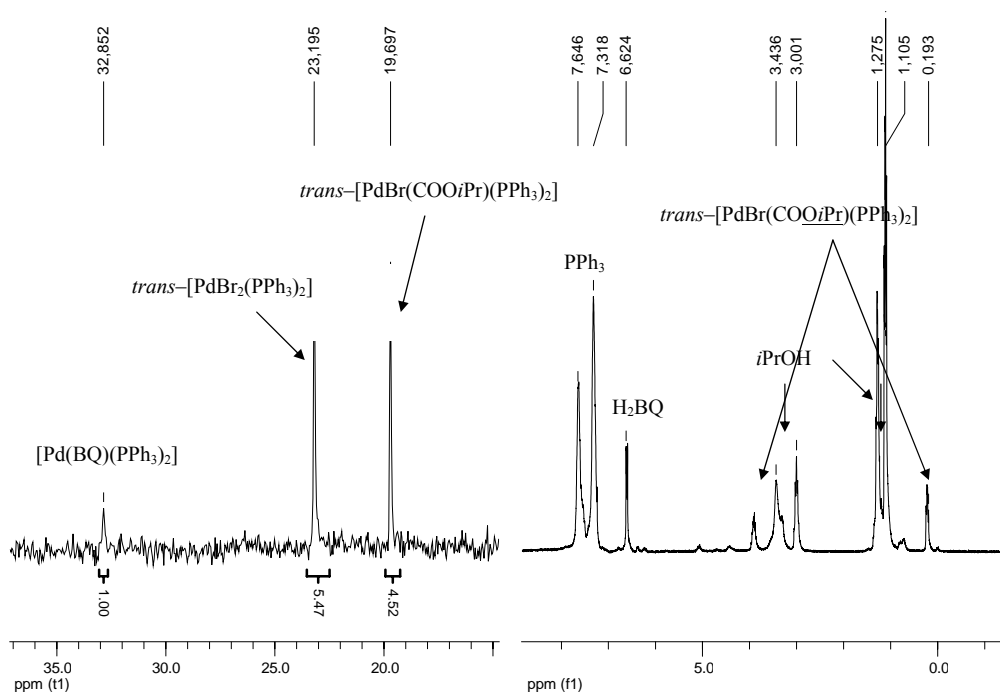


Figure 5. ¹H and ³¹P{¹H} spectra of the recovered yellow solid **2** in CD₃OD at r. t..

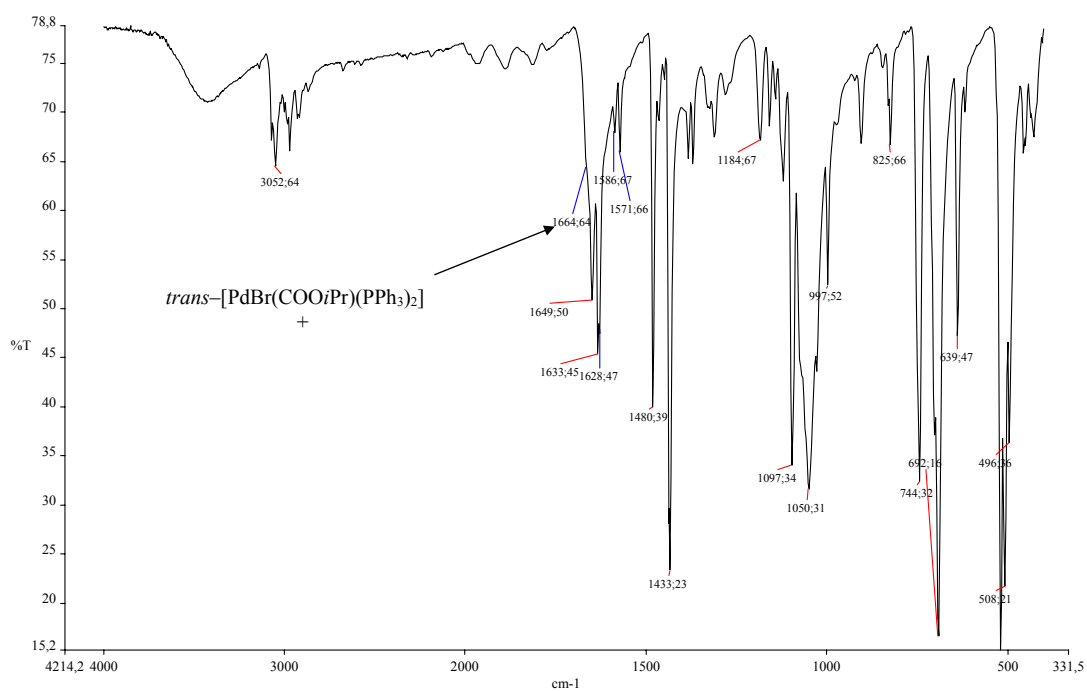


Figure 6. IR in KBr of the recovered yellow solid 2.

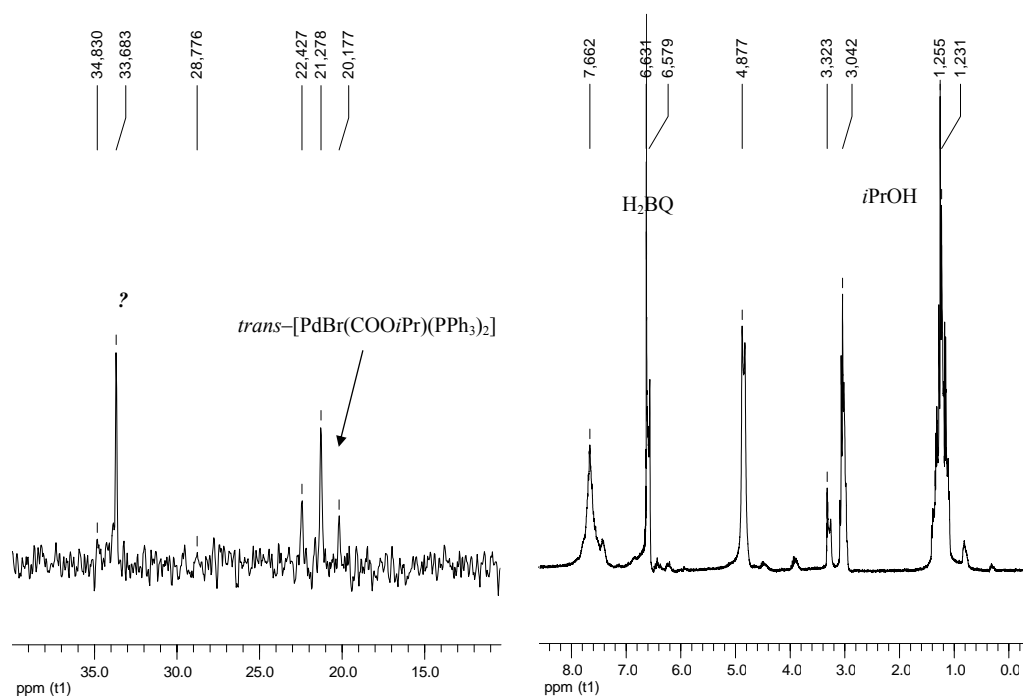


Figure 7. 1H and $^{31}P\{^1H\}$ spectra of the recovered brown solid 3 in CD_3OD at r. t..

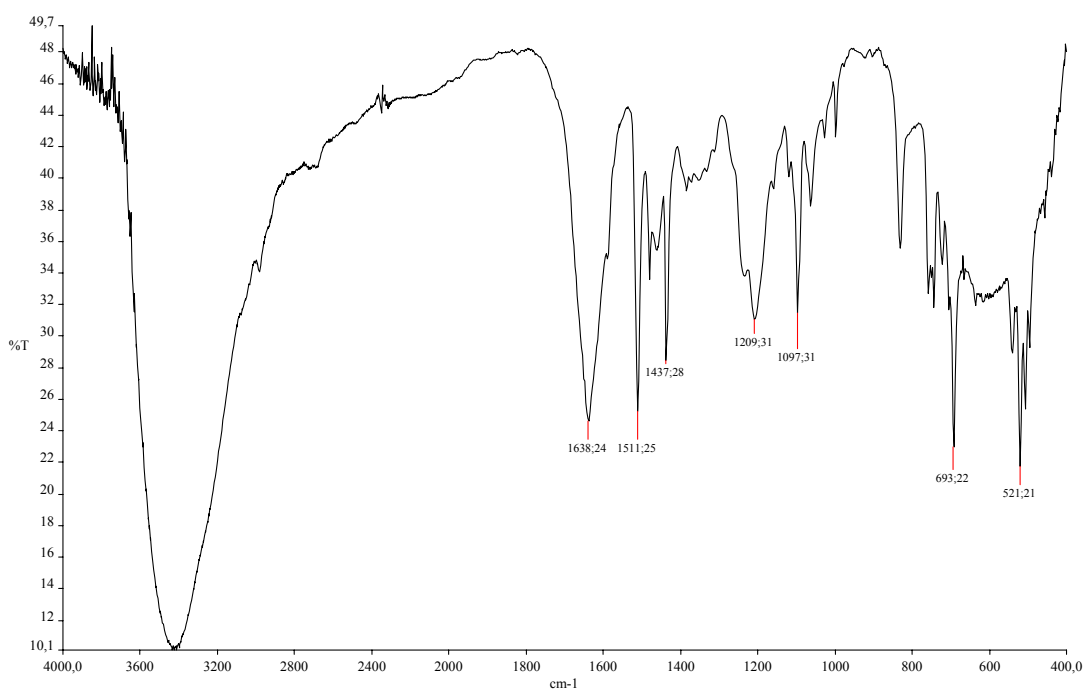
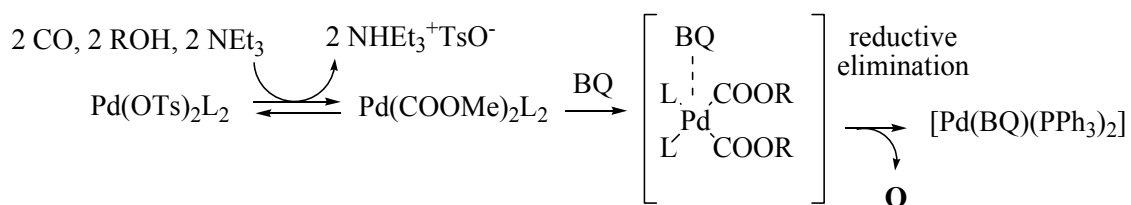


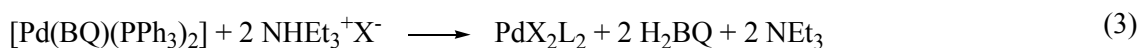
Figure 8. IR in KBr of the recovered brown solid **3**.

Product forming step and attempted reformation of the precursor. The major product of the oxidative carbonylation of *i*PrOH is the corresponding oxalate, which is likely formed from a dicarboisopropoxy–Pd(II) species. In Chapter 3 it has been reported that BQ favors the reductive elimination of DMO from *trans*–[Pd(COOMe)₂(PPh₃)₂], probably favoring also the formation of a species having two Pd(COO*i*Pr)₂ moieties in *cis*– position. Scheme 2 shows a simplified pathway for the formation of DMO starting from the precursor *cis*–[Pd(OTs)₂(PPh₃)₂], in which [Pd(BQ)(PPh₃)₂]₂ is also formed.



Scheme 2. Pathway for the formation of DMO from starting from *cis*–[Pd(OTs)₂(PPh₃)₂].

Since this chapter deals with the oxidative carbonylation of *i*PrOH using the precursor *trans*-[PdBr₂L₂], we planned to study some model reactions related to this system. However, this precursor revealed to be not so reactive like the cationic complex *cis*-[Pd(OTs)₂L₂]. Moreover, several attempts to isolate a dicarboisopropoxy complex were unsuccessful. Therefore, we studied the reactivity of NHEt₃⁺Br⁻ with the system obtained after the product forming step from *trans*-[Pd(COOMe)₂(PPh₃)₂], which should close the catalytic cycle when using the precursor *trans*-[PdBr₂L₂] in the presence of NEt₃:



In a HP-NMR tube *trans*-[Pd(COOMe)₂(PPh₃)₂] (0.005 mmol) and BQ (Pd/BQ = 1/10) were dissolved in CD₂Cl₂. The solution was pressurized with 4 atm of CO. All the operations were carried out at -78 °C. As shown in Figure 9, the complex is stable in solution from -78 °C up to 25 °C, temperature at which new signals appear attributed to [Pd(BQ)(PPh₃)₂]₂ and *trans*-[Pd(COOMe)(OMe)(PPh₃)₂]. At this temperature the formation of oxalate becomes evident (*ca.* 10–15%) (this was already described in Chapter 3). At this point the NMR tube was again cooled down to -78 °C after which BrNHEt₃ was added (Pd/N = 1/2) and CO was readmitted (4 atm). No significant change was observed warming up to 25 °C, but at 40 °C the signals of [Pd(BQ)(PPh₃)₂]₂ and *trans*-[Pd(COOMe)(OMe)(PPh₃)₂] disappear. No other change has been observed increasing the temperature even up to 60 °C. It has been expected the formation of *trans*-[PdBr₂(PPh₃)₂] has been expected to occur (reaction (3)). The ¹H NMR spectrum showed the signals of H₂BQ and NEt₃, however the ³¹P{¹H} spectrum did not show the signal of the expected *trans*-[PdBr₂(PPh₃)₂] (23.3 ppm in CD₂Cl₂ at 40 °C).* In any case, BrNHEt₃ interacts with [Pd(BQ)PPh₃]₂.

* There were signals of unidentified species at *ca.* 27 ppm and 22 ppm.

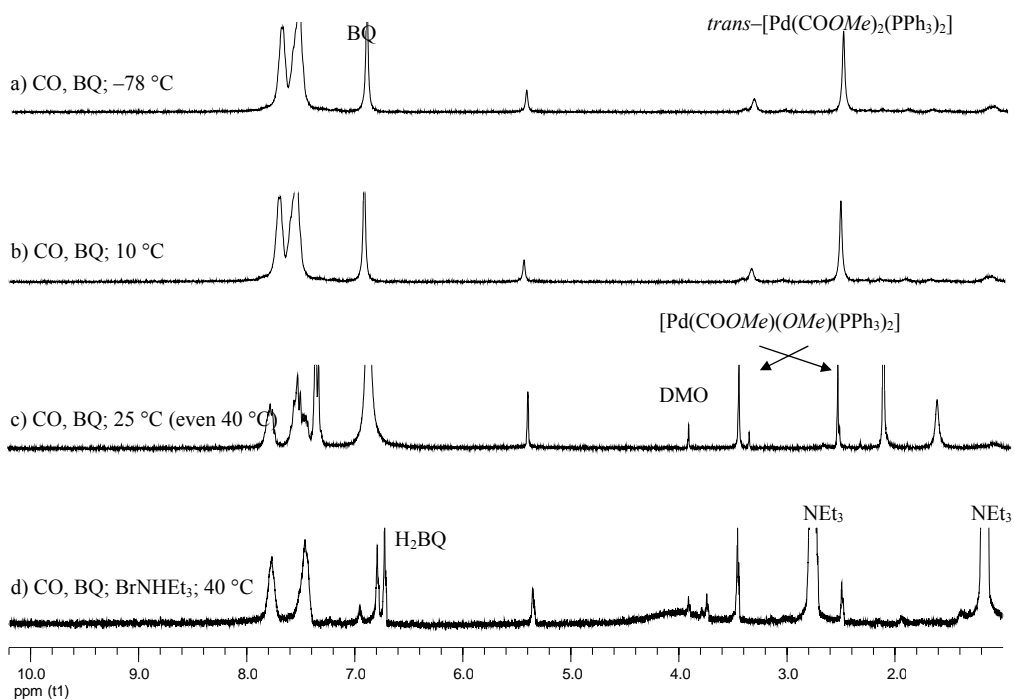
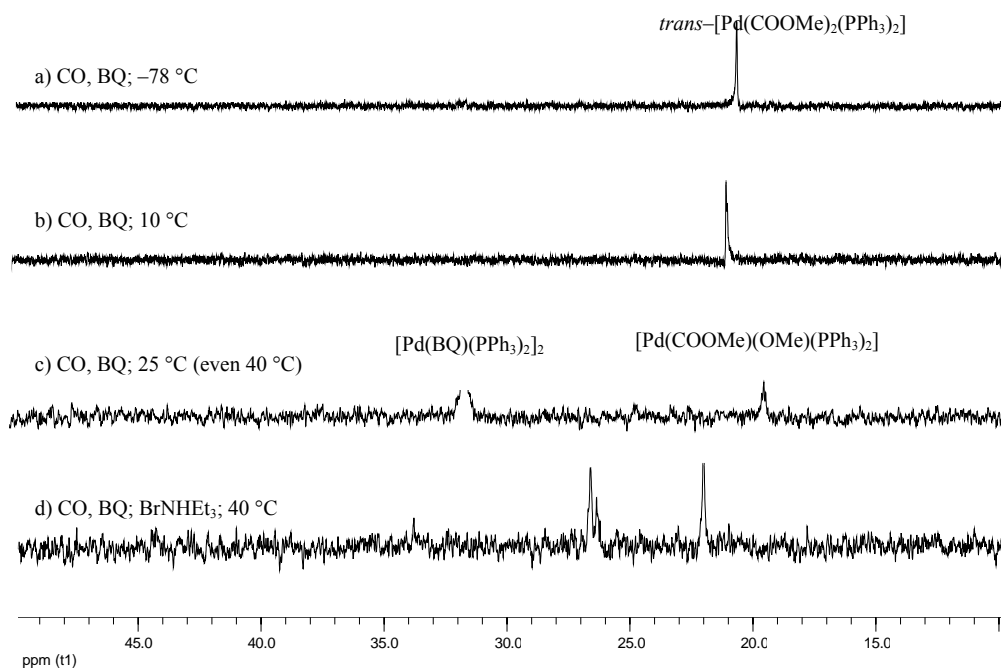
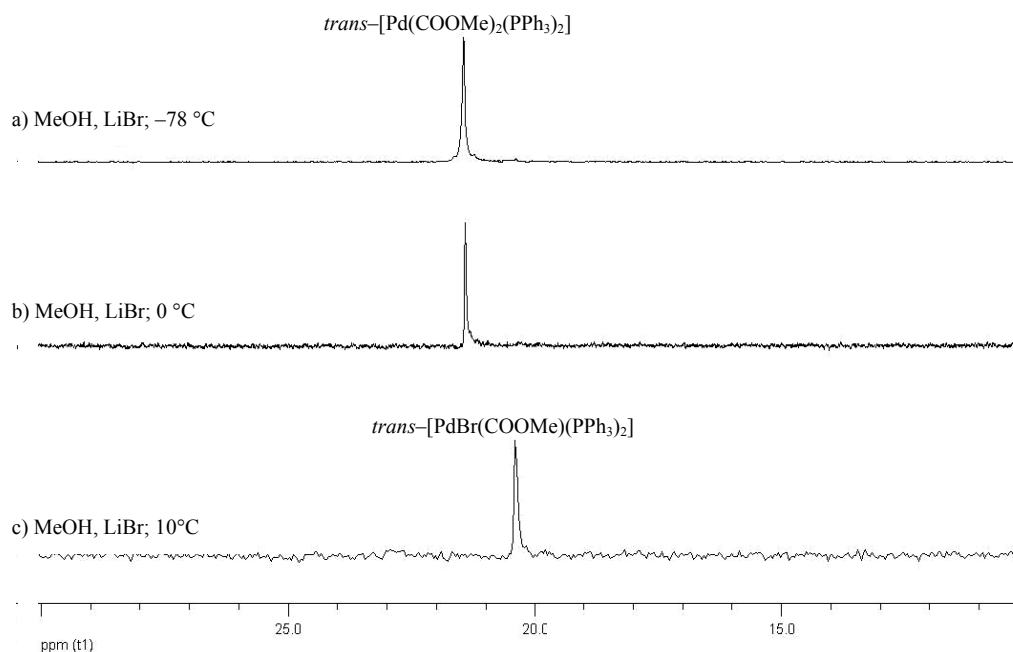


Figure 9. Selected $^{31}\text{P}\{^1\text{H}\}$ and ^1H NMR spectra in CD_2Cl_2 of the reactivity of *trans*- $[\text{Pd}(\text{COOMe})_2(\text{PPh}_3)_2]$.

Reactivity with LiBr. The promoting effect of LiBr was unexpected, because Br^- is a strongly coordinating ligand. We suggested that this anion may coordinate Pd(0) species thus favoring its reoxidation. In addition, we suggest that this anion may favor the isomerisation from *trans* to *cis* of dicarboxy species, thus favoring the reductive elimination of O. In order to check this latter hypothesis the reactivity of *trans*-[Pd(COOMe)₂(PPh₃)₂] with LiBr was studied. A solution of LiBr (0.010 mmol) in 0.15 mL MeOH was added to a solution of *trans*-[Pd(COOMe)₂(PPh₃)₂] in CD₂Cl₂ (Pd/Br = 1/2) in a NMR tube at -78 °C. As shown in Figure 10 *trans*-[Pd(COOMe)₂(PPh₃)₂] at 10 °C is converted to *trans*-[PdBr(COOMe)(PPh₃)₂]. A closer inspection into the ¹H spectrum shows that the H(PPh₃)/H(COOCH₃) intensity ratio lowers from *ca.* 6/30 to 3/30, without appearance of any other species having -COOMe groups, such as for example carbonate or oxalate.



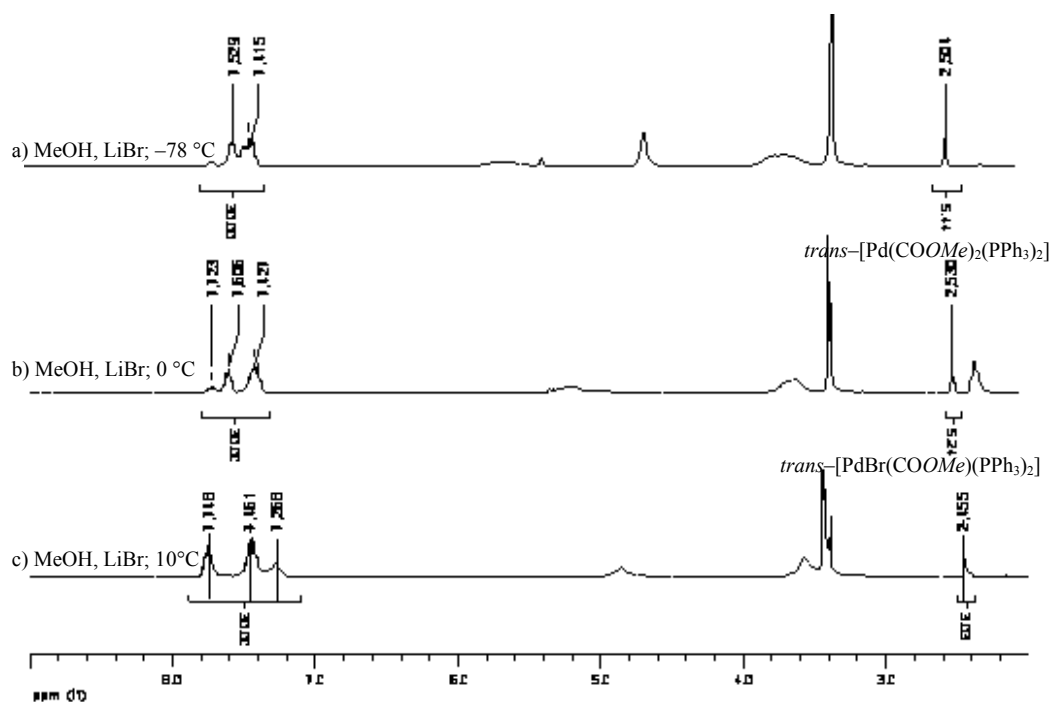
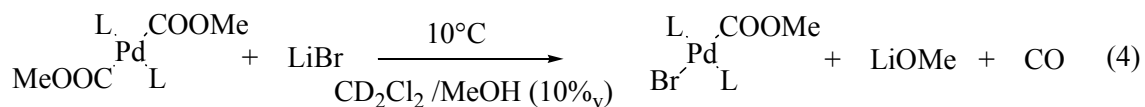


Figure 10. Selected $^{31}\text{P}\{^1\text{H}\}$ and ^1H NMR spectra in CD_2Cl_2 of the reactivity of *trans*- $[\text{Pd}(\text{COOMe})_2(\text{PPh}_3)_2]$ with LiBr.

Therefore, Br^- interacts with the palladium centre however without formation of oxalate, but rather with loss of a COOMe ligand (4). However, it should be noticed that this occurs in the NMR tube under relatively low pressure.



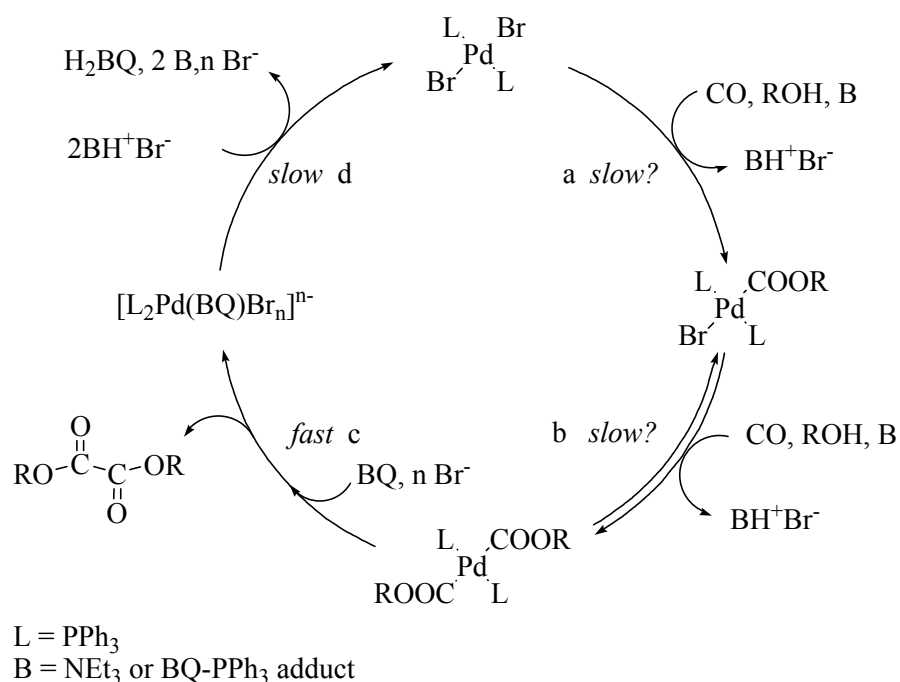
As matter of fact, under the conditions of Graph 3 (85 atm, 90 °C), the rate of formation of **O** increases upon increasing the Br/Pd ratio, whereas the formation of **C** is little influenced and remains low. These facts suggest that at high CO pressure the loss of a COOMe moiety might occurs only to a minor extent, if not at all.

Proposed catalytic cycle. Scheme 3 shows a simplified catalytic cycle for the oxidative carbonylation of *i*PrOH catalyzed by *trans*-[PdBr₂(PPh₃)₂]. Three complexes were detected after catalysis, *i. e.* the precursor, *trans*-[PdBr(COO*i*Pr)(PPh₃)₂] and [Pd(BQ)(PPh₃)₂]₂ when using a low BQ/Pd ratio in experiments carried in an autoclave at high pressure and temperature. These complexes might be involved in the slow step of catalysis.

In the absence of BQ *trans*-[PdBr(COO*i*Pr)(PPh₃)₂] is stable. In fact, it has been synthesized in high yield when the precursor is treated with CO in *i*PrOH in the presence of NEt₃ at 80–90 °C under 40–80 atm of CO. Under these conditions it is stable for several hours, without formation of **O**, **C** or **A**. However, in the presence of BQ high catalytic activity is observed. Even higher activity can be achieved in the presence of LiBr. Br⁻ might add to the precursor or to *trans*-[PdBr(COO*i*Pr)(PPh₃)₂], thus preventing the coordination of the reacting molecules to the metal centre and inhibiting the catalysis, which is the opposite of what observed. Therefore, it is unlikely that these complexes represent a resting state.

[Pd(BQ)(PPh₃)₂]₂ has been detected also when all BQ was consumed, so it is also rather stable. Br⁻ might coordinate this Pd(0) complex to form anionic Pd(0) complexes of the type [PdBr(BQ)(PPh₃)₂]⁻ or [PdBr₂(BQ)(PPh₃)₂]²⁻.^{*} The negative charge of these Pd(0) complexes might make their reoxidation easier. Is this the slow step of the catalysis?

^{*} For the reoxidation of Pd(0) species see also Chapter 3.



Scheme 3. Simplified mechanism of the oxidative carbonylation of alkanol toward oxalate catalyzed by Pd(II) complexes in presence of BQ and B and LiBr.

Conclusions

The activity and selectivity toward oxalate of the oxidative carbonylation of *i*PrOH catalyzed by PdX₂L₂ are strongly influenced by the nature of X, L and promoters (NEt₃, LiBr, L, etc.). Higher catalytic performance toward **O** is obtained using Pd(II) catalyst precursor with strongly coordinating X (Br) and in presence of the base. Additional L, which gives an adduct with BQ, and LiBr enhance the catalytic activity, but have a minor effect on the formation of **C**. The Br⁻ anion might *i*) coordinate the Pd(0) formed in the product forming step, thus enhancing its reoxidation and *ii*) favor the isomerisation from *trans* to *cis* of the intermediate complexes.

Experimental section

Instrumentation and materials

All reactions were carried out using standard Schlenk techniques under an atmosphere of argon. Chemicals were purchased from Sigma–Aldrich, Acros Chimica, Strem Chemicals and Eurisotop. The IR spectra were recorded in nujol mull or in KBr on a Nicolet FTIR instrument mod. Nexus. NMR spectra were recorded on Bruker 300 MHz spectrometers. ^{31}P spectra were measured ^1H decoupled. All ^1H chemical shifts are reported relative to the residual proton resonance in the deuterated solvents. ^{31}P signals were referenced to an 85 % aqueous solution of H_3PO_4 . NMR under pressure was performed using a special glass tube (resistant up to 13 atm) purchased from the Wilmad Lab Glass. GC analysis was performed on: a) Hewlett–Packard Model 6890 chromatograph fitted with HP5, 30 m \times 0.32 μm \times 0.25 μm column (detector: FID; carrier gas: N_2 , 0.7 mL/min; oven: 40 $^\circ\text{C}$ (3.5 min) to 250 $^\circ\text{C}$ at 15 $^\circ\text{C}/\text{min}$). b) Hewlett–Packard Model 5890 Series II chromatograph fitted with 20 % Carbowax 20 M on 80–100 mesh Chromosob W, 1 m \times 2.3 mm ID packed column (detector: FID; carrier gas: N_2 ; 25 mL/min; oven: 80 $^\circ\text{C}$). Carbon monoxide (purity higher than 99%) was supplied by SIAD Spa (Italy). The PPh_3 , ($z\text{Y}-\text{C}_6\text{H}_4$) $_3\text{P}$ ($z = o, m, p$; $\text{Y} = \text{CH}_3, \text{CH}_3\text{O}, \text{F}$), [o,o' (CH_3O) $_2(\text{C}_6\text{H}_3)$] $_3\text{P}$) PdCl_2 , LiCl , LiBr , LiI , BrNHET_3 , NEt_3 , and anhydrous solvent ($i\text{PrOH}$ and MeOH) were purchased from commercial sources and used as received. 1,4–benzoquinone (BQ) was purified before use from ethyl ether. $\text{PdCl}_2(\text{PhCN})_2$ ¹² and *trans*– $[\text{PdCl}_2(\text{PPh}_3)_2]$,¹³ *trans*– $[\text{Pd}(\text{OAc})_2(\text{PPh}_3)_2]$,¹⁴ *trans*– $[\text{Pd}(\text{OTs})_2(\text{PPh}_3)_2]$ ¹⁵, *cis*– $[\text{Pd}(\text{C}_2\text{O}_4)(\text{PPh}_3)_2]$ (*cfr.* Chapter 2) and *trans*– $[\text{Pd}(\text{COOMe})_2(\text{PPh}_3)_2]$ (*cfr.* Chapter 3) were prepared according to literature procedures.

Preparation of the complexes

Synthesis of $[\text{PdCl}_2\text{L}_2]$ ($\text{L} = (z\text{Y}-\text{C}_6\text{H}_4)_3\text{P}$ ($z = o, m, p$; $\text{Y} = \text{CH}_3, \text{CH}_3\text{O}, \text{F}$); [o,o' (CH_3O) $_2(\text{C}_6\text{H}_3)$] $_3\text{P}$). To a solution of $[\text{PdCl}_2(\text{PhCN})_2]$ (77 mg, 0.20 mmol) in 5 mL of

EtOH a solution of the ligand (0.44 mmol) in 5 mL of Et₂O was added dropwise. After 20 min under stirring at room temperature the solution was concentrated at *ca.* 2 mL and Et₂O (20 mL) was added. The microcrystalline solid that was formed was filtered off, washed with Et₂O and dried under vacuum.

trans-[PdCl₂(*o*CH₃-PPh₃)]. Yield: 96 %. Elem. anal. Calcd for C₄₂H₄₂Cl₂O₆P₂Pd: C, 57.19; H, 4.80; Found: C, 57.23 ; H, 4.76 .

trans-[PdCl₂(*m*CH₃-PPh₃)]. Yield: 95 %.

trans-[PdCl₂(*p*CH₃-PPh₃)]. Yield: 93 %.

trans-[PdCl₂(*o*MeO-PPh₃)]. Yield: 97 %.

trans-[PdCl₂(*m*MeO-PPh₃)]. Yield: 96 %.

trans-[PdCl₂(*p*MeO-PPh₃)]. Yield: 93 %.

trans-[PdCl₂(*o,o'*MeO-PPh₃)]. Yield: 95 %.

trans-[PdCl₂(*p*F-PPh₃)]. Yield: 94 %.

Synthesis of [PdBr₂L₂] (L = PPh₃, (zY-C₆H₄)₃P (z = *o*, *m*, *p*; Y= CH₃, MeO, F), [*o,o'*(MeO)₂(C₆H₃)₃P). To a suspension of [PdCl₂L₂] (0.10 mmol) in 5 mL of anhydrous *i*PrOH/CHCl₃ (1/1) a solution of LiBr (2.4 mmol) and ligand (0.2 mmol) in 5 mL of *i*PrOH was added. After 2 h under stirring at room temperature the solution was concentrated to half volume and Et₂O (*ca.* 5 mL) was added. The formed microcrystalline solid was filtered off, washed several time (*ca.* 3–4) with *i*PrOH and Et₂O, and dried under vacuum.

trans-[PdBr₂(PPh₃)]. Yield: 96 %. Elem. anal. Calcd for C₃₆H₃₀Br₂P₂Pd: C, 54.68; H, 3.82; Found: C, 53.61 ; H 3.92 .

trans-[PdBr₂(*o*CH₃-PPh₃)]. Yield: 89 %.

trans-[PdBr₂(*m*CH₃-PPh₃)]. Yield: 95 %.

trans-[PdBr₂(*p*CH₃-PPh₃)]. Yield: 96 %..

trans-[PdBr₂(*o*MeO-PPh₃)]. Yield: 90 %.

trans-[PdBr₂(*m*MeO-PPh₃)]. Yield: 91 %.

trans-[PdBr₂(*p*MeO-PPh₃)]. Yield: 97 %.

trans-[PdBr₂(*o,o'*MeO-PPh₃)]. Yield: 92 %.

trans-[PdBr₂(*p*F-PPh₃)]. Yield: 93 %.

Synthesis of *cis*-[Pd(SO₄)(PPh₃)₂]. To a 0.1 mmol of *trans*-[Pd(OAc)₂(PPh₃)₂] in 20 mL EtOH a slight excess of H₂SO₄ was added dropwise. After *ca.* 10 minutes a yellow solid precipitated. The suspension was stirred for 30 more minutes. After adding 20 mL petrol ether, the solid was collected on a filter, washed with H₂O, EtOH, petroleum ether and dried under vacuum. Yield 80 %.

Synthesis of *trans*-[PdBr(COO*i*Pr)(PPh₃)₂]. A mixture of *trans*-[PdBr₂(PPh₃)₂] (0.1 mmol), PPh₃ (0.1 mmol) and NEt₃ (0.2 mmol) in 6 ml of *i*PrOH was added to a glass bottle which was placed into an autoclave. The autoclave was purged with CO and pressurized with 50 atm of the same gas at room temperature. After heating at 80 °C for 4 h under stirring, the autoclave was cooled to room temperature and depressurized. The microcrystalline product was separated by filtration, washed with the alkanol and dried under vacuum. Yield 82 %. IR (KBr): 1665 s (ν_{CO}), 1042 br (ν_{COC}) cm⁻¹.

Synthesis of H₂BQ–BQ adduct

BQ (1 mmol) and H₂BQ (1 mmol) were dissolved, under argon atmosphere, in 20 mL of MeOH and the solution was refluxed under stirring. Immediately a black solid precipitated. The suspension was stirred for 3 h more. After this time the solid was collected on a filter, washed MeOH and dried under vacuum. IR (KBr): 1630 br cm⁻¹. The NMR data is reported in Table 5.

Table 5. ^1H and $^{31}\text{P}\{^1\text{H}\}$ NMR data of the synthesized compound.

<i>Compound</i>	$\delta^1\text{H}$ NMR [ppm]	$\delta^{31}\text{P}\{^1\text{H}\}$ NMR [ppm]
<i>trans</i> -[PdCl ₂ (PPh ₃) ₂]	7.73–7.22 (m, 30 H, Ph)	24.5 (s)
<i>trans</i> -[PdBr ₂ (PPh ₃) ₂]	7.75–7.21 (m, 30 H, Ph)	23.2 (s)
<i>trans</i> -[PdCl ₂ (yCH ₃ -PPh ₃) ₂] ^a y = <i>meta</i>	7.69–7.12 (m, 24 H, Ph)	25.2 (s)
	2.35 (s, 18 H, CH ₃ -Ph)	
	<i>para</i> 7.61–7.22 (m, 24 H, Ph)	23.0 (s)
	2.39 (s, 18 H, CH ₃ -Ph)	
<i>trans</i> -[PdBr ₂ (yCH ₃ -PPh ₃) ₂] y = <i>orto</i>	7.36–7.18 (m, 24 H, Ph)	23.5 (brs)
	2.40 (s, 18 H, CH ₃ -Ph)	
	<i>meta</i> 7.62–7.23 (m, 24 H, Ph)	23.7 (s)
	2.34 (s, 18 H, CH ₃ -Ph)	
<i>trans</i> -[PdCl ₂ (yMeO-PPh ₃) ₂] y = <i>orto</i>	7.581–7.16 (m, 24 H, Ph)	21.5 (s)
	2.37 (s, 18 H, CH ₃ -Ph)	
	7.72–6.89 (m, 24 H, Ph)	12.5 (s)
	3.70 (s, 18 H, MeO-Ph)	
<i>trans</i> -[PdBr ₂ (yMeO-PPh ₃) ₂] y = <i>orto</i>	7.41–6.96 (m, 24 H, Ph)	26.6 (s)
	3.72 (s, 18 H, MeO-Ph)	
	<i>para</i> 7.63–6.92 (m, 24 H, Ph)	20.8 (s)
	3.83 (s, 18 H, MeO-Ph)	
<i>trans</i> -[PdBr ₂ (yMeO-PPh ₃) ₂] y = <i>orto</i>	7.42–6.78 (m, 24 H, Ph)	11.3 (s)
	3.52 (s, 18 H, MeO-Ph)	
	<i>meta</i> 7.42–6.83 (m, 24 H, Ph)	25.7 (s)
	3.76 (s, 18 H, MeO-Ph)	
<i>trans</i> -[PdCl ₂ (<i>o,o'</i> MeO-PPh ₃)]	7.62–6.91 (m, 24 H, Ph)	19.5 (s)
	3.83 (s, 18 H, MeO-Ph)	
	7.56–6.64 (m, 18 H, Ph)	1.5 (s)
	3.61 (s, 36 H, MeO-Ph)	
<i>trans</i> -[PdBr ₂ (<i>o,o'</i> MeO-PPh ₃)]	7.57–6.45 (m, 18 H, Ph)	2.8 (s)
	3.62 (s, 36 H, MeO-Ph)	
<i>trans</i> -[PdCl ₂ (pF-PPh ₃) ₂]	7.66–7.11 (m, 24H, Ph)	22.2 (s)
<i>trans</i> -[PdBr ₂ (pF-PPh ₃) ₂]	7.69–7.09 (m, 24 H, Ph)	20.9 (s)

<i>cis</i> -[Pd(SO ₄)(PPh ₃) ₂]	7.66–6.94 (m, 30 H, Ph)	35.0 (s)
<i>trans</i> -[PdBr(COO <i>i</i> Pr)(PPh ₃) ₂]	7.75–7.41 (m, 30 H, Ph)	20.04 (s)
	3.66 (m, 1 H, OCH)	
	0.32 (d, 6 H, CH ₃)	
H ₂ BQ–BQ adduct	7.26–6.72 (m, H, Ar)	

NMR spectra were taken in CDCl₃ at r. t. Abbreviations: s, singlet; d, doublet; brs, broad singlet. ^(a) with *o*CH₃–PPh₃ the complexes is not soluble.

Catalytic oxidative carbonylation of *i*PrOH

Typically, 5 mL of a solution of NEt₃ in *i*PrOH was introduced into a *ca.* 20 mL glass bottle containing 0.001 mmol of catalyst precursor and the desired amount of ligand and BQ. The glass bottle was then placed in an autoclave of *ca.* 50 mL volume. The autoclave was first purged several times (4–5) with CO, then pressurized and heated to the desired pressure and temperature. The solution was stirred with a magnetic bar. After the desired reaction time the autoclave was rapidly cooled to 0 °C and then slowly depressurized. The solution was analyzed by GC using *n*–undecane and toluene as internal standards.

Reactivity of *trans*-[PdBr₂(PPh₃)₂] in oxidative carbonylation conditions

Trans-[PdBr₂(PPh₃)₂] (0.1 mmol), BQ, LiBr and eventually NEt₃ (Pd/Br/NEt₃/BQ = 1/4/2/5) were added to 5 mL of anhydrous *i*PrOH in a glass bottle introduced in a *ca.* 70 mL autoclave. After purging with CO, the autoclave was pressurized with 70 atm of CO at 25 °C and then warmed up to the reaction temperature, 90 °C, and maintained at this temperature for 1 hours. At the end of the reaction the autoclave was quickly cooled down to 0 °C and vented. The solution was analyzed by GC. When in absence of NEt₃, a yellow precipitate formed (70,2 mg) was collected on a filter, washes with *i*PrOH and dried under vacuum. When in presence also of NEt₃ the yellow solid (52.2 mg) formed by removing the solvent under vacuum and adding MeOH. The solid was separated by filtration. From the solution, after removing MeOH by

vacuum, a brown pitchy residue was recovered. In both case the solids recovered were analyzed by IR and NMR.

High pressure NMR experiments

It has been used the same procedure already discussed in Chapter 3.

References

- (1) Current, S. P. *J. Org. Chem.* **1983**, *48*, 1779.
- (2) Pearson, D. M. ; Waymouth R. M. *Organometallics* **2009**, *28*, 3896.
- (3) (a) Amatore, C.; Azzabi, M.; Jutand, A. *J. Am. Chem. Soc.* **1991**, *113*, 8375. (b) Negishi, E.; Takahashi, T.; Akiyoshi, K. *J. Chem. Soc., Chem. Commun.* **1986**, 1338.
- (4) (a) Popp, B. V.; Thorman, J. L.; Sthal, S. S. *J. Mol. Catal. A: Chem.* **2006**, *251*, 2. (b) Amatore, C.; Bensalem, S.; Ghalem, S.; Jutand, A.; Fenech, D.; Galia, A.; Silvestri, G. C. *R. Chimie* **2004**, *7*, 737. (c) Amatore, C. and Jutand, A. *Acc. Chem. Res.* **2000**, *33*, 314.
- (5) (a) Pearson, R. G. *J. Am. Chem. Soc.* **1963**, *85*, 3533. (b) Ho, T. L. *Chem. Rev.* **1975**, *75*, 1.
- (6) Calò, V.; Giannoccaro, P.; Nacci, A.; Monopoli, A. *J. Organomet. Chem.* **2002**, *645*, 152.
- (7) van Leeuwen, P. W. N. M., Zuideveld, M. A.; Swennenhuis, B. H. G.; Freixa, Z.; Kamer, P. C. J.; Goubitz, K.; Fraanje, J.; Luitz, M.; Spek, A. L. *J. Am. Chem. Soc.* **2003**, *125*, 5523.
- (8) Dekker, G.P.C.M.; Buijjs, A.; Elsevier, C.J.; van Leeuwen, P.W.N.M.; Smeets, W.J.J.; Spek, A.L.; Wang, Y.F. and Stam, C.H. *Organometallics* **1992**, *11*, 1937.
- (9) Wilkins, R. G. *Kinetics and mechanism of reactions of transition metal complexes*, Wilkins, R. G, Ed.; VCH, **1991**.
- (10) Khabibulin, V. R.; Kulik, A. V.; Oshanina, I. V.; Bruk, L. G.; Temkin, O. N.; Nosova, V. M.; Ustynyuk, Y. A.; Bel'skii, V. K.; Stash, A. I.; Lysenko, K. A.; Antipin, M. Y. *Kinet. Katal.* **2007**, *48*, 228.
- (11) (a) Arshad, M.; Beg, A.; M. S. Siddiquiri, M. S. *Tetrahedron* **1966**, *22*, 2203. (b) Ramirez, F. and Dershowitz, S. *J. Am. Chem. Soc.* **1956**, *78*, 5614.
- (12) Doile, J. R.; Slade, P. E.; Jonassen, H. B. *Iorg. Synth.* **1960**, *6*, 216.

-
- (13) Jenkins, J. M.; Verkade, J. C. *Inorg. Synth.* **1968**, *11*, 108.
- (14) Stephenson, T. A.; Morehouse, S. M.; Powell, A. R.; Heffer, J. P.; Wilkinson, G. *J. Chem. Soc.* **1965**, 3632.
- (15) Cavinato, G.; Vavasori, A.; L. Toniolo, L.; Dolmella, A. *Inorg. Chim. Acta* **2004**, *357*, 2737.

Chapter 5

Pd(II)–Diphosphine Catalysts for the Oxidative Carbonylation of Alkanols

Introduction

The previous chapter dealt with the study of monophosphine complexes for the catalytic oxidative carbonylation of alkanols, in particular with the results achieved using the catalyst precursors *trans*-[PdX₂(PPh₃)₂] (X = Br, Cl, OAc, OTs; X₂ = C₂O₄, SO₄) in *i*PrOH. The highest catalytic activity was obtained with the use of X = Br, and it was even higher in the presence of added LiBr. Substituted phenyl rings of the PPh₃ ligand revealed that steric effects have a major role with respect to the electronic ones.

Diphosphines may have a marked role in the catalysis, in particular those retaining a *cis*-coordination during the whole course of catalysis. In fact, the elementary migration steps of the catalytic cycle require that the interacting moieties occupy two coordination sites in *cis*-position, which is better guaranteed with *cis*-ligating diphosphines. Moreover, they may stabilize the transition state of the rate-limiting step, thus enhancing the catalytic activity.

To the best of our knowledge, up to now no investigation has appeared in the literature reporting the use of diphosphine-based catalysts for the oxidative carbonylation of alkanols.

Hereafter, we present catalytic and mechanistic studies concerning the use of catalyst precursors of the type *cis*-[PdX₂(P∩P)] for this reaction.

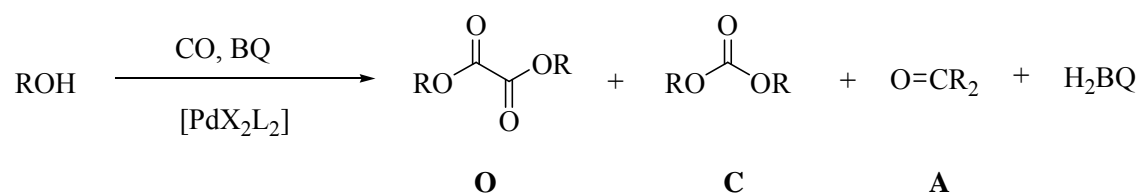
Results and discussion

Influence of the anion of the catalyst precursor [PdX₂(dppf)] (dppf = 1,1'-bis(diphenylphosphino)ferrocene

In Chapters 2, 3 and 4 it was reported that when using Pd(II)-monophosphine complexes higher catalytic activity can be achieved in the presence of NEt₃, because the base favors the formation of Pd-COOR intermediates. In addition, it was found that no decomposition to palladium metal was observed even under relatively severe conditions (90 °C, 90 atm, 3 hours) when catalysis was carried out in *i*PrOH (Chapter 4). It was also found that when using this alcohol the mass balance between reagents and products fitted reasonably well (20 %). For these reasons we chose to carry out the catalysis in *i*PrOH and in the presence of NEt₃ also in the present investigation.

Preliminary results showed that dppf-based catalysts were more active than those with other diphosphines. Therefore, the precursors [PdX₂(dppf)] (X or X₂ = TsO,^{*} SO₄, AcO, C₂O₄, Cl) were used in order to study the influence of the anion on the activity and selectivity.

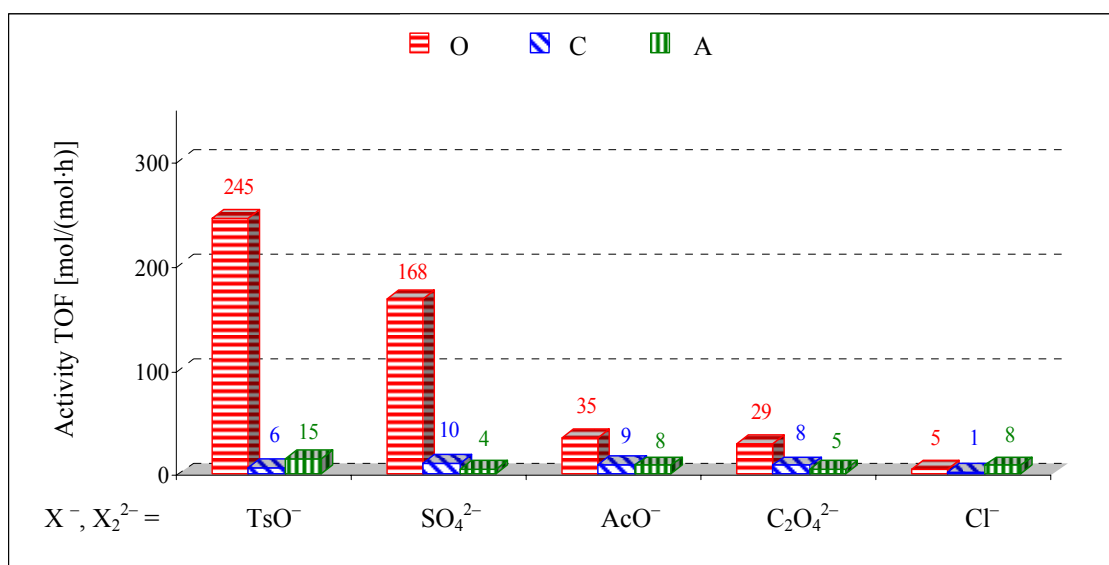
The major product was diisopropyl oxalate (**O**), while diisopropyl carbonate (**C**) was also formed. Moreover, a side reaction occurred which led to the formation of acetone (**A**).



Scheme 1. Products of the oxidative carbonylation of *i*PrOH.

^{*} This actual precursor is the cationic mono-aquo complex *cis*-[Pd(OTs)(H₂O)(dppf)](TsO).

Graph 1 shows that the TOF for **O** is influenced significantly by the coordinating properties of the anion X. The most weakly coordinating TsO gives the highest TOF to oxalate. This result is not surprising since strongly coordinating anions compete with CO and the alcohol for coordination, a prerequisite for the formation of the products. However, this behavior is the opposite of that observed with monophosphine-based precursors [PdX₂(PPh₃)₂], in which case the highest catalytic activity was achieved with X = Br and the lowest with TsO (Chapter 4).



Graph 1. Effect of the anion on the activity using *cis*-[PdX₂(dppf)]. Conditions: [Pd] = 2·10⁻⁴ mol/L, Pd/BQ/NEt₃ = 1/700/2, P_{CO} = 80 atm, T = 80 °C, 1 h, 5 mL anhydrous *i*PrOH.

With a strong coordinating anion such as Cl⁻ both activity and selectivity toward the formation of **O** are significantly depressed, whereas the TOF for the formation of **C** and **A** are less influenced. A reasonable explanation is the following. According to a schematic view (Scheme 2 cycles 1, 2 and 3), the formation of the products occurs through a Pd-OR intermediate which is common to all three products. β-Hydride elimination from Pd-OR gives a Pd(0) species and the side product **A**. Oxidation of the Pd(0) by BQ and HX gives back the catalyst.

If a migratory insertion of coordinated CO in the Pd-OR bond takes place before β-hydride elimination, a monocarboalcoxy intermediate Pd-COOR is formed. Attack of ROH,

most likely coordinated to Pd(II),¹ gives **C** and Pd(0), which is oxidized by BQ to the initial Pd(II).

For the formation of **O** it is necessary that a dicarbomethoxy species is formed before formation of **C** occurs. Going from TsO⁻ to Cl⁻ the activity toward **C** and **A** is little influenced, but instead there is a dramatic lowering of the TOF toward **O**. This suggests that once a Pd-COOR intermediate is formed, Cl⁻ competes more strongly than TsO⁻ for the coordination of another molecule of ROH or CO necessary to give the Pd(COOR)₂ species leading to the formation of **O**. This might be due to the electron withdrawing properties of the COOR ligand (Chapter 2), which may make the displacement of the Cl⁻ more difficult.

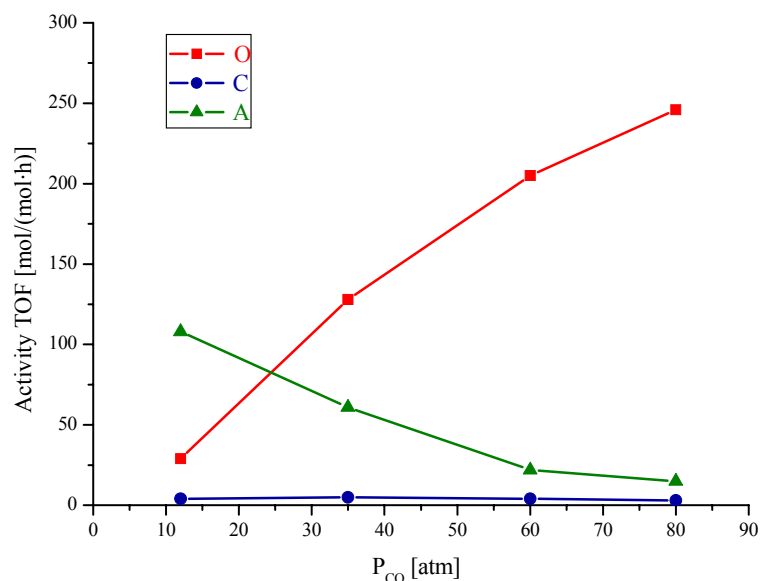
Effect of the pressure of carbon monoxide

Table 1 and Graph 2 show that upon increasing the pressure of CO the activity and the selectivity toward oxalate increases (TOF = 246 h⁻¹ at 80 atm), with a concomitant decrease of the formation of acetone. Instead, the formation of carbonate is little influenced and remains low (max 3 % selectivity).

Table 1. Effect of P_{CO} on the activity of the oxidative carbonylation reaction using *cis*-[Pd(OH₂)(OTs)(dppf)](TsO)

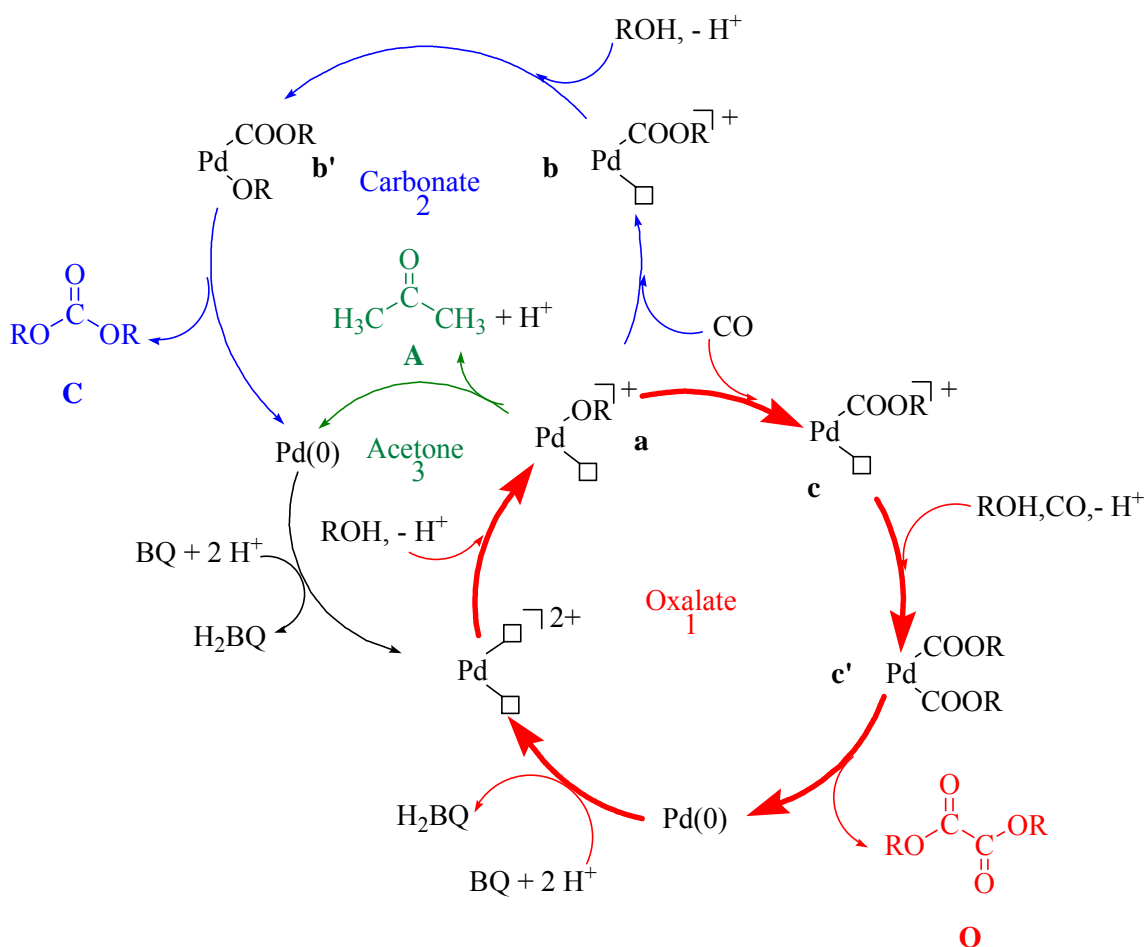
<i>Entry</i>	<i>P_{CO}</i> [atm]	<i>Activity TOF</i> [mol/(mol*h)]			<i>Selectivity</i> [%]		
		<i>O</i>	<i>C</i>	<i>A</i>	<i>O</i>	<i>C</i>	<i>A</i>
1	80	246	3	15	93	1	6
2	60	205	4	22	89	2	10
3	35	128	5	61	66	3	32
4	12	29	4	108	20	3	76

Conditions: [Pd] = 2·10⁻⁴ mol/L, Pd/BQ/NEt₃ = 1/700/2, 80 °C, 1 h, 5 mL anhydrous *i*PrOH.



Graph 2. Effect of P_{CO} on the activity of the oxidative carbonylation reaction using *cis*-[Pd(OH₂)(OTs)(dppf)](TsO). For the conditions see Table 1.

The trends of Graph 2 suggest that the formation of **O** is connected to that of **A** and that they interfere hardly with the formation of **C**. A reasonable explanation might be the following. Acetone forms through β -hydride elimination from the Pd-OR species **a**. Alternatively, this species inserts CO giving two different Pd(COOR) isomers, **b** and **c**. Species **b** is the most abundant also at relatively low CO pressure, so that its concentration is not much affected by it. **b** interacts with ROH giving intermediate Pd(COOR)(OR) (**b'**), which gives **C** and Pd(0) in a relatively slow step. Species **c** interacts with CO and ROH giving intermediate Pd(COOR)₂ (**c'**) which yields **O** and Pd(0). The CO pressure influences significantly the equilibrium between **a** and **c**, so that upon increasing the CO pressure the selectivity toward **O** increases at the expenses of **A**. Pd(0) is reoxidized by BQ and HX. Scheme 2 shows the proposed catalytic cycles.



Scheme 2. Proposed catalytic cycles for the formation of **O**, **C** and **A** ($R = iPr$).

Influence of the natural bite angle of the diphosphine ligands

The “natural bite angle” is defined as the preferred chelation angle determined by the ligand backbone only.² A wider backbone will tend to make the P–M–P angle larger and in this way it will change both the electronic and steric properties of the bidentate ligand.

The natural bite angle β_n is calculated by means of molecular mechanics, using a dummy atom for the metal that has no angular preferences and that is characterized in MM2 calculation by a metal–to–phosphorus distance, and stretching, bending (the M–P–M bending is set to zero), and dihedral force constants. In Figure 1 the metal is represented by a dot. A dummy metal atom is necessary to pull the lone pairs of the electrons and the substituent on the

phosphorus atoms in the right direction and to simulate the constraints imposed on the ligand backbone by the metal atom in a complex as exemplified by the picture for dppe on the right.³

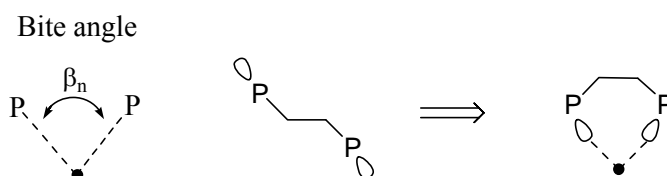


Figure 1. The bite angle explained.

In crystal structures the angles found may show a similar trend as the calculated angles β_n , but they do not have necessarily the same values.³

When chelating diphosphine-based catalysts are used the bite angle² may be a key parameter since it may influence significantly both activity and selectivity. Comprehensive examples have been published in the last two decades,^{3b, c; 4} including many attempts to rationalize the so called “bite angle effect”.⁵

As mentioned above, an increment of the bite angle can exert two distinct effects: i) it increases the effective steric bulk and ii) it electronically favors or disfavors certain geometries.^{5b} For instance, considering palladium complexes, using wide bite angle diphosphines, the *cis*–*trans* equilibrium is shifted in favor of the *trans* species.¹ An extreme case is observed with SPANphos, typically considered a *trans* diphosphine, which form *cis*–complexes only when extremely *cis*–enforcing conditions are present.⁶

By NMR investigations on *cis*–[Pd(OAc)₂(DPEphos)] it was possible to obtain information about the coordination geometry. Indeed, the complexes show only one signal in ³¹{¹H}P NMR at room temperature. However, at low temperature (below –40 °C) a multiplicity of broad and sharp signals was observed as shown in Figure 2, which suggests the occurrence of *cis*–*trans* isomerisation (Scheme 3). These equilibrium are probably favored by the formation of a palladium–oxygen bond in the *trans* cationic complex; the nearby oxygen atom can indeed

stabilize the ionic intermediate that can be formed during the interchange from the *cis*- to *trans*-neutral complexes. Similar results has been reported by using methyl palladium complexes with Xantphos type ligands.⁷

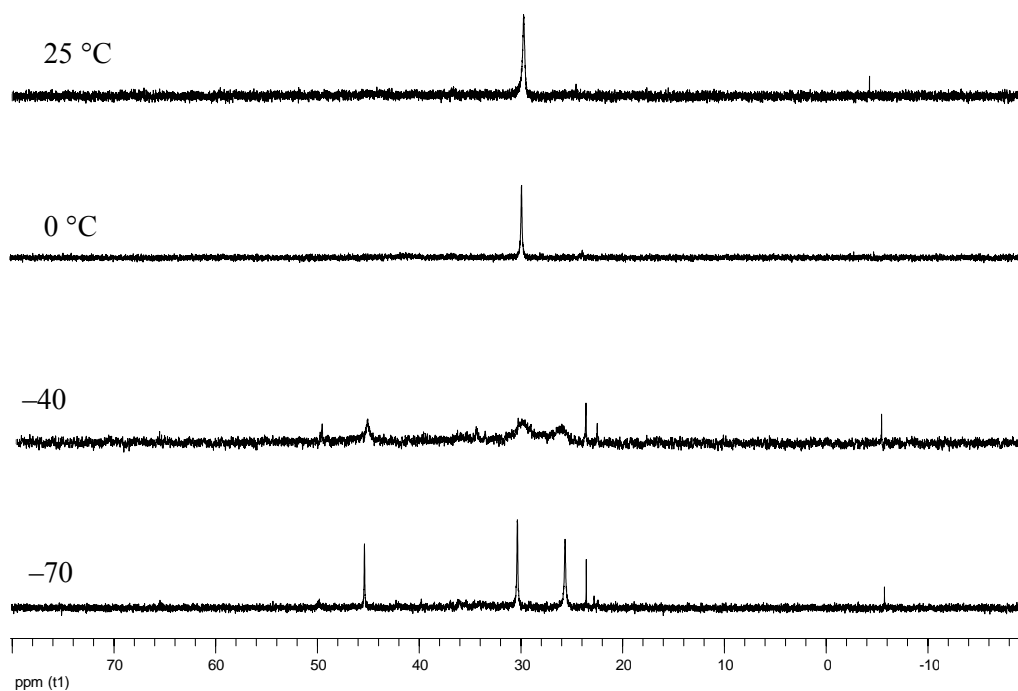
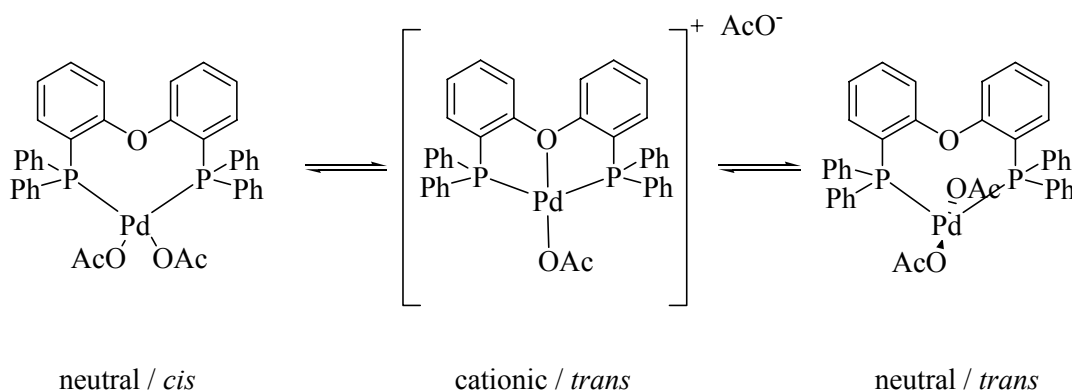


Figure 2. Variable temperature $^{31}\text{P}\{^1\text{H}\}$ NMR spectra of *cis*-[Pd(OAc)₂(DPEphos)] in CD₂Cl₂.



Scheme 3. Possible pathway for the *cis*-*trans* isomerisation.

The selected ligands cover a wide range of bite angles, from the narrowest of the series dppe, typically a *cis*-chelating diphosphine, to SPANPhos to the other extreme (Figure 3). The main goal was the understanding of the factors ruling the activity and selectivity. In Table 2 and Graph 3 the results obtained using *cis*-[Pd(OH₂)_n(OTs)_{2-n}(P∩P)](TsO)_n (n = 0, 1; P∩P = dppe, dppp, dppb, dppf, DPEphos, Xantphos) and *trans*-[Pd(OTs)₂(SPANphos)] are presented.

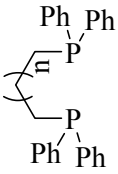
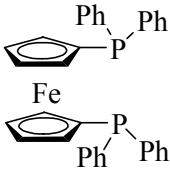
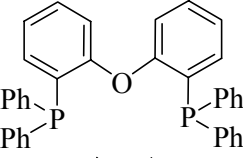
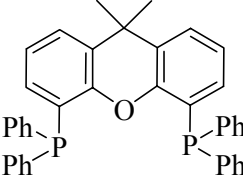
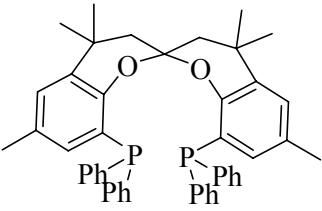
			β_n^a [°]
	n = 0	dppe	78.1
	1	dppp	86.2
	2	dppb	98.7
		dppf	99.1
		DPEphos	102.9
		Xantphos	110.0
		SPANphos	171.9 ^b

Figure 3. Diphosphine ligands used in this study. ^a The natural bite angle (β_n) are taken from ref.4g. ^b Extracted from the X-ray structure of *trans*-[PdCl₂(SPANphos)].⁸

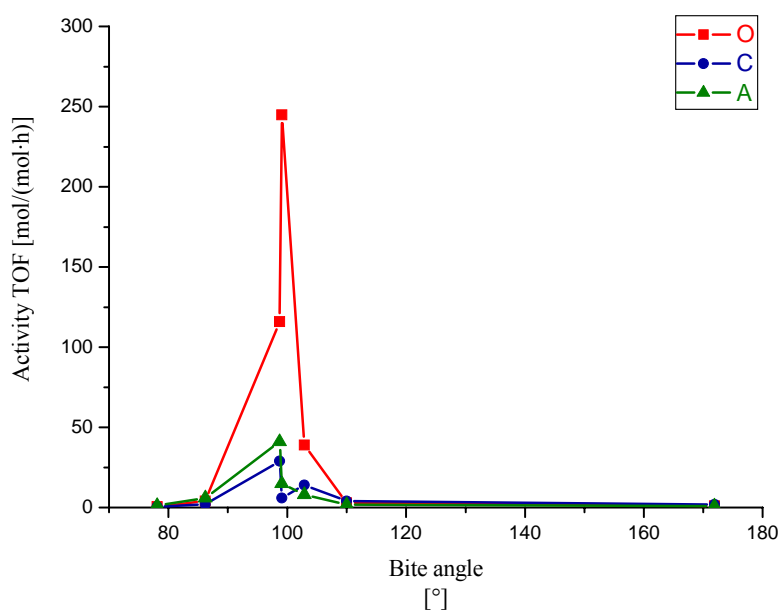
The results are reported in Table 2 and Graph 3. Both the activity and the selectivity toward oxalate depend strongly on the bite angle. Dppf presents the optimal value, whereas narrower or wider bite angles are detrimental. Bite angles of around 100° appear to be an ideal compromise. Similar bite angle effects were reported in literature when studying C–C reductive

elimination reactions using palladium complexes^{3a, d}, although for these reactions slightly wider bite angles were optimal, *e.g.* DPEphos or Xantphos.^{4g, h} Thus, the observed trend suggests that also for the present reaction the slow step of the catalytic cycle for the formation of oxalate is the reductive elimination of two COOR ligands from a dicarboalkoxy species.

Table 2. Effect of P∩P bite angle on the oxidative carbonylation

Entry	ligand	β_n^a [°]	Activity TOF [mol/(mol*h)]			Selectivity [%]		
			O	C	A	O	C	A
1	dppe	78.1	0.6	0.5	1.3	25	20	55
2	dppp	86.2	4.0	2.0	5.9	33	17	50
3	dppb	98.7	116	29	41	62	16	22
4	dppf	99.1	245	6	15	92	2	6
5	DPEphos	102.9	39	14	8	64	23	13
6	Xantphos	110.0	3.0	4.1	1.8	34	46	20
7	SPANphos	171.9 ^b	1.1	1.9	0.9	29	49	22

Conditions: [Pd] = 2.10⁻⁴ mol/L, Pd/BQ/NEt₃ = 1/700/2, P_{CO} = 80 atm, T = 80 °C, 1 h, 5 mL anhydrous *i*PrOH.



Graph 3. Bite angle effect on the activity. For the conditions see Table 2 above reported.

Electronic and steric effects of the diphosphine ligand

In order to better rationalize the steric and electronic effects it is useful to introduce here the concepts developed by Tolman.⁹ For phosphorus ligands the cone angle θ (Figure 4) is defined as the apex angle of a cylindrical cone, centred at 2.28 Å from the centre of the P atom, which touches the outermost atom of the model. The electronic parameter χ is based on the difference in the IR frequencies of $\text{Ni}(\text{CO})_3\text{L}$ and the reference compound $\text{Ni}(\text{CO})_3(\text{PtBu}_3)$. Both these parameters are widely accepted for monodentate ligands, but could be used also for defining, with good approximation, steric and electronic parameters of the bidentate ligands.

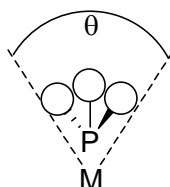


Figure 4. Tolman cone angle θ .

The electronic and the steric effects on the activity and selectivity were studied by comparing the catalytic performance of a dppf-based catalyst (the most active among those reported) with that of catalysts with modified ferrocenyl ligands having electron donating or withdrawing groups. These are shown in Figure 5.

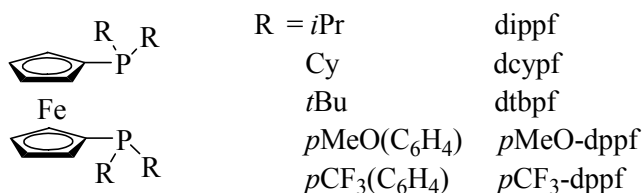


Figure 5. Modified ferrocenyl–diphosphine ligands.

The results are reported in Table 3, together with those relevant to the dppf-based catalyst for comparative purposes. The catalytic activity and selectivity are affected by both electronic and steric properties. The comparison between aryl and alkyl ferrocenyl ligands clearly shows

that the electronic parameters play a major role in controlling the activity toward oxalate. In particular the aryl ferrocenyl ligands with electron-withdrawing substituents (pCF_3) strongly inhibits the catalysis, whereas the ligand with electron-releasing groups ($pMeO$) presents a slightly accelerating effect (entries 1–3). The results reported in Table 2 suggested that for the dppf system the reductive elimination of oxalate might be the rate determining step. If this were true also for the pCF_3 -dppf ligand then a higher activity would be expected, which is not the case. Indeed, this ligand, though presenting a favorable bite angle for the reductive elimination, depresses strongly the catalytic activity. For this ligand the rate limiting step might be the reoxidation of Pd(0) that is formed in the product forming step. With the other two ligands, $pMeO$ -dppf or dppf, it seems unlikely that the rate determining step is the reoxidation one, because the activity does not differ significantly. Other hypotheses may be suggested, but in the absence of more significant data, this discussion may appear a little speculative.

Table 3. Oxidative carbonylation reaction using ferrocenyl modified ligands

Entry	$P\text{C}P$	θ^a steric parameter	χ^a electronic parameter	Activity TOF			Selectivity		
				[mol/(mol*h)]			[%]		
				O	C	A	O	C	A
1	PCF_3 -dppf	145	20.50	4	8	10	18	36	45
2	dppf	145	13.25	245	6	15	92	2	6
3	$pMeO$ -dppf	145	10.50	291	7	5	96	2	6
4	dippf	160	3.45	3.5	1.0	1.1	62	18	20
5	dcypf	170	1.40	1.7	2.2	4.3	21	27	52
6	dtbpf	182	0.00	0.9	1.3	3.7	16	21	62

Conditions: $[Pd] = 2 \cdot 10^{-4}$ mol/L, Pd/BQ/ $NEt_3 = 1/700/2$, $P_{CO} = 80$ atm, $T = 80$ °C, $t = 1$ h, 5 mL anhydrous $iPrOH$. ^a Tolman's cone angle θ and the χ values are taken from reference 9 and 10, respectively, considering the corresponding PAR_3 .

In order to gain some insights on the reoxidation step, the activity of the dppf-based catalyst was studied using different BQ/Pd ratios and for different reaction times.

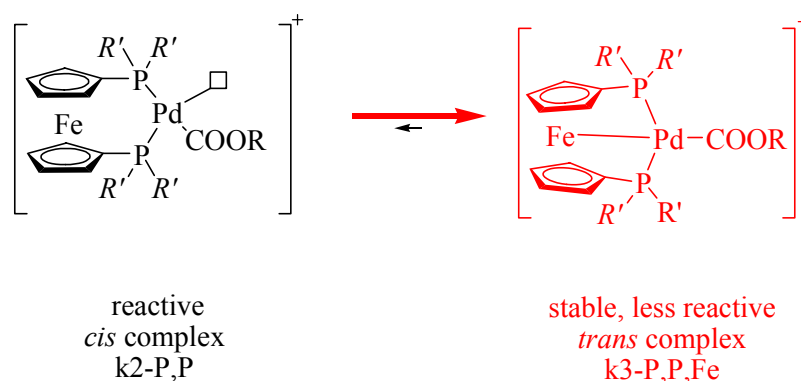
Table 4. Influence of BQ/Pd ratio on the oxidative carbonylation performance of *cis*-[Pd(OH₂)(OTs)(dppf)](TsO)

Entry	BQ/Pd [mol/mol]	time [h]	Activity TON [mol/mol]			Selectivity [%]		
			O	C	A	O	C	A
1	1400	1	253	6	13	93	2	5
2	1000	1	253	6	12	93	2	4
3	900	1	248	5	10	94	2	4
4	700	1	245	6	15	92	2	6
5	600	1	250	5	16	92	2	6
6	500	1	247	4	15	93	2	6
7	1400	2	537	11	25	94	2	4
8	700	2	543	9	31	93	2	5
9	1400	3	846	16	49	93	2	5

Conditions: [Pd] = $2 \cdot 10^{-4}$ mol/L, Pd/NEt₃ = 1/2, P_{CO} = 80 atm, T = 80 °C, t = 1h, 5 mL anhydrous *i*PrOH.

The results show that the activity toward **O** does not depend on the BQ/Pd initial ratio (entries 1–6) and exhibits a linear trend with time (entries 4, 7 and 1, 8, 9). These results suggest that in the rate determining step either i) uncoordinated BQ is not involved or ii) all palladium (or most of it) is present as a species in which Pd(0) is coordinated also by BQ, for instance [Pd(BQ)(P∩P)], which might represent a resting state. It is worth mentioning that when using *trans*-[PdBr₂(PPh₃)₂] as precursor it has been suggested that the oxidation of [Pd(BQ)(PPh₃)₂] (arising from [Pd(COOMe)₂(PPh₃)₂] and BQ in the product-forming step) might be the slow step of the catalytic cycle (Chapter 4).

All the explanations given above seem in contrast with the results obtained using the more basic alkyl ferrocenyl ligands (dippf, dcypf, dtbpf; entries 4–6 in Table 3). However, it should be considered that these ligands may also coordinate through a *k*3-P,P,Fe bonding mode, which is favored when electron-withdrawing COOMe ligand is formed as shown in Scheme 4.¹¹



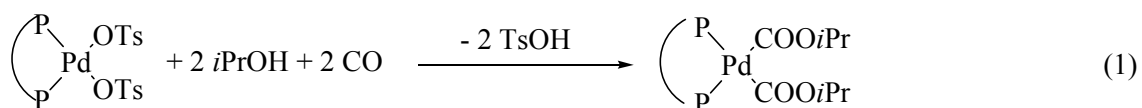
Scheme 4. Formation of Fe–Pd dative bond ($R' = t\text{Bu}, i\text{Pr}, \text{Cy}$).

Thus, there might be an equilibrium between the more stable *k3*-P,P,Fe isomer and the more active *k2*-P,P one. The dative Fe–Pd bond changes the geometry of the complexes from *cis* to *trans* and this may be a key factor that makes these complexes less active. In other words the concentration of the effective catalyst might be only a fraction of the amount indicated in Table 3 (2×10^{-4} mol/L).

It is interesting to observe that, within the dppf, dcypf, dtbpf series (entries 4–6 in Table 3), the increase of the steric hindrance favors the formation of acetone, the least bulky product and involving β -hydrogen elimination, the reaction requiring less space.

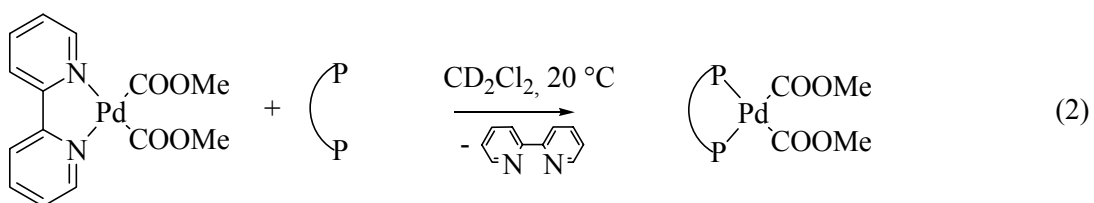
Reactivity of $[\text{Pd}(\text{COOR})_2(\text{P}\curvearrowright\text{P})]$

With the aim to gain more insights in the role of the dicarboalkoxy species that gives **O**, we tried their synthesis under conditions close to those used in catalysis, *i. e.* from $[\text{Pd}(\text{OTs})_2(\text{P}\curvearrowright\text{P})]$ dissolved in *i*PrOH, under carbon monoxide, either in the presence or absence of NEt_3 , but always in the absence of BQ.



However, in spite of the wide spectrum of conditions we checked, all attempts gave unsatisfactory results. In contrast, through the same procedure used for the synthesis of *trans*-[Pd(COOMe)₂(PPh₃)₂] in MeOH (Chapter 2), it was possible to isolate two complexes, *cis*-[Pd(COOMe)₂(P∩P)] (P∩P = dppe, and dppp). For the other diphosphines all attempts were unsuccessful even when starting from a temperature as low as - 78 °C. In particular, several attempts were made to isolate the corresponding complex with dppf. In none of the attempts dicarbomethoxy complex was formed, nor did we observe the formation of DMO, DMC, or formaldehyde. These facts suggest that the dppf complex undergoes reduction to Pd(0) before a carbomethoxy species may form (*cf.* Chapter 3, Scheme 1). It is worth noting that in catalysis, *i. e.* in the presence of BQ, the dppf precursor gives the best performance (Table 2). Thus, it is BQ that makes the difference.

The reactivity of preformed *cis*-[Pd(COOMe)₂(P∩P)] (P∩P = dppe, dppp) was studied by NMR spectroscopy. The dppe complex in CD₂Cl₂ at 25 °C remained intact after 24 hours, whereas the dppp one (0.01 mmol in 1 mL) gave 80 % of DMO and unidentified Pd complexes. The same results were observed when a dipyriddy dicarbomethoxy complex, prepared separately,¹² was made to react with a diphosphine in an NMR tube. The formation of the corresponding *cis*-[Pd(COOMe)₂(P∩P)] was immediate and complete (reaction 2).



After 24 hours only the dppp complex decomposed giving 80 % oxalate. Thus these P∩P complexes present the same reactivity either in the presence or in the absence of bipy.

Therefore, in order to study the reactivity of the other hypothetical *cis*-[Pd(COOMe)₂(P∩P)] complexes that could not be synthesized, we followed the way through reaction 2. The results are reported in Table 5.

Table 5. Reactivity of [Pd(COOMe)₂(P∩P)] formed *in situ* through reaction 2

<i>Entry</i>	<i>ligand</i>	β_n^a [°]	<i>Stability</i>	<i>time</i>	<i>Conversion toward O</i> [%]
1	dppe	78.1	stable	24 h	0
2	dppp	86.2	moderately stable	24h	80
3	dppb	98.7	unstable	immediately	100
4	dppf	99.1	unstable ^b	immediately ^b	100 ^b
5	DPEphos	102.9	unstable	immediately	100
6	Xantphos	110.0	unstable	immediately	100
7	SPANphos	171.9 ^c	stable	24 h	0

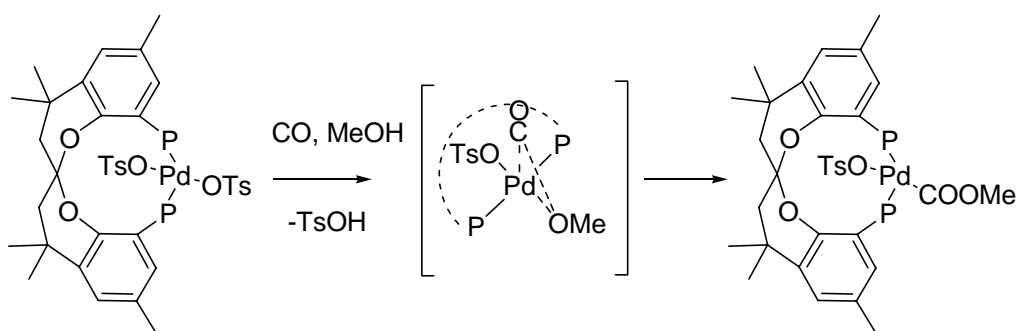
Conditions: [Pd] = 1·10⁻² molL⁻¹, T = 25 °C, 1 mL anhydrous CD₂Cl₂. ^a The natural bite angle (β_n) are taken from ref 4g. ^b Even at -78 °C and at 50 atm of CO. ^c Extracted from the X-ray structure of *trans*-[PdCl₂(SPANphos)].⁸

The reactivity of these complexes provided us with very valuable information. Compared to the others, the dppe- and dppp-dicarbomethoxy complexes are stable. These results and the poor performance of the dppe- and dppp-based catalysts (Table 2) indicate that with these diphosphines the reductive elimination of oxalate might be the slow step of the catalysis.

When using wider bite angle diphosphines, the dicarboalkoxy complexes are unstable and they decompose immediately to oxalate and Pd(0)(P∩P) (except with SPANphos). This indicates that the reductive elimination might not be the slow step, contrary to what suggested above.

Only with SPANphos the formation of oxalate has not been observed even after 24 hours. This fact was initially attributed to the formation of a *trans*- palladium compound such as *trans*-[Pd(COOMe)₂(SPANphos)] unable to eliminate oxalate. However the nature of the complexes formed *in situ* has not been determined. In order to gain more insights, the reactivity of *trans*-[Pd(OTs)₂(SPANphos)] was studied by VT ³¹P and ¹H NMR spectroscopy under conditions closer to those of catalysis (MeOH/CD₂Cl₂ = 1/10, v/v, P_{CO} = 5 atm). At -78 °C the

monocarbomethoxy complex $trans$ -[Pd(COOMe)(OTs)(SPANphos)] is formed, which is stable even in presence of NEt_3 up to $60^\circ C$. Above this temperature decomposition takes place, however without formation of dimethyloxalate, dimethylcarbonate or formaldehyde. No dicarboalkoxy Pd-complexes were observed either. We suppose that the formation of $trans$ -monocarbomethoxy species occurs through a five-coordinated intermediate in which the CO and MeO are in cis position so they can react to give a Pd-COOMe moiety (Scheme 5). Probably, the formation of this species stabilizes the square-planar $trans$ -[Pd(COOMe)(OTs)(SPANphos)] complex, thus preventing further transformation (*i. e.* its conversion to dicarboalkoxy species and oxalate or formation of dimethylcarbonate by alcoholysis).



Scheme 5. Putative mechanism of the formation of $trans$ -[Pd(COOMe)(OTs)(SPANphos)].

The fact that reductive elimination takes place immediately with Xantphos or DPEphos seems in contrast with the poor catalytic performance obtained with these wide bite angle bidentates. This observation makes us to suppose that in these cases the difficult step of the catalysis is the formation of a dicarboalkoxy species or of any species that lead to their formation. This behavior was also observed for C-C cross coupling and hydrocyanation reactions using palladium and a similar diphosphine ligand series, for which wider bite angles gave rise to side reactions before the palladium bis hydrocarbyl intermediate could form.^{4 g, h.}

Conclusions

The oxidative carbonylation of *i*PrOH catalyzed by $[\text{PdX}_2(\text{P}\cap\text{P})]$ gives the corresponding oxalate, the major product, and carbonate. Acetone is also formed as a minor by-product. The catalytic performance is strongly influenced by the diphosphine ligand properties (bite angle, electronic and steric parameters), the nature of the anion and the pressure of carbon monoxide. Specifically, high activity and selectivity toward oxalate are achieved with weakly coordinating anions, $\text{P}\cap\text{P}$ ligands with a relatively wide bite angle capable of maintaining *cis*- geometry, and under relatively high CO pressure. The best results were obtained with *cis*- $[\text{Pd}(\text{OTs})_2(p\text{MeO}-\text{dppf})]$. These results and those on the reactivity of the dicarboalkoxy species of the type *cis*- $[\text{Pd}(\text{COOMe})_2(\text{P}\cap\text{P})]$ suggest that the slow step of the catalysis is related to the nature of $\text{P}\cap\text{P}$. For dppe, dppp the reductive elimination of oxalate in the product forming step may be rate limiting, while for dppb, dppf and substituted-dppf this might be the reoxidation step. For DPEphos and Xantphos the formation of dicarboalkoxy species may be hampered, as stoichiometric reactions show that the reductive elimination of oxalate from a biscarbomethoxy palladium complex is very fast.

The importance of the *cis*- chelation has been shown studying the reactivity of the SPANphos-based catalyst, the poorest performer. Although in this case the monocarbomethoxy complex *trans*- $[\text{Pd}(\text{COOMe})(\text{OTs})(\text{SPANphos})]$ can be isolated, catalysis does not occur to a significant extent probably because the *trans* geometry does not favor the steps required for the advancement of the catalysis.

Experimental section

Instrumentation and materials

All reactions were carried out using standard Schlenk techniques under an atmosphere of argon. Chemicals were purchased from Sigma–Aldrich, Acros Chimica, Strem Chemicals and Eurisotop. NMR spectra were recorded on Bruker 400 and 500 MHz spectrometers. ^{31}P and ^{13}C spectra were measured ^1H decoupled. All ^1H and ^{13}C chemical shifts are reported relative to the residual proton resonance in the deuterated solvents. ^{31}P signals were referenced to an 85 % aqueous solution of H_3PO_4 . NMR under pressure was performed using a 5 mm sapphire HP–NMR tube with titanium head. Infrared spectra were recorded on a Nicolet FT–IR spectrophotometer. Mass spectra were run by MALDI–TOF on a Bruker Daltonics Autoflex spectrometer. X–ray analysis were recorder on a Bruker–Nonius diffractometer equipped with a APPEX 2 4K CCD area detector, a FR591 rotating anode with $\text{Mo}_{\text{K}\alpha}$ radiation, Montel mirrors as monochromator and a Kryoflex low temperature device ($T = 100 \text{ K}$). GC analysis was performed on: a) Hewlett–Packard Model 6890 chromatograph fitted with HP5, $30 \text{ m} \times 0.32 \mu\text{m} \times 0.25 \mu\text{m}$ column (detector: FID; carrier gas: N_2 , 0.7 mL/min ; oven: $40 \text{ }^\circ\text{C}$ (3.5 min) to $250 \text{ }^\circ\text{C}$ at $15 \text{ }^\circ\text{C/min}$). b) Hewlett–Packard Model 5890 Series II chromatograph fitted with 20 % Carbowax 20 M on 80–100 mesh Chromosob W, $1 \text{ m} \times 2.3 \text{ mm ID}$ packed column (detector: FID; carrier gas: N_2 ; 25 mL/min ; oven: 80°C). Carbon monoxide (purity 99.9 %) was supplied by Carbueros Metálicos. The dppe, dppp, dppb, dppf, dippf, dtbpf, dcyph, Xantphos, DPEphos, $(p\text{OCH}_3\text{--C}_6\text{H}_4)_2\text{PCl}$, $(p\text{CF}_3\text{--C}_6\text{H}_4)_2\text{PCl}$, PdCl_2 , $\text{Pd}(\text{OAc})_2$, $\text{Ag}(\text{OTs})$, $\text{TsO}\cdot\text{H}_2\text{O}$, NEt_3 , TMDA, *n*–BuLi, Na_2SO_4 , and anhydrous solvent (acetone, THF, CH_2Cl_2 , *n*–hexane and Et_2O) were purchased from commercial sources and used as received. 1,4–benzoquinone (BQ) was purified before use from ethyl ether. Dry *i*PrOH and MeOH were obtained by distillation over Mg and I_2 and stored over 4 \AA molecular sieves under argon. Dry CDCl_3 and CD_2Cl_2 were distilled over P_2O_5 and stored over 4 \AA molecular sieves under Ar. *p*OMe–dppf,¹³ SPANphos,⁸ *cis*–

$[\text{Pd}(\text{OAc})_2(\text{dppp})]$,¹⁴ *cis*- $[\text{Pd}(\text{OH}_2)(\text{OTs})(\text{dppp})](\text{TsO})$,¹⁴ $[\text{PdCl}_2(\text{CH}_3\text{CN})_2]$,¹⁵ *cis*- $[\text{PdCl}_2(\text{dppf})]$,¹⁶ and *cis*- $[\text{Pd}(\text{COOMe})_2(\text{dipy})]$ ¹² were prepared according to literature procedures.

Catalytic oxidative carbonylation of *i*PrOH

Typically, 5 mL of a solution of *i*PrOH and NEt_3 was introduced into a *ca.* 15 mL glass bottle, previously evacuated by a Ar flow, containing 0.001 mmol of catalyst precursor and the desired amount of BQ. The glass bottle was then placed in an autoclave of *ca.* 50 mL volume, previously evacuated by a vacuum pump, under Ar flow. The autoclave was first purged several (4–5) times with CO, then pressurized and heated to the desired pressure and temperature. The solution was stirred with a magnetic bar. After the desired reaction time the autoclave was rapidly cooled to 0 °C and then slowly depressurized. The solution was analyzed by GC using *n*-undecane and toluene as internal standard.

Preparation of the ligand

The diphosphine ligand is oxygen sensitive. This ligand was synthesized and manipulated under an argon atmosphere.

Synthesis of *p*CF₃-dppf. To a solution of ferrocene (0.24 g, 1.3 mmol) in *n*-hexane (7 mL) were quickly added *n*-BuLi (0.18 g, 2.8 mmol) and TMDA (0.31 g, 2.7 mmol) and the resulting solution was stirred at 60 °C for 1h. The heating bath was removed, and 3 mL of dry THF was added. The dark brown suspension was cooled to –78 °C and a solution of (*p*CF₃-C₆H₄)₂PCl (1.00 g, 2.8 mmol) in THF (2 mL) was added within 10 min. The reaction mixture was allowed to warm and was stirred overnight at room temperature. The solvent was removed *in vacuo*, at the residual was added Et₂O 20 mL and the insoluble solid was removed by filtration. The filtrate was washed with degassed water. The organic layer was dried over Na₂SO₄ and the solvent was removed *in vacuo*. *p*CF₃-dppf was purified by rotative

chromatography on silica gel using *n*-hexane. The crude products were recrystallized from *n*-hexane. Yield: (215 mg) 20 %. ^1H NMR (400 MHz, CDCl_3 , 25 °C): δ 7.57 (d, $J = 7.70$ Hz, 8 H), 7.40 (t, $J = 7.70$ Hz, 8 H), 4.34 (t, $J = 1.81$ Hz, 4H), 4.00 (q, $J = 1.81$ Hz, 4H). $^{31}\text{P}\{^1\text{H}\}$ NMR (161 MHz, CDCl_3 , 25 °C): δ -13.65. ^{13}C NMR (100 MHz, CDCl_3 , 25 °C): 133.6 (d, $J = 19.3$ Hz), 125.0 (m), 77.21 (s), 77.8 (d, $J = 14.5$ Hz), 72.7 (m). MALDI-MS: 826.1 $[\text{M}]^+$.

Preparation of the complexes

All the operations were made in argon atmosphere by Schlenk technique using anhydrous solvents. In Table 6 the ^1H and $^{31}\text{P}\{^1\text{H}\}$ NMR data of the synthesized complexes are reported.

Synthesis of *cis*-[Pd(OAc)₂(P∩P)] (P∩P = dppe, dppb, dppf, dippf, dtbpf, dcypf, pCF₃-dppf, DPEphos, Xantphos). To a suspension Pd(OAc)₂ (0.4 mmol) in acetone (3 mL) was dropwise added a solution of P∩P (0.4 mmol) in acetone (5 mL) within 10 min under stirring at room temperature. A precipitate formed in a few seconds. This suspension was concentrated to half volume and *n*-hexane (20 mL) was added under vigorous stirring. The microcrystalline solid was filtered off, washed with *n*-hexane and dried under vacuum.

cis-[Pd(OAc)₂(dppe)]. The general procedure was used except that the ligand was dissolved in acetone/ CH_2Cl_2 (1/1, 5 mL). Yield: 98 %. IR: $\nu(\text{OAc})$ 1613, 1580, 1369, 1319 cm^{-1} . MALDI-MS: 563.1 $[\text{M} - \text{AcO}]^+$.

cis-[Pd(OAc)₂(dppb)]. The general procedure was used except that the ligand was dissolved in acetone/ CH_2Cl_2 (1/1, 5 mL). Yield: 98 %. IR: $\nu(\text{OAc})$ 1615, 1570, 1403, 1317 cm^{-1} . MALDI-MS: 591,1 $[\text{M} - \text{AcO}]^+$.

cis-[Pd(OAc)₂(dppf)]. The general procedure was used except that the ligand was dissolved in acetone/THF (1/1, 5 mL). Yield: 89 %. IR: $\nu(\text{OAc})$ 1612, 1580, 1364, 1306 cm^{-1} . MALDI-MS: 719.0 $[\text{M} - \text{AcO}]^+$.

cis-[Pd(OAc)₂(dippf)]. The general procedure was used except that the ligand was dissolved in acetone/THF (1/1, 5 mL). Yield: 66 %. IR: $\nu(\text{OAc})$ 1613, 1574, 1359, 1307 cm⁻¹. MALDI-MS: 583.1 [M - AcO⁻]⁺.

cis-[Pd(OAc)₂(dtbpf)]. The general procedure was used except that the ligand was dissolved in THF (5 mL). Yield: 52 %. IR: $\nu(\text{OAc})$ 1625, 1310 cm⁻¹. MALDI-MS: 639.1 [M - AcO⁻]⁺.

cis-[Pd(OAc)₂(dcypf)]. Yield: 63 %. IR: $\nu(\text{OAc})$ 1620, 1604, 1360, 1297 cm⁻¹. MALDI-MS: 723.2 [M - AcO⁻]⁺.

cis-[Pd(OAc)₂(*p*CF₃-dppf)]. Yield: 69 %. IR: $\nu(\text{OAc})$ 1560, 1540, 1397, 1319 cm⁻¹. MALDI-MS: 991.0 [M - AcO⁻]⁺.

cis-Pd(OAc)₂(DPEphos). The general procedure was used except that the ligand was dissolved in THF (5 mL). Yield: 90 %. IR: $\nu(\text{OAc})$ 1613, 1581, 1363, 1310 cm⁻¹. MALDI-MS: 703.1 [M - AcO⁻]⁺.

cis-Pd(OAc)₂(Xantphos). The general procedure was used except that the ligand was dissolved in CH₂Cl₂ (5 mL). Yield: 78 %. IR: $\nu(\text{OAc})$ 1568, 1387 cm⁻¹. MALDI-MS: 743.1 [M - AcO⁻]⁺.

Synthesis of [PdCl₂(P∩P)] (P∩P = *p*CF₃-dppf, *p*MeO-dppf, SPANphos). In literature several procedures for the synthesis of these complexes are reported. For instance, *trans*-[PdCl₂(SPANphos)] was obtained by reaction of [PdCl₂(cod)] (cod = 1,5-cyclooctadiene) with stoichiometric amounts of SPANphos.⁸ I followed a similar procedure but using [PdCl₂(CH₃CN)₂] as palladium precursor. To a solution of [PdCl₂(CH₃CN)₂] (0.3 mmol) in 5 mL of CH₂Cl₂ was dropwise added a solution of the ligand (0.3 mmol) in 5 mL of CH₂Cl₂. After 30 min under stirring at room temperature the solution was concentrated at *ca.* 2 mL and Et₂O (20 mL) was added. The formed microcrystalline solid was filtered off, washed with Et₂O and dried under vacuum.

cis-[PdCl₂(*p*CF₃-dppf)]. Crystals of this complexes suitable for a single-crystal diffraction were obtained by recrystallisation from CH₂Cl₂ and Et₂O. Yield: 74 %. MALDI-MS: 966.9 [M - Cl]⁺.

cis-[PdCl₂(*p*MeO-dppf)]. Yield: 79 %. MALDI-MS: 815.0 [M - Cl]⁺.

trans-[PdCl₂(SPANPhos)]. Yield: 85 %. MALDI-MS: 845.2 [M - Cl]⁺.

Synthesis of [Pd(OH₂)_n(OTs)_{2-n}(P∩P)](TsO)_n (n = 0, 1; P∩P = dppe, dppb, dppf, dippf, dtbpf, dcypf, *p*CF₃-dppf, DPEphos, Xantphos, *p*MeO-dppf, SPANphos). Two different methods have been employed for the synthesis of these complexes. Method A: the [Pd(OAc)₂(P∩P)] complexes is treated with two equivalents of TsOH·H₂O to form the title complexes as already proposed by our groups for the synthesis of *cis*-[Pd(OH₂)(OTs)(dppp)](TsO).¹⁴ Method B: it has been used as standard procedure of synthesis.^{11a, 17} The title complexes is formed by treating the [PdCl₂(P∩P)] with Ag(OTs). TsO⁻ is a labile ligand and it can be displaced from the coordination sphere of the palladium by the water present in the system forming, probably only in the solid state, the cationic mono *aquo* complexes. Indeed in solution the ³¹P{¹H} NMR spectra of these *cis* complexes indicates that the two phosphorus atoms are equivalent (singlet signal) probably due to the fast exchange of labile water, TsO⁻ or solvent. To determine the formation of the cationic or the neutral complexes is crucial the interpretation of the H₂O¹⁸ and TsO¹⁹ signals in the IR spectra.

Method A. To a suspension of [Pd(OAc)₂(P∩P)] (0.2 mmol) in acetone (3 mL) was added dropwise a solution of TsOH·H₂O (0.4 mmol) in acetone (3 mL). After 15 minute stirring at room temperature the solution was concentrated to half volume and was added to *n*-hexane (20 mL) under vigorous stirring. The formed microcrystalline solid was filtered off, washed with *n*-hexane and dried under vacuum.

cis-[Pd(OH₂)(OTs)(dppe)](TsO). Yield 80 %. IR: ν(OH₂) 3225, ν(TsO) 1242, 1220, 1029, 1004, 998 cm⁻¹. MALDI-MS: 675.1 [M - H₂O - TsO]⁺.

cis-[Pd(OH₂)(OTs)(dppb)](TsO). Yield 78 %. IR: $\nu(\text{OH}_2)$ 3650, 3514; $\nu(\text{TsO})$ 1255, 1221, 1031, 1009, 996 cm⁻¹. MALDI-MS: 703.1 [M - H₂O - TsO⁻]⁺.

cis-[Pd(OH₂)(OTs)(dppf)](TsO)₂. Yield: 87 %. IR: $\nu(\text{OH}_2)$ 3422, $\nu(\text{TsO})$ 1222, 1031, 1007, 998 cm⁻¹. MALDI-MS: 831.0 [M - H₂O - TsO⁻]⁺.

cis-[Pd(OH₂)(OTs)(dippf)](TsO). Yield: 66%. MALDI-MS: 695.1 [M - H₂O - TsO⁻]⁺.

cis-[Pd(OH₂)(OTs)(dtbpf)](TsO). Yield: 82 %. IR: $\nu(\text{H}_2\text{O})$ 3394, $\nu(\text{TsO})$ 1279, 1239, 1031, 1007, 983 cm⁻¹. MALDI-MS: 751.2 [M - H₂O - TsO⁻]⁺.

cis-[Pd(OTs)₂(dcypf)]. Yield: 75 %. IR: $\nu(\text{OTs})$ 1234, 1030, 1007 cm⁻¹. MALDI-MS: 855.2 [M - TsO⁻]⁺.

cis-[Pd(OTs)₂(*p*CF₃-dppf)]. Yield: 71 %. IR: $\nu(\text{OTs})$ 1249, 1030, 1004 cm⁻¹. MALDI-MS: 1103.0 [M - TsO⁻]⁺.

cis-[Pd(OTs)₂(DPEphos)]. Yield: 82 %. IR: $\nu(\text{TsO})$ 1218, 1029, 997 cm⁻¹. MALDI-MS: 816.4 [M - TsO⁻]⁺.

cis-[Pd(OH₂)(OTs)(Xantphos)](TsO). Yield: 70 %. IR: $\nu(\text{OH}_2)$ 3438, $\nu(\text{TsO})$ 1257, 1227, 1034, 1011, 1001 cm⁻¹. MALDI-MS: 855.1 [M - H₂O - TsO⁻]⁺.

Method B. Ag(OTs) (0.2 mmol) was dissolved in 10 mL of MeOH with the exclusion of light, then [PdCl₂(P \cap P)] (0.1 mmol) dissolved in 10 mL of CH₂Cl₂ was added. The mixture was stirred at room temperature for 2 h. AgCl was filtered off through Celite, the solvent was evaporated under reduced pressure, the solid was dissolved again in minimum volume of acetone (*ca.* 1–2 mL) and the formed solution was added to *n*-hexane (20 mL) under vigorous stirring. The formed microcrystalline solid was filtered off, washed with *n*-hexane and dried under vacuum.

cis-[Pd(OTs)₂(*p*MeO-dppf)]. Yield: 78 %. IR: $\nu(\text{OTs})$ 1255, 1027, 1009 cm⁻¹. MALDI-MS: 951.1 [M - TsO⁻]⁺.

trans-[Pd(OTs)₂(SPANPhos)]. Yield: 80 %. IR: ν (OTs) 1223, 1030, 1009 cm⁻¹. MALDI-MS: 981.2 [M - TsO⁻]⁺.

Synthesis of *cis*-[Pd(C₂O₄)(dppf)]. To a suspension of *cis*-[Pd(OAc)₂(dppf)] (0.25 mmol) in ethanol (8 mL) was added dropwise a solution of H₂C₂O₄·2H₂O (0.28 mmol) in acetone (5 mL). After 20 minutes stirring at room temperature the solution was added Et₂O (20 mL) and the formed microcrystalline solid was filtered off, washed with H₂O, Et₂O and dried under vacuum. Yield: 80 %. IR: ν (C₂O₄) 1697, 1676, 1357, 780 cm⁻¹. Elem anal. Calcd for C₃₆H₂₈O₄P₂FePd: C, 57.74; H, 3.77; Found: C, 57.76 ; H, 3.99.

Synthesis of *cis*-[Pd(SO₄)(dppf)]·H₂O. To a suspension of [Pd(OAc)₂(dppf)] (0.25 mmol) in ethanol (3 mL) was added dropwise a solution of H₂SO₄ (0.3 mmol) in ethanol (1 mL). After 20 minutes stirring at room temperature 20 mL of Et₂O were added to the solution, and the formed microcrystalline solid was filtered off, washed with Et₂O and dried under vacuum. Yield: 86 %. IR: ν (H₂O) 3656, 3495, ν (SO₄) 1260, 1142, 1099, 897 cm⁻¹. Elem anal. Calcd for C₃₄H₃₀O₅P₂SFePd: C, 52.70; H, 3.90; S, 4.13; Found: C, 52.89; H, 3.65; S, 4.05.

Synthesis of *cis*-[Pd(COOMe)₂(P∩P)] (P∩P = dppe, dppp). *cis*-[Pd(OH₂)(OTs)(P∩P)](TsO) (0.1 mmol) was dissolved in 2 mL of MeOH and the solution was pressurized with carbon monoxide (2 atm) at 0 °C for 10 minutes under stirring. The reaction mixture turned from yellow to brown. NEt₃ (0.8 mmol) was then added while stirring along 10 more minutes. The light brown solid that formed was collected on a filter, washed with MeOH, Et₂O and dried under vacuum.

cis-[Pd(COOMe)₂(dppe)]. Yield: 80 %. IR: ν (C=O) 1627, 1653 cm⁻¹. Elem anal. Calcd for C₃₀H₃₀O₄P₂Pd: C, 57.84; H, 4.85; Found: C, 57.98 ; H, 4.65.

cis-[Pd(COOMe)₂(dppp)]. Yield: 86 %. IR: ν (C=O) 1622, 1647cm⁻¹. Elem anal. Calcd for C₃₁H₃₂O₄P₂Pd: C, 58.46; H, 5.06; Found: C, 57.82; H, 5.18.

Synthesis of *trans*-[Pd(COOMe)(OTs)(SPANphos)]. A 5 mm sapphire HPNMR tube was charged under Ar with a solution of *trans*-[Pd(OTs)₂(SPANphos)] (5 mg, 0.004 mmol) in 0.5 mL of CD₂Cl₂ with 10 % of MeOH and pressurized with 10 atm of CO at -78 °C.

In situ NMR study on the preparation of [Pd(COOMe)₂(P∩P)] (P∩P = dppe, dppp, dppb, dppf, DPEphos, Xantphos, SPANphos) by exchange reaction. A NMR tube was charged under Ar with a solution of *cis*-[Pd(COOMe)₂(dipy)] (2.5 mg, 0.007 mmol) in 0.2 mL of CD₂Cl₂ at which was added, at -78 °C, a solution of the desired P∩P (0.007 mmol) dissolved in 0.2 mL of CD₂Cl₂. The reaction was followed by ³¹P{¹H} and ¹H NMR spectroscopy. When dppf was used the 5 mm sapphire HPNMR tube was used and the solution was pressurized with 30 atm of CO at -78°C and the reaction was followed by variable-temperature ³¹P{¹H} and ¹H NMR spectroscopy.

Table 6. ¹H and ³¹P{¹H} NMR data of the synthesized complexes

<i>Complexes</i>	<i>δ¹H NMR</i> <i>[ppm]</i>	<i>δ³¹P{¹H} NMR</i> <i>[ppm]</i>
<i>cis</i> -[Pd(OAc) ₂ (dppe)]	7.93–7.27 (m, 20H, Ar) 2.25 (m, 4H, CH ₂) 1.66 (s, 6H, OAc)	59.15 (s)
<i>cis</i> -[Pd(OAc) ₂ (dppb)]	7.67–6.93 (m, 20H, Ar) 3.47 (m, 4H, CH ₂) 1.65 (s, 6H, OAc) 1.19 (m, 4H, CH ₂)	26.58 (s)
<i>cis</i> -[Pd(OAc) ₂ (dppf)]	7.99–7.39 (m, 20H, Ar) 4.42, 4.39 (s, 8H, Cp) 1.40 (s, 6H, OAc)	30.8 (s)
<i>cis</i> -[Pd(OAc) ₂ (dippf)]	4.66, 4.48 (s, 8H, Cp) 2.50 (m, 4H, <i>i</i> Pr) 1.99 (s, 6H, OAc) 1.65, 1.33 (dd, J _{PH} = 17.00 Hz,	61.74 (s)

	$J_{\text{PH}} = 7.05 \text{ Hz}, 24\text{H}, i\text{Pr}$	
<i>cis</i> –[Pd(OAc) ₂ (dtbpf)]	4.90–4.20 (m, 8H, Cp) 1.60–1.12 (m, 42H, OAc, <i>t</i> But).	62.81 (s)
<i>cis</i> –[Pd(OAc) ₂ (dcypf)]	4.63, 4.48 (s, 8H, Cp) 1.95–0.92 (m, 50H, OAc, Cy)	52.03 (s)
<i>cis</i> –[Pd(OAc) ₂ (<i>p</i> CF ₃ –dppf)]	7.98–7.52 (m, 16H, Ar) 4.78, 4.35 (s, 8H, Cp) 1.30 (s, 6H, OAc)	28.33 (s)
<i>cis</i> –[Pd(OAc) ₂ (DPEphos)]	7.66–6.12 (m, 28H, Ar) 1.32 (m, 6H, OAc)	28.14 (s)
<i>cis</i> –[Pd(OAc) ₂ (Xantphos)]	7.61–6.90 (m, 26H, Ar) 1.78 (s, 6H, C(CH ₃) ₂) 1.27 (m, 6H, OAc)	30.55 (s)
<i>cis</i> –[PdCl ₂ (<i>p</i> CF ₃ –dppf)]	8.09–7.77 (m, 8H, Ph) 4.58, 4.31 (s, 8H, Cp)	36.48 (s)
<i>cis</i> –[PdCl ₂ (<i>p</i> MeO–dppf)]	7.86–6.97 (m, 16H, Ph) 4.42, 4.23 (s, 8H, Cp) 3.89 (s, 12H, OMe)	34.33 (s)
<i>trans</i> –[PdCl ₂ (SPANPhos)]	8.03–7.19 (m, 22H, Ar) 6.55 (m, 2H, Ar) 2.70 (d, $J_{\text{HH}} = 13.82 \text{ Hz}$, 2H, H3a, H3a’) 2.14 (s, 6H, CH ₃ 4a, CH ₃ 4a’) 2.06 (d, $J_{\text{HH}} = 13.82 \text{ Hz}$, 2H, H3b, H3b’) 1.50 (s, 6H, CH ₃ 4b, CH ₃ 4b’) 1.41 (s, 6H, CH ₃ 6, CH ₃ 6’)	20.60 (s)
<i>cis</i> –[Pd(OH ₂)(OTs)(dppe)](TsO)	7.88–7.23 (m, 28H, Ar) 2.47 (m, 4H, CH ₂) 2.24 (s, 6H, CH ₃ –TsO)	67.80 (s)
<i>cis</i> –[Pd(OH ₂)(OTs)(dppb)](TsO)	7.73–6.89 (m, 28H, Ar) 3.45 (m, 4H, CH ₂) 2.30 (s, 6H, CH ₃ –TsO)	34.46 (s)

	1.17 (m, 4H, CH ₂)	
<i>cis</i> -[Pd(OH ₂)(OTs)(dppf)](TsO) ₂	8.04 – 6.87 (m, 28H, Ar)	47.06 (s)
	4.46, 4.26 (s, 8H, Cp)	
	2.24 (s, 6H, CH ₃ -TsO)	
<i>cis</i> -[Pd(OH ₂)(OTs)(dippf)](TsO)	7.63–7.11 (m, 8H, Ar)	83.62 (s)
	4.83, 4.62 (s, 8H, Cp)	
	2.70 (m, 4H, <i>i</i> Pr)	
	2.35 (s, 6H, CH ₃ -TsO)	
	1.73, 1.39 (dd, J _{PH} = 16.93 Hz, J _{PH} = 9.89 Hz, 24H, <i>i</i> Pr)	
<i>cis</i> -[Pd(OH ₂)(OTs)(dtbpf)](TsO) ^a	7.77–7.22 (m, 8H, Ar)	90.01 (s)
	4.90–4.21 (m, 8H, Cp)	
	2.41 (s, 6H, CH ₃ -TsO)	
	1.71–1.19 (m, 36H, <i>t</i> But)	
<i>cis</i> -[Pd(OTs) ₂ (dcypf)] ^a	7.74, 7.19 (s, 8 H, Ar)	76.90 (s)
	4.82, 4.64 (s, 8H, Cp)	
	2.40 (s, 6H, CH ₃ -TsO)	
	1.85–1.30 (m, 44H, Cy)	
<i>cis</i> -[Pd(OTs) ₂ (<i>p</i> CF ₃ -dppf)] ^a	8.15–7.01 (s, 24H, Ar)	37.16 (s)
	4.80, 4.70 (s, 8H, Cp)	
	2.35 (s, 6H, CH ₃ -TsO)	
<i>cis</i> -[Pd(OTs) ₂ (DPEphos)]	7.67–6.73 (m, 36H, Ar)	29.47 (s)
	2.36 (s, 6H, CH ₃ -TsO)	
<i>cis</i> -[Pd(OH ₂)(OTs)(Xantphos)](TsO)	7.91–6.95 (m, 34H, Ar)	45.21 (s)
	2.26 (s, 6H, CH ₃ -TsO)	
	1.83 (s, 6H, C(CH ₃) ₂)	
<i>cis</i> -[Pd(OTs) ₂ (<i>p</i> MeO-dppf)] ^a	7.89–6.94 (s, 24H, Ar)	45.72 (s)
	4.67, 4.56 (s, 8H, Cp)	
	3.88 (s, 12H, CH ₃ O)	
	2.34 (s, 6H, CH ₃ -TsO)	
<i>trans</i> -[Pd(OTs) ₂ (SPANPhos)]	8.33–6.77 (m, 32H, Ar)	δ 38.20 (s)
	2.36 (s, 6H CH ₃ -TsO)	
	2.31 (s, 6H, CH ₃ 4a, CH ₃ 4a')	
	2.27 (d, J _{HH} = 14.17 Hz, 2H,	

	H3a, H3a')	
	1.53 (d, $J_{\text{HH}} = 14.17$ Hz, 2H, H3b, H3b')	
	1.30 (s, 6H, CH ₃ 4b, CH ₃ 4b')	
	1.26 (s, 6H, CH ₃ 6, CH ₃ 6')	
<i>cis</i> -[Pd(C ₂ O ₄)(dppf)]	7.77–7.47 (m, 20H, Ar)	34.04 (s)
	3.72, 3.58 (s, 8H, Cp)	
<i>cis</i> -[Pd(SO ₄)(dppf)]·H ₂ O	7.75–7.27 (m, 20H, Ar)	41.71 (s)
	4.54, 4.40 (s, 8H, Cp)	
<i>cis</i> -[Pd(COOMe) ₂ (dppe)]	7.73–7.30 (m, 20H, Ar)	38.81 (s)
	3.43 (s, 6H CH ₃)	
	2.38–2.32 (m, 4H, CH ₂).	
<i>cis</i> -[Pd(COOMe) ₂ (dppp)]	7.56–7.38 (m, 20H, Ar)	0.25 (s)
	3.00 (s, 6H CH ₃)	
	2.50 (m, 4H, CH ₂)	
	1.92 (m, 2H, CH ₂) ppm.	
<i>trans</i> -[Pd(COOMe)(OTs)(SPANphos)]	7.65–6.47 (m, 32H, Ar)	15.92 (d)
^b	3.13 (s, 3H, COOCH ₃)	9.19 (d)
	2.35 (s, 6H, CH ₃ -TsO)	($J_{\text{PP}} = 180$ Hz)
	2.15 (s, 6H, CH ₃ 4a, CH ₃ 4a')	
	2.08 (m, 2H, H3a, H3a')	
	1.53–1.19 (m, 12H, H3b + H3b' + CH ₃ 4b + CH ₃ 4b' + CH ₃ 6 + CH ₃ 6').	

NMR spectra ¹H (400 MHz) and ³¹P{¹H} (161 MHz) were taken in CD₂Cl₂ at 25 °C.

Abbreviations: s, singlet; d, doublet; brs, broad singlet. ^(a) with *o*-CH₃-PPh₃ the complexes is not soluble.

^(a) NMR spectra ¹H (500 MHz) and ³¹P{¹H} (201 MHz) were taken in CD₂Cl₂ at –70 °C. ^(b) as ^(a) but in CD₂Cl₂/10% MeOH.

References

- (1) van Leeuwen, P. W. N. M.; Zuideveld, M. A.; Swennenhuis, B. H. G.; Freixa, Z.; Kamer, P. C. J.; Goubitz, K.; Fraanje, J.; Luitz, M.; Spek, A. L. *J. Am. Chem. Soc.* **2003**, *125*, 5523.
- (2) Casey, C. P. and Whiteker, G. T. *Isr. J. Chem.* **1990**, *30*, 299.
- (3) (a) Birkholz, M. N.; Freixa, Z.; van Leeuwen, P. W. N. M. *Chem. Soc. Rev* **2009**, *38*, 1099. (b) van Leeuwen, P. W. N. M.; Kamer, P. C. J.; Reek, J. N. H.; Dierkes, P. *Chem. Rev.* **2000**, *100*, 2741. (c) Dierkes, P.; van Leeuwen, P. W. N. M. *J. Chem. Soc., Dalton Trans.* **1999**, 1519. (d) Marcone, J. E.; Moloy, K. J. *J. Am. Chem. Soc.* **1998**, *120*, 8527.
- (4) (a) Freixa, Z.; Van Leeuwen, P. W. N. M. "Bite Angle Effects of Diphosphines in Carbonylation Reactions" in "Modern Carbonylation Methods" L. Kollár, Ed; Wiley-VCH, **2008**, 1. (b) van Haaren, R. J.; van Strijdonck, G. P. F.; Oevering, H.; Reek, J. N. H.; Kamer, P. C. J.; van Leeuwen, P. W. N. M. *Eur J Inorg Chem* **2001**, 837. (c) Kamer, P. C. J.; van Leeuwen, P. W. N. M.; Reek, J. N. H. *Acc. Chem. Res.* **2001**, *34*, 895. (d) van der Veen, L. A.; Keeven, P. H.; Schoemaker, G. C.; Reek, J. N. H.; Kamer, P. C. J.; van Leeuwen, P. W. N. M.; Lutz, M.; Spek, A. L. *Organometallics* **2000**, *19*, 872. (e) van der Veen, L. A.; Boele, M. D. K.; Bregman, F. R.; Kamer, P. C. J.; van Leeuwen, P. W. N. M.; Goubitz, K.; Fraanje, J.; Schenk, H.; Bo, C. *J. Am. Chem. Soc.* **1998**, *120*, 11616. (f) Kamer, P. C. J.; Reek, J. N. H.; van Leeuwen, P. W. N. M. *Chemtech* **1998**, *28*, 27. (g) Kranenburg, M.; Kamer, P. C. J.; van Leeuwen, P. W. N. M. *Eur. J. Inorg. Chem.* **1998**, 155 (h) Kranenburg, M.; Kamer, P. C. J.; van Leeuwen, P. W. N. M.; Vogt, D.; Keim, W. *J. Chem. Soc., Chem. Commun.* **1995**, 2177. (i) Kranenburg, M.; van der Burgt, Y. E. M.; Kamer, P. C. J.; van Leeuwen, P. W. N. M. *Organometallics* **1995**, *14*, 3081. (j) Casey, C.

-
- P.; Whiteker, G. T.; Melville, M. G.; Petrovich, L. M.; Gavney Jr., J. A.; Powell, D. R. *J. Am. Chem. Soc.* **1992**, *114*, 5535.
- (5) (a) van Zeist, W.-J.; Visser, R.; Bickelhaupt, F. M. *Chem. Eur. J.* **2009**, *15*, 6112. (b) Freixa, Z.; van Leeuwen, P. W. N. M. *Dalton Trans.* **2003**, 1980 (c) Carbó, J. J.; Maseras, F.; Bo, C.; van Leeuwen, P. W. N. M. *J. Am. Chem. Soc.* **2001**, *123*, 7630.
- (6) Jimenez-Rodríguez, C.; Roca, F. X.; Bo, C.; Benet-Buchholz, J.; Escudero-Adan, E. C.; Freixa, Z.; van Leeuwen, P. W. N. M. *Dalton Trans* **2006**, 268.
- (7) Zuideveld, M.; Swennenhuis, B. H. G.; Boele, M. D. K.; Guari, Y.; van Strijdonck, G. P. F.; Reek, J. N. H.; Kamer, P. C. J.; Goubitz, K.; Fraanje, J.; Lutz, M.; Spek, L.; van Leeuwen, P. W. N. M. *J. Chem. Soc. Dalton Trans.* **2002**, 2308.
- (8) Freixa, Z.; Beentjes, M. S.; Batema, G. D.; Dieleman, C. B.; van Strijdonck, G. P. F.; Reek, J. N. H.; Kamer, P. C. J.; Fraanje, J.; Goubitz, K.; van Leeuwen, P. W. N. M. *Angew. Chem. Int. Ed.* **2003**, *42*, 1284.
- (9) Tolman, C. A. *Chem. Rev.* **1977**, *77*, 313.
- (10) Bartik, T.; Himmler, T.; Schulte, H.; Seevogel, K. *J. Organomet. Chem.* **1984**, *272*, 29.
- (11) (a) Bianchini, C.; Meli, A.; Oberhauser, W.; Parisel, S.; Passaglia, E.; Ciardelli, F.; Gusev, O. V.; Kal'si, A. M.; Vologdin, N. *Organometallics* **2005**, *24*, 1018. (b) Zuideveld, M. A.; Swennenhuis, B. H. G.; Kamer, P. C. J.; van Leeuwen, P. W. N. M. *J. Organomet. Chem.* **2001**, *637-639*, 805.
- (12) (a) Santi, R.; Romano, A. M.; Garrone, R.; Millini, R. *J. Organomet. Chem.* **1998**, *566*, 37 (b) Giannoccaro, P.; Ravasio, N.; Aresta, M. *J. Organomet. Chem.* **1993**, *451*, 243. (c) Smith, G. D.; Hanson, B.E.; Merola, J. S.; Waller, F. J. *Organometallics* **1993**, *12*, 568.
- (13) Ogasawara, M.; Takizawa, K.; Hayashi, T. *Organometallics* **2002**, *21*, 4853.
- (14) Benetollo, F.; Bertani, R.; Bombieri, G.; Toniolo, L. *Inorg. Chim. Acta* **1995**, *233*, 5.

-
- (15) (a) Noskowska, M.; Sliwinska, E.; Duczmal, W. *Transit. Metal. Chem.* **2003**, *28*, 756. (b) Andrews, M. A.; Tony, C.; Chang, T.; Cheng, C. W. F.; Emge, T. J.; Kelly, K. P.; Koetzle, T. F. *J. Am. Chem. Soc.* **1984**, *106*, 5913.
- (16) (a) Butler, I. R.; Cullen, W. R.; Kim, T. J.; Rettig, S. J.; Trotter, J. *Organometallics* **1985**, *4*, 972. (b) Hayashi, T.; Konishi, M.; Kobori, Y.; Kumada, M.; Higuchi, T.; Hirotsu, K. *J. Am. Chem. Soc.* **1984**, *106*, 158.
- (17) (a) Bianchini, C.; Meli, A.; Oberhauser, W.; Segarra, A. M.; Claver, C.; Suarez, E. J. G. *J. Mol. Catal. A: Chem.* **2007**, *265*, 292. (b) Gustev, O. V.; Kalsin, A. M.; Peterleintner, M. G.; Petrovskii, P. V.; Lyssenko, K. A.; Akhmedov, N. G.; Bianchini, C.; Meli, A.; Oberhauser, W. *Organometallics* **2002**, *21*, 3637. (c) Fochi, F.; Jacopozzi, P.; Wagelius, E.; Rissanen, K.; Cozzini, P.; Mastrantoni, E.; Fisicaro, E.; Manini, P.; Fokkens, R.; Dalcanale, E. *J. Am. Chem. Soc.* **2001**, *123*, 7539.
- (18) Vicente, J.; Arcas, A. *Coordin. Chem. Rev.* **2005**, *249*, 1135.
- (19) Amadio, E.; Cavinato, G.; Dolmella, A.; Ronchin, L.; Toniolo, L.; Vavasori, A. *J. Mol. Catal. A: Chem.* **2009**, *298*, 103.

Short Final Comment

As mentioned in the General Introduction, we were initially interested in the study of the oxidative alkoxy carbonylation of ethene. However, since the reaction occurred also with formation of carbonate and oxalate, we decided to take into consideration also the study of the simpler system, *i. e.* the oxidative carbonylation of the alkanol. The aim was to take advantage of the knowledge gained by studying this system for studying later the oxidative carbonylation of ethylene. It turned out that the study was more challenging than expected (and also more interesting, at least for us). It took practically all the time of my thesis and yet much remains to be investigated.

Abstract/Riassunto

Student: EMANUELE AMADIO

Matriculation number: 955382

PhD: CHEMICAL SCIENCES

Cycle: XXII

Title of PhD thesis: *OXIDATIVE CARBONYLATION OF ALKANOLS CATALYZED BY Pd(II)-PHOSPHINE COMPLEXES*

The complexes *trans*-[Pd(COOR)(OH₂)(PPh₃)₂](TsO) (R = Me, Et, *n*Pr, *i*Pr, *n*Bu, *i*Bu, *sec*Bu) and *trans*-[Pd(COOR)_nX_{2-n}(PPh₃)₂] (R = Me, n = 1, 2; X = ONO₂, ONO, OTs, Br. R = *i*Pr, n = 1, X = Cl, Br) have been synthesised and characterised. Most of them have been used as catalyst precursors for the oxidative carbonylation of MeOH, selective to dimethyloxalate, using *p*-benzoquinone (BQ) as an oxidant. BQ changes properties of the reaction centre. When using *i*PrOH in place of MeOH, high activity and selectivity toward diisopropylxalate have been achieved using *trans*-[PdX₂(PAr₃)₂] with strongly coordinating X (Br), in presence of a base (NEt₃ or PAr₃-BQ adduct) and of an excess of LiBr. The slow step of the catalysis (RDS) might be the reoxidation of Pd(0), which is formed in the product-forming step. Using [PdX₂(P∧P)] the best performance has been achieved with weakly coordinating X (TsO) and using P∧P of relatively wide bite angle but with *cis*-geometry. The RDS is related to the nature of P∧P.

Sono stati sintetizzati e caratterizzati i complessi *trans*-[Pd(COOR)(OH₂)(PPh₃)₂](TsO) (R = Me, Et, *n*Pr, *i*Pr, *n*Bu, *i*Bu, *sec*Bu) e *trans*-[Pd(COOR)_nX_{2-n}(PPh₃)₂] (R = Me, n = 1, 2; X = ONO₂, ONO, OTs, Br. R = *i*Pr, n = 1, X = Cl, Br). Molti sono stati utilizzati come precursori

catalitici nella carbonilazione ossidativa di MeOH, selettiva a dimetilossalato, impiegando *p*-benzoquinone (BQ) come ossidante. Il BQ modifica le proprietà del centro di reazione. Con *i*PrOH al posto di MeOH si ottengono elevate attività e selettività a diisopropilossalato utilizzando *trans*-[PdX₂(PAr₃)₂] con X fortemente coordinanti (Br), in presenza di base (NEt₃ o PAr₃-BQ) e di LiBr in eccesso. Lo stadio lento della catalisi (RDS) potrebbe essere la riossidazione del Pd(0) che si forma nello stadio di formazione dell'ossalato. Con [PdX₂(P∩P)] le migliori prestazioni sono state ottenute con X debolmente coordinanti (TsO) e con P∩P ad angolo di morso relativamente ampio ma di geometria *cis*. L' RDS dipende da P∩P.

Signature of the student
